Energy, Mines and
Resources Canada

Énergie, Mines et
Ressources Canada

CANMET

Canada Centre for
Mineral and Energy
Technology

Centre canadien de la
technologie des
minéraux et de l'énergie

**Mining
Research
Laboratories**

**Laboratoires
de recherche
minière**

Canada

THE GEOLOGICAL AND ENGINEERING CLASSIFICATION OF NEPEAN SANDSTONE

B. GORSKI
CANADIAN MINE TECHNOLOGY LABORATORY

MRL 89-118(TR)

SEPTEMBER 1989

Carleton University - Fall term 1989

Integrated Science 60.399: Independent Study

Chairman: I.S. Pressman (Integrated Sciences Studies)

Faculty Supervisor: A.P.S. Selvadurai (Chairman of Civil Engineering)

MICROMEDIA

[illegible] (CANMET)

[illegible]

209 pp

90-02554/

THE GEOLOGICAL AND ENGINEERING CLASSIFICATION OF NEPEAN SANDSTONE

by

B. Gorski*

ABSTRACT

A rock substance may be classified differently depending on the scientific discipline involved in the study. Geologists, mining, and civil engineers require certain information about a rock substance for different reasons. Rock may be classified by age, mineralogy, physical and mechanical properties. The object of this study is to bring together a method of rock classification based on geological and engineering properties. Nepean sandstone was selected for this study as it is readily available and sufficient data exists to compare with the test results of this study.

---

*Rock Mechanics & Equipment Development Technologist,
Canadian Mine Technology Laboratory, Mining Research Laboratories,
CANMET, Energy, Mines and Resources Canada, Ottawa, Canada

CLASSIFICATION GÉOLOGIQUE ET D'INGÉNIERIE DU GRÈS DE NEPEAN

par

B. Gorski*

RÉSUMÉ

Un matériel rocheux peut être classifié de différentes façons, en fonction de la discipline scientifique impliquée dans une étude. Géologues, ingénieurs miniers et civils requièrent certaines informations techniques concernant un matériel rocheux pour différentes raisons. Une roche peut être classifiée en fonction de son âge géologique, sa minérologie ou ses propriétés physiques et mécaniques. L'objectif de cette étude est d'élaborer une méthode de classification du roc basée sur ses propriétés géologiques et physiques comme matériau d'ingénierie. Le grès de Nepean fut choisi à cause de sa disponibilité et que sufisamment de résultats existent pour comparer avec les résultats de tests de cette étude.

---

*Technologiste en mécanique des roches et technique de développement,
Laboratoire canadian de la technologie miniére, Laboratoires de recherche miniére,
CANMET, Énergie, Mines et Ressources Canada, Ottawa, Canada.

TABLE OF CONTENTS

Page

ABSTRACT i

RÉSUMÉ ii

1. INTRODUCTION 1

2. GENERAL METHODOLOGY 3

  2.1 REGIONAL GEOLOGY 3

  2.2 LABORATORY CORE DRILLING 3

  2.3 PHYSICAL PROPERTIES 4

  2.4 MECHANICAL PROPERTIES 4

3. GEOLOGICAL DETERMINATIONS 5

  3.1 SITE SELECTION 5

  3.2 SITE GEOLOGY 7

  3.3 MEGASCOPIC ANALYSES 7

  3.4 MICROSCOPIC ANALYSES 10

  3.5 ROCK CLASSIFICATION 10

4. SPECIMEN PREPARATION 15

  4.1 CUTTING AND LAPPING 15

  4.2 OVEN DRYING AND DIMENSIONING 19

  4.3 STRAIN GAUGING 19

5. PHYSICAL ROCK PROPERTY TESTS 19

  5.1 SPECIMEN SELECTION 19

  5.2 POROSITY MEASUREMENT 19

  5.3 P - WAVE MEASUREMENT 22

6. MECHANICAL ROCK PROPERTY TESTS 24

  6.1 MTS 815 ROCK MECHANICS TEST SYSTEM 24

    6.1.1 Component design 24

    6.1.2 Theory of operation 31

  6.2 BRAZILIAN TENSILE STRENGTH TESTS 35

  6.3 UNIAXIAL COMPRESSIVE STRENGTH TESTS 35

    6.3.1 Load control tests 37

    6.3.2 Circumferential control tests 39

  6.4 TRIAXIAL COMPRESSIVE STRENGTH TESTS 39

    6.4.1 Single stage load control tests 42

    6.4.2 Single stage circumferential control tests 42

    6.4.3 Multi stage circumferential control tests 43

6.5 CONFINED CONSTANT HEAD PERMEABILITY TEST 44
7. EXPERIMENTAL TEST RESULTS 46
7.1 POROSITY DATA 46
7.2 LONGITUDINAL WAVE VELOCITY DATA 46
7.3 BRAZILIAN TENSILE STRENGTH DATA 46
7.4 UNIAXIAL DATA - LOAD CONTROL 46
7.5 UNIAXIAL DATA - CIRCUMFERENTIAL CONTROL 48
7.6 SINGLE STAGE TRIAXIAL DATA - LOAD CONTROL 48
7.7 SINGLE STAGE TRIAXIAL DATA - CIRCUMFERENTIAL CONTROL . 48
7.8 MULTI STAGE TRIAXIAL DATA - CIRCUMFERENTIAL CONTROL . 51
7.9 CONSTANT HEAD PERMEABILITY DATA - CONFINED 51
8. ANALYSIS AND DISCUSSIONS OF TEST RESULTS 51
8.1 STATISTICAL TREATMENT OF DATA 51
8.1.1 Mean and standard deviation equations 51
8.1.2 Least squares linear regression equations 54
8.1.3 Least squares non linear regression equations 54
8.2 FACTORS EFFECTING STRENGTH TEST RESULTS 55
8.2.1 Specimen end restraint 55
8.2.2 Specimen length to diameter ratios 56
8.2.3 Specimen size 56
8.2.4 Specimen moisture content 56
8.2.5 Rate of loading 56
8.2.6 Intrinsic property effects 56
8.2.7 Jacketing effects 58
8.3 POROSITY 58
8.4 PERMEABILITY 58
8.5 BRAZILIAN TENSILE STRENGTH 58
8.6 UNIAXIAL COMPRESSIVE STRENGTH 58
8.7 YOUNG'S MODULUS 59
8.8 POISSON'S RATIO 59
8.9 PEAK STRAIN 59
8.10 RESIDUAL UNIAXIAL COMPRESSIVE STRENGTH 59
8.11 TRIAXIAL COMPRESSIVE STRENGTH 59
8.12 RESIDUAL TRIAXIAL COMPRESSIVE STRENGTH 60
8.13 LOAD VS CIRCUMFERENTIAL STRAIN RATE CONTROLLED TESTS 60
8.14 MOHR CIRCLE ANALYSIS 61

8.15 HOEK AND BROWN FAILURE ENVELOPE ANALYSES 61
8.16 MOHR-COULOMB FAILURE ENVELOPE ANALYSES 66
8.17 COMPUTER ANALYSES 67
9. CONCLUSIONS AND RECOMMENDATIONS 67
10. REFERENCES 75

TABLES

1 Specimen Selection Data 21
2 Porosity/Velocity Measurements 23
3 Brazilian Tensile Strength 36
4 Uniaxial Compressive Test Results 38
5 Triaxial Test Results 41
6 Permeability Test Results 45
7 Intact Failure Envelope Material Constants 63
8 Residual Failure Envelope Material Constants 63
9 Intact Failure Envelope Parameters 64

FIGURES

1 CMTL rock mechanics test system 2
2 Geographic location of quarry 6
3 Talus rock location 8
4 Upper quarry floor 8
5 Core-drilling of test block 9
6 Cored test specimens 9
7 Highland 91 cm rock saw 11
8 Rock face displaying erosional surface 11
9 Rock face displaying cross-bedding 12
10 Sandstone classification 12
11 Zeiss Microscope with Icon camera attached 13
12 Magnified thin section 80x 14
13 Water cooled 200 mm saw 16
14 Prepared test specimens 16
15 Lapping machine 17
16 Dial gauge tolerance plate 18
17 Oven, weigh scale, and desiccator 18

18 Gauged test specimen and strain indicators 20
19 Immersion porosity apparatus 20
20 Velocity measurement apparatus 23
21 Hydraulic power supply 25
22 Load frame and triaxial chamber 26
23 Confinement and pore/permeability pressure subsystem 28
24 Controller, function generator, and data display 29
25 Micro-consoles, temperature controller, and PDP 11/73 30
26 X-Y1-Y2 recorder, printer, plotter, and terminal 32
27 Principle of closed loop control 32
28 Flow chart of factors affecting rock failure in a stiff machine 33
29 Fast response, closed loop, servo-controlled test system 33
30 Complete uniaxial compressive stress-strain plots 34
31 Control modes versus rock brittleness 34
32 Brazilian test set-up 36
33 Uniaxial load control test set-up 38
34 Triaxial test set-up 40
35 Permeability test set-up 45
36 Tested Brazilian specimens 47
37 Tested uniaxial specimens - load control 47
38 Tested uniaxial specimens - circumferential control 49
39 Tested triaxial specimens - load control - σ_3=10MPa 49
40 Tested triaxial specimens - load control - σ_3=20MPa 50
41 Tested triaxial specimens - load control - σ_3=30MPa 50
42 Tested triaxial specimens - circumferential control - σ_3=10MPa 52
43 Tested triaxial specimens - circumferential control - σ_3=20MPa 52
44 Tested triaxial specimens - circumferential control - σ_3=30MPa 53
45 Tested triaxial specimens - multi stage circumferential control 53
46 Rock face displaying iron oxide groundwater staining 57
47 Rock face displaying high quartzite content and cross-bedding 57
48 Hoek and Brown Mohr circle analyses 62
49 Hoek and Brown graphical stress representation 65
50 Hoek and Brown load control single stage failure envelope 68
51 Hoek and Brown circumferential control single stage failure envelope 69
52 Hoek and Brown circumferential control multi-stage failure envelope 70
53 Mohr-Coulomb load control single stage failure envelope 71

54 Mohr-Coulomb circumferential control single stage failure envelope 72
55 Mohr-Coulomb circumferential control multi-stage failure envelope 73

APPENDICES

A Uniaxial tests - load control 77
  A-1 Stress vs. strain - axial strain gauges 78
  A-2 Stress vs. strain - circumferential strain gauges 82
  A-3 Lpost.bas - MTS Basic 86
  A-4 Uplot.bas - MTS Basic 91
B Uniaxial tests - circumferential control 94
  B-1 Stress vs. strain - axial strain gauges 95
  B-2 Stress vs. strain - axial lvdts 99
  B-3 Stress vs. strain - circumferential strain gauges 103
  B-4 Stress vs. strain - circumferential extensometer 107
C Single stage triaxial tests - load control 111
  C-1 Stress vs. strain - axial lvdts 112
  C-2 Stress vs. strain - circumferential extensometer 123
  C-3 Lmulti.bas - MTS Basic 134
  C-4 Tplot.bas - MTS Basic 138
D Single stage triaxial tests - circumferential control 141
  D-1 Stress vs. strain - axial lvdts 142
  D-2 Stress vs. strain - circumferential extensometer 153
E Multi stage triaxial tests - circumferential control 164
  E-1 Stress vs. strain - axial lvdts 165
  E-2 Stress vs. strain - circumferential extensometer 170
  E-3 Stress vs. confining pressure 175
F Additional software 180
  F-1 Mean.for - Fortran 77 181
  F-2 Slope.bas - MTS Basic 183
  F-3 Failure.for - Fortran 77 186
  F-4 Perm.bas - MTS Basic 194
G Geologic rock classification 196
  G-1 Sedimentary rock classification 197
  G-2 Igneous rock classification 199
  G-3 Metamorphic rock classification 201

1. INTRODUCTION

The pursuit of precious metals dates back to prehistoric man. As surface ore deposits depleted, the need to excavate into rock masses in search of precious metals increased. In times past if groundwater influx or rock falls were too frequent in an underground excavation, the mining activity would be terminated. Previous mining methods were labour intensive with no regard for safety to the miners. As time progressed advancements in technology led to mechanization of mining methods and man found himself excavating deeper into the bowels of the earth in search of ore. Such deep workings saw the need for stability in excavations so that miners could work safely in advancing stopes.

The safe design of underground openings in rock masses requires the use of rock mechanics principles. Prior to excavation the physical and mechanical properties of the rock mass must be determined. This requires both a geological and an engineering approach in mine design. Parameters used in determining rock mass behaviour as excavation progresses are determined from in situ tests and laboratory tests.

Considerable advancement has been made in standardizing test methods used for classifying rock masses based on their physical and mechanical rock properties. The standardized tests have been used extensively in Canadian mine design. Test methods used in this study conform to those test methods suggested by the Commission on Testing Methods, International Society for Rock Mechanics, Brown, (1981). Novel test methods used will be described further on in this paper.

Rock Mechanics tests have become highly specialized and sophisticated test equipment is used. The Department of Energy, Mines, and Resources Canada (EMR) has established such a unique Rock Mechanics Test Laboratory and it is situated in Ottawa. This test facility is called The Canadian Mine Technology Laboratory (CMTL) and is a section of the division of The Mining Research Laboratories (MRL). CMTL has recently updated the laboratory by acquiring a $1,000,000.00 computer controlled servo-hydraulic rock mechanics test system (fig. 1). To date this test system is the only one of its kind in Canada.

It is felt that the data that exists to date across Canada on the mechanical properties of various rock types should be consolidated and published. Such information would be of interest to the practicing geologist or geotechnical engineer. This data would be updated as more data is received.

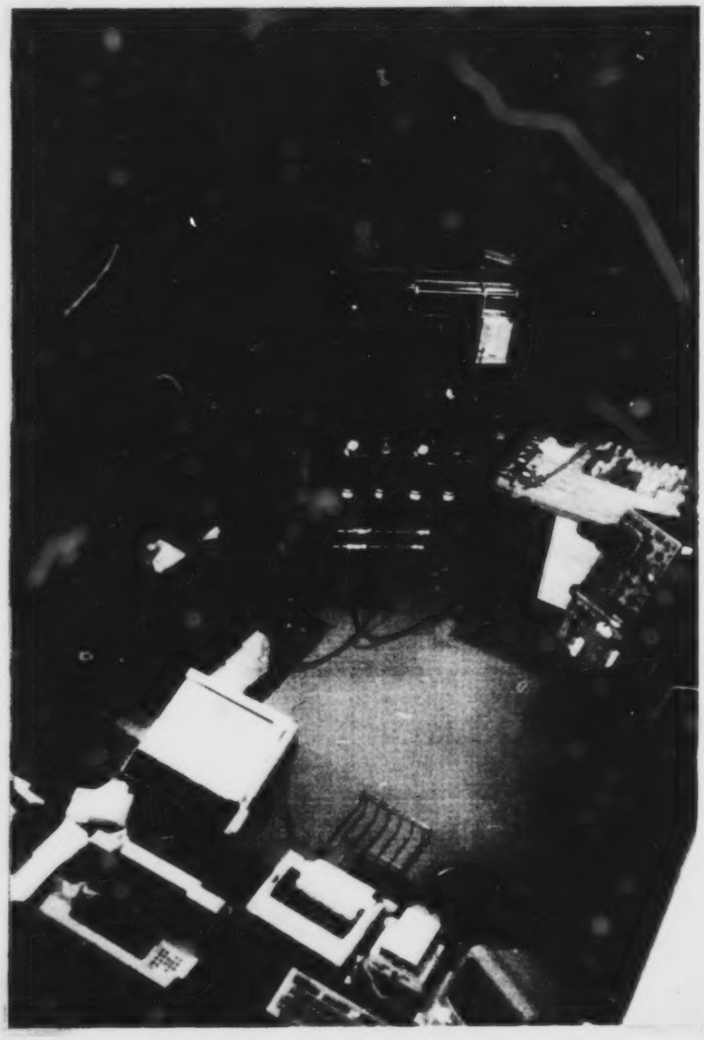

Fig. 1 CMTL rock mechanics test system

Publication of mechanical rock properties requires a rational and systematic approach to testing prior to data presentation. The formulation of a standard testing sequence and the presentation of the data is the object of this independent study. Variations in test methods and their effects on results will also be discussed. Sandstone from the Ottawa area was selected for testing in this study. The Rock Mechanics Test Facility at CMTL was used to undertake the actual test program.

This paper first defines the geological approach used. The engineering approach is then defined. The actual fieldwork and testing is then detailed. The data is then compiled and discussed including the theoretical basis.

2. GENERAL METHODOLOGY

2.1 REGIONAL GEOLOGY

Field drilling for assaying purposes is generally undertaken to determine the profitability of mining at a specific site.

Site drilling of rock strata for subsequent laboratory testing requires documentation of the following information:

General site geology
Dip of strata
Strike of strata
Borehole collar geodetic elevation
Borehole collar latitude and longitude
Borehole depth
Borehole dip and strike
Core logging by depth
Core % recovery

2.2 LABORATORY CORE LOGGING

Laboratory core logging details further those observations taken in the field and confirms stratigraphic classification. Megascopic features are recorded as follows:

Fracture spacing
Un-conformities
Lithology (igneous, sedimentary, metamorphic)
Lithology by depth
Bedding thickness
Bedding features

Bedding inclination
Hardness
Weathering
Colour
Grain sorting
Grain roundness
Grain shape
Matrix

Thin sections of major rock units are prepared from representative core both perpendicular and parallel to the core axis. Petrographic descriptions of the rock units are then recorded based on thin section microscopic analysis. Magnified thin sections are photographed for future reference. Microscopic analysis supplements megascopic descriptions including the following:

Grain mineralogy ratios
Matrix type
Grain maturity
Crystallization
Grain size

2.3 PHYSICAL PROPERTIES

Rock core units are separated by lithology for preparation prior to testing. The rock core specimens are cut to specified lengths and end lapped to within tolerances. The specimens are then oven dried, weighed, and their dimensions recorded. The physical properties are then determined as follows:

Bulk dry density
Saturated bulk density - immersion technique
Porosity
Void ratio
Grain density
Dry longitudinal wave velocity
Saturated longitudinal wave velocity
Confined constant head water permeability

2.4 MECHANICAL PROPERTIES

Mechanical properties of selected specimens are determined from the following sequence of tests:

Brazilian tensile strength - load control
Uniaxial compressive strength - load control
Uniaxial compressive strength - circumferential displacement control
Triaxial compressive strength - load control
Triaxial compressive strength - circumferential displacement control
Multi-stage triaxial compressive strength - circumferential displacement control

The mechanical properties are then calculated as follows:

Tensile strength
Ultimate uniaxial compressive strength
Young's modulus
Poisson's ratio
Peak strain
Triaxial compressive strength
Cohesion
Angle of internal friction
Angle of failure
Shear stress
Normal stress
Hoek and Brown intact failure envelope
Mohr-Coulomb intact failure envelope
Hoek and Brown residual failure envelope
Mohr-Coulomb residual failure envelope

3. GEOLOGICAL DETERMINATIONS

3.1 SITE SELECTION

Campbell's quarry located in Bell's Corners was selected as the site for retrieval of Nepean sandstone test specimens. The abandoned quarry at one time was the major source of sandstone building stone used in the construction of the Parliament Buildings. The quarry is located within the confines of NCC property adjacent to the Bells Corners CANMET Research Complex. The approximate geographic location of the quarry is 45° 19' 11" North latitude and 75° 52' 11" East longitude (fig. 2).

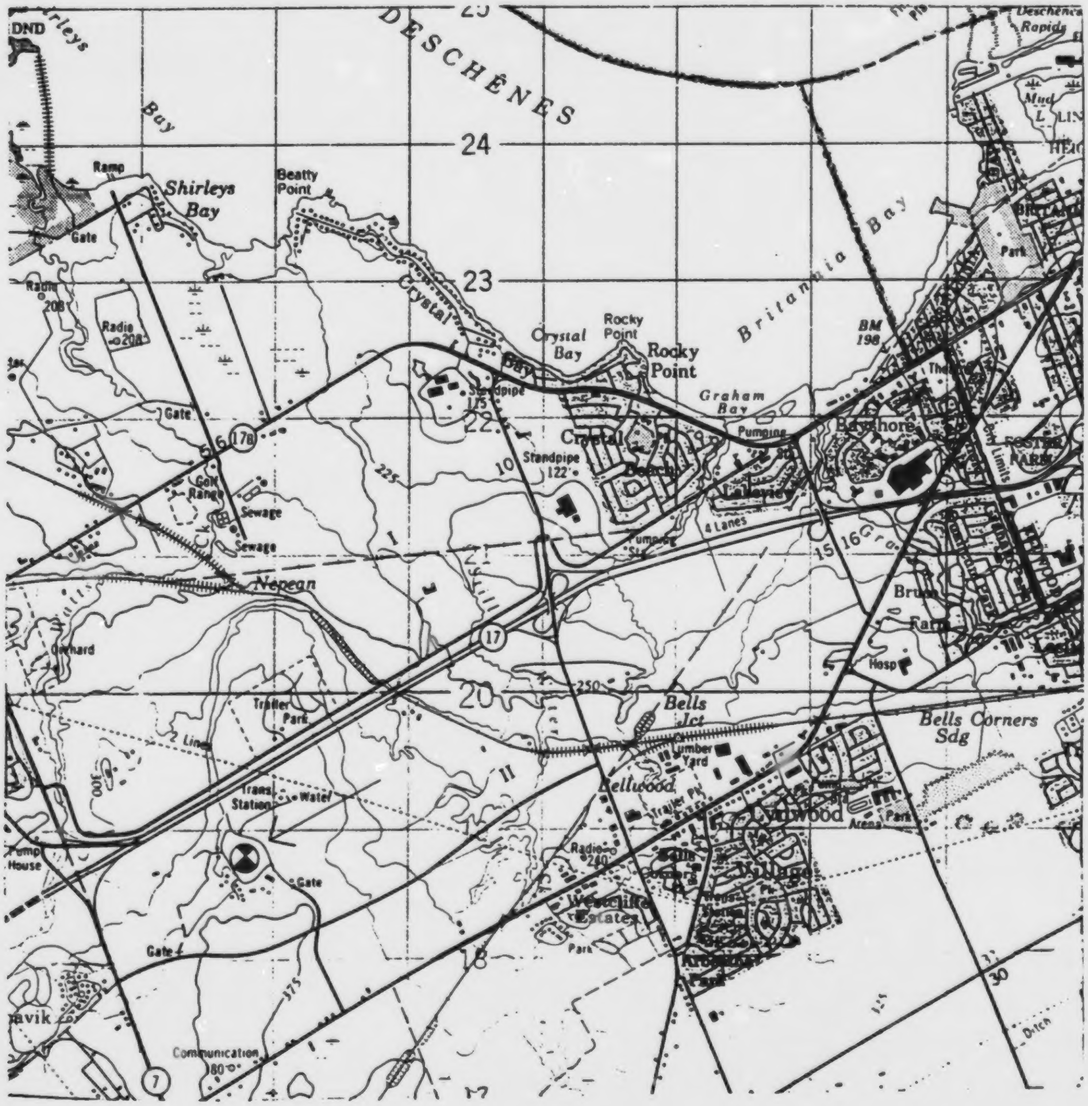
DND
DESCHÊNES
Deschênes Rapids
Mud L
Bay
24
Ramp
Shirleys Bay
Beatty Point
Gate
23
Radio 208
Radio 208
Crystal
Crystal Bay
Rocky Point
Rocky Point
Britannia Bay
BM 198
Graham Bay
Standpipe 175
22
Crystal Beach
Bayshore
Pumping Sta
Lakeview
Gate
178
Golf Range
Sewage
Sewage
225
10
Standpipe 122
FOSTER PARK
Park
City Limits
4 Lanes
Pumping Sta
15
16
Nepean
17
Bruce Farm
Hosp
Orchard
20
250
Bells Jct
Bells Corners Sdg
Trailer Park
Lines
Lumber Yard
Bellwood
Trans Station
Water
Lynwood
Arena
Park
Trailer Pk
Pump House
Gate
Radio 240
Bells Corners
Village
Westcliffe Estates
Park
Arlington Park
Gate
18
375
30
325
Ditch
Communication 380
7
17

Fig. 2 Geographic location of quarry

The geodetic elevation of the quarry floor was estimated to be 105 m. A sandstone block was selected from talus rock fringing the north-east part of the quarry (fig. 3). The dimensions of the rock specimen were 48 x 38 x 28 cm deep.

3.2 SITE GEOLOGY

Site geology is best described by Wilson, (1956). The Nepean Formation is the oldest member of the Paleozoic strata. It is thin to thick-bedded, coarse-grained, cream-coloured, silica sandstone, weathering grey with irregular brown stains. Where silica forms the cementing material it is hard with thin bands of pure quartzite. Near the top where the cement is calcareous or of iron oxide it disintegrates after long exposure. Since the formation was deposited on an irregular surface it has a wide range in thickness, the maximum known thickness being 85 meters. The Nepean has been formerly correlated with the Potsdam of New York, and it is assumed to be of Upper Cambrian age. It appears to be un-fossiliferous in the Ottawa area, and its age is not definitely known. There is no discernible break between the Nepean and the March formation above it. It is possible that the Nepean sandstone was laid down in an advancing Ordovician sea.

In the quarry many joint planes are inclined perpendicular to the horizontal (fig. 4). Joint planes occurred in the rock due to shrinkage during solidification. Ripple marks are close and asymmetric indicating shallow water deposition near shore by breaking waves, where top water was carried forward by the wind. Dark spots of iron material are observable indicating percolating water which dissolved the oxidized material and carried it through the porous sandstone re-depositing it en route. Some dark streaks are observed in irregular concentric circles suggestive of cross-bedding. Three thin bands of quartzite each approximately 5 mm thick are located within the cored segment of the test block. This was confirmed during coring by reduction in the recovery speed when the thin layers were encountered due to their increased hardness. Generally the composition of the test block was found to be medium grained white quartz sandstone with increasing quartzite content from top to bottom.

3.3 MEGASCOPIC ANALYSES

The sandstone sample was transported to the CMTL laboratory in preparation for subsequent testing. The block was core-drilled perpendicular to the bedding using an Ibarmia drill equipped with a water swivel (fig. 3). A 45 mm diameter thin wall diamond impregnated core barrel was used to extract 35 cylindrical test specimens having length to diameter ratios of at least 3 to 1 (fig. 4). Specimens were core-drilled at 1136 rpm with an advancing thrust of 4 kN regulated by an air intensifier.

Fig. 3 Talus rock location

Fig. 4 Upper quarry floor

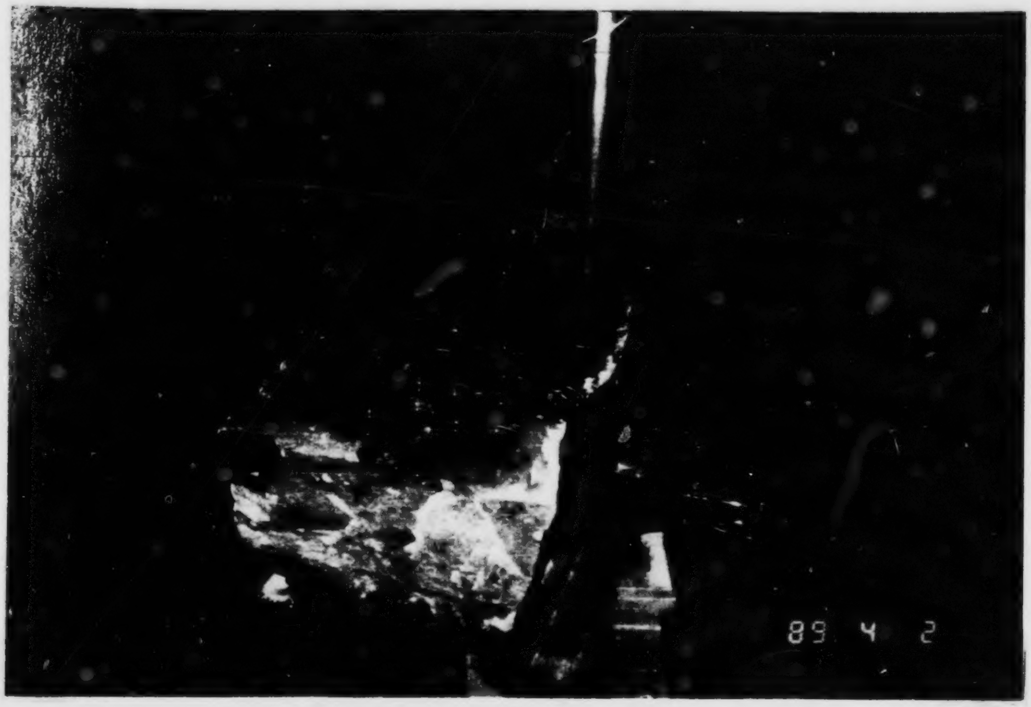

Fig. 5 Coredrilling of test block

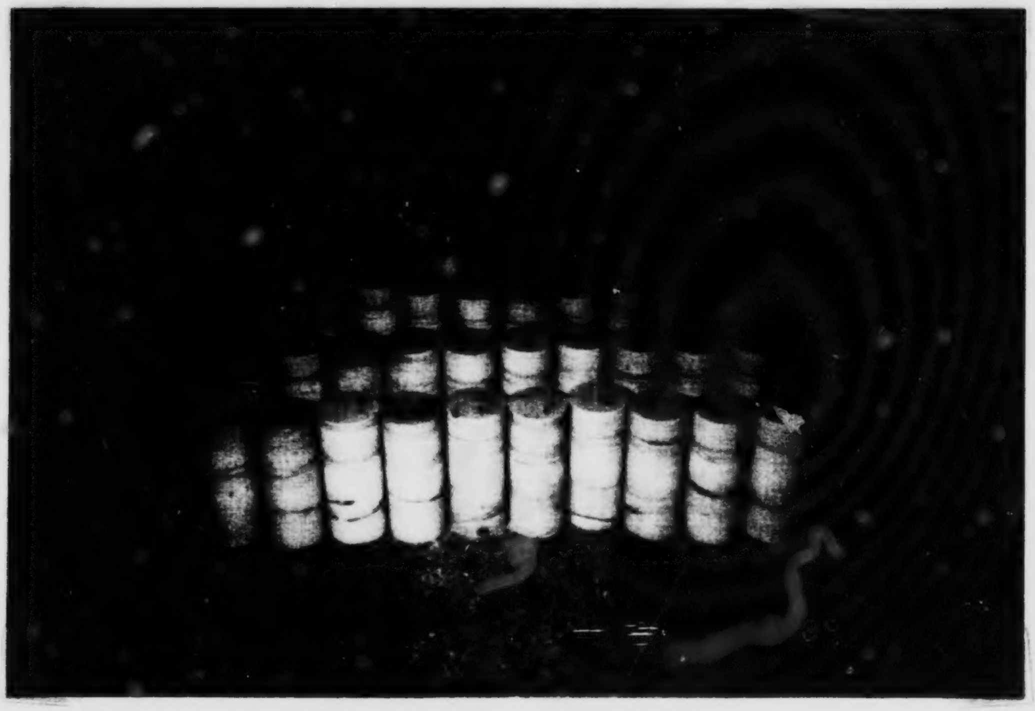

Fig. 6 Cored test specimens

Once cored the block was cut into 4 segments by cutting in two vertical planes at right angles to each other and perpendicular to the bedding. A Highland Park 91 cm diameter diamond rock saw cooled with Almag cutting fluid was used to cut the rock (fig. 7). The cuts were performed to facilitate the determination of megascopic features based on fresh surfaces. The faces were displayed 'top up'. A prominent asymmetric erosional surface was observed across the base of the region cored (fig. 8). Below and above the erosional surface cross bedding was well defined by the presence of dark streaks separating the bedding planes (fig. 9).

3.4 MICROSCOPIC ANALYSES

Petrographic analysis was conducted using a standard Zeiss microscope. A thin section of Nepean sandstone on loan from Carleton University's department of Earth Sciences was used for microscopic analyses. The sandstone was classified according to Gilbert, (1982), (fig. 10). The sandstone was classified as a super-mature quartz arenite. The quartz arenite is well sorted, displaying well rounded quartz grains averaging 0.14 mm in diameter. Little or no calcite cement matrix was evident and quartz cement over-growths were confirmed by bands of tiny bubbles. Tangential grain contacts were observed with some grains displaying diametral cracks.

The magnified thin section was photographed with a 35 mm Zeiss Ikon camera equipped with a Zeiss microscope adapter (fig. 11). The thin section was photographed at a magnification of 80X (fig. 12).

3.5 ROCK CLASSIFICATION

An ideal classification of rocks should include petrography, genesis, and chemical composition, and should group together genetically related rocks. The classification of rocks as proposed by R. B. Travis of The Colorado School of Mines, (1955), is considered to be adequately encompassing in this regard. The proposed rock classifications for sedimentary, metamorphic, and igneous rocks are reproduced in table form in Appendix G. Methods used by geologists in determining rock nomenclature are extensively documented and discussion thereof will not lend itself to this paper.

Based on microscopic and megascopic analysis and supplemented with the geology of the area as detailed by A. E. Wilson, the sandstone may be classified as follows according to R. B. Travis and The North American Stratigraphic Code:

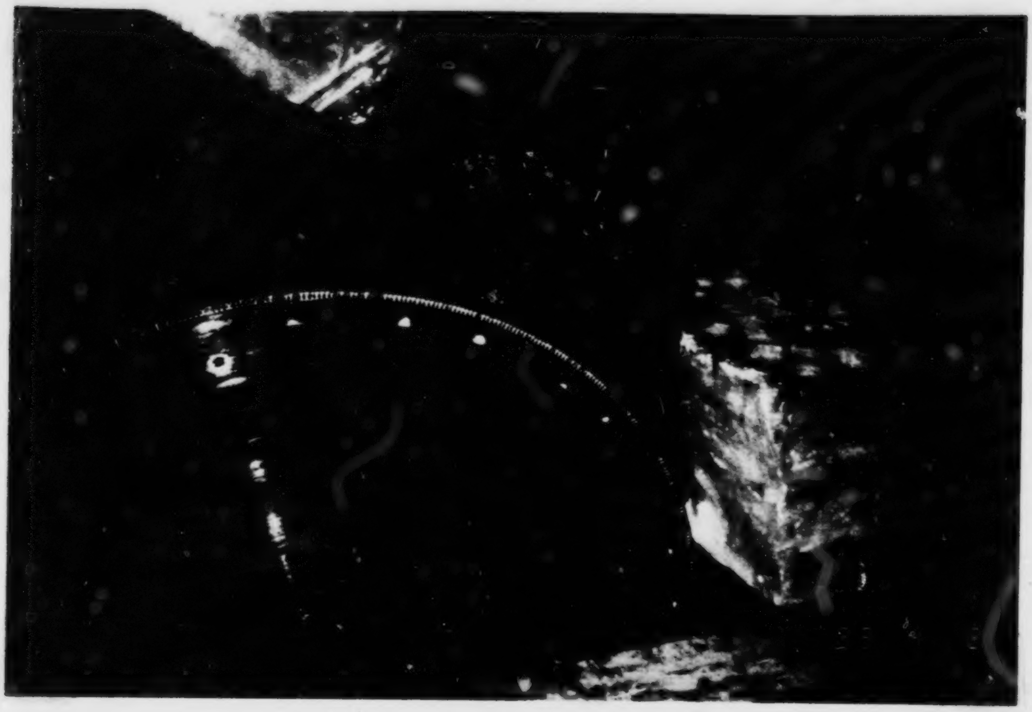

Fig. 7 Highland 91 cm rock saw

Fig. 8 Rock face displaying erosional surface

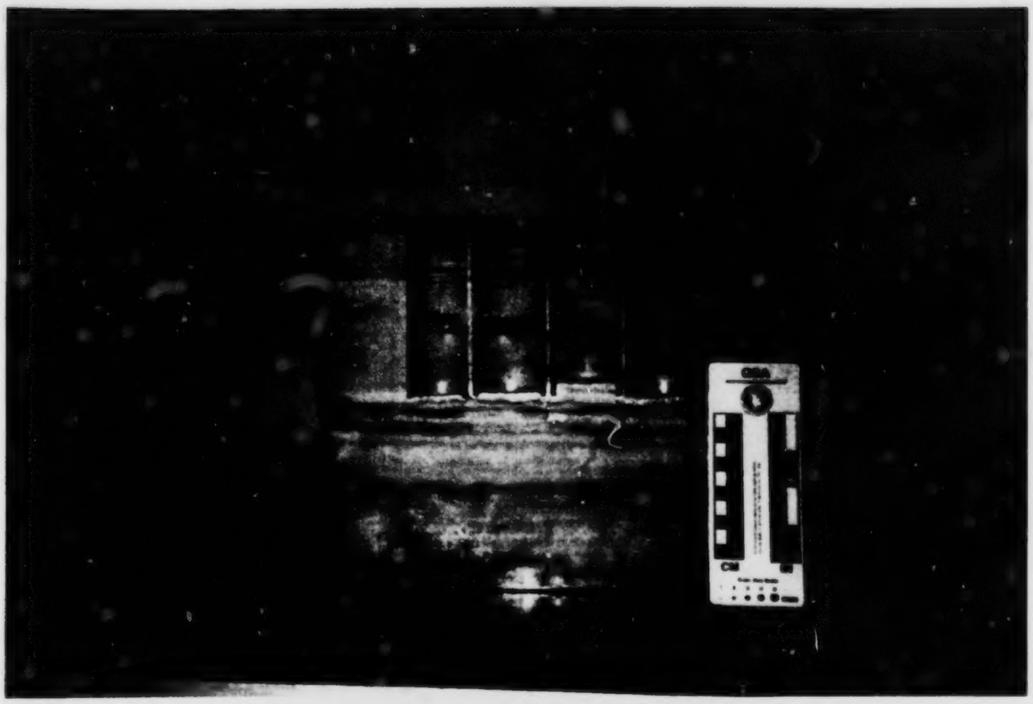

Fig. 9 Rock face displaying crossbedding

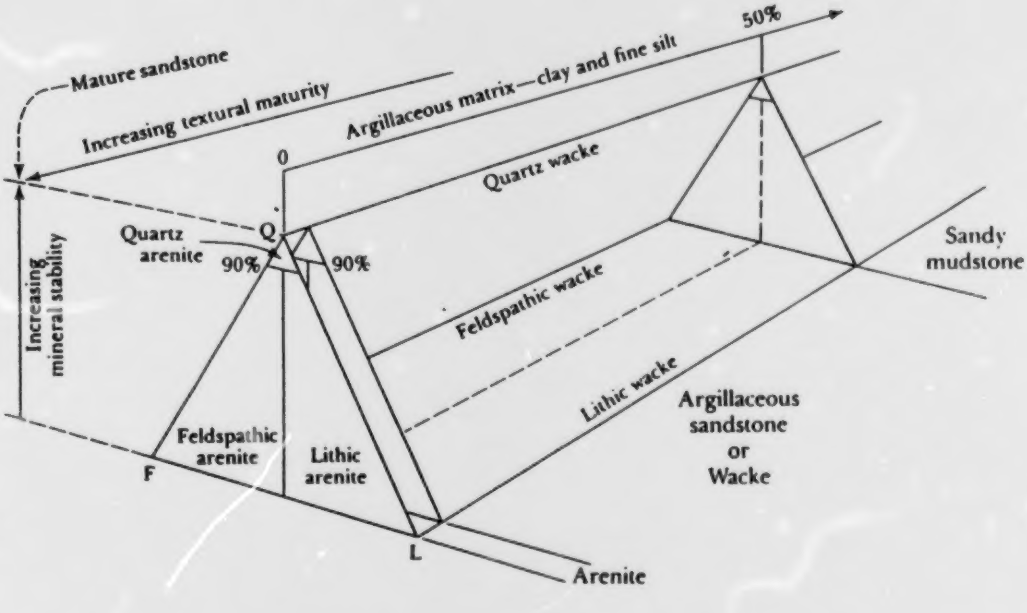
50%
Mature sandstone
Increasing textural maturity
Argillaceous matrix—clay and fine silt
0
Quartz wacke
Q
Quartz arenite
90%
90%
Increasing mineral stability
Feldspathic wacke
Sandy mudstone
Lithic wacke
Argillaceous sandstone or Wacke
Feldspathic arenite
Lithic arenite
F
L
Arenite

Fig. 10 Sandstone classification (Gilbert, 1982)

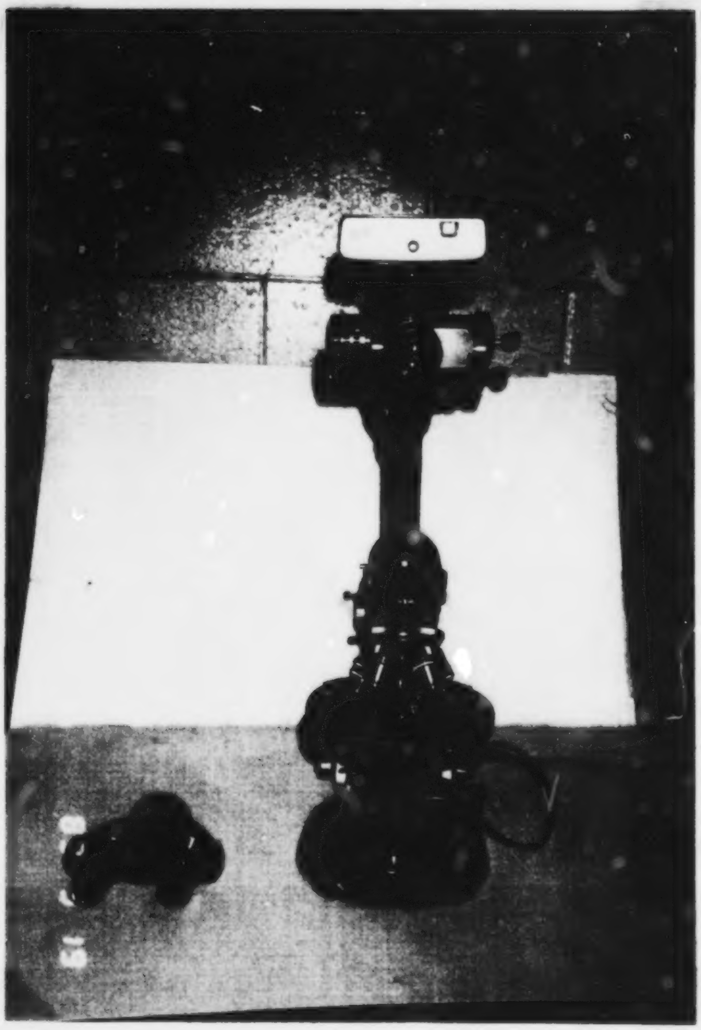

Fig. 11 Zeiss Microscope with Icon camera attached

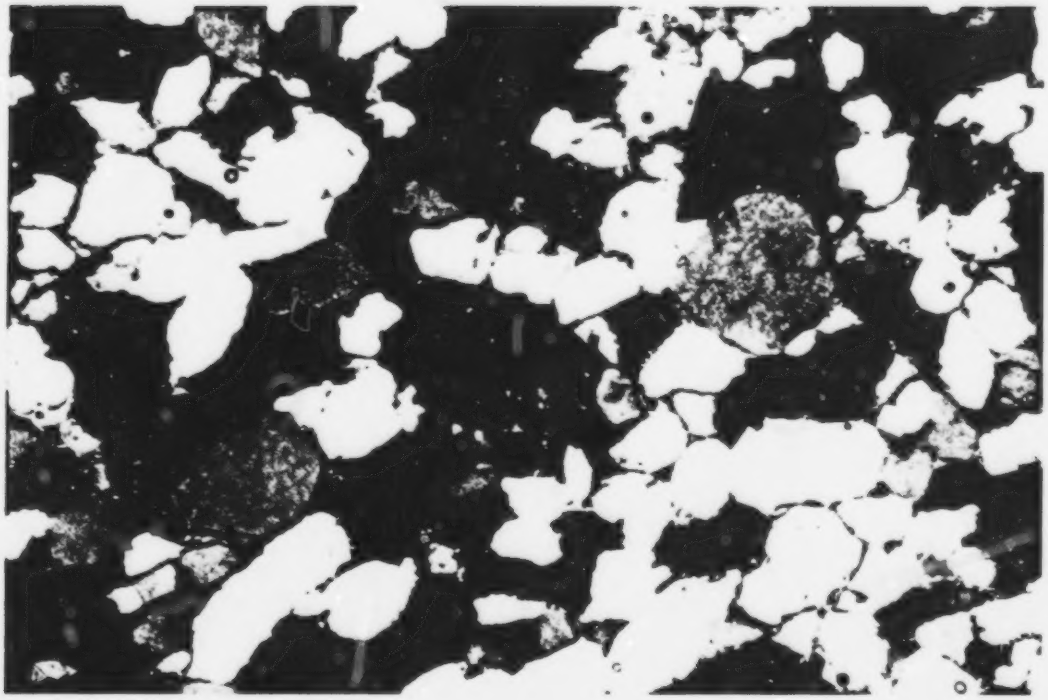

Fig. 12 Magnified thin section 80x

Genetic - Sedimentary
Texture - Clastic allogenic
Color - White
Structure - Ripple marks
Grain size - 0.14 mm diameter
Grain shape - well rounded
Sorting - well sorted
% Quartz - >90%
Sandstone classification - Quartz arenite (Quartz sandstone)
Era - Paleozoic
Age - Upper Cambrian
Period - Chazy
Formation - Nepean

4. SPECIMEN PREPARATION

4.1 CUTTING AND LAPPING

The coring technique method used was described under megascopic analysis. The proper combination of peripheral speed versus diamond cutting force was dependent on the rock hardness and water flushing rate. Down feed force was maintained using an air intensifier equipped with an air regulator. The method adjusts automatically to variable rock hardness encountered in the run. Fixed gear driven drills over-stress diamond core drills when advancing in hard rock and cause premature wearing of the core bit.

Once cored the specimens were cut to approximate test lengths using a Felker Di-Met water cooled 200 mm diamond saw (fig. 13). Brazilian test specimens were cut to a length to diameter ratio of 1:2, uniaxial and triaxial specimens to 2.3:1, and the permeability test specimen was cut to 1:1 (fig. 14). Once cut the specimens were end lapped (fig. 15). The lapping machine laps both ends of the rock specimen simultaneously. A water-carborundum grit slurry is used as the grinding medium. The lapping method is a single step process whereby a rock specimen ends are prepared flat, parallel, and perpendicular to the axis of the core to within .025 mm tolerance. Finished tolerances were confirmed with a dial gauge and surface plate (fig. 16). Cylindrical surfaces were confirmed as being true therefore cylindrical grinding techniques were not necessary.

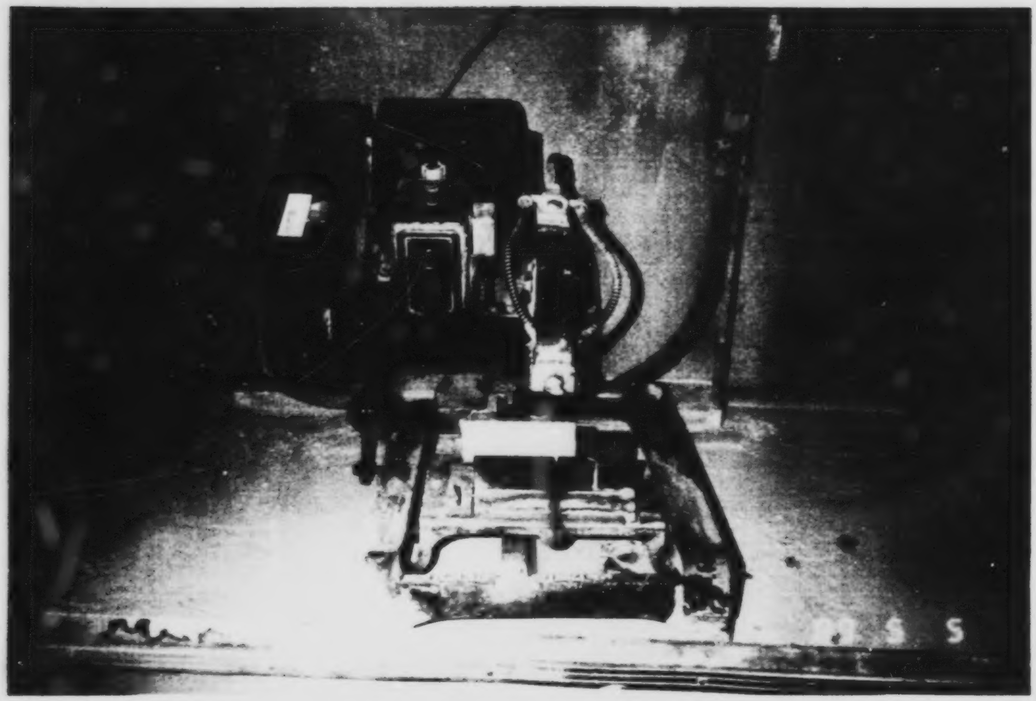

Fig. 13 Water cooled 200 mm saw

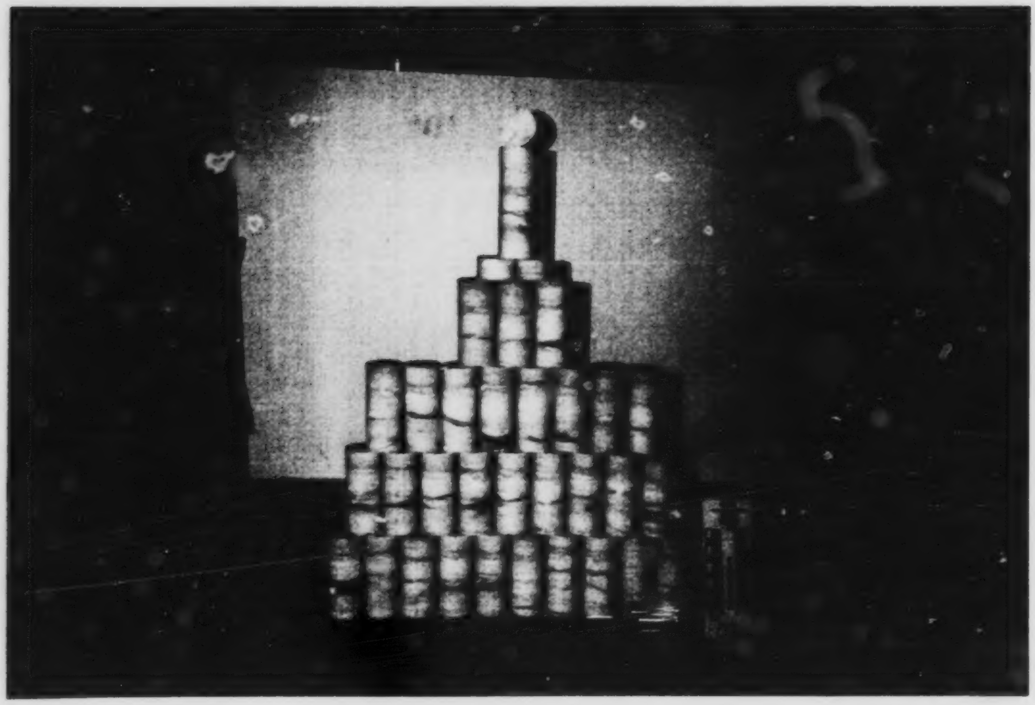

Fig. 14 Prepared test specimens

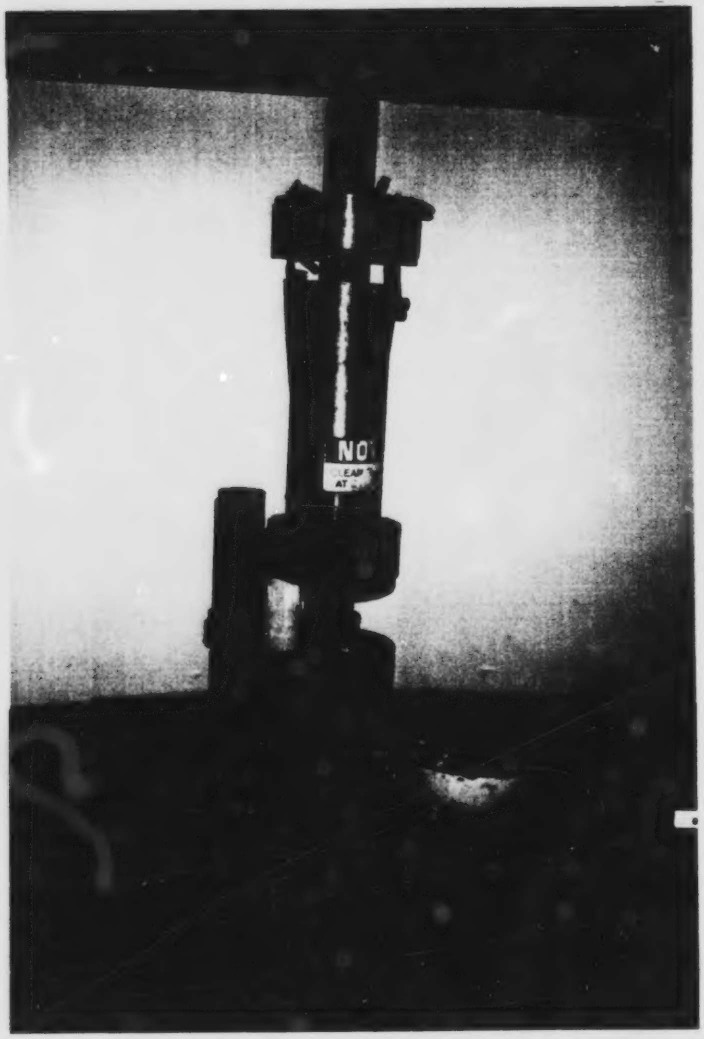

Fig. 15 Lapping machine

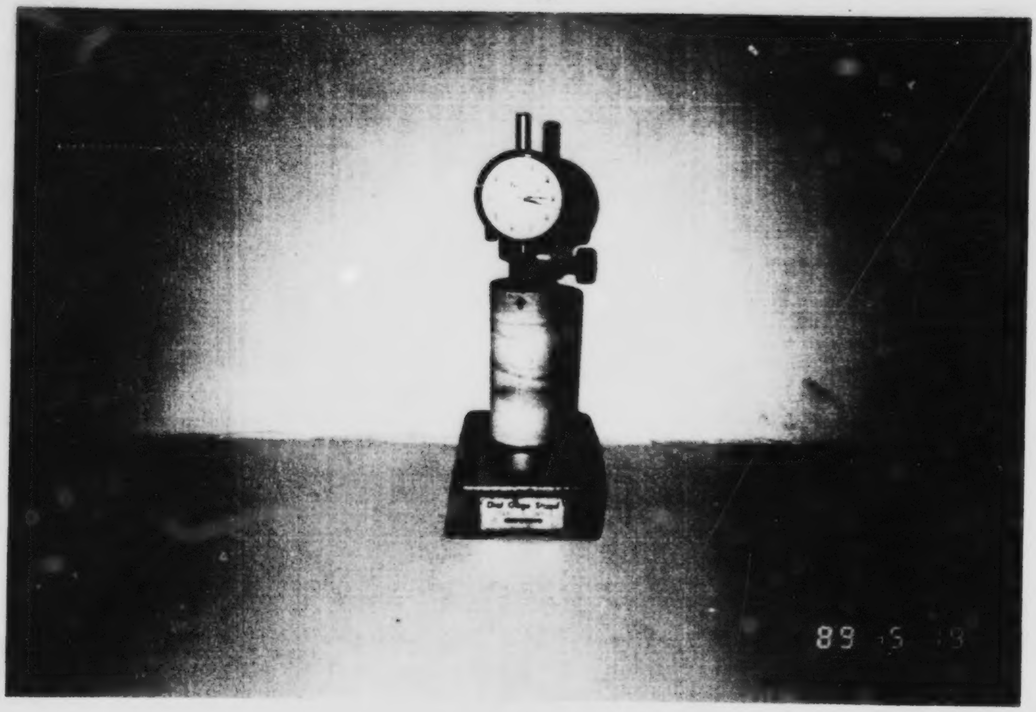
Dial Gauge Stand
89 5 19

Fig. 16 Dial gauge tolerance plate

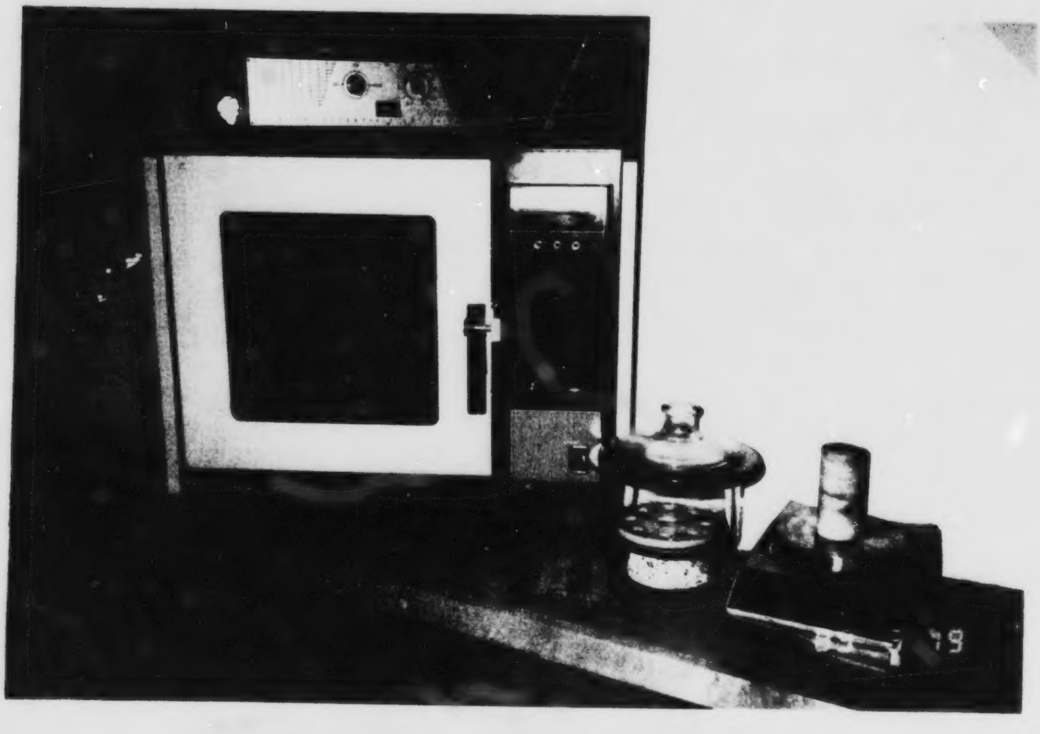

Fig. 17 Oven, weigh scale, and desiccator

4.2 OVEN DRYING AND DIMENSIONING

Lapped specimens were washed clean of grit residue and then dried and evacuated using a Fisher model 282 isotemp vacuum oven. The heating rate was regulated so as not to exceed 1° C per minute. Excessive heating rates and high temperature levels are known to induce micro-fracturing as confirmed by Simmons et al, (1978). The specimens were oven dried at a temperature of 50° C for 3 hours. Dried specimens were then weighed using a Mettler PC 2000 electronic balance accurate to within 0.01 grams. Physical dimensions were taken using a vernier caliper accurate to within 0.02 mm. The measured specimens were then stored in desiccator prior to testing (fig. 17).

4.3 STRAIN GAUGING

Uniaxial test specimens were strain gauged using SR4 120 ohm strain gauges. The strain gauges provide the means to monitor rock deformation during testing. The strain gauges were bonded to the cylindrical surfaces of the rock at mid height. The gauges were bonded to the rock surfaces using Permabond 910 adhesive, a one component cyanoacyrlate ester. For every specimen four gauges were applied. Two gauges were aligned parallel to the axis of the core and diametrically opposed. The other two gauges were aligned perpendicular to the axis of the core and diametrically opposed. The two pairs of gauges were then wired in series separate circuits (fig. 18). The series circuits provide an averaging of strain read-outs.

5. PHYSICAL ROCK PROPERTY TESTS

5.1 SPECIMEN SELECTION

Three specimens were selected for each triaxial, uniaxial, and brazilian test series. Spare specimens were placed on reserve and used in instances of invalidated tests. Table 1 displays the actual test sequences including coding, test type, specimen length, and specimen bulk dry density. All specimens were of 44.80 mm in diameter.

5.2 POROSITY MEASUREMENT

This test is intended to measure the porosity, the dry density, and related properties of a rock specimen in the form of specimens of regular geometry.

Porosity measurements were conducted on specimens N31 and N35. The bulk dry densities were calculated from those measurements described under oven drying and dimensioning. The specimens were then evacuated in a chamber for four hours (fig. 19).

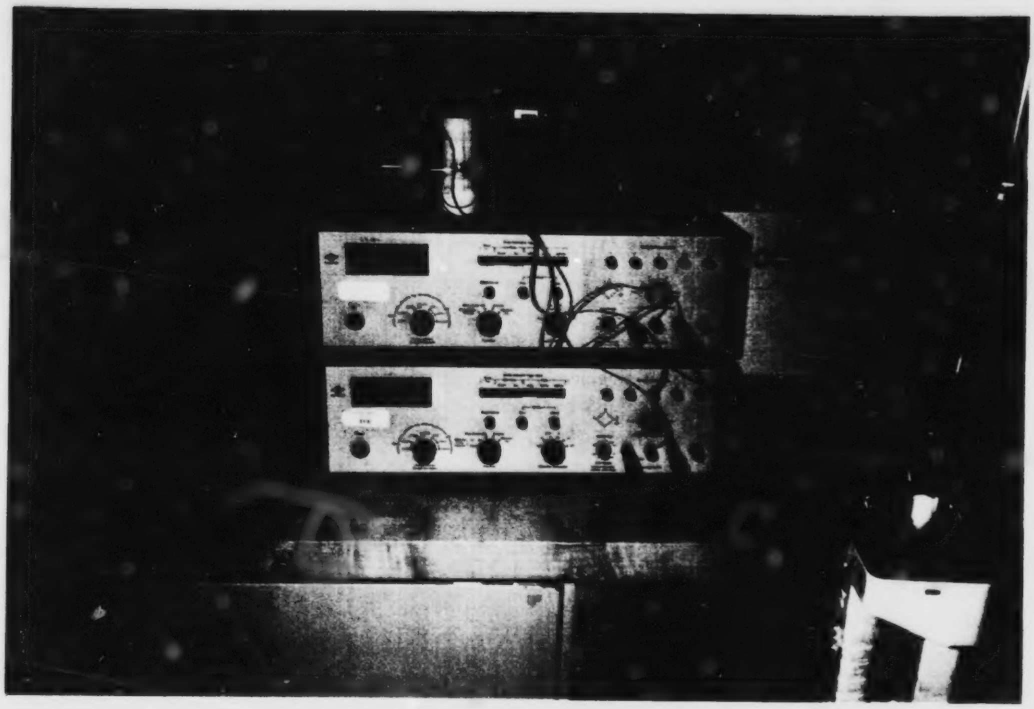

Fig. 18 Gauged test specimen and strain indicators

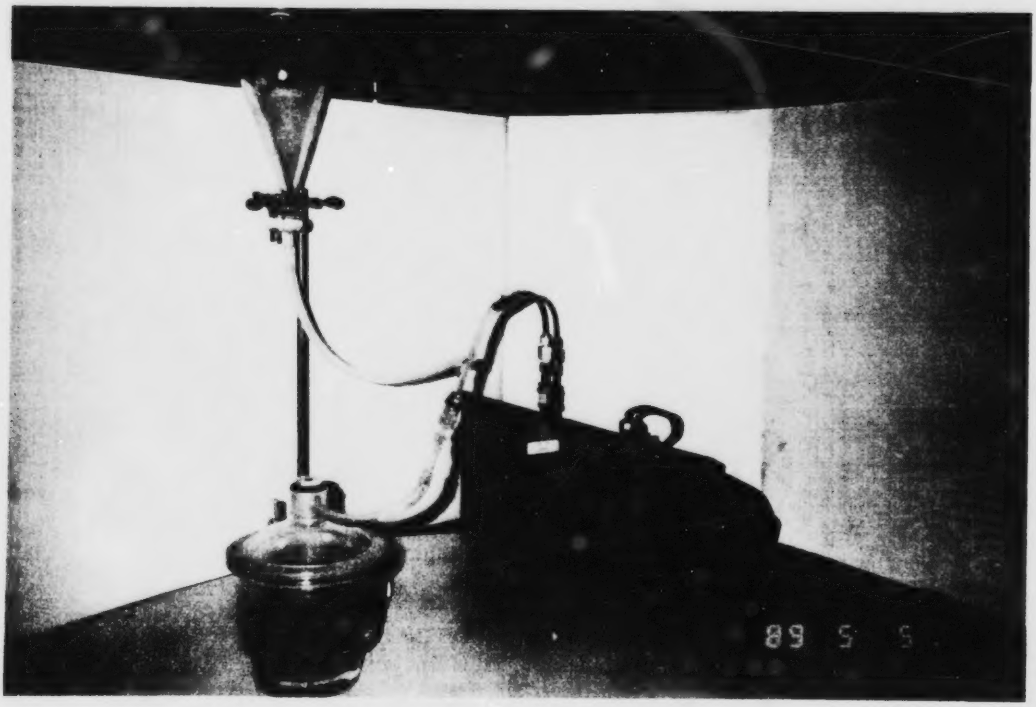

Fig. 19 Immersion porosity apparatus

Table 1 Specimen Selection Data

Sample Number	Test Type	Control Mode	σ_3 (MPa)	l_o (mm)	M_d (g)	γ_d (g/cm^3)
N1	Uniaxial	Load	0.0	104.20	394.74	2.403
N2	Uniaxial	Load	0.0	102.84	385.70	2.379
N3	Uniaxial	Load	0.0	104.00	396.02	2.416
					mean	2.399±0.019
N4	Uniaxial	Circumferential	0.0	104.88	396.22	2.397
N5	Uniaxial	Circumferential	0.0	103.26	391.10	2.403
N6	Uniaxial	Circumferential	0.0	103.20	388.39	2.388
					mean	2.396±0.008
N7	Single stage triaxial	Load	10.0	104.66	396.55	2.404
N8	Single stage triaxial	Load	10.0	104.30	395.75	2.407
N9	Single stage triaxial	Load	10.0	103.26	392.68	2.413
					mean	2.408±0.005
N10	Single stage triaxial	Load	20.0	104.86	399.15	2.415
N11	Single stage triaxial	Load	20.0	103.54	397.29	2.434
N12	Single stage triaxial	Load	20.0	102.96	389.42	2.399
					mean	2.416±0.018
N13	Single stage triaxial	Load	30.0	104.30	398.30	2.423
N14	Single stage triaxial	Load	30.0	104.00	393.30	2.399
N15	Single stage triaxial	Load	30.0	103.90	391.42	2.390
N16	Single stage triaxial	Load	30.0	103.40	395.98	2.429
					mean	2.410±0.019
N17	Single stage triaxial	Circumferential	10.0	104.10	394.91	2.407
N18	Single stage triaxial	Circumferential	10.0	104.30	394.69	2.401
N19	Single stage triaxial	Circumferential	10.0	104.10	392.35	2.391
					mean	2.400±0.008
N20	Single stage triaxial	Circumferential	20.0	103.64	391.37	2.396
N21	Single stage triaxial	Circumferential	20.0	104.20	392.64	2.390
N22	Single stage triaxial	Circumferential	20.0	104.20	391.68	2.385
					mean	2.390±0.006
N23	Single stage triaxial	Circumferential	30.0	104.50	398.89	2.422
N24	Single stage triaxial	Circumferential	30.0	104.30	397.38	2.417
N25	Single stage triaxial	Circumferential	30.0	104.42	395.84	2.405
N26	Single stage triaxial	Circumferential	30.0	103.46	390.07	2.392
					mean	2.409±0.013
N27	Multi stage triaxial	Circumferential	10,20,30	102.64	385.22	2.381
N28	Multi stage triaxial	Circumferential	10,20,30	103.54	396.15	2.427
N29	Multi stage triaxial	Circumferential	10,20,30	104.87	392.72	2.387
N30	Multi stage triaxial	Circumferential	10,20,30	103.94	394.06	2.405
					mean	2.400±0.021
N31	P-wave/Porosity	N/A	0.0	104.24	397.57	2.420
N32	Brazilian	Load	0.0	25.76	98.62	2.429
N33	Brazilian	Load	0.0	25.28	93.68	2.351
N34	Brazilian	Load	0.0	25.50	97.00	2.413
					mean	2.398±0.041
N35	Permeability/Porosity	Load	10,20,30	44.00	169.78	2.448
				total	mean	2.403±0.018

The specimens were then submerged in de-aired water while under constant vacuum for one hour. The specimens were then surface dried and weighed. Porosity measurements were conducted at a room temperature of 21° C. The following properties were then determined.

$\gamma_d = \frac{M_d}{V}$

where,

γ_d = Bulk dry density (g/cm^3)

V = Bulk volume (cm^3)

M_d = Dry mass (g)

$V_v = \frac{M_s - M_d}{\gamma_w}$

where,

V_v = Pore volume (cm^3)

M_s = Saturated mass (g)

M_d = Dry mass (g)

γ_w = Density of water (g/cm^3)

$n = \frac{100 V_v}{V}$

where,

n = Porosity %

The calculated physical quantities are listed in Table 2.

5.3 P - WAVE MEASUREMENT

This test is intended as a method to determine the velocity of propagation of elastic waves in laboratory rock testing, using the ultrasonic pulse method.

P-wave measurements were conducted on specimen N31 (fig. 20). Three determinations were made and averaged for both the dry state and wet state. The ultrasonic pulse method was used, in which a mechanical impulse is imparted to the specimen and the time required for a mechanical transient pulse to traverse the length of the specimen is used to calculate the velocity with the following formula:

$V_p = l/t$

where,

V_p = Longitudinal wave velocity (km/s)

l = Wave travel distance (km)

t = Travel time (s)

Table 2 Porosity/Velocity Measurements

Sample Number	V (cm^3)	M_s (g)	M_d (g)	n (%)	G_s (g/cm^3)	v_s (km/s)	v_d (km/s)
N31	164.314	411.60	397.57	8.5	2.65	4.66	4.09
N35	69.357	175.18	169.78	7.8	2.65		

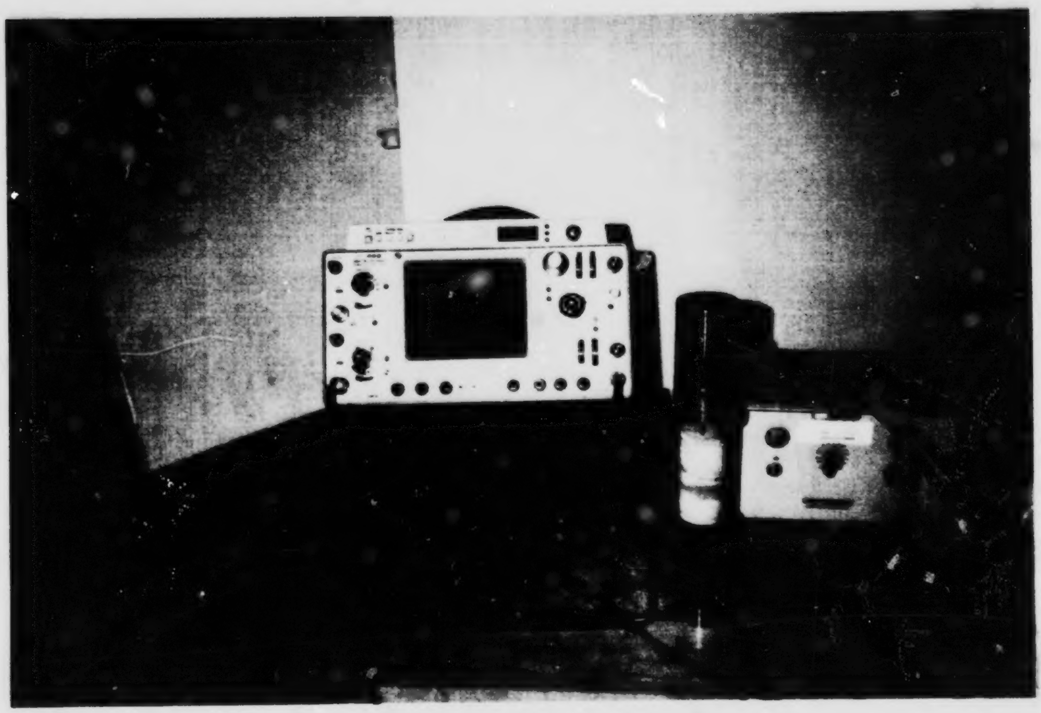

Fig. 20 Velocity measurement apparatus

A Tektronix model 468 digital storage scope was used to display the wave form and measure the travel time. A Terrametrics Pulse Generator equipped with piezo electric P-wave pulsing and sensing heads were used to generate the mechanical pulse. Water was used to couple the sensing heads to the specimen ends. The determined velocities are listed in Table 2.

6. MECHANICAL ROCK PROPERTY TESTS

6.1 MTS 815 ROCK MECHANICS TEST SYSTEM

Brazilian, uniaxial, triaxial, and permeability tests were conducted using a computer controlled servo-hydraulic test system. The 815 Rock Mechanics Test System was manufactured by Materials Test Systems, USA. The MTS test system comprises many hydraulic, mechanical and electronic components. The individual components will be described briefly as to their function.

6.1.1 Component design

The load frame is of fixed cross-head design and is rated 4.5 MN compressive load (fig. 22). The actuator is double acting, servo-hydraulic and has a maximum stroke of 100 mm. The actuator is equipped with a linear variable differential transducer for stroke control and a delta-p pressure transducer for load control. Two 5 gpm servo-valves and a hydraulic service manifold control actuator hydraulic fluid flow.

The hydraulic power supply is rated at 10 gpm (fig. 21). A heat exchanger uses water to cool the hydraulic oil. System interlocks shut down the pump if hydraulic fluid exceeds 40° C or if the hydraulic fluid level in the reservoir drops by a preset amount.

The triaxial cell is rated up to 150 MPa confinement pressure at an elevated temperature of 200° C maximum (fig. 20 cell raised). The cell is equipped with a 2.22 MN rated load cell, 3 linear variable differential transducers (lvdt), end platens, heat shroud, heater, permeability/pore pressure porting, thermocouples, circumferential extensometers, and a hydraulic lift mechanism. Feed-throughs are provided for all electrical signals including two spare strain channels. The load cell may be used for load control and lvdt #1 may be used for stroke control. The triaxial chamber may accommodate rock specimens having maximum dimensions of 100 mm in diameter, and 200 mm in length. Specimens are jacketed in teflon or polyolefin heat shrink tubing.

Fig. 21 Hydraulic power supply

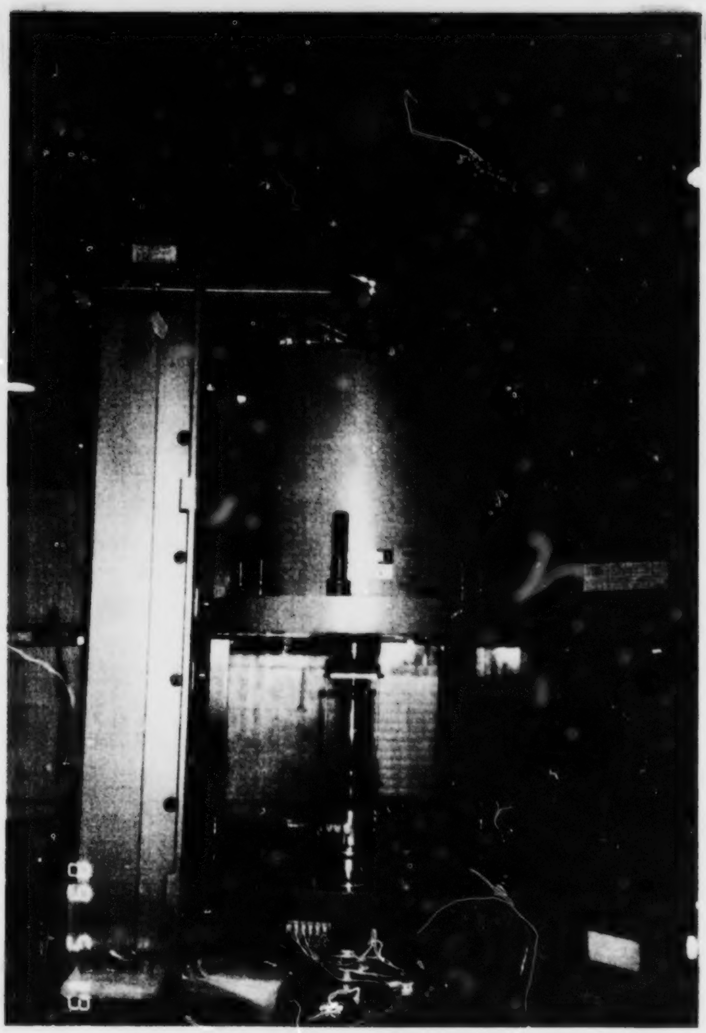

Fig. 22 Load frame and triaxial chamber

Confining pressure is generated using a 150 MPa rated intensifier with 1150 cm^3 of high fluid pressure output. The intensifier is equipped with two 5 gpm servo-valves, a hydraulic service manifold, a pressure transducer, a displacement transducer, and a confining fluid reservoir. Confinement pressure may be applied or controlled via the pressure transducer or the displacement transducer. The permeability/pore pressure unit is identical to the confining pressure unit except that water is used and the maximum fluid output is 980 cm^3 (fig. 23).

The controller provides all the controls necessary for conducting tests in local control and set-up for computer controlled tests. Control may be selected as either load, stroke, or circumferential displacement control for tests. Adjustments to conditioners, dc errors, valve balance and dither may be undertaken also. Control may be offset or interlocks enabled. Signals are accessible to peripheral devices. Control modes are equipped with four selectable ranges (fig. 24 panel 448.85).

Any two of six channels may be displayed on the panel with one channel being reserved for external input. Units may be scaled directly. Max/min, and peak/valley signals may also be displayed (fig. 24 panel 464.80).

The front panel function generator is used for local control tests (fig. 24 panel 410.80). Any one of the three control modes may used versus time to generate a sine wave, square wave or ramp.

Two micro-consoles are provided. One is for the confining pressure subsystem, and the other is for the permeability pressure subsystem. The micro-consoles function basically the same as the controller. For either system, intensifier stroke or pressure may be selected as the control mode. In addition the confining pressure micro-console houses the conditioners, for the three lvdts (fig. 25 panel 458.20).

The temperature controller may be operated manually or by computer control (fig. 25 panel 409.80). The controller is used to control power output to the heater element thereby imparting heat to the confining fluid in the triaxial chamber. The internal heater element has a maximum temperature rating of 200° C.

The test processor contains devices used to provide computer controlled operation of the servo-hydraulic test system. With built in MTS multi-user Basic software, the functions provided are command signal generation, data acquisition and handling, monitoring and control of the operation of other system components, initiation of computer interrupt routines upon the detection of certain programmed events, and communication with the system controllers and associated system control software.

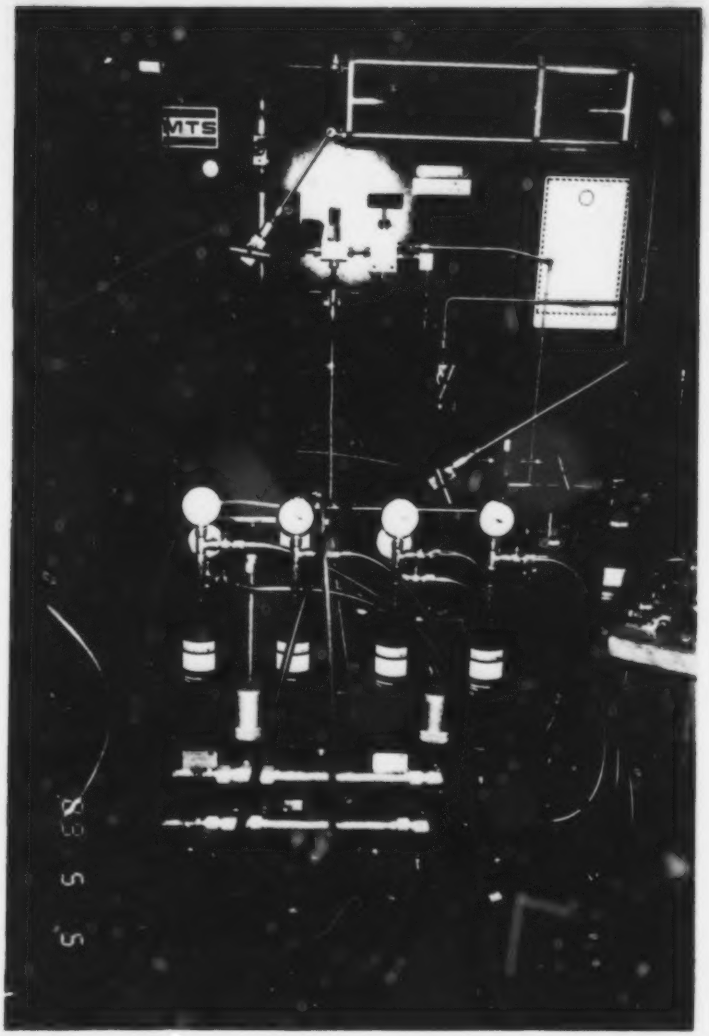

Fig. 23 Confinement and pore/permeability pressure subsystem

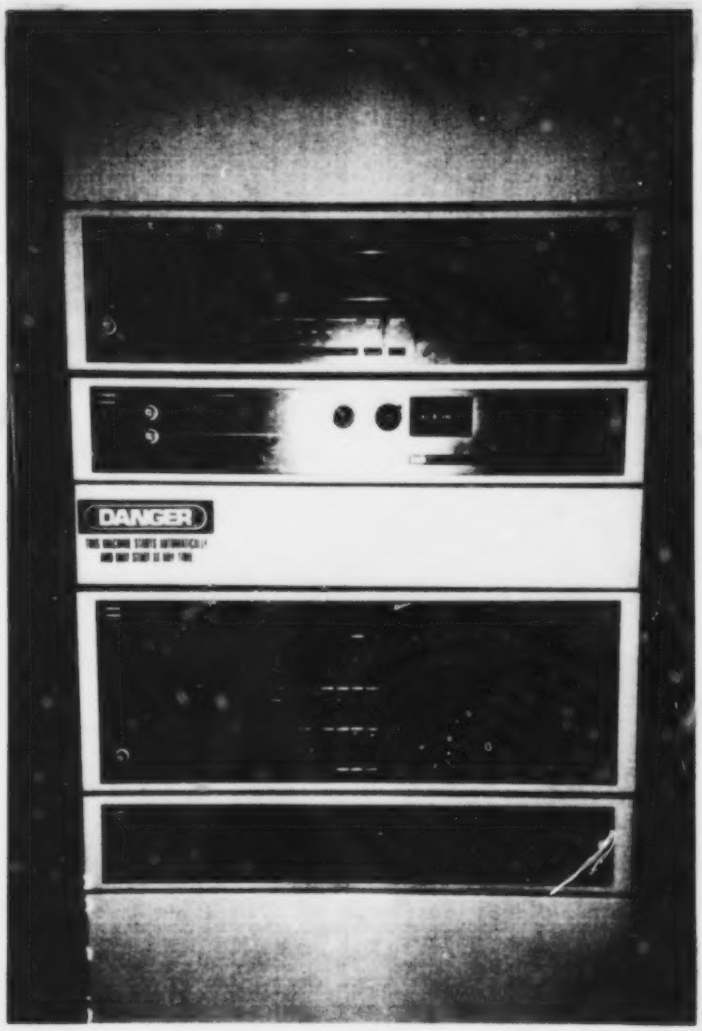

Fig. 24 Controller, function generator, and data display

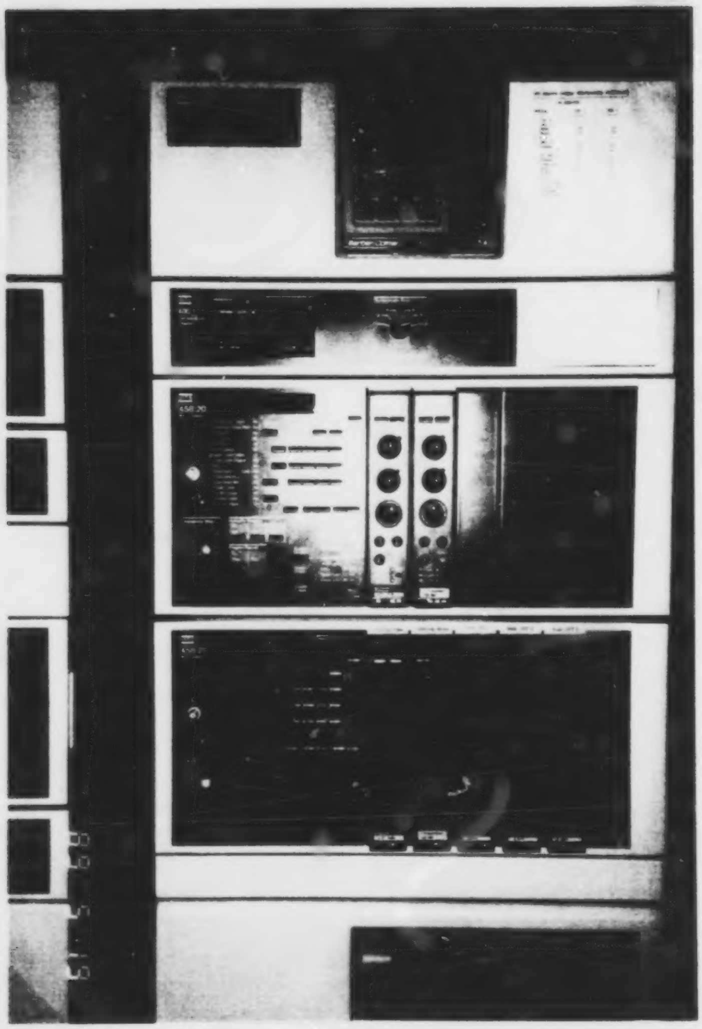

Fig. 25 Micro-consoles, temperature controller, and PDP 11/73

A PDP 11/73 computer is an integral part of the test system. The computer comes equipped with a 512 kilo-byte MOS memory, a RD52 31 megabyte Winchester hard disk, and a RX50 Dual 400 kilo-byte floppy disk drive. Peripherals include two DEC VT240 graphics terminals, DEC LA50 printer, and a DEC LVP16 digital 6 pen plotter (fig. 26). The computer uses RT-11 as the operating system. MTS Basic is used to enable the development of automated test programs. The language is interactive and allows the real-time modification of tests, correction of mistakes, and resumption of program execution without recompiling.

Additional peripherals include a Hewlett-Packard 7046B X-Y1-Y2 recorder (fig. 26) and two Bruel and Kjaer 1526 strain indicators (fig.18).

6.1.2 Theory of operation

The MTS test system incorporates closed loop servo-hydraulics to control post-peak failure of cylindrical rock specimens (fig. 27). The required response time of the servo-controller system, used for closed loop control, is dependent on the stiffness of the loading frame, and the rate of failure propagation within the rock specimen, Hudson et al, (1971). The best test results are obtained with test systems possessing the faster control loops, minimal test stacks, minimal hydraulic ram fluid, and stiffer frames (fig. 28).

The closed loop servo-hydraulic MTS test system is capable of controlling changes in test specimen load, circumferential displacement, axial displacement, confining pressure, and pore/permeability pressure (fig. 29 stroke control). Any one or combination of these parameters may be measured with the appropriate transducer, and used as the feedback signal in the control loop. The feedback signal becomes the independent variable for test control. The servo-controller compares the feedback signal with a program signal provided by a digital programmable function generator, and provides an error signal proportional to the difference between them. The error signal is amplified to become the servo-valve command signal. The signal then drives the servo spool valve in the appropriate direction thereby varying the hydraulic fluid flow rate to the hydraulic actuator which in turn drives the actuator in the appropriate direction to reduce the the error to zero.

Load is not a satisfactory feedback signal for post-failure testing of rock specimens (fig. 30). Using load as a feedback parameter will not permit the control of a test beyond the maximum load carrying capability of the specimen (point A in fig. 30). At that point, the programmed load will exceed the specimen strength and there will be a sudden complete failure as the loading actuator tries to maintain load.

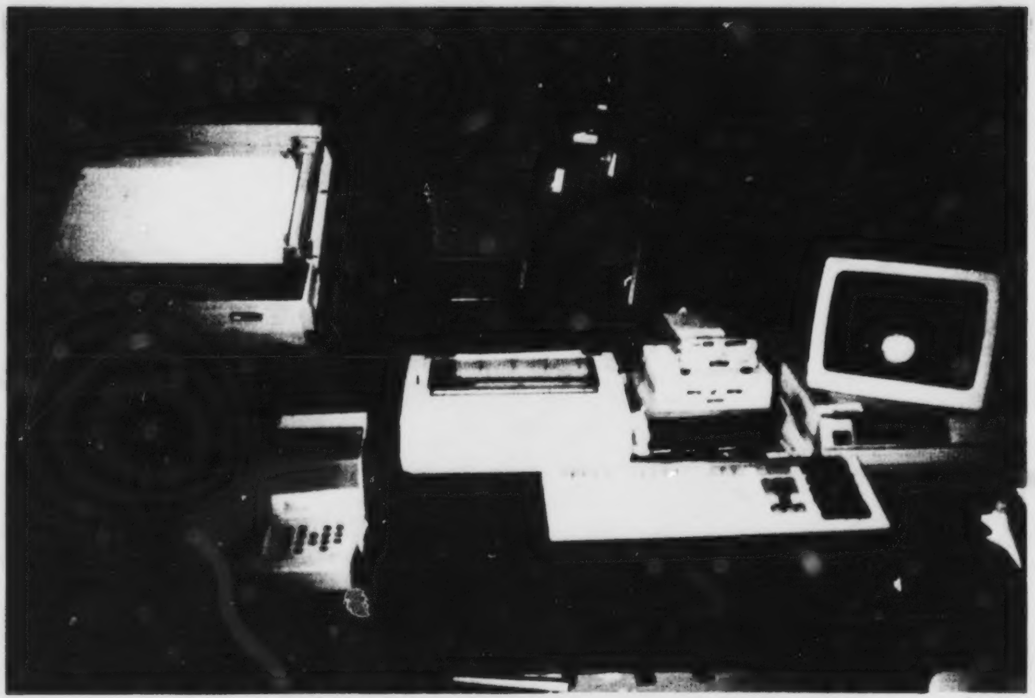

Fig. 26 X-Y1-Y2 recorder, printer, plotter, and terminal

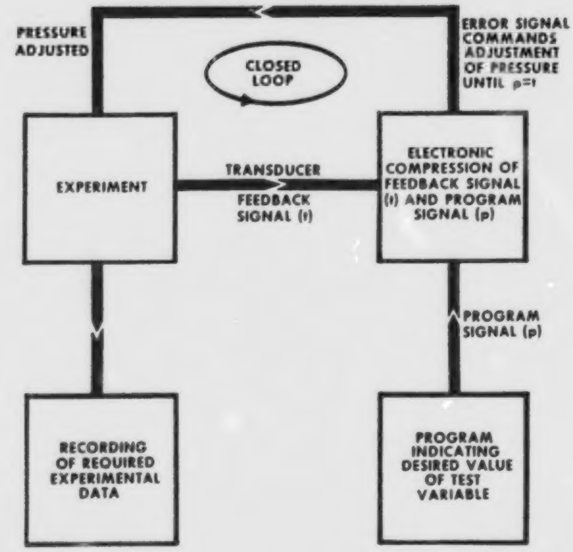
PRESSURE ADJUSTED
CLOSED LOOP
ERROR SIGNAL COMMANDS ADJUSTMENT OF PRESSURE UNTIL p=r
EXPERIMENT
TRANSDUCER
FEEDBACK SIGNAL (r)
ELECTRONIC COMPRESSION OF FEEDBACK SIGNAL (r) AND PROGRAM SIGNAL (p)
PROGRAM SIGNAL (p)
RECORDING OF REQUIRED EXPERIMENTAL DATA
PROGRAM INDICATING DESIRED VALUE OF TEST VARIABLE

Fig. 27 Principle of closed loop control

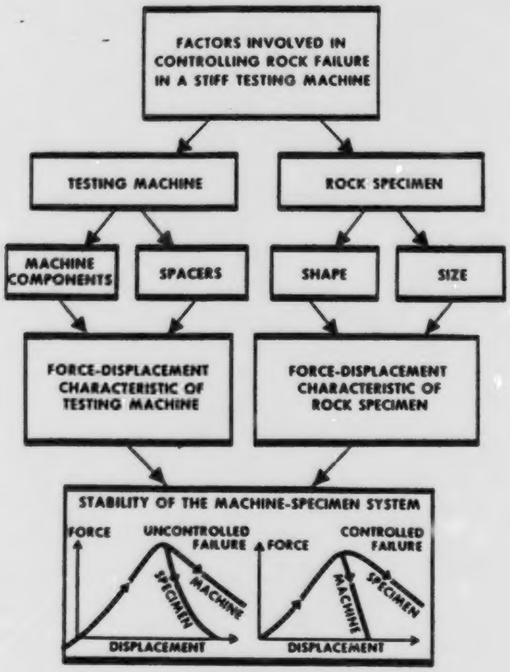
FACTORS INVOLVED IN CONTROLLING ROCK FAILURE IN A STIFF TESTING MACHINE
TESTING MACHINE
ROCK SPECIMEN
MACHINE COMPONENTS
SPACERS
SHAPE
SIZE
FORCE-DISPLACEMENT CHARACTERISTIC OF TESTING MACHINE
FORCE-DISPLACEMENT CHARACTERISTIC OF ROCK SPECIMEN
STABILITY OF THE MACHINE-SPECIMEN SYSTEM
FORCE
UNCONTROLLED FAILURE
SPECIMEN
MACHINE
DISPLACEMENT
FORCE
CONTROLLED FAILURE
MACHINE
SPECIMEN
DISPLACEMENT

Fig. 28 Flow chart of factors affecting rock failure in a stiff machine

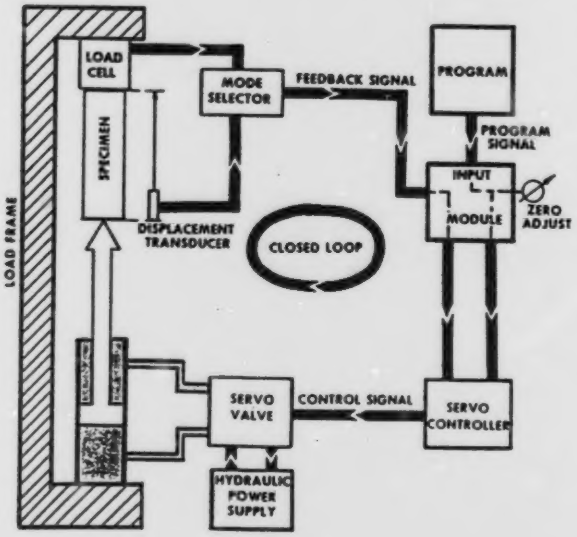
LOAD CELL
SPECIMEN
LOAD FRAME
MODE SELECTOR
FEEDBACK SIGNAL
PROGRAM
PROGRAM SIGNAL
INPUT
MODULE
ZERO ADJUST
DISPLACEMENT TRANSDUCER
CLOSED LOOP
SERVO VALVE
CONTROL SIGNAL
SERVO CONTROLLER
HYDRAULIC POWER SUPPLY

Fig. 29 Fast response, closed loop, servo-controlled test system

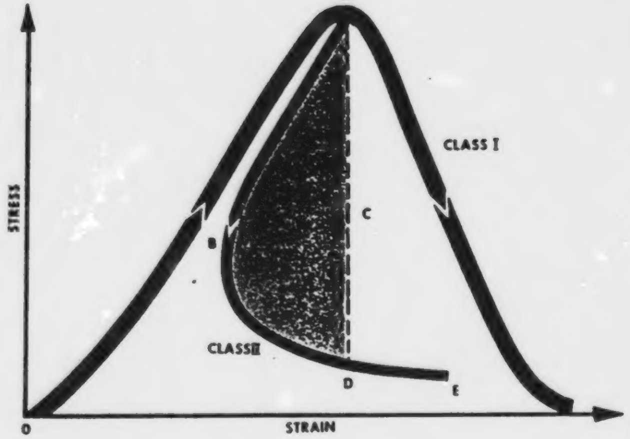

Fig. 30 Complete uniaxial compressive stress-strain plots

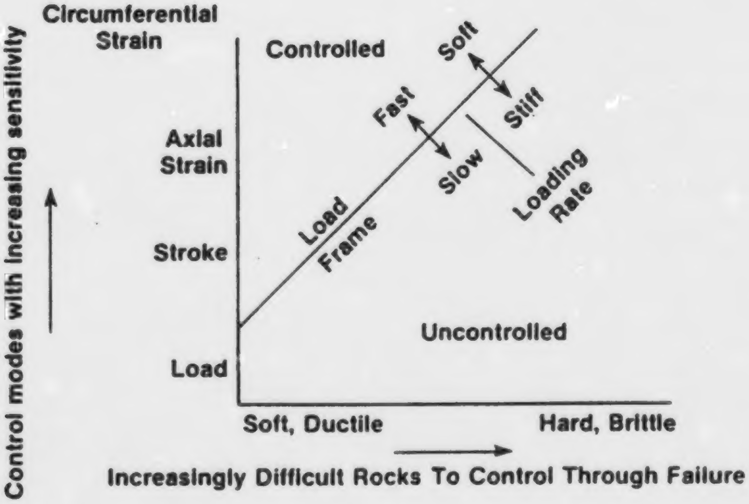
Circumferential Strain
Axial Strain
Stroke
Load
Controlled
Uncontrolled
Soft
Stiff
Fast
Slow
Load Frame
Loading Rate
Soft, Ductile
Hard, Brittle
Control modes with increasing sensitivity
Increasingly Difficult Rocks To Control Through Failure

Fig. 31 Control modes versus rock brittleness

The use of a circumferential transducer as the feedback signal for control provides the most sensitive means of detecting specimen failure. Formation of cracks at failure causes much more lateral strain than specimen axial displacement (fig. 31). Circumferential strain in rock specimens normally provides a reliable monotonically increasing relationship and analog signal for failure control. The specimen thus is controlled to dilate uniformly while load and axial strain can be monitored independently as failure progresses.

6.2 BRAZILIAN TENSILE STRENGTH TESTS

This method of test is intended to measure indirectly the uniaxial tensile strength of a rock specimen of regular geometry. The test is mainly intended for classification and characterization of intact rock.

Brazilian tensile strength tests were conducted on specimens N32, N33, and N34. These specimens were cut and prepared from the same core stick in order to determine the variation in strength over the standard length of all specimens cored for the test program. The specimens were loaded at diametrically opposed ends using the MTS 815 Rock Mechanics Test System (fig. 32). The specimens were loaded to failure in load control using a load rate of 0.5 kN/s. Computer software was written to run the test and acquire data real time. The same software depending on user input was used for load control and circumferential displacement control uniaxial compressive strength tests. The computer program is called Lpost.bas and a printout is contained in Appendix A-3. The tensile strength of the specimens were calculated using the following formula.

$$\sigma_t = \frac{2P}{\pi D t}$$

where,

σ_t = Brazilian tensile strength (MPa)
P = Load at failure (N)
D = Diameter (mm)
t = Thickness (mm)

The tensile strengths are listed in Table 4.

6.3 UNIAXIAL COMPRESSIVE STRENGTH TESTS

This method of test is intended to determine stress-strain curves, Young's modulus, Poisson's ratio, and the uniaxial compressive strength of a rock specimen of regular geometry. The test is mainly intended for strength classification and characterization of intact rock.

Table 3 Brazilian Tensile Strength

Sample Number	γ_d (g/cm^3)	Failure Load (kN)	σ_t (MPa)
N32	2.429	14.688	-8.09
N33	2.351	8.641	-4.85
N34	2.413	13.526	-7.53
mean			-6.82
std.dev.			±1.73

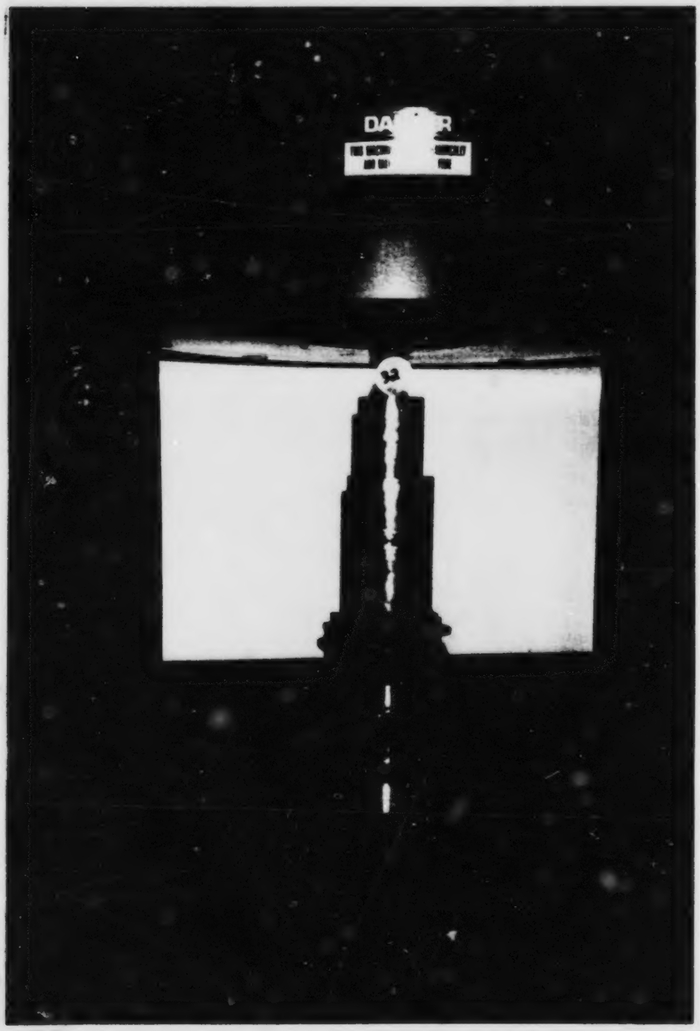

Fig. 32 Brazilian test set-up

6.3.1. Load control tests

Uniaxial compressive strength tests were conducted on specimens N1, N2, and N3. The specimens were loaded to failure in load control using the MTS 815 test system (fig. 33). Violent failure was anticipated at peak strength for specimens tested in load control. Lvdts and the circumferential extensometer were not used in this set of tests to avoid the risk of being damaged. Prior to testing the specimens were jacketed with heat shrink tubing as a means of containing the rock fragments during failure. Strain gauges were used to measure specimen axial and circumferential strain during the test. The specimen strain gauge circuits were connected to the strain indicators to form the active circuit of a 1/2 arm Wheatstone bridge configuration. The compensating or dummy arm comprised strain gauges of identical gauge factor. Real time analog signals from the strain indicators were wired directly to the MTS data acquisition system. Specimen load was measured using the load cell. The specimens were loaded using computer control at a loading rate of 1 kN/s (0.634 MPa/s). Load, axial strain, and circumferential strain data were sampled and stored every second. Real time plots of specimen axial load versus axial displacement were displayed using the HP plotter. Rock material constants were calculated as follows:

$\epsilon_a = \frac{\Delta l}{l_o}$

where,

ϵ_a = Strain

l_o = Original specimen length (mm)

Δl = Change in specimen length (mm)

$Q_u = \frac{10P}{A_o}$

where,

Q_u = Ultimate uniaxial compressive strength (MPa)

P = Ultimate compressive load (kN)

A_o = Original cross-sectional area (cm^2)

$E_a = \frac{\Delta\sigma}{1000\Delta\epsilon_a}$

where,

E_a = Young's tangent modulus at $.5Q_u$ (GPa)

1000 = conversion to GPa

$\Delta\sigma$ = Axial stress component (MPa)

$\Delta\epsilon_a$ = Axial strain component (ϵ)

$\nu = \frac{\Delta\epsilon_d}{\Delta\epsilon_a}$

where,

ν = Poisson's ratio at $.5Q_u$

$\Delta\epsilon_a$ = Axial tangent strain component (ϵ)

$\Delta\epsilon_d$ = Circumferential tangent strain component (ϵ)

Table 4 Uniaxial Compressive Test Results

Sample Number	γ_d (g/cm^3)	Q_u (MPa)	ϵ_{peak} (%)	E (GPa)	ν	t_p (s)
N1	2.403	147.68	0.51	39.45	0.55	233
N2	2.379	140.88	0.48	37.19	0.68	222
N3	2.416	158.58	0.44	43.91	0.41	251
mean		149.05	0.48	40.18	0.55	235
std.dev.		±8.93	±0.04	±3.42	±0.14	±15
N4	2.397	145.08	0.44(0.44)	39.70(39.31)	0.50(0.48)	1353
N5	2.403	141.59	0.49(0.45)	37.92(40.29)	0.53(0.50)	1845
N6	2.388	140.86	0.46(0.45)	37.27(38.03)	0.31(0.32)	1230
mean		142.51	0.46(0.45)	38.30(38.17)	0.45(0.43)	1476
std.dev.		±2.26	±0.03(±0.06)	±1.26(±1.04)	±0.12(±0.10)	±325

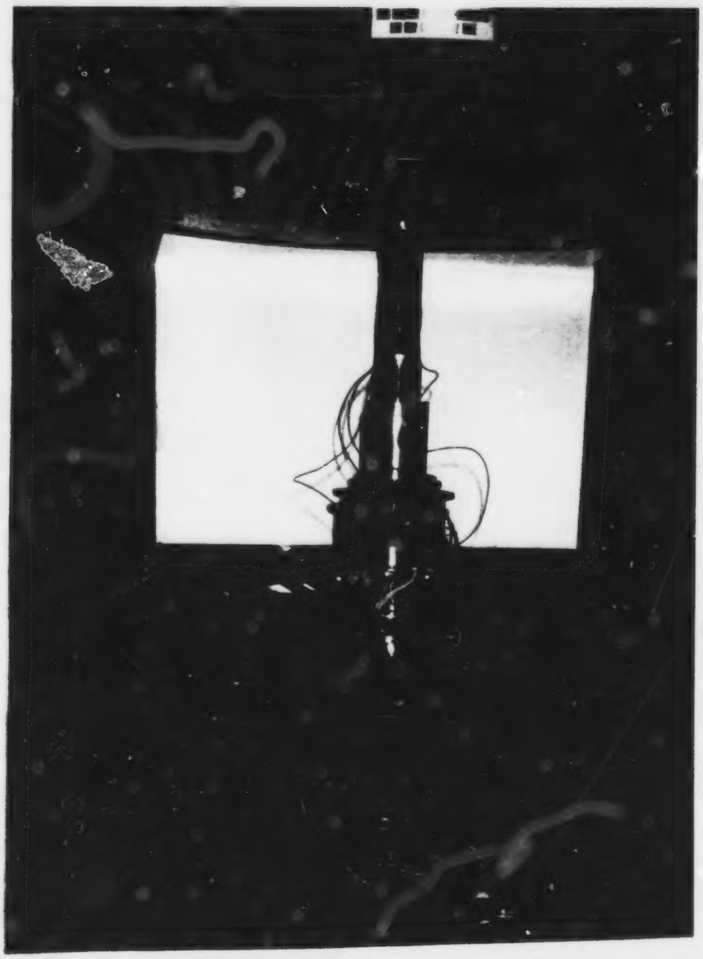

Fig. 33 Uniaxial load control test set-up

The preceding formulas were written into software used to conduct the tests in computer control, and the calculated material constants were automatically displayed upon test completion. Material constants were calculated using MTS Basic. The computer program was named Lpost.bas, (Appendix A-3). The test results are contained in Table 4.

6.3.2 Circumferential control tests

Post-failure rock properties are of interest to the mining engineer. Deep excavations in rock have been observed to be stable even though the mine pillars have partially failed over time. Circumferential displacement control tests were undertaken to observe the behaviour of rock specimens in the post-failure region of the tests. As loading rates were considerably less in this test method over that of load control tests, variation of peak strengths may be compared between both test methods.

Specimens N4, N5, and N6 were tested using circumferential displacement control. The specimens were uniaxially loaded in load control, at a rate of 1 kN/s (0.634 MPa/s). When the circumferential dilation of the specimen reached 0.02 mm magnitude the axial load was reduced by 20%. The control mode was then switched over to circumferential displacement control. The test was then continued, at a circumferential strain rate of 2.17 $\mu\epsilon/s$, to a maximum of 0.91 mm displacement. The rate was then automatically increased to 6.77 $\mu\epsilon/s$ to a maximum of 3.81 mm displacement. The test was continued through peak strength until the residual strength was visually established, as indicated by a plateau in the graph recorded by the X-Y1-Y2 recorder. The test was then terminated. During the test, data was acquired every 3 seconds and stored for later recall. Data sampled comprised signals from axial strain gauges, circumferential strain gauges, load cell, circumferential extensometer, and the 3 lvdts. Computer software used for test control and rock material constant determinations, was common to load control tests. The test results are contained in Table 4.

6.4 TRIAXIAL COMPRESSIVE STRENGTH TESTS

This test is intended to measure the strength of cylindrical rock specimens subjected to triaxial compression (fig. 34). This provides the values necessary to determine the strength envelope, and from this the value of the internal friction angle, and the 'apparent' cohesion may be calculated.

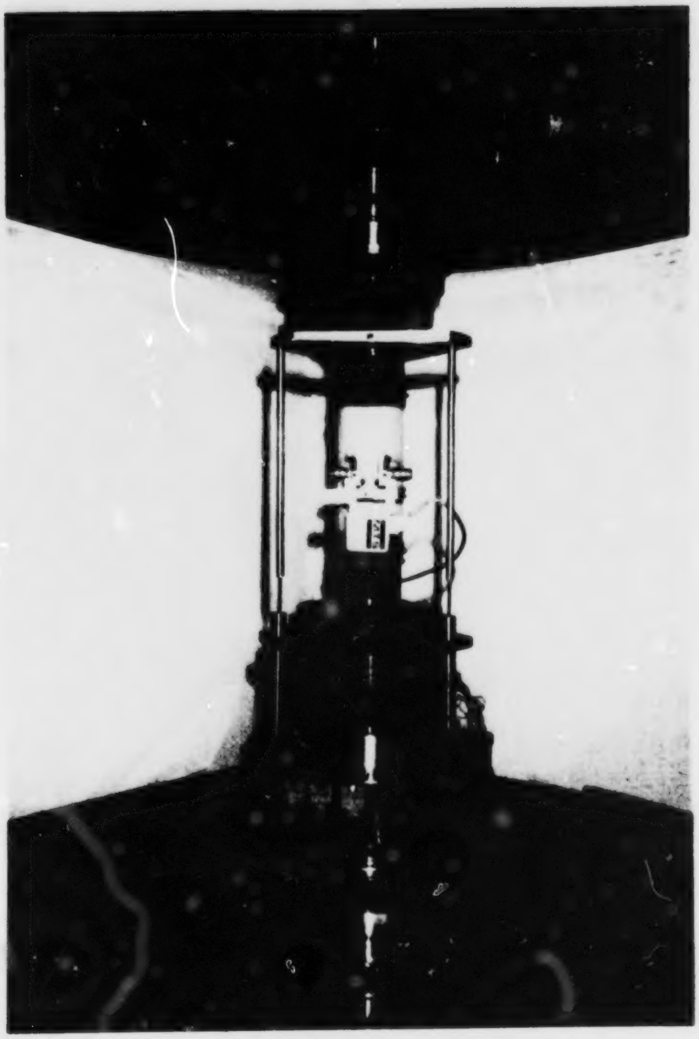

Fig. 34 Triaxial test set-up

Table 5 Triaxial Test Results

Sample		Identification			σ_3=10.0	MPa	σ_3=20.0	MPa	σ_3=30.0	MPa	Residual	
Sample Number	γ_d (g/cm^3)	E (GPa)	ν	t_p (s)	σ_1 (MPa)	ϵ_{peak} (%)	σ_1 (MPa)	ϵ_{peak} (%)	σ_1 (MPa)	ϵ_{peak} (%)	σ_{1r} (MPa)	σ_{3r} (MPa)
N7	2.404	45.90	0.48	443	251.71	0.78						
N8	2.407	47.12	0.36	456	258.97	0.80						
N9	2.413	47.82	0.28	468	265.95	0.79						
N10	2.415	49.27	0.27	621			352.82	1.26				
N11	2.434	51.14	0.26	656			372.48	1.04				
N12	2.399	48.37	0.35	592			336.36	0.99				
N13	2.423	50.32	0.26	713					405.31	1.07		
N14	2.399			280					(159.03)	(0.58)		
N15	2.390	46.43	0.41	662					376.16	1.13		
N16	2.429	50.97	0.25	726					412.67	1.11		
mean					258.88	0.79	353.89	1.10	398.05	1.10		
std.dev.					±7.12	±0.01	±18.08	±0.14	±19.31	±0.03		
N17	2.407	46.61	0.47	3216	241.06	0.81					103.24	10.0
N18	2.401	47.53	0.48	3264	247.06	0.83					100.43	10.0
N19	2.391	46.78	0.44	2955	238.05	0.80					107.70	10.0
N20	2.396	49.66	0.23	2220			324.64	1.02			126.39	20.0
N21	2.390	47.21	0.47	3045			304.01	0.99			146.63	20.0
N22	2.385	46.72	0.39	3066			310.79	1.02			112.73	20.0
N23	2.422	50.01	0.32	1632					384.39	1.06		
N24	2.417	50.63	0.23	1371					387.01	1.10	189.15	30.0
N25	2.405	49.65	0.31	2475					388.56	1.17	178.78	30.0
N26	2.392	46.73	0.32	3066					362.60	1.20	169.68	30.0
mean					242.06	0.81	313.15	1.01	380.64	1.13		
std.dev.					±4.59	±0.02	±10.51	±0.02	±12.15	±0.06		
N27	2.381	44.30	0.43	1365	218.39	0.68	293.16	0.92	345.65	1.13	174.43	30.0
N28	2.427	48.87	0.24	1275	262.65	0.71	345.17	0.94	418.58	1.22	163.77	30.0
N29	2.387	46.71	0.43	1500	232.53	0.69	290.16	0.85	368.99	1.17	193.21	30.0
N30	2.405	44.28	0.18	1065	249.19	0.76	320.67	0.98	385.75	1.26	138.54	30.0
mean					240.69	0.71	312.29	0.92	379.74	1.20		
std.dev.					±19.31	±0.04	±25.87	±0.05	±30.67	±0.06		

6.4.1 Single stage load control tests

Three series of load control triaxial tests were conducted as follows: specimens N7, N8, and N9 at a confinement of 10 MPa; specimens N10, N11, and N12 at a confinement of 20 MPa; and specimens N13, N14, N15, and N16 at a confinement of 30 MPa. Software was written common to all triaxial tests. The computer program was called Lmulti.bas, (Appendix C-3).

The specimens were triaxially loaded, in load control, by the simultaneous application of axial load and confining pressure, at a stress rate of 0.634 MPa/s. When the desired confining pressure of the test was reached, axial loading was continued until specimen failure occurred at peak strength. The test was then terminated. Data was sampled every second and comprised signals from the load cell, the circumferential extensometer, the 3 lvdts, and the confinement pressure transducer. Rock material constants were calculated as follows:

$$\sigma_1 = \frac{10P}{A_o}$$

where,

σ_1 = Triaxial strength (MPa)
P = Failure load (kN)
A_o = Original cross-sectional area (cm^2)
σ_3 = Confining pressure (MPa)

The test results are contained in Table 5.

6.4.2 Single stage circumferential displacement control tests

Three series of circumferential displacement control tests were conducted as follows: specimens N17, N18, and N19 at a confinement of 10 MPa; specimens N20, N21, and N22 at a confinement of 20 MPa; and specimens N23, N24, N25, and N26 at a confinement of 30 MPa.

The specimens were triaxially loaded in load control, by the simultaneous application of axial load and confining pressure, at a stress rate of 0.634 MPa/s. When the desired confining pressure of the test was reached, axial loading was continued, at a stress rate of 0.634 MPa/s, while the confining pressure was kept constant. When the circumferential displacement of the specimen reached 0.02 mm magnitude the axial load was reduced by 20%. The control mode was then switched over to circumferential displacement control. The test was continued at circumferential strain rate of 2.17 $\mu\epsilon$/s, to a maximum of 0.91 mm displacement. The rate was then automatically increased to 6.77 $\mu\epsilon$/s to a maximum of 3.81 mm displacement. The confining pressure was held constant through the peak strength until the residual strength was visually established, as indicated by a plateau in the graph recorded by the X-Y1-Y2 recorder. The specimen was then further dilated to a maximum of 3.81 mm circumferential displacement, while the confining pressure was linearly reduced to zero within the time period of 60 seconds. This last phase of the test was performed to retrieve residual strength data. Data was sampled every 3 seconds. The signals sampled were common to load control triaxial tests, including the test software.

6.4.3 Multi stage circumferential displacement control tests

This test was first proposed by Kovari and Tisa, (1975). The test measures the strength of a single rock specimen subjected to several levels of triaxial compression. Post failure residual strength properties are also determined.

Four specimens were tested using this method. Specimens N27, N28, N29, and N30 were tested, each at successive confining pressures of 10, 20, and 30 MPa. Software and data sampling was common to the single stage series.

The specimens were triaxially loaded in load control mode, by the simultaneous application of axial load and confining pressure, at a stress rate of 0.634 MPa/s. When the desired confining pressure of the first stage was reached, the axial loading was continued, at a stress rate of 0.634 MPa/s, while holding the confining pressure constant. When circumferential dilation of the specimen had reached 0.02 mm magnitude the axial load was reduced by 20%. The control mode was then switched over to circumferential displacement control. The test was continued, at a circumferential strain rate of 2.17 $\mu\epsilon/s$, to a maximum of 0.91 mm displacement. The rate was then automatically increased to 6.77 $\mu\epsilon/s$, to a maximum of 3.81 mm displacement.

The test continued until an imminent failure was detected, as indicated by plateauing of specimen axial load. The desired confining pressure of the second stage was then automatically applied, and so on, until the procedure was completed for each predetermined increment of confining pressure.

The confining pressure of the last stage was held through the peak strength until the residual strength was established, as indicated by a plateau in the graph recorded by the X-Y1-Y2 recorder. The specimen was then further dilated to a maximum of 3.81 mm displacement, while the confining pressure was linearly reduced to zero within the time period of 60 seconds. The test results are contained in Table 5.

6.5 CONFINED CONSTANT HEAD PERMEABILITY TEST

This method is intended to measure directly the water permeability of a rock specimen of regular geometry at different levels of confinement.

Permeability tests were conducted on specimen N35. Initially, specimen dimensions, dry density, and saturated density measurements were performed (Table 2). The specimen was then jacketed with bicycle tubing. The tubing was clamped to the permeability end platens using O - rings. Stainless steel tubing was connected to the permeability platen ports. The assembly was then transferred to the MTS triaxial chamber (fig. 35). The specimen was triaxially loaded, in load control, by the simultaneous application of axial load, confining pressure, and upstream permeability pressure, at a stress rate of 0.634 MPa/s. Once equilibrium was attained, axial load and confinement pressure was held constant. Downstream specimen permeability was vented to atmosphere through a volume calibrated glass bore. While holding upstream water pressure constant, the volume of water displaced through the glass bore over time was recorded. The procedure was then repeated for the next level of confinement and upstream pressure. The test was performed at 3 levels of confinement and 3 levels of upstream pressure (Table 5). Rock permeability was determined as follows:

$$k = \frac{Ql_o}{A_o 10207(h_i - h_f)t}$$

where,

k = Permeability (cm/s)

Q = Volume of water displaced (cm^3)

l_o = Specimen length (cm)

A_o = Specimen cross-sectional area (cm^2)

h_i = Upstream pressure (MPa)

h_f = Downstream pressure (MPa)

t = Flow time (s)

10207 = Conversion of h_i, h_f to head (cm)

$$k_{eff} = \frac{Ql_o}{A_o 10207(\sigma_3 - h_i - h_f)t}$$

where,

k_{eff} = Effective Permeability (cm/s)

σ_3 = Confinement pressure (MPa)

Computer software, Perm.bas, was written to perform the test in computer control (Appendix F-4).

Table 6 Permeability Test Results

Sample Number	l_o (cm)	A_o (cm^2)	t (s)	Q (cm^3)	σ_3 (MPa)	P_{up} (MPa)	P_{down} (MPa)	k_{eff} (cm/s)
N35	4.400	15.763	34.2	0.400	10.0	5.0	0.0	6.40×10^{-8}
			29.5	0.400	20.0	10.0	0.0	3.71×10^{-8}
			13.7	0.400	30.0	15.0	0.0	5.32×10^{-8}

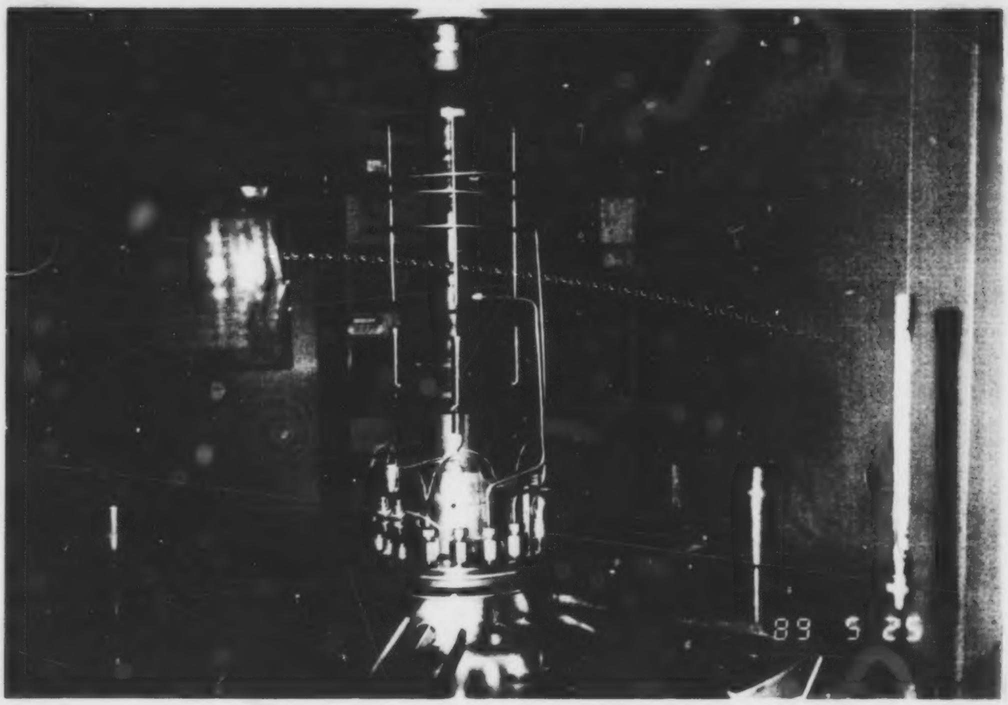

Fig. 35 Permeability test set-up

7 EXPERIMENTAL TEST RESULTS

7.1 POROSITY DATA

Porosities n were calculated as 8.5 % for specimen N31, and 7.8 % for specimen N35 (Table 2). Grain density G_s was calculated to be 2.65 g/cm^3 for both specimens. The lower porosity of specimen N35 was confirmed by it's corresponding greater bulk dry density γ_d (Table 2). The calculated grain densities and porosities agree with values determined by Hewitt, (1964). The values confirm that saturation was 100 % therefore all pores are connected.

7.2 LONGITUDINAL WAVE VELOCITY DATA

Longitudinal wave velocities were calculated as 4.66 km/s (saturated), v_s, and 4.09 km/s (dry), v_d, for specimen N31 (Table 2). Data published by Belanger et al, (1980), record velocities of 4.14 ±0.48 km/s, v_d, for the same formation. The greater value of saturated velocity confirms the presence of pores within the specimen.

7.3 BRAZILIAN TENSILE STRENGTH DATA

The mean tensile strength σ_t for specimens N32-N34 was calculated as -6.82 ±1.73 MPa. Individual specimens confirmed greater strength with increasing bulk dry density γ_d (Table 3). The tested specimens are shown in figure 36. Hewitt, (1964) lists a tensile strength value of -11.17 MPa for sandstone adjacent to Campbell's quarry.

7.4 UNIAXIAL DATA - LOAD CONTROL

The uniaxial compressive strength results, Q_u, for specimens N1-N3 are listed in Table 4. The values are in close agreement with those published by Hewitt, (1964). The results indicated increased strength values for specimens of greater bulk density, γ_d. Peak axial strains, ϵ_{peak}, at peak strength, are values obtained from axial strain gauge signals. Young's modulus values, E, were calculated from load cell and axial strain gauge signals. Poisson's ratio, ν, was calculated using axial and circumferential strain gauge signals. E and ν were calculated at a $.5Q_u$ line tangent to the stress-strain plots. Test duration time to peak strength in seconds, t_p, were also recorded. Appendix A-1 provides plots of stress versus axial strain using axial strain gauge signals. Appendix A-2 provides plots of stress versus circumferential strain using circumferential strain gauge signals. The plots were generated using the LVP16 6 pen plotter. The computer programs written in MTS Basic to run the tests, Lpost.bas, and to generate the plots, Uplot.bas, are contained in Appendix A-3 and A-4. The tested specimens are shown in figure 37.

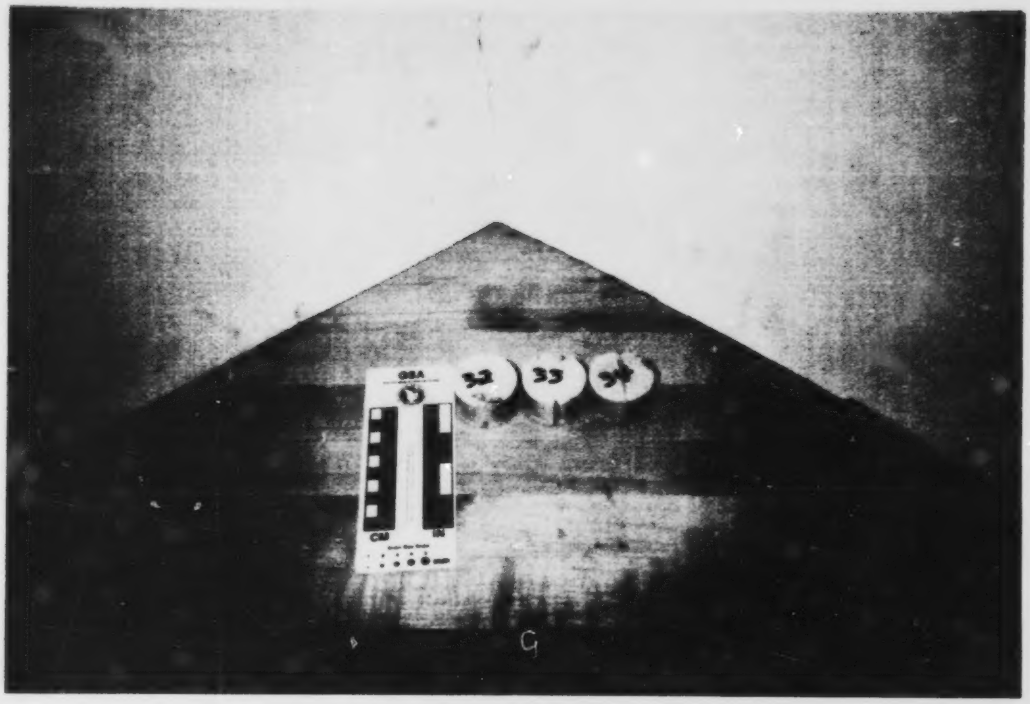

Fig. 36 Tested Brazilian specimens

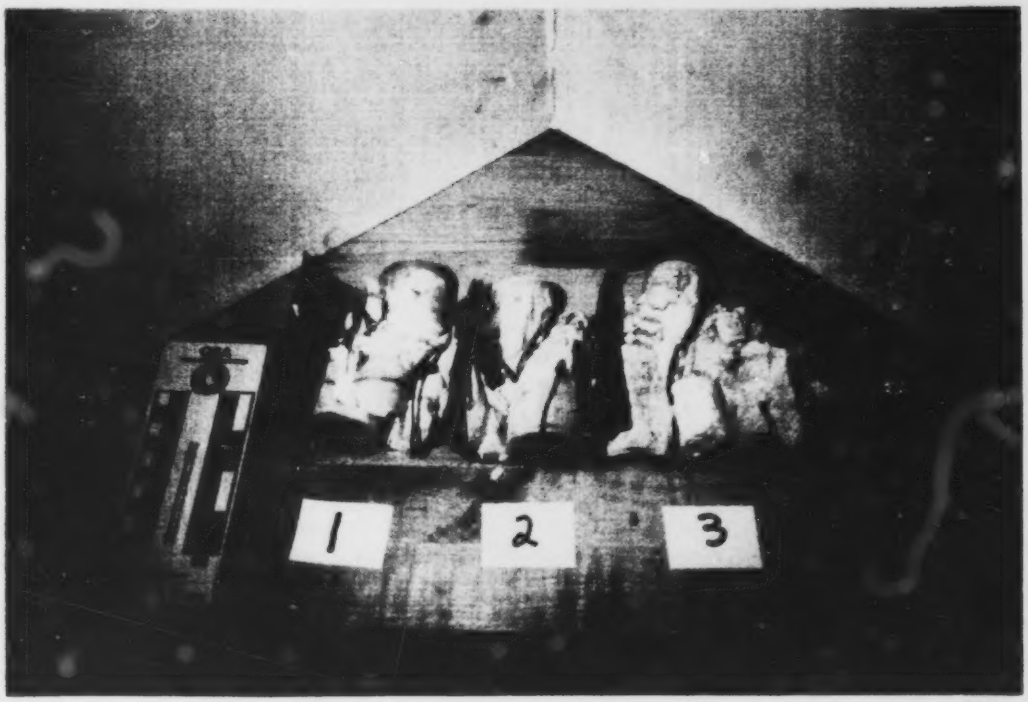

Fig. 37 Tested uniaxial specimens - load control

7.5 UNIAXIAL DATA - CIRCUMFERENTIAL CONTROL

The uniaxial compressive strength results, Q_u, for specimens N4-N5 are listed in Table 4. Values of ϵ_{peak}, E, ν, and t_p were calculated using those methods described under item 7.4. The additional results shown in brackets were calculated using signals from the 3 linear variable differential transducers, and the circumferential extensometer. The computer programs used were also common to the load control uniaxial tests. Appendix B-1 provides plots of stress versus axial strain using axial strain gauge signals. Appendix B-2 provides stress-plots using averaged axial lvdt strain signals. The axial and circumferential strain gauge signals failed in the post-peak region of tests due to specimen fracture propagation. Lvdt signals were corrected for end platen correction located within the sensing length. Appendix B-3 provides plots using circumferential strain gauge signals. Appendix B-4 provides plots using the circumferential extensometer strain signals. The tested specimens are shown in figure 38.

7.6 SINGLE STAGE TRIAXIAL DATA - LOAD CONTROL

The triaxial compressive strength results for specimens N7-N16 are contained in Table 5. The major principle stress values, σ_1, were calculated using signals from the triaxial load cell. The minor principle stress values were calculated using signals from the confinement pressure intensifier. The test series conducted at σ_3=30 MPa, was supplemented with an additional test due to invalidated test results from specimen N14. Confining fluid pressure punctured the jacket enclosing specimen N14 and subsequently saturated the specimen with oil. Values of E, ν, t_p, ϵ_{peak}, were calculated using those methods described in item 7.5 excluding the use of strain gauges. All specimens failed violently at peak strength. Appendix C-1 provides plots of stress versus axial strain using averaged axial lvdt strain signals. Appendix C-2 provides plots using circumferential extensometer signals. Computer software written in MTS Basic to run the test, Lmulti,bas, and to generate the plots, Tplot.bas, are contained in Appendix C-3 and C-4. The tested specimens are shown in figures 39 to 41.

7.7 SINGLE STAGE TRIAXIAL DATA - CIRCUMFERENTIAL CONTROL

The triaxial compressive strength results for specimens N17-N26 are contained in Table 5. The test series conducted at σ_3=30 MPa, was supplemented with an additional test due to oil intrusion of specimen N23 during the post-peak portion of the test. Material properties were calculated using the same methods outlined in item 7.6. Residual values were determined from the post-failure plateau portion of the tests.

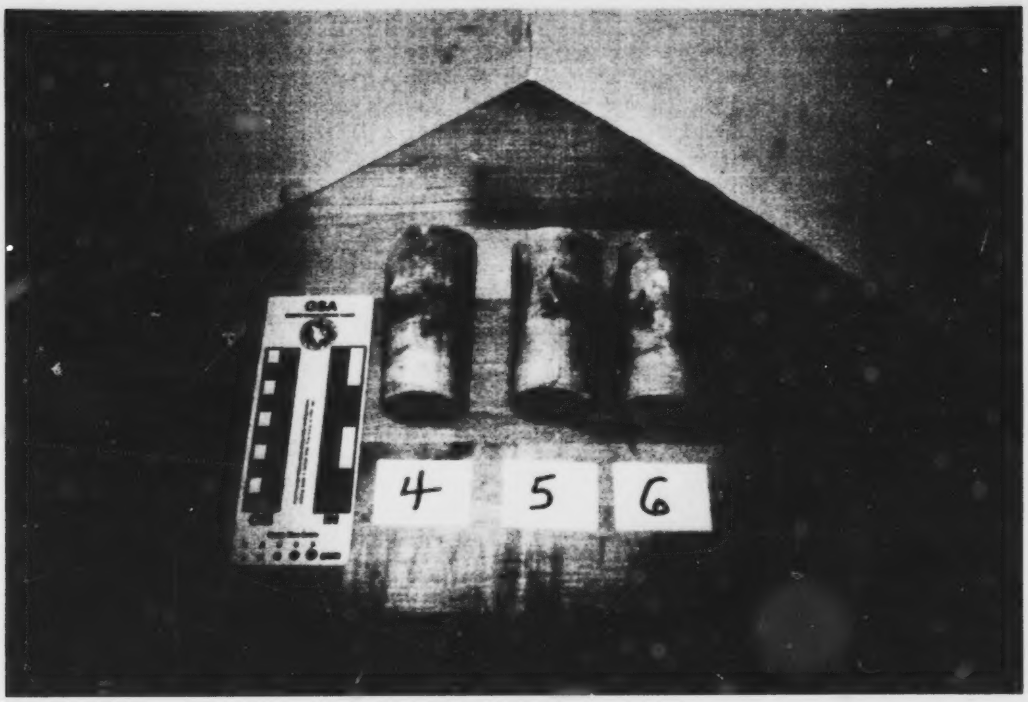

Fig. 38 Tested uniaxial specimens - circumferential control

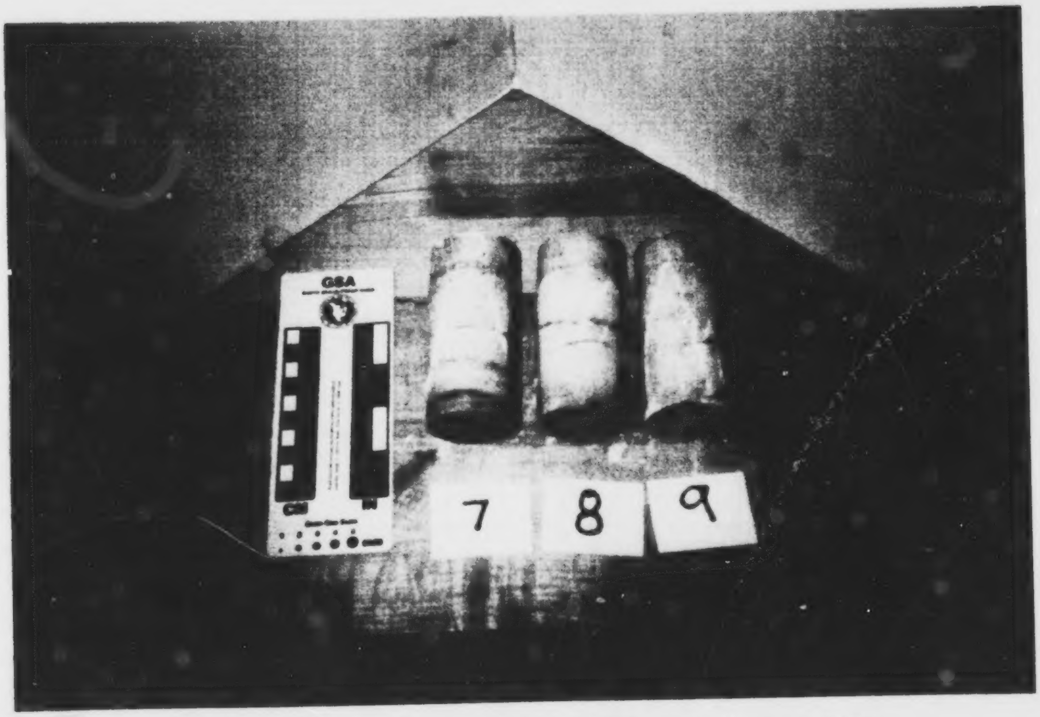

Fig. 39 Tested triaxial specimens - load control- σ_3=10MPa

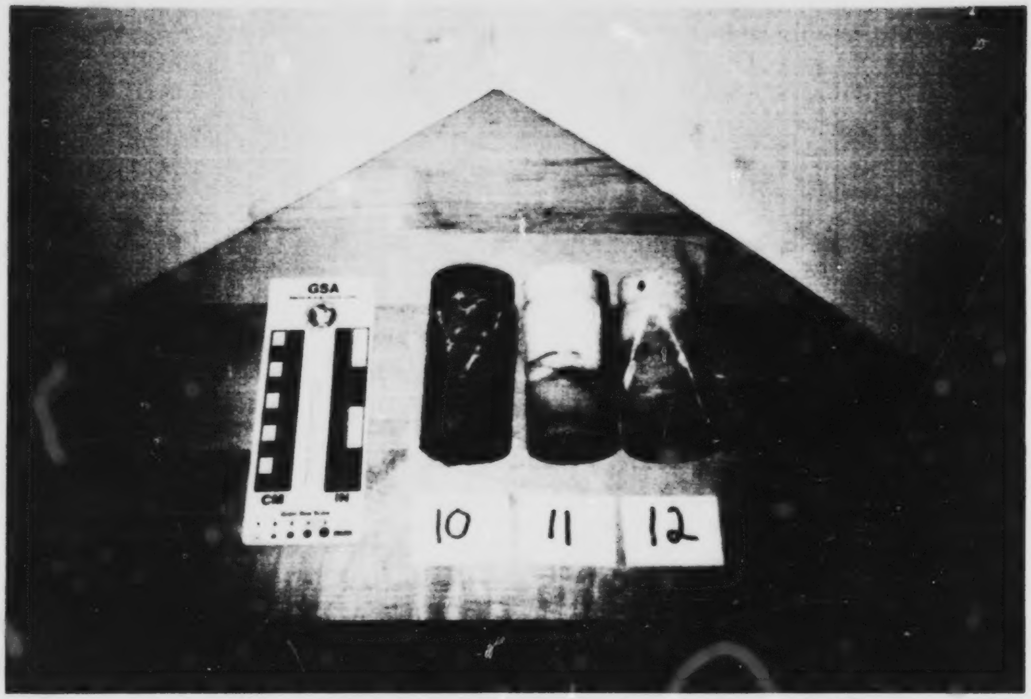
GSA
CM
IN
10
11
12

Fig. 40 Tested triaxial specimens - load control - σ_3=20MPa

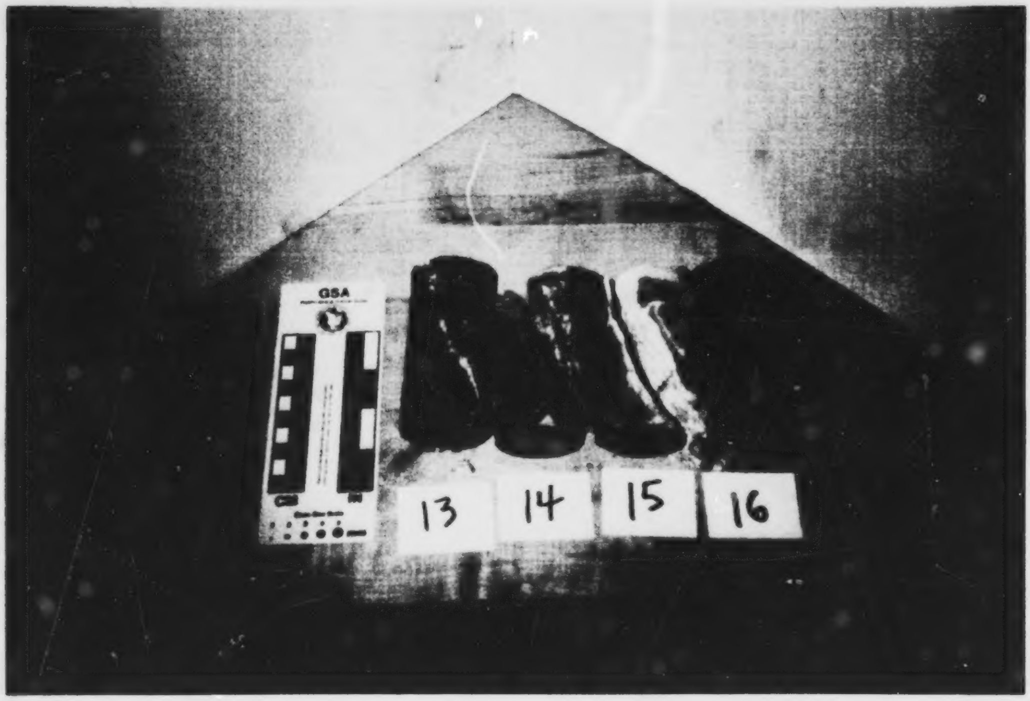
GSA
CM
IN
13
14
15
16

Fig. 41 Tested triaxial specimens - load control - σ_3=30MPa

Appendices D-1 and D-2 provide plots of stress versus axial lvdt strain, and stress versus circumferential extensometer strain, respectively. The computer programs used were common to the load control triaxial tests. The tested specimens are shown in figures 42 to 44.

7.8 MULTI STAGE TRIAXIAL DATA - CIRCUMFERENTIAL CONTROL

The triaxial compressive strength results for specimens N27-N30 are contained in Table 5. The test series was supplemented with an additional test due to oil intrusion of specimen N28 during the residual strength portion of the test. Values of E, ν, and t_p were determined for the first stage of confining pressure for each test. Residual values were determined for the last stage of each test. Appendices E-1, E-2 and E-3 provide plots of stress versus axial lvdt strain, stress versus circumferential extensometer strain, and stress versus confining pressure, respectively. The computer programs used were common to the load control triaxial tests. The tested specimens are shown in figure 45.

7.9 CONSTANT HEAD PERMEABILITY DATA - CONFINED

The permeability values for specimen N35 are contained in Table 6. The mean permeability was calculated to be 5.14 x 10^{-8} cm/s.

8 ANALYSIS AND DISCUSSIONS OF TEST RESULTS

8.1 STATISTICAL TREATMENT OF DATA

8.1.1 Mean and standard equations

All test series excluding permeability, porosity, and velocity tests were tested in populations of N=3. The mean and standard deviation of selected test series data were calculated according to the following equations:

Mean $$\overline{x} = \frac{\sum_{i=1}^{n} x_i}{n}$$

and

Standard deviation $$\sigma_x = \sqrt{\frac{\sum_{i=1}^{n}(\overline{x}-x)^2}{n-1}}$$

Computer software was written using Fortran to calculate the mean and standard deviation. The program listing, Mean.for, is contained in Appendix F-1.

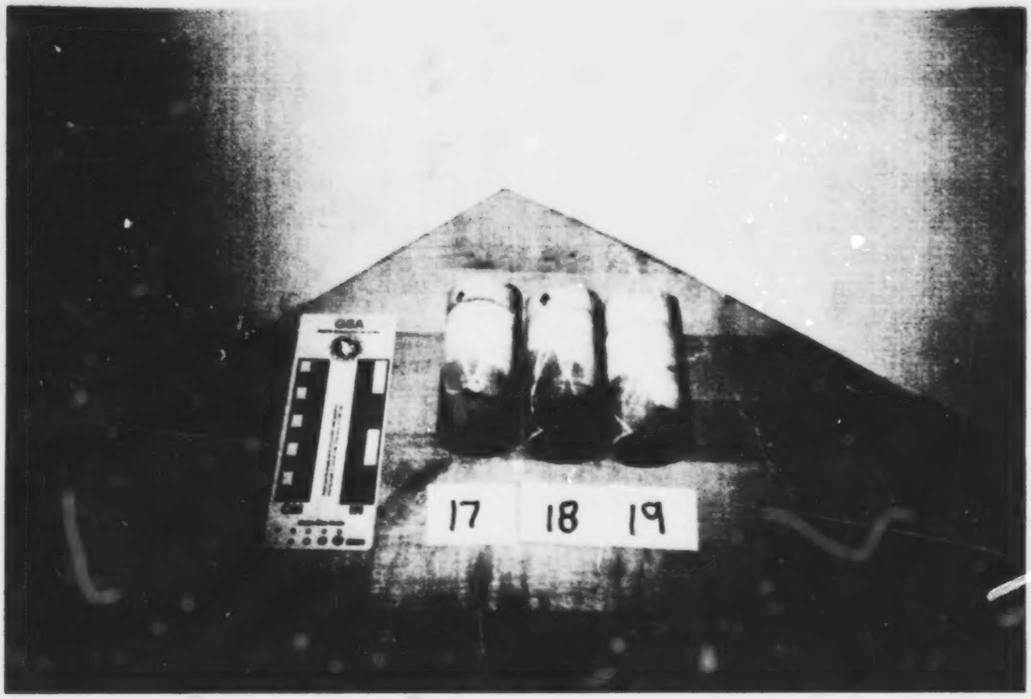
GSA
CM
IN
17
18
19

Fig. 42 Tested triaxial specimens - circumferential control - σ_3=10MPa

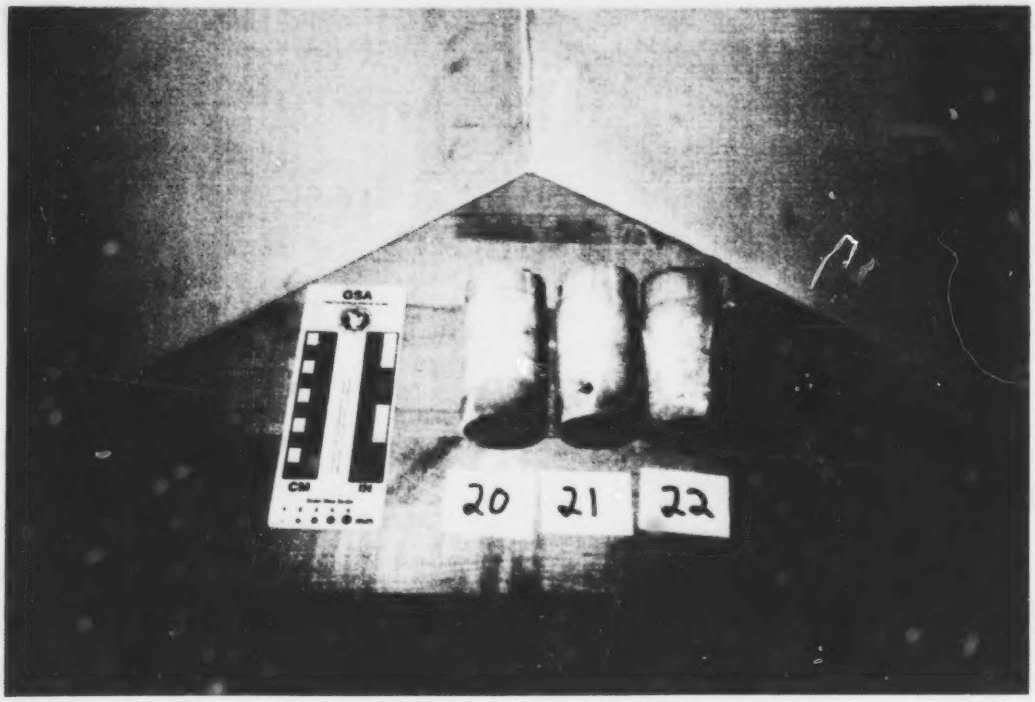
GSA
CM
IN
20
21
22

Fig. 43 Tested triaxial specimens - circumferential control - σ_3=20MPa

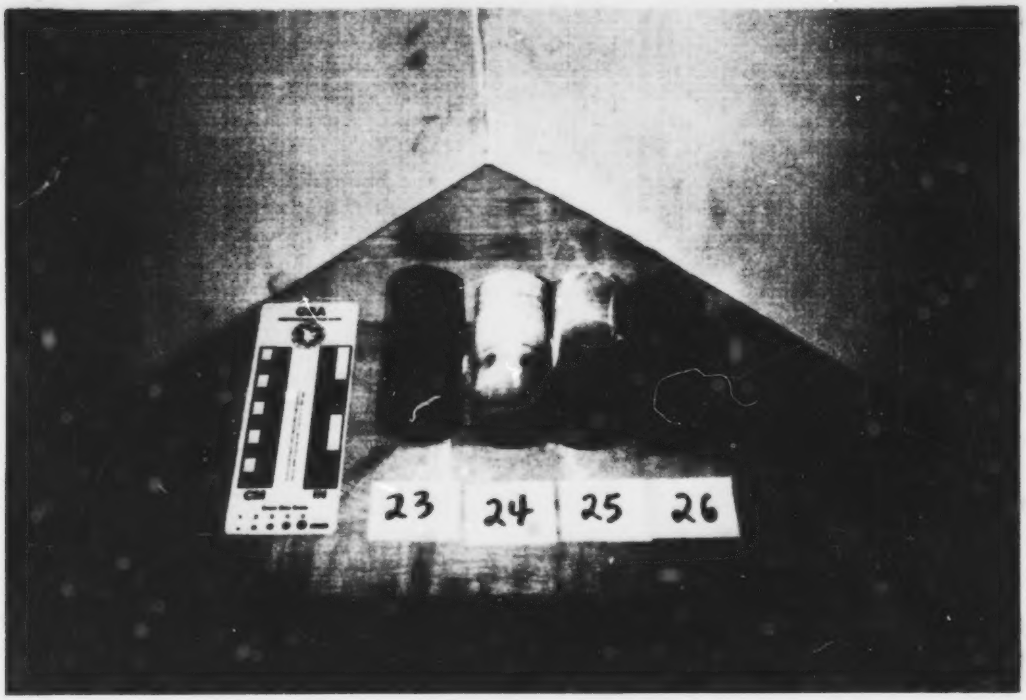

Fig. 44 Tested triaxial specimens - circumferential control - σ_3=30MPa

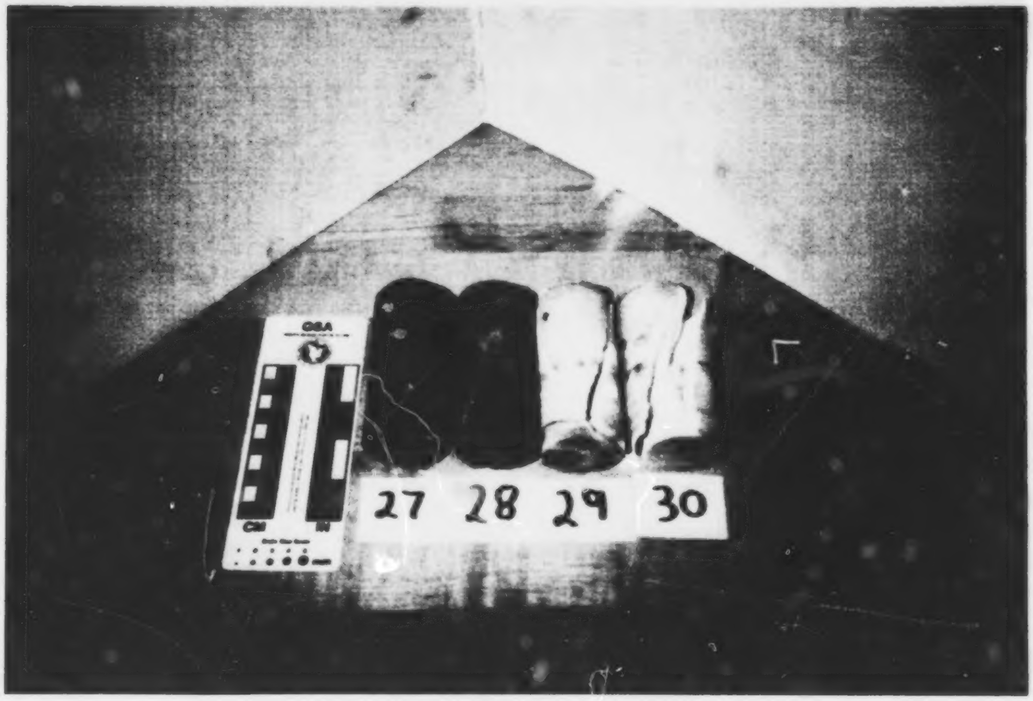

Fig. 45 Tested triaxial specimens - multi stage circumferential control

8.1.2 Least squares linear regression equations

Least squares linear regression fitting methods were used to fit platen compression versus load data, and shear stress versus normal stress data. The following equations were used:

Normal equation $\sum y = na + b\sum x$
where,

$$\sum xy = a\sum x + b\sum x^2$$

$$a = \frac{\sum x^2 \sum y - \sum x \sum xy}{n\sum x^2 - (\sum x)^2}$$

$$b = \frac{n\sum xy - \sum x \sum y}{n\sum x^2 - (\sum x)^2}$$

Least squares calculations were written into the MTS Basic program, Slope.bas, which was used to calculate corrections to end platens due to compression. The program listing is contained in Appendix F-2. Linear regression formulas were also written into the Fortran program, Failure.for, to fit shear stress versus normal stress values. The program is listed in Appendix F-3.

8.1.3 Least squares non linear regression equations

Hoek and Brown, (1980) developed the following empirical relationship between the principle stresses associated with the failure of rock:

$$\sigma_1 = \sigma_3 + \sqrt{m\sigma_c\sigma_3 + s\sigma_c^2}$$

where,

σ_1 = Major principle stress at failure (MPa)
σ_3 = Minor principle stress (MPa)
$\sigma_c = Q_c$ = Intact uniaxial compressive strength (MPa)
m = Constant dependent on cohesion and friction angle
s = Constant dependent on tensile strength

The formula may be rewritten as follows:

$$y = m\sigma_c x + s\sigma_c^2$$

where,

$y = (\sigma_1 - \sigma_3)^2$

and

$x = \sigma_3$

For intact rock, $s = 1$ and the uniaxial compressive strength, σ_c, and the material constant m are given by the following equations:

$$\sigma_c^2 = \frac{\sum y_i}{n} - [\frac{\sum x_i y_i - \frac{\sum x_i \sum y_i}{n}}{\sum x_i^2 - \frac{(\sum x_i)^2}{n}}]\frac{\sum x_i}{n}$$

$$m = \frac{1}{\sigma_c}[\frac{\sum x_i y_i - \frac{\sum x_i \sum y_i}{n}}{\sum x_i^2 - \frac{(\sum x_i)^2}{n}}]$$

x_i and y_i are successive data pairs and n is the total number of such pairs.

The coefficient of determination, r^2, is calculated as follows:

$$r^2 = \frac{[\sum x_i y_i - \frac{\sum x_i \sum y_i}{n}]^2}{[\sum x_i^2 - \frac{(\sum x_i)^2}{n}][\sum y_i^2 - \frac{(\sum y_i)^2}{n}]}$$

For broken or heavily jointed rock, the strength of the intact rock pieces, Q_u, is determined from uniaxial compressive strength tests, and this value is then used for σ_c in the equation. The value of m for the broken or heavily jointed rock is calculated as shown previously, and s is calculated as follows:

$$s = \frac{1}{\sigma_c^2}[\frac{\sum y_i}{n} - m\sigma_c\frac{\sum x_i}{n}]$$

8.2 FACTORS EFFECTING STRENGTH TEST RESULTS

8.2.1 Specimen end restraint

Uniaxial and triaxial tests were conducted with end bearing platens having the same diameter as the test specimen. Platens produce a lateral restraint at the specimen ends due to dissimilar coefficients of friction, and this lateral stress inhibits crack growth. Initial fracture extension occurs near the center of the specimen, where axial stress is greatest and the lateral constraint is a minimum, Paul and Gangal, (1966).

8.2.2 Specimen length to diameter ratios

Length to diameter ratios of 2.5 - 3.0 are recommended for compressive strength tests Mogi, (1966). Lesser ratios tend to show increased strength values, whereas greater ratios do not increase the compressive strength significantly and may fail due to elastic instability. For the test series conducted, length to diameters of 2.3 to 1 were used.

8.2.3 Specimen size

The strength of specimens usually decreases with increase in their size to some limiting diameter, Hoskins and Horino, (1969). Maximum strengths were established for specimens 50 mm in diameter in their study. For the test series conducted, specimen diameters were 44.8 mm.

8.2.4 Specimen moisture content

Price, (1960), conducted tests on certain sandstones with different percentages of moisture and reported a significant decrease in strength with increase in moisture. This effect is seen to increase with specimens having less porosity. For the test series conducted, specimens were oven dried and evacuated, and then allowed to stand in laboratory air prior to testing.

8.2.4 Rate of loading

Houpert, (1970) investigated the effect of the loading rate on compressive strength of granite. His results revealed an increase in strength with increase in loading rate. For the test series conducted, several different loading rates were used and their effects on compressive strength values will be discussed further on in this study.

8.2.5 Intrinsic property effects

Rocks containing quartz as the binding material are the strongest followed by calcite, Price, (1960). Fine grained rocks exhibit higher strength, Brace, (1961), and the compressive strength decreases with increase in porosity, Price, (1960). The quartz sandstone tested in this study was poorly cemented with quartz overgrowths, and the quartz grains averaged 0.17 mm in diameter. The sandstone porosity averaged 8.5 %. The quartz grains were sufficiently small in size such that averaging of strain properties using strain gauges having grid lengths of 11.7 mm was automatic.

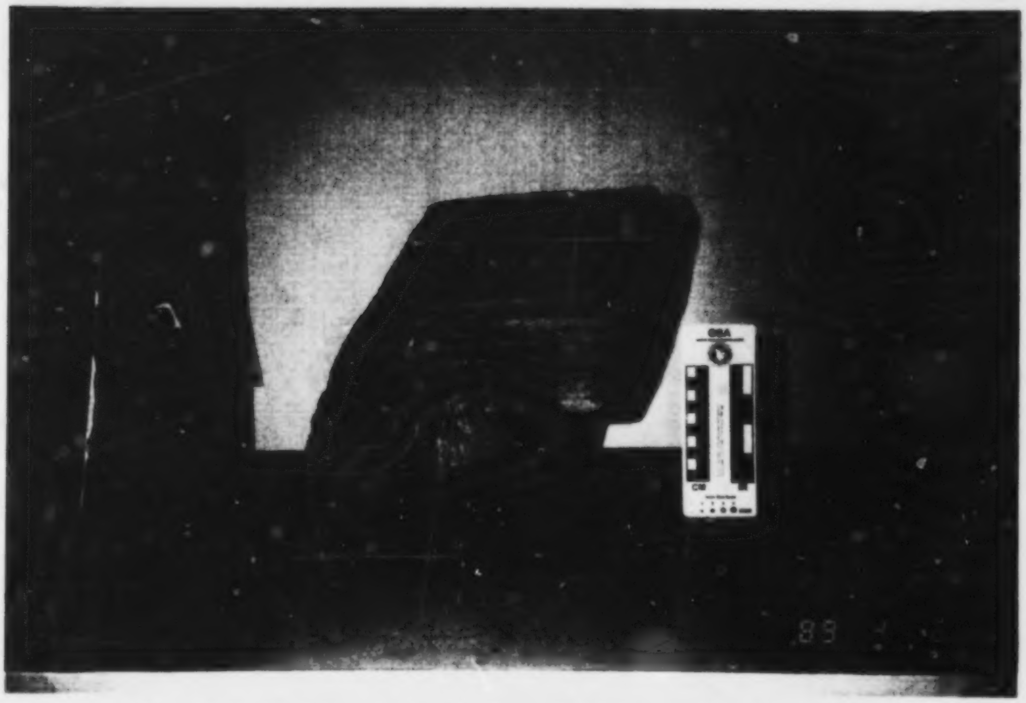

Fig. 46 Rock face displaying iron oxide groundwater staining

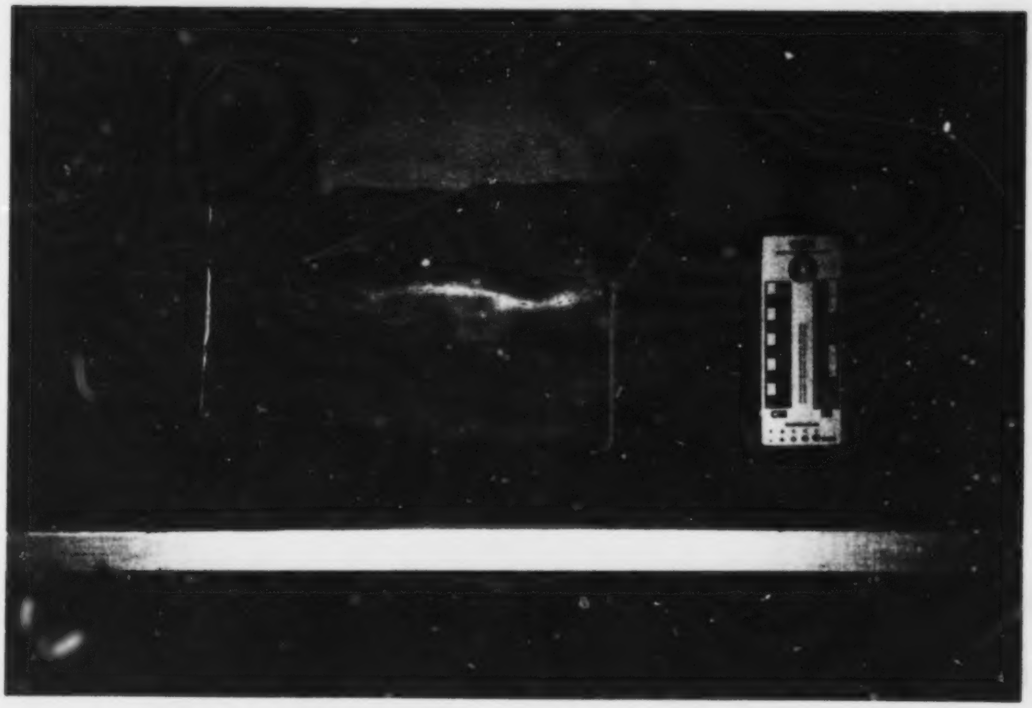

Fig. 47 Rock face displaying high quartzite content and cross-bedding

8.2.6 Jacketing effects

Triaxial test specimens were jacketed with polyolefin heat shrink tubing as the means to prevent confinement oil intrusion into rock specimens. The jackets were seen to induce some measure of confinement to the specimen during extreme dilation in the post failure region of tests. These effects were not investigated and are considered to be negligible as the jackets are relatively elastic. The jacket material compresses during application of confinement pressure, and this effect caused a strain shift in the circumferential extensometer readout. The strain shift was calculated to be 0.000016 ϵ per 1 MPa of applied confinement pressure.

8.3 POROSITY

The calculated porosity of specimens N35 and N31, and the subsequent calculated grain density confirms the absence of interstitial cement. Groundwater movement within the rock pores probably diluted and washed out the calcite cement. The remaining cement comprises quartz over-growths.

8.4 PERMEABILITY

The calculated effective permeability of N35, did not vary appreciably with different levels of confinement or with different upstream pressures. The value calculated is within the range reported for other comparable sandstones tested by Serafim, (1968). Figure 46 displays a saw cut face of Nepean sandstone acquired from another site. The displayed iron oxide patterns confirms the ability of water to migrate vertically through the rock pores. Figure 47 displays another sandstone sample from the same site. Lack of internal iron oxide staining was attributed to the high silica content of the rock (quartzite), known to be relatively impervious in the absence of fractures.

8.5 BRAZILIAN TENSILE STRENGTH

The brazilian test specimens split diametrically according to theory, Hawkes et al, (1971). The calculated ratio of Q_u to σ_t was 22. According to Griffith's theory, (1924), this value should be 8. The discrepancy may be attributed to the inhomogeniety and non-isotropic characteristics of the sandstone specimens. Further to this, the specimens lacked degree of intactness, as matrix cement was minimal.

8.6 UNIAXIAL COMPRESSIVE STRENGTH

The uniaxial strength, Q_u, results using circumferential control, were 4.6 % lower than those achieved with the load control method. The lower strength may be attributed in part to the lower mean specimen density, γ_d, (Table 4). The reduction in strength is mainly attributed to the reduced strain rate used in the circumferential control method. The time, t_p, taken to attain peak strength using circumferential control was 6 times greater than the load control method.

8.7 YOUNG'S MODULUS

Young's Modulus, E, results using circumferential control, were 5 % lower than those achieved with the load control method, (Table 4). The lower values are attributed mainly to those reasons explained under item 8.6. The calculated values agreed well, whether calculated using bonded strain gauge signals, or lvdt signals.

8.8 POISSON'S RATIO

Poisson's ratio, ν, results using circumferential control, were 22 % lower than those achieved with the load control method, (Table 4). The lower values were attributed mainly to those reasons explained under item 8.6. Typically, sandstones possess Poisson values of 0.30. The calculated values were in the order of 0.50. The higher values were attributed to the poor cementing of the quartz grains, the degree of grain roundness, and the lack of grain interlocking. The grains were seen to displace at grain contacts under load, and the degree of grain fracturing was small. The calculated values agreed well, whether calculated using bonded strain gauge signals, or lvdt signals.

8.9 PEAK STRAIN

Peak strain, ϵ_{peak}, results using circumferential control, were 4.3 % lower than those achieved with the load control method, (Table 4). The lower values were attributed mainly to those reasons explained under item 8.6. The plots provided in Appendices A-1, A-2, B-1, and B-3 using strain gauges signals were applicable up to peak strength values. Post-peak signals were erroneous as the strain gauges have failed, or are imparting signals from rock fragments not being strained. The calculated values of ϵ_{peak} agree well, whether calculated using bonded strain gauges, or lvdt signals.

8.10 RESIDUAL UNIAXIAL COMPRESSIVE STRENGTH

Post-failure uniaxial test results were recorded for circumferential control tests. The results of these tests indicate no measurable residual strength, Q_{ur}, for specimens tested in the unconfined state, (Appendices B-2 and B-4).

8.11 TRIAXIAL COMPRESSIVE STRENGTH

The results of triaxial tests (Table 5) confirmed increasing triaxial strength with increasing confining pressure applied. Values of E, ν, and ϵ_{peak} were calculated using signals from the lvdts, load cell, and the circumferential extensometer. Circumferential control results were found to be lower than load control results. Depending on the level of confinement used, triaxial strengths calculated using the circumferential method, were from 4.6 to 13.0 % less than the load control method. The differences are mainly attributed to those reasons discussed under item 8.6. The results of circumferential control single stage and multi stage triaxial tests were in agreement with each other. Values of E, ν, t_p, ϵ_{peak}, σ_1, and σ_{1r} increased with increasing confining pressure.

The confinement levels used were determined based on the known stratigraphy of the area. Maximum thicknesses of lithological units and previous glacial history information were used to determine the maximum overburden pressure the sandstone may have been subjected to. Lower levels of confinement were then also determined for testing purposes. The determinations were made based on the following geologic information, Belanger et al, (1980).

Rockcliffe formation	γ_d=2.49	h=50m	γh=1.22MPa
Billings formation	γ_d=2.62	h=90m	γh=2.31MPa
Carlsbad formation	γ_d=2.62	h=165m	γh=4.24MPa
Russell & Queenstone formations	γ_d=2.64	h=30m	γh=0.78MPa
Ottawa formation	γ_d=2.69	h=210m	γh=5.54MPa
Eastview formation	γ_d=2.65	h=6m	γh=0.16MPa
St. Martin formation	γ_d=2.69	h=12m	γh=0.32MPa
Oxford formation	γ_d=2.72	h=75m	γh=2.00MPa
March formation	γ_d=2.58	h=10m	γh=0.25MPa
Nepean formation	γ_d=2.52	h=85m	γh=2.10MPa
Glacial ice	γ_d=1.00	h=610m	γh=5.98MPa
Total overburden pressure			24.90MPa

8.12 RESIDUAL TRIAXIAL COMPRESSIVE STRENGTH

Post-failure triaxial test results were recorded for circumferential control tests. The results of these tests indicate increasing residual strength with increasing confining pressure, (Appendices D-1, D-2, E-1, and E-2).

8.13 LOAD VERSUS CIRCUMFERENTIAL STRAIN RATE CONTROLLED TESTS

Uniaxial and triaxial compressive strength tests conducted in load control exhibited higher peak strengths than those conducted in circumferential control. The slower strain rates used in circumferential control allowed specimen micro-fracture initiation to propagate more extensively at lower loads. This confirmed the time-depend behaviour of micro-fracturing of rock specimens under load.

8.14 MOHR CIRCLE ANALYSIS

Various theories relative to the stress situation in a rock mass at the time of failure have been proposed and used. The failure of a rock mass is in closest accordance with the tenets of the Mohr theory of failure. According to the Mohr theory, a material fails along the plane at which the angle between the resultant of the normal and shearing stresses is a maximum. From several triaxial tests conducted at different levels of confining pressure, a locus of points representing shear stress versus normal stress at failure are determined through which a tangent line may be fitted. This line is called the Mohr envelope or failure envelope. The existence of a linear failure envelope was predicted by Coulomb, so if the envelope is linear it is referred to as the Mohr-Coulomb failure envelope. The angle of the of the failure envelope line to the normal is equal to the angle of internal friction.

Hoek and Brown developed an empirical relationship between the principal stresses associated with the failure of rock. This relationship was developed based on failure theories first proposed by Griffith, (1924) and later modified by McClintock and Walsh, (1962). The relationship may be used to plot the maximum stress conditions graphically for a rock mass in the form of a Mohr diagram. The derived failure envelope is curved rather than linear. Figure 48 depicts Mohr circle analyses using the Hoek and Brown method for determining the failure envelope, (upper envelope), and the residual envelope, (lower envelope).

Triaxial data and uniaxial data were analyzed using both the Mohr-Coulomb and Hoek and Brown methods. Data were separated into load control tests, single stage circumferential control tests, and multi-stage circumferential control tests for purposes of analyses. The results of these analyses are presented in Tables 7, 8, and 9.

8.15 HOEK AND BROWN FAILURE ENVELOPE ANALYSES

The Hoek and Brown empirical relationship is described under item 8.1.3. Figure 49 displays the graphical representation of stress conditions for failure of intact rock. Balmer, (1952) expressed the equation for a system of Mohr circles as :

$$(\sigma_n - 0.5(\sigma_1 + \sigma_3))^2 + \tau^2 = 0.25(\sigma_1 - \sigma_3)^2$$

Substitution of Hoek and Brown's into Balmer's equations gives:

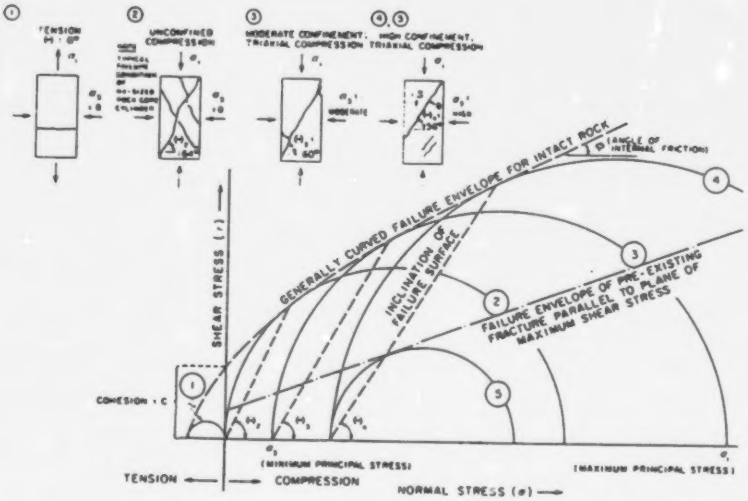
①
TENSION
② UNCONFINED COMPRESSION
③ MODERATE CONFINEMENT, TRIAXIAL COMPRESSION
④,⑤ HIGH CONFINEMENT, TRIAXIAL COMPRESSION
σ_1
σ_3 = 0
σ_3 = MODERATE
σ_3 = HIGH
60°
30°
GENERALLY CURVED FAILURE ENVELOPE FOR INTACT ROCK
φ (ANGLE OF INTERNAL FRICTION)
INCLINATION OF FAILURE SURFACE
FAILURE ENVELOPE OF PRE-EXISTING FRACTURE PARALLEL TO PLANE OF MAXIMUM SHEAR STRESS
SHEAR STRESS (τ)
COHESION = C
1
2
3
4
5
σ_3 (MINIMUM PRINCIPAL STRESS)
σ_1 (MAXIMUM PRINCIPAL STRESS)
TENSION
COMPRESSION
NORMAL STRESS (σ)

The Mohr concept of rock strength relating shear strength components, cohesion (c), and angle of internal friction (ϕ) to imposed stress. Shown are five typical examples of engineering property tests on NX-sized rock core; (1) tension, (2) unconfined compression, (3) triaxial compression at moderate confinement, (4) triaxial compression at high confinement, and (5) triaxial compression at high confinement with fracturing present.

Fig. 48 Hoek and Brown Mohr circle analyses

Table 7 Intact Failure Envelope Material Constants

Includes Uniaxial Series		*Hoek and Brown* $\sigma_1 = \sigma_3 + \sqrt{m\sigma_c\sigma_3 + s\sigma_c^2}$				*Mohr − Coulomb* $\tau = c + \sigma_n tan\phi$		
Test Series	Control Mode	m	s	Q_c (MPa)	r^2	c (MPa)	ϕ (°)	r^2
Single stage triaxial	Load	24.93	1.00	156.15	0.98	28.36	51.6	0.99
Single stage triaxial	Circumferential	24.18	1.00	140.57	1.00	26.23	50.8	0.99
Multi stage triaxial	Circumferential	24.17	1.00	139.94	1.00	26.14	50.8	0.99

Table 8 Residual Failure Envelope Material Constants

Circumferential Displacement Control		*Hoek and Brown* $\sigma_1 = \sigma_3 + \sqrt{m\sigma_c\sigma_3 + s\sigma_c^2}$				*Mohr − Coulomb* $\tau = c + \sigma_n tan\phi$		
Test Series	Residual Used	m_r	s_r	Q_u (MPa)	r^2	c_r (MPa)	ϕ (°)	r^2
Single stage triaxial	Plateau data	4.72	0.04	142.51	0.91	8.00	41.0	0.99
Single stage triaxial	All data	3.97	0.00	142.51	0.74	3.31	42.0	1.00
Single stage triaxial	$\sigma_3 = 10MPa$	5.47	0.00	142.51	0.96	3.69	44.7	1.00
Single stage triaxial	$\sigma_3 = 20MPa$	3.33	-0.00	142.51	0.82	3.11	40.6	1.00
Single stage triaxial	$\sigma_3 = 30MPa$	3.92	0.00	142.51	0.71	3.29	41.9	1.00
Multi stage triaxial	All data	3.62	0.00	142.51	0.85	3.20	41.3	1.00

Table 9 Intact Failure Envelope Parameters

	Test Results			*Hoek and Brown* $\sigma_1 = \sigma_3 + \sqrt{m\sigma_c\sigma_3 + s\sigma_c^2}$						*Mohr − Coulomb* $\tau = c + \sigma_n tan\phi$					
Specimens	σ_1 (MPa)	σ_3 (MPa)	θ (°)	τ (MPa)	σ_n (MPa)	σ_1 (MPa)	c (MPa)	ϕ (°)	θ (°)	τ (MPa)	σ_n (MPa)	σ_1 (MPa)	c (MPa)	ϕ (°)	θ (°)
N1-N3	149.05	0.0	79	39.61	10.80	156.15	21.28	60	75	50.59	17.61	162.92	28.36	52	71
N7-N9	258.88	10.0	73	76.38	35.85	261.62	29.48	53	71	73.10	35.45	245.41	28.36	52	71
N10-N12	353.89	20.0	70	105.26	59.54	339.75	37.19	49	69	95.61	53.29	327.91	28.36	52	71
N13-N16	398.05	30.0	70	130.08	82.33	405.72	44.31	46	68	118.12	71.13	410.41	28.36	52	71
N4-N6	142.51	0.0		36.09	9.97	140.57	19.42	59	75	46.55	16.59	147.26	26.23	51	70
N17-N19	242.06	10.0	78	71.72	34.85	241.87	27.46	52	71	68.30	34.33	226.04	26.23	51	70
N20-N22	313.15	20.0	69	99.37	58.28	316.25	34.95	48	69	90.04	52.08	304.82	26.32	51	70
N23-N26	380.64	30.0	70	123.05	80.78	378.94	41.84	45	68	111.79	69.83	383.60	26.32	51	70
N4-N6	142.51	0.0		35.94	9.94	139.94	19.34	59	75	46.38	16.54	146.62	26.14	51	70
N27-N28	240.69	10.0	71	71.53	34.80	241.10	27.38	52	71	68.10	34.28	225.28	26.14	51	70
N27-N28	312.29	20.0	71	99.14	58.23	315.35	34.86	48	69	89.82	52.03	303.94	26.14	51	70
N27-N28	379.74	30.0	71	122.77	80.71	377.93	41.74	45	68	111.54	69.77	382.60	26.14	51	70

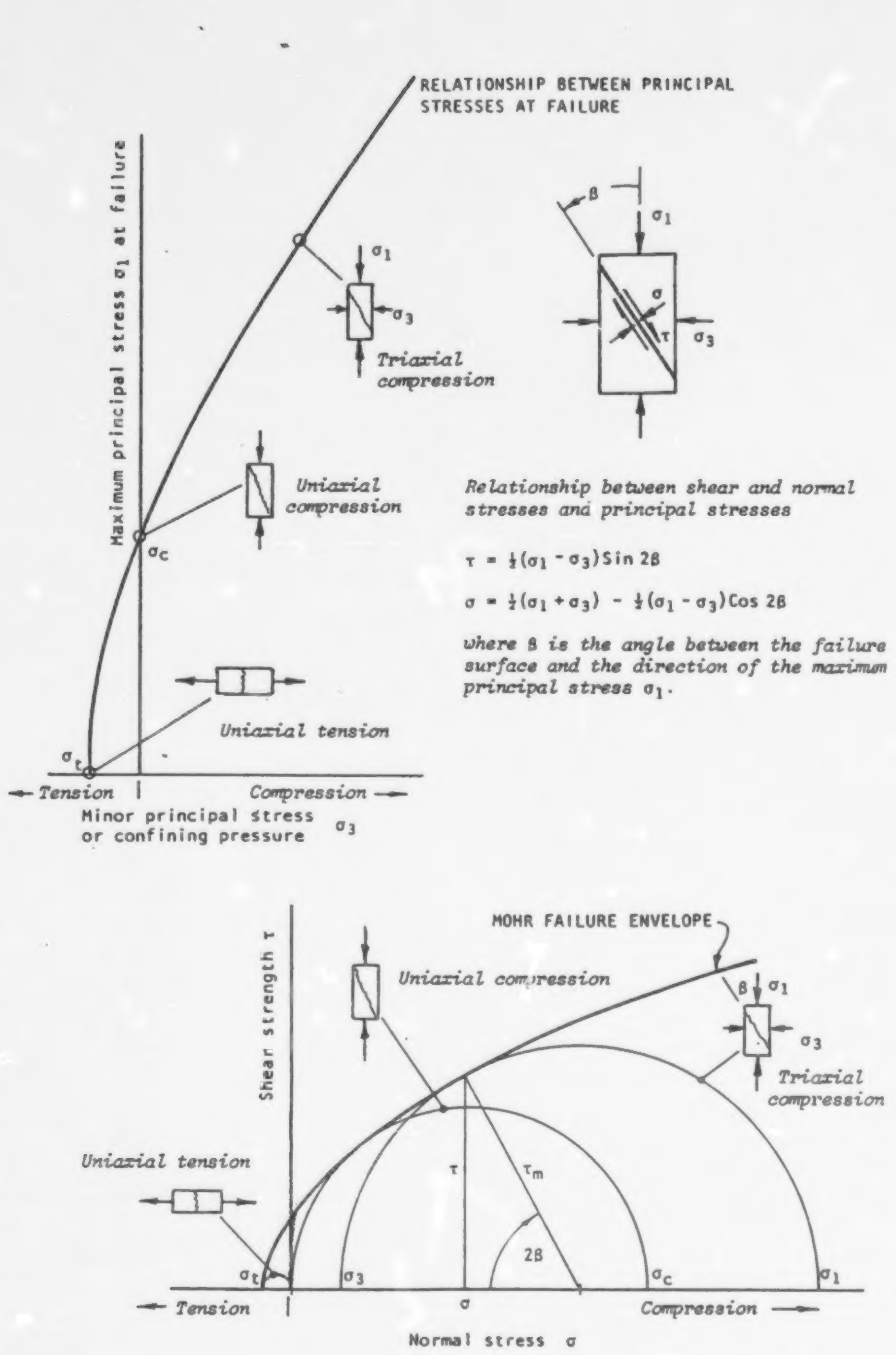
RELATIONSHIP BETWEEN PRINCIPAL STRESSES AT FAILURE
Maximum principal stress σ_1 at failure
σ_1
σ_3
Triaxial compression
β
σ
τ
Uniaxial compression
σ_c
Relationship between shear and normal stresses and principal stresses
$\tau = \frac{1}{2}(\sigma_1 - \sigma_3)\sin 2\beta$
$\sigma = \frac{1}{2}(\sigma_1 + \sigma_3) - \frac{1}{2}(\sigma_1 - \sigma_3)\cos 2\beta$
where β is the angle between the failure surface and the direction of the maximum principal stress σ_1.
Uniaxial tension
σ_t
Tension
Compression
Minor principal stress or confining pressure σ_3
MOHR FAILURE ENVELOPE
Shear strength τ
Uniaxial compression
β
σ_1
σ_3
Triaxial compression
Uniaxial tension
τ
τ_m
2β
σ_t
σ_3
σ_c
σ_1
Tension
σ
Compression
Normal stress σ

Fig. 49 Hoek and Brown graphical stress representation

$$\sigma_n = \sigma_3 + \frac{\tau_m^2}{\tau + m\sigma_c/8}$$

$$\tau = (\sigma_n - \sigma_3)\sqrt{1 + m\sigma_c/4\tau_m}$$

where,

$$\tau_m = 0.5(\sigma_1 - \sigma_3)$$

and the failure angle is defined by

$$Sin2\theta = \frac{\tau}{\tau_m}$$

Using these equations the Hoek and Brown failure envelope and residual envelope may be generated using the empirical relationship. The coefficient of friction may also be determined and the cohesion intercept.

The calculated values of m, s, Q_c, and r^2 are displayed in Table 7. Table 8 displays the corresponding residual values. Values of m did not vary significantly regardless of test method. The values of $s = 1$ confirmed the rock tested was intact. Values of Q_c were less for circumferential control tests confirming the influence of the slower loading rates. Values of s_r were generally calculated to be zero confirming the non-intact state of the rock when extended into the post-failure region of the tests. This was confirmed by the low calculated values of residual strength, m_r.

8.16 MOHR - COULOMB FAILURE ENVELOPE ANALYSES

The Mohr-Coulomb failure envelope relationship is expressed as follows:

$$\tau = c + \sigma_n tan\phi$$

where,

$$\frac{\sigma_1 + \sigma_c}{\sigma_3 + \sigma_c} = tan^2(45 + \phi/2)$$

and

$$\sigma_1 = \sigma_3 tan^2(45 + \phi/2) + \frac{c(tan^2(45+\phi/2)-1)}{tan\phi}$$

and the failure angle is

$$\theta = 45 + \phi/2$$

Table 7 displays the calculated values of c, ϕ, and r^2. The corresponding values for the residual case are displayed in Table 8. Cohesion strength was higher for the load control tests confirming the effect of the faster load rate used to reduce the fracture initiation prior to failure. The residual cohesion strength was lower indicating the higher degree of fracturing present. The lower residual failure angle indicates the advanced degree of shearing of asperities along the shear plane. The higher residual cohesion strength recorded for plateau data, indicates the lesser extent to which the rock has been fractured at that point of the test.

8.17 COMPUTER ANALYSES

Fortran software was used for Hoek and Brown and Mohr-Coulomb envelope analyses, and subsequent graphical presentation. The computer program Failure.for is contained in Appendix F-3. Subsequent plotting of data was performed using Dataplot software. Figure 50 displays Hoek and Brown failure envelope analyses for load control single stage tests. Figure 51 displays Hoek and Brown failure envelope analyses for circumferential control single stage tests. Figure 52 displays Hoek and Brown failure envelope analyses for circumferential control multi-stage tests. Figures 53, 54, and 55 display in the same sequence analyses using the Mohr-Coulomb failure envelope method.

This same data is displayed in numerical form in Table 9. By perusal of Table 9, comparisons may be made between actual test results and the corresponding results derived from both the Hoek and Brown, and Mohr-Coulomb failure envelope analyses. For circumferential control tests, the Hoek and Brown results for σ_1 and θ were in close agreement with actual test results. The load control results using the Hoek and Brown method were slightly higher than actual.

For circumferential tests, the Mohr-Coulomb results skewed slightly higher than actual test results for σ_1. This was due to the fact that Mohr-Coulomb analyses uses a linear relationship whereas actual test data indicates a curved failure envelope should be used. For load control tests the Mohr-Coulomb results for σ_1 were more skewed than those determined for circumferential control tests.

In comparing Hoek and Brown to Mohr-Coulomb results, it was confirmed that the Hoek and Brown method approximated the actual test results more closely. This was due to the non-linear fitting method used in the Hoek and Brown method.

9. CONCLUSIONS AND RECOMMENDATIONS

Geologically, Nepean sandstone may be classified as a sedimentary mature quartz arenite having well sorted and well rounded 0.14 mm diameter quartz grains displaying quartz overgrowths. The Nepean Formation dates to Upper Cambrian age of Paleozoic era and the Chazy period. The absence of interstitial silica cement confirms the extent of weathering subjected to the formation.

Physically, Nepean sandstone has a bulk dry density of 2.40 g/cc and a grain density of 2.65 g/cc. The sandstone porosity is 8.10 %. The compressional wave velocity of the rock is in the order of 4.66 km/s. The average confined permeability was calculated to be 5.14 $cm/10^{-8}$. Evidence of decreasing permeability with increasing confinement pressure was not confirmed.

HOEK AND BROWN FAILURE ENVELOPE

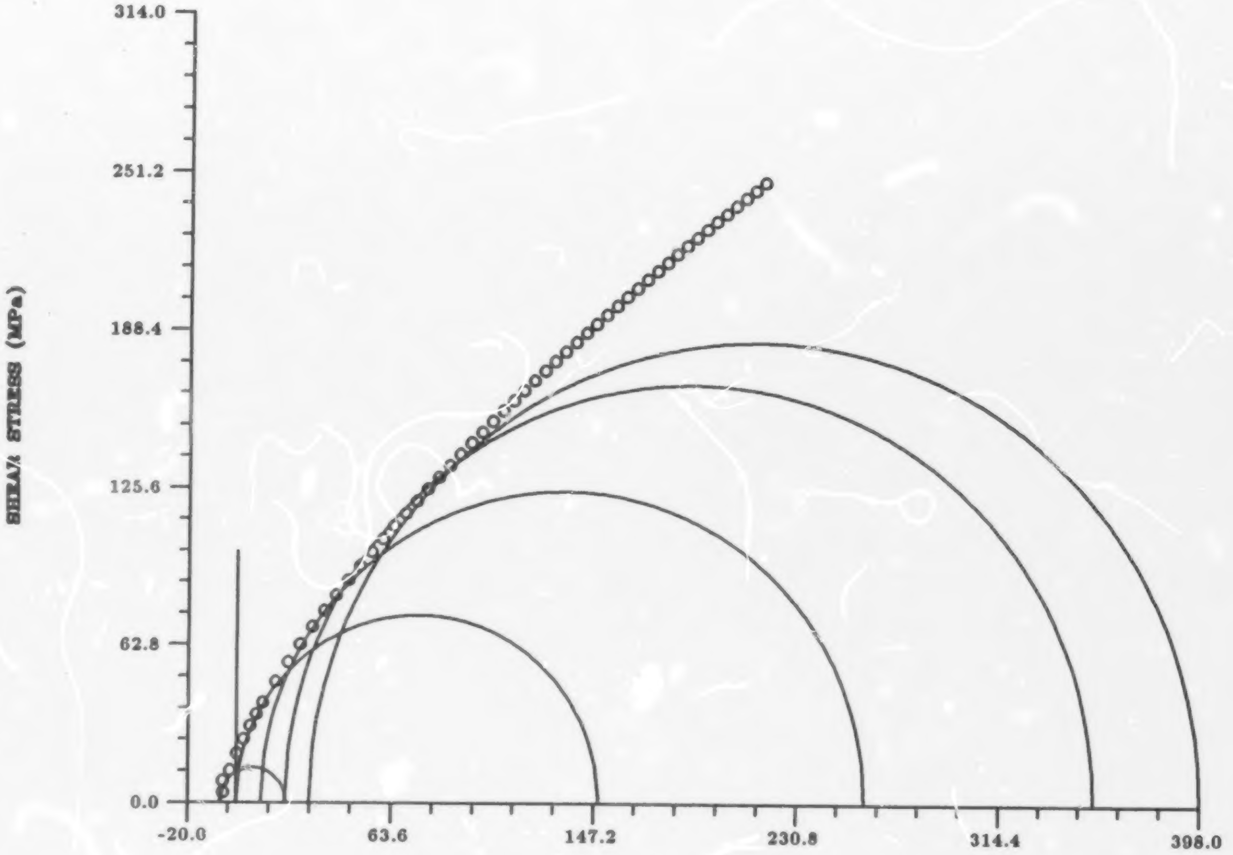

NEPEAN SANDSTONE

Fig. 50 LOAD CONTROL SINGLE STAGE TRIAXIAL

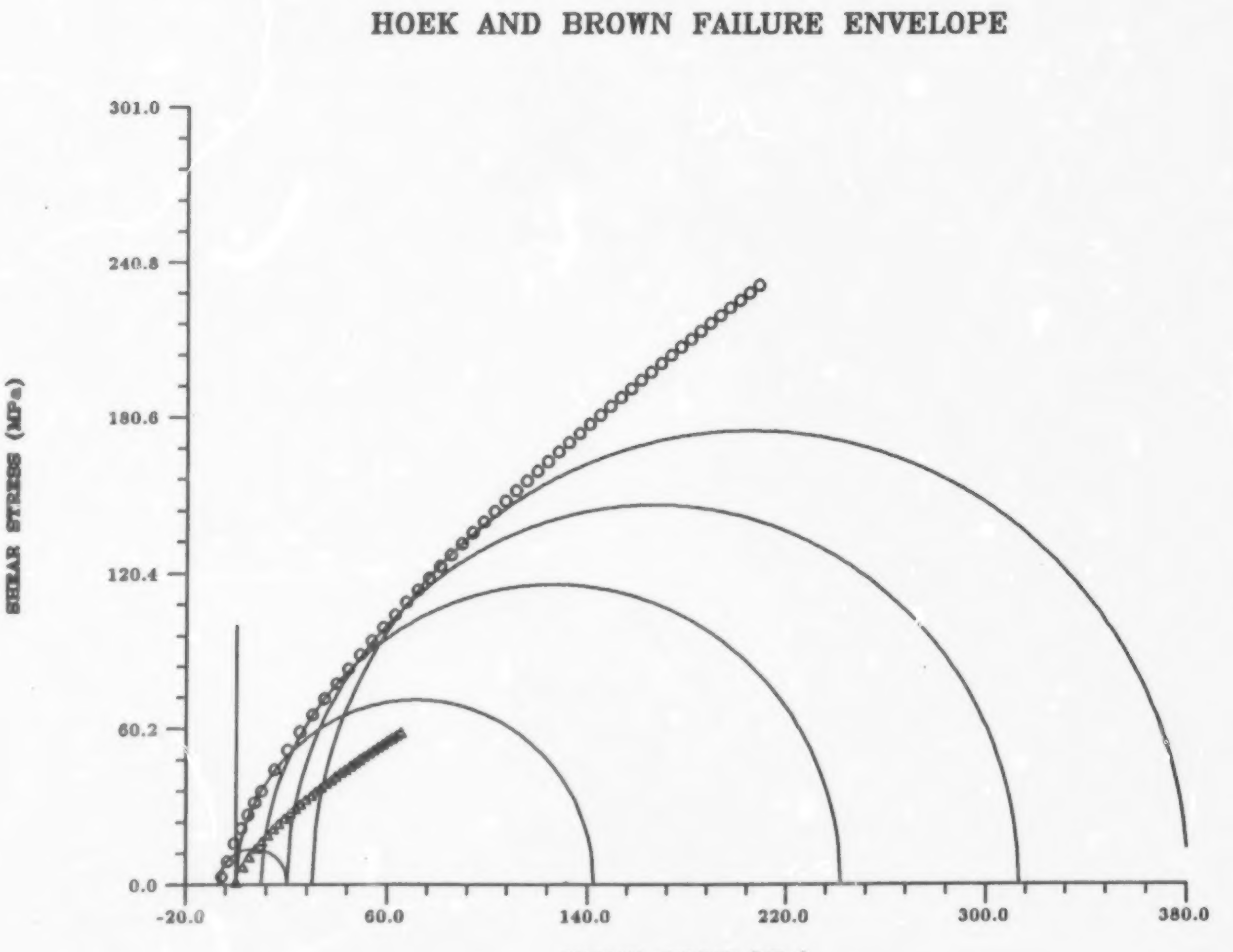

Fig. 51 NEPEAN SANDSTONE – ALL RESIDUAL DATA
CIRCUMFERENTIAL DISPLACEMENT CONTROL SINGLE STAGE TRIAXIAL

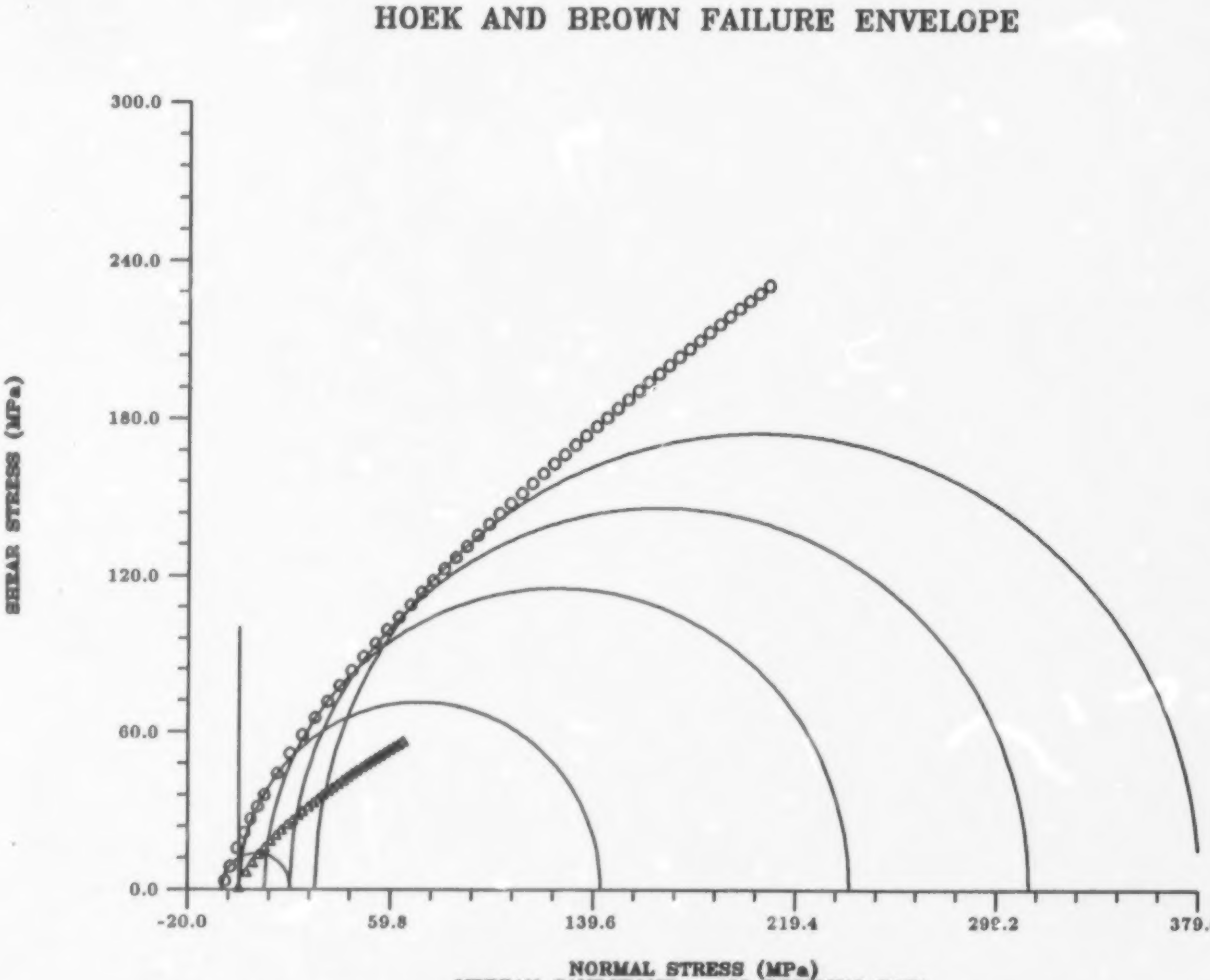

Fig. 52 NEPEAN SANDSTONE - ALL RESIDUAL DATA
CIRCUMFERENTIAL DISPLACEMENT CONTROL MULTI STAGE TRIAXIAL

MOHR - COULOMB FAILURE ENVELOPE

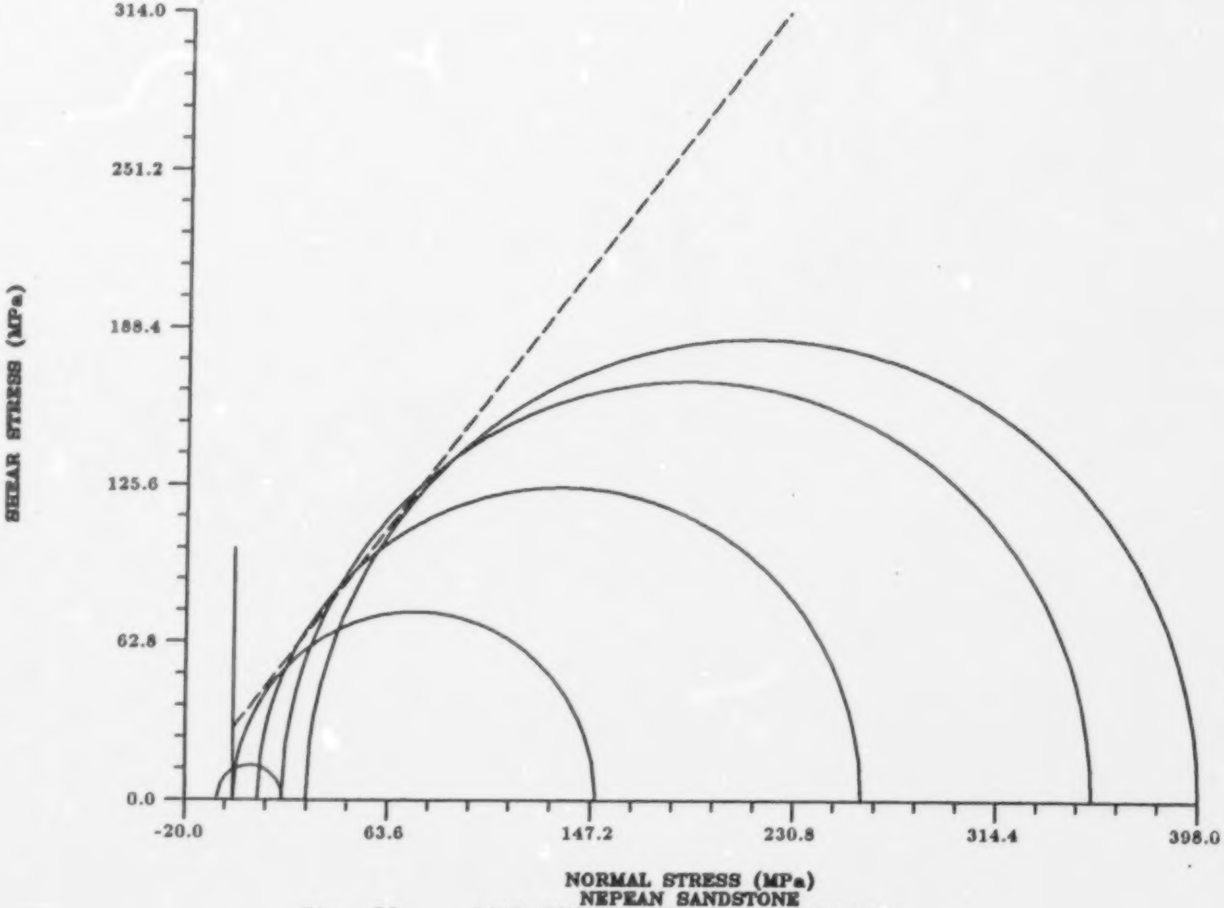

NEPEAN SANDSTONE

Fig. 53 LOAD CONTROL SINGLE STAGE TRIAXIAL

MOHR – COULOMB FAILURE ENVELOPE

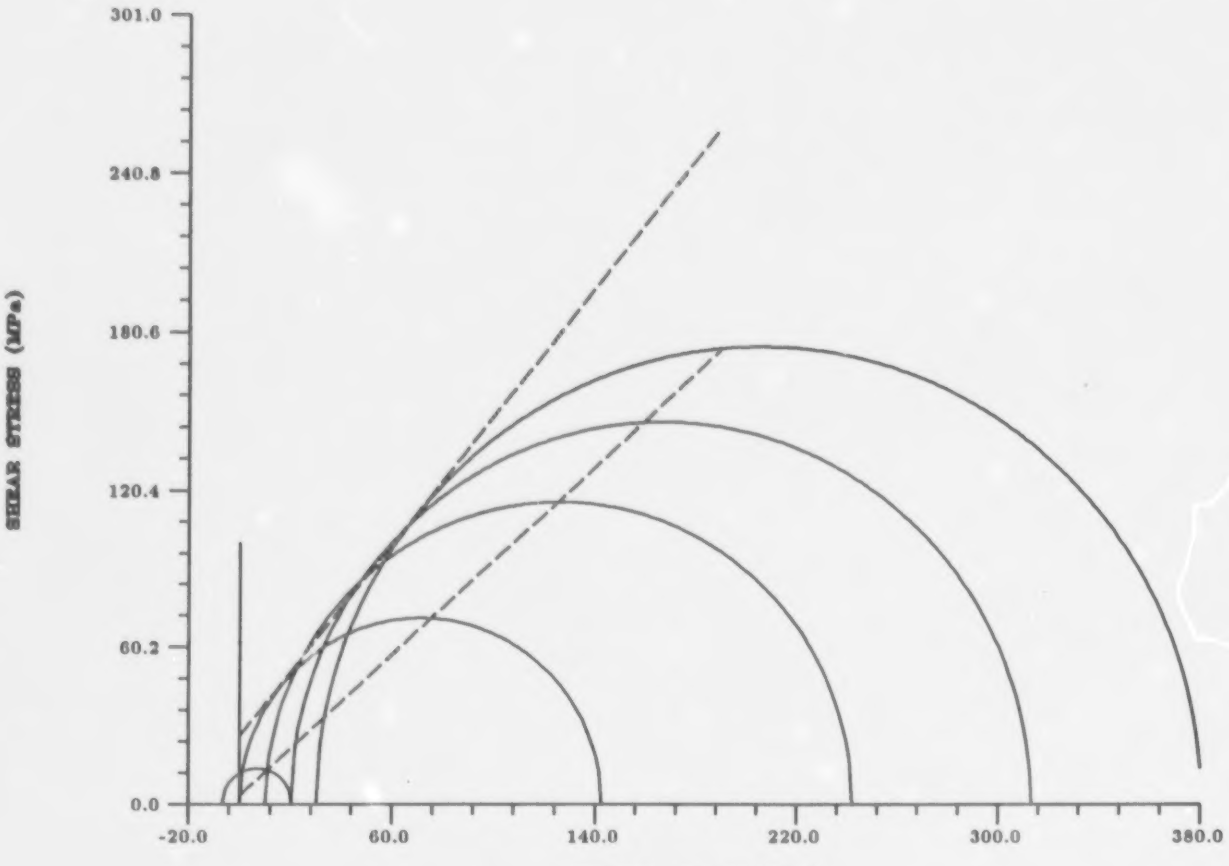

NORMAL STRESS (MPa)
NEPEAN SANDSTONE – ALL RESIDUAL DATA
Fig. 54 CIRCUMFERENTIAL DISPLACEMENT CONTROL SINGLE STAGE TRIAXIAL

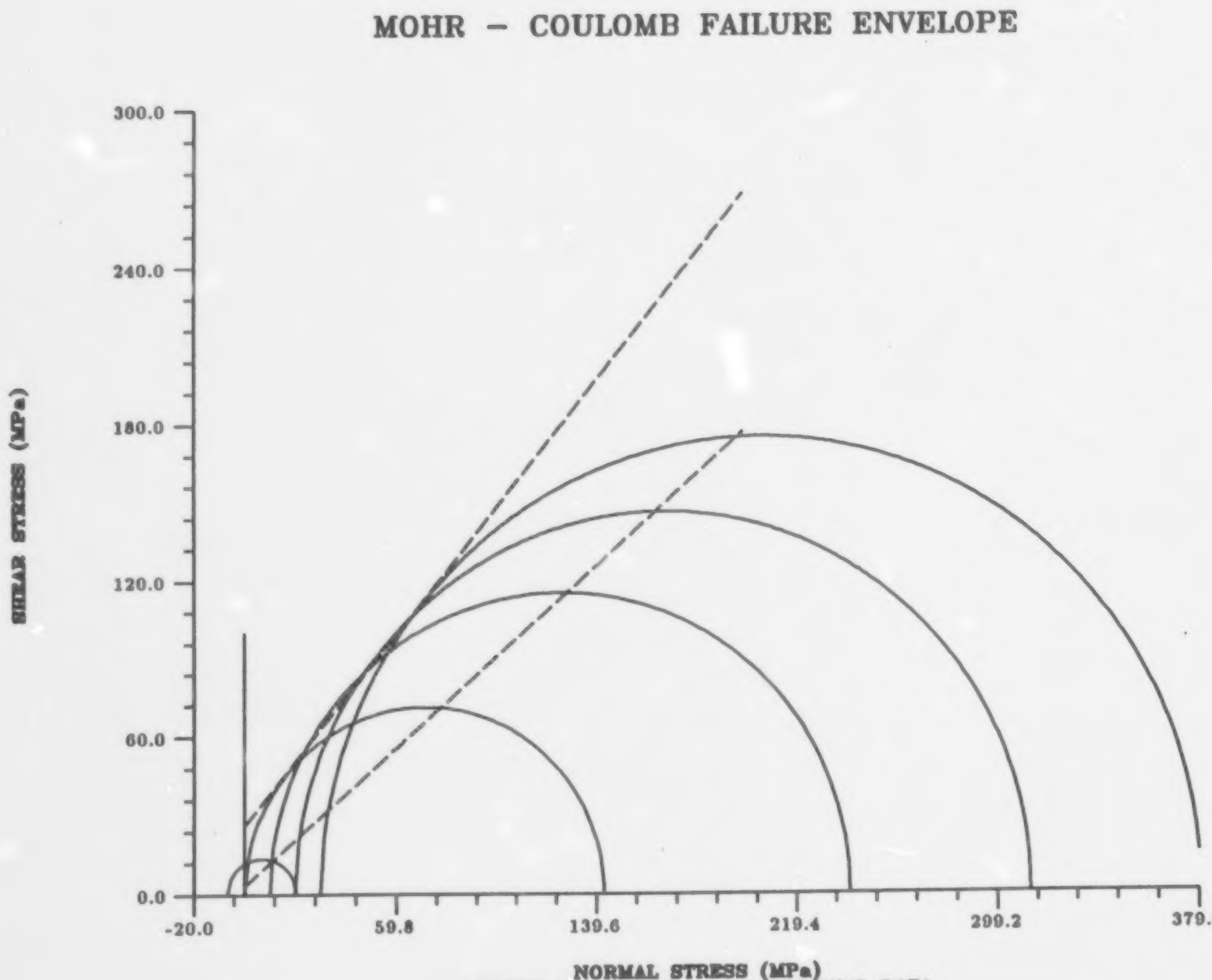

Fig. 55 NEPEAN SANDSTONE - ALL RESIDUAL DATA
CIRCUMFERENTIAL DISPLACEMENT CONTROL MULTI STAGE TRIAXIAL

Mechanically, Nepean sandstone has a mean tensile strength of -6.82 MPa. The mean ultimate uniaxial strength was calculated to be 145.78 MPa based on both test control methods. The mean Young's modulus was 39.24 GPa and the mean Poisson's ratio was calculated to be 0.50. Triaxially, Young's modulus and the triaxial strength increased with increasing confinement pressure while Poisson's ratio decreased. Regardless of test type, strengths decreased with decreasing bulk density. Peak strengths were marginally less for circumferential control tests over those conducted in load control.

Using Hoek and Brown failure envelope analyses, m and s were calculated to be 24.43 and 1.0 respectively for intact specimens. For residual analyses, m_r and s_r were calculated to be 4.17 and 0.00 respectively. The analyses confirmed the actual failure envelopes to be curved and not linear as assumed in Mohr-Coulomb analyses. The Hoek and Brown method confirmed that the failure angle decreases with increasing confinement pressure according to theory and as confirmed by actual measurements. The Mohr-Coulomb method results in a constant failure angle, (Table 9). The angle of internal friction of the Nepean sandstone ranged between 45 and 60 degrees depending on the level of confinement pressure.

Sufficient data has been compiled in this study on Nepean sandstone for it to be included in a national rock property data base file. The organization of such a data base file was not the object of this study. This study tried to present a systematic method of determining the mechanical properties of a rock substance while at the same time ensuring the rock material was adequately described and analysed from a geologic standpoint. Further to this, engineering failure criteria has been determined using two different failure theories and in this regard it is proposed to use the superior Hoek and Brown method instead of the Mohr-Coulomb method. Both load control and circumferential control tests methods were used in determining the rock material strength properties. Of these two methods it is proposed that the circumferential strain control multi-stage triaxial test method be used in subsequent rock property tests. This test method requires less tests while at the same time allowing the residual strength rock properties to be determined. The Brazilian test method of determining the tensile strength of a rock substance was found to be questionable as uniaxial to tensile strength ratios of 20:1 were calculated. According to Hoek and Brown (1980) a ratio of 8:1 is realistic. Based on the test results in this report it is recommended that Brazilian tensile strengths not be used when undertaking failure envelope analyses. Further to this, high Hoek and Brown m values should be used with caution as they do not necessarily equate to stronger intact rock. The m value should only be used for conditions within the intervals of the test confinement pressures used and in concert with the actual uniaxial strength of the rock material. The results should also be corrected for any confirmed subsequent anisotropy relative to the orientation of the anticipated stress field.

10. REFERENCES

1. Balmer, G. (1952): "A general analytical solution for Mohr's envelope", Amer. Soc. Testing Materials, Vol. 52, pp.1260-1271.

2. Belanger, J.R., Harrison, J.E. (1980): "Regional geoscience information: Ottawa-Hull", E.M.R, Geological Survey of Canada, Paper 77-11, 17p.

3. Brace, W.F. (1960): "Dependence of fracture strength of rocks on grain size", Proc. 4th Symp. Rock Mech., Univ. Park, Penn., pp.99-103.

4. Brown, E.T. (1981): "Rock characterization testing and monitoring", ISRM, Pergamon Press, London, England, 211p.

5. Gilbert, C.M. (1982): "Petrography, an introduction to the study of rocks in thin sections", 2nd. ed., W.H. Freeman and Company, San Francisco, Fig. 13.1, p.327.

6. Griffith, A.A. (1924): "Theory of Rupture", Proc. 1st Int. Cong. Applied Mech., pp.55-63.

7. Hawkes, I., Mellor, M. (1971): "Measurement of tensile strength of rock strength by diametral compression of discs and annuli", Eng. Geol., Vol. 5, pp.173-225.

8. Hewitt, D.F. (1964): "Building stones of Ontario", Ontario Department of Mines, Industrial Mineral Report No. 17, 57p.

9. Hoek, E., Brown, E.T. (1980): "Underground excavations in rock", Int. Min. Met., London, 527p.

10. Hoskins, J.R., Horino, F.G. (1969): "Influence of spherical head size and specimen diameters on the uniaxial compressive strength of rocks", U.S.B.M.R.I. 7234, 16p.

11. Houpert, R. (1970): "The uniaxial compressive strength of rocks", Proc. 2nd Cong. Int. Soc. Rock Mech., Belgrade, pp.49-55.

12. Hudson, J.A., Crouch, S.L., Fairhurst, C. (1971): "Soft, stiff and servo controlled testing machines", Dept. of Civil and Mineral Engineering, University of Minnesota, MTS 160.03-01, Minnesota, 23p.

13. Kovari, K., Tisa, A. (1975): "Multiple failure state and strain controlled triaxial tests", Rock Mechanics, Vol. 7, No. 1, Springer-Verlag, pp.17-33.

14. McClintock, F.A., Walsh, J.B. (1962): "Friction on Griffith cracks in rocks under pressure", Int. Cong. on Applied Mech., Berkeley, pp.1015-1021.

15. Mogi, P. (1962): "The influence of the dimensions of specimens on the fracture strength of rocks", Bull. Earthquake Res. Inst., Tokyo Univ., Vol. 40, pp.175-185.

16. Paul, G., Gangal, M. (1966): "Initial and subsequent fracture curves for biaxial compression of brittle materials", Proc. 8th Symp. Rock Mech., Minneapolis, Minn., pp.113-141.

17. Price, N.J. (1960): "The compressive strength of coal measure rocks", Coll. Eng., Vol. 37, pp.283-292.

18. Serafim, J.L. (1968): "Influence of insterstitial water on the behaviour of rock masses", Rock Mechanics in Engineering Practice, K.G. Stagg and O.C. Zienkiewicz, London, Wiley, pp.55-97.

19. Simmons, G., Cooper, H.W. (1978): "Thermal cycling cracks in three igneous rocks", Int. J. Rock Mech. Min. Sci. & Geomech., Abstract, Vol. 15, Pergamon Press, pp.145-148.

20. Travis, R.B. (1955): "Classification of rocks", Colorado School of Mines, Quarterly, Vol. 50, No. 1, 98p.

21. Wilson, A.E. (1956): "A guide to the geology of the Ottawa district", The Canadian Field Naturalist, Monograph, Vol. 70, No. 1, 68p.

APPENDIX A

Uniaxial tests - load control

APPENDIX A-1

Stress vs. strain - axial strain gauges

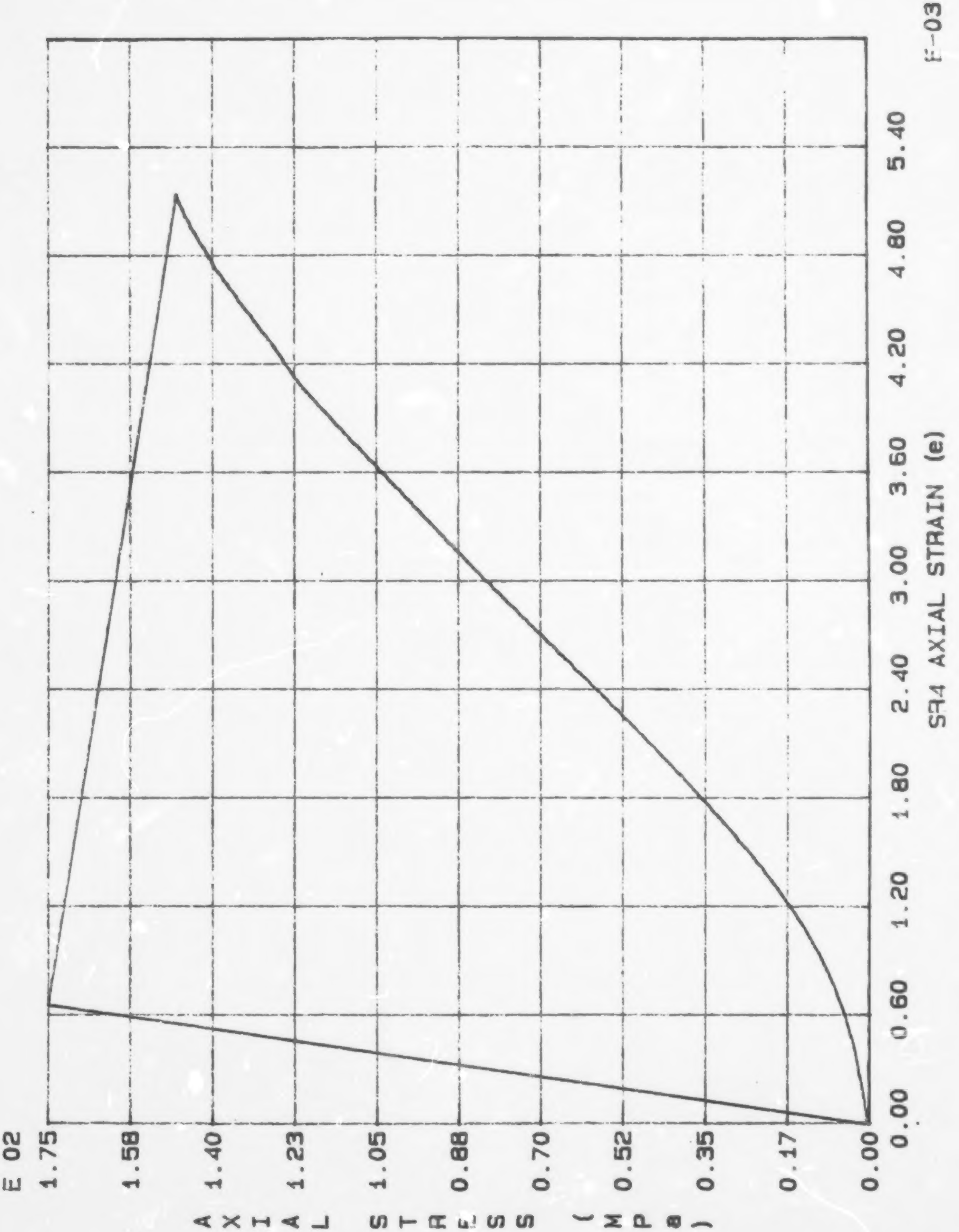
E 02
1.75
1.58
1.40
1.23
1.05
0.88
0.70
0.52
0.35
0.17
0.00
AXIAL STRESS (MPa)
0.00
0.60
1.20
1.80
2.40
3.00
3.60
4.20
4.80
5.40
E-03
SR4 AXIAL STRAIN (e)
N1

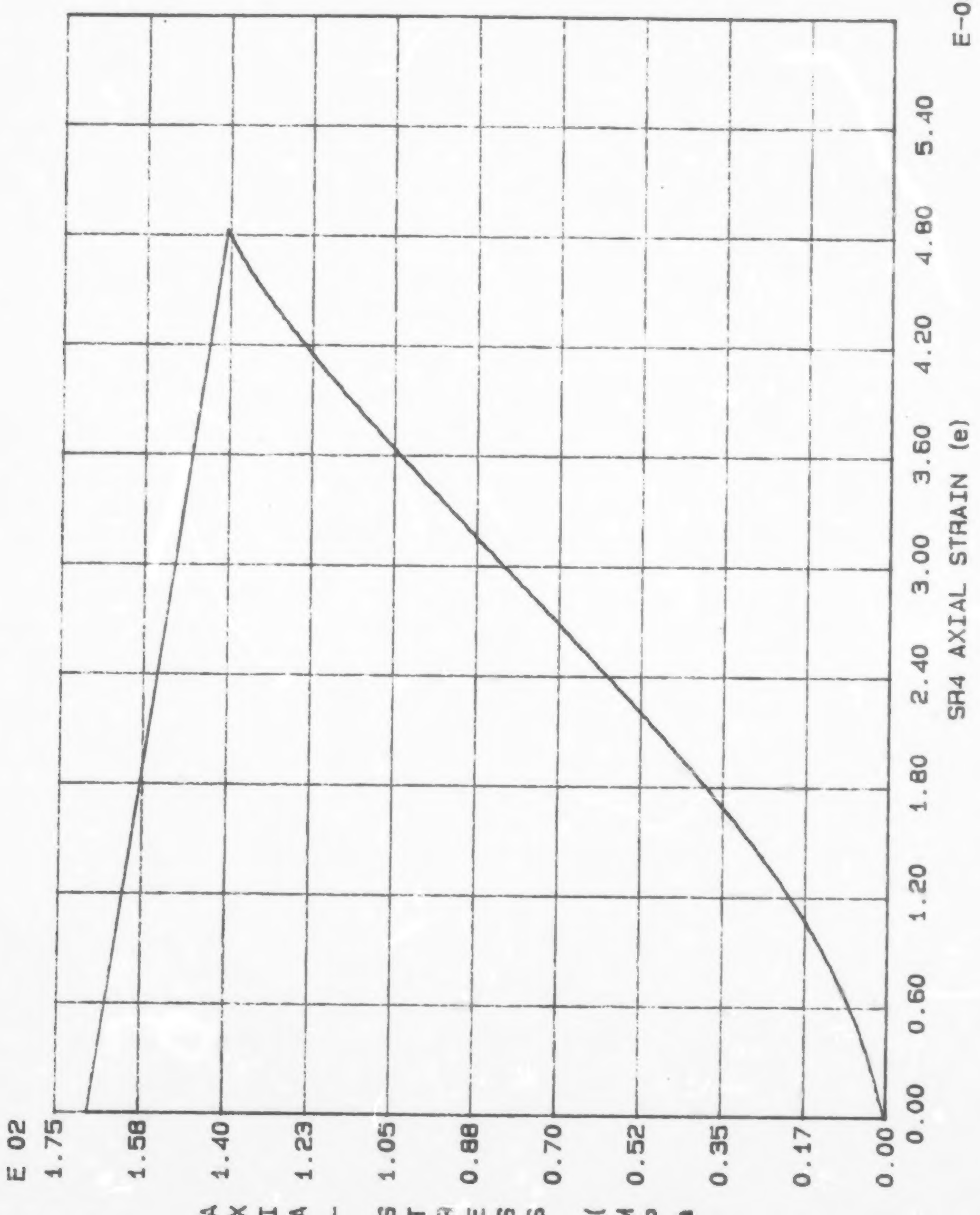
E-03
0.00
0.60
1.20
1.80
2.40
3.00
3.60
4.20
4.80
5.40
SR4 AXIAL STRAIN (e)
N2
E 02
1.75
1.58
1.40
1.23
1.05
0.88
0.70
0.52
0.35
0.17
0.00
AXIAL STRESS

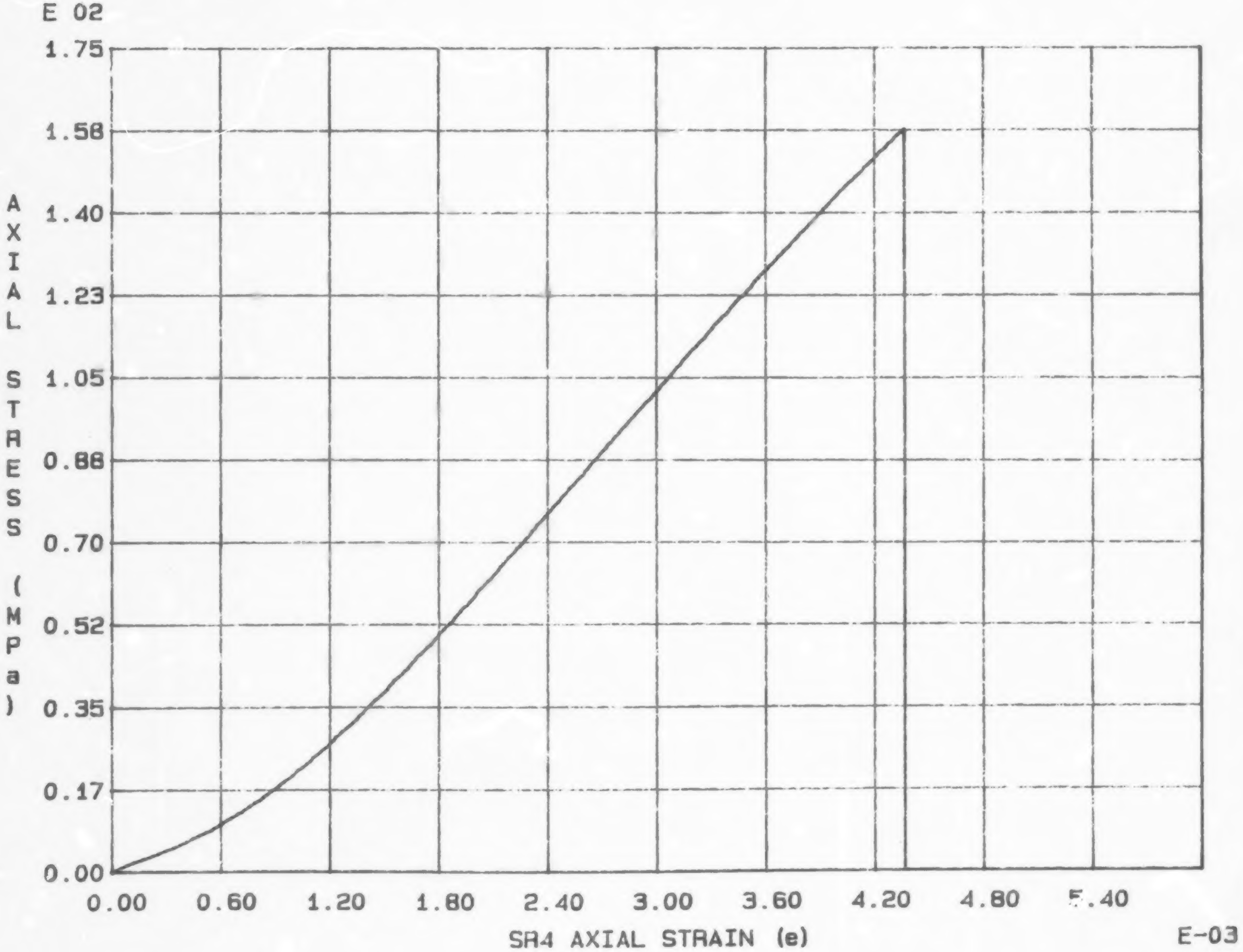
E 02
1.75
1.58
1.40
1.23
1.05
0.88
0.70
0.52
0.35
0.17
0.00
AXIAL STRESS (MPa)
0.00
0.60
1.20
1.80
2.40
3.00
3.60
4.20
4.80
5.40
SR4 AXIAL STRAIN (e)
E-03

N3

APPENDIX A-2

Stress vs. strain - circumferential strain gauges

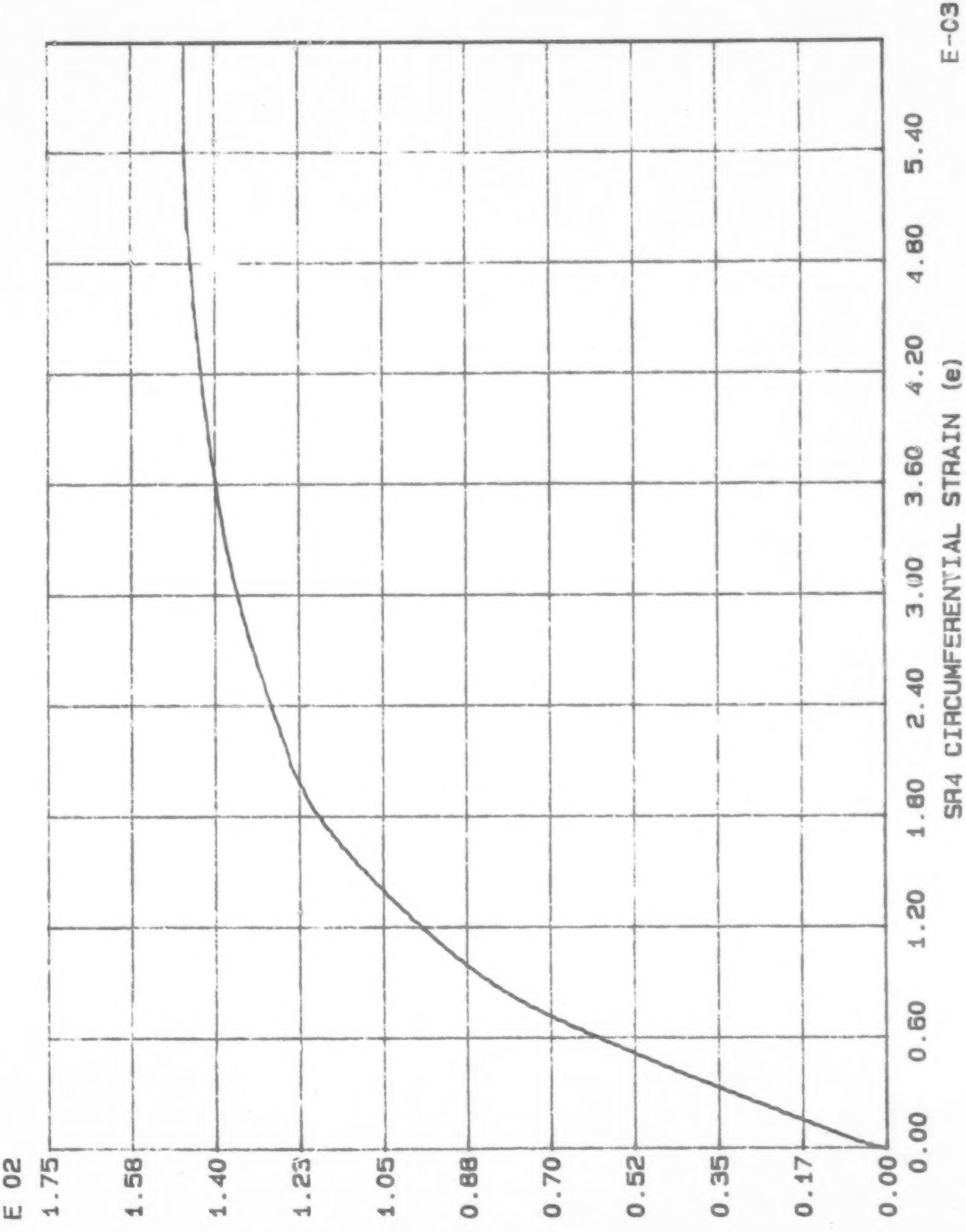
E 02
1.75
1.58
1.40
1.23
1.05
0.88
0.70
0.52
0.35
0.17
0.00
AXIAL STRESS (MPa)
0.00
0.60
1.20
1.80
2.40
3.00
3.60
4.20
4.80
5.40
E-03
SR4 CIRCUMFERENTIAL STRAIN (e)
N1

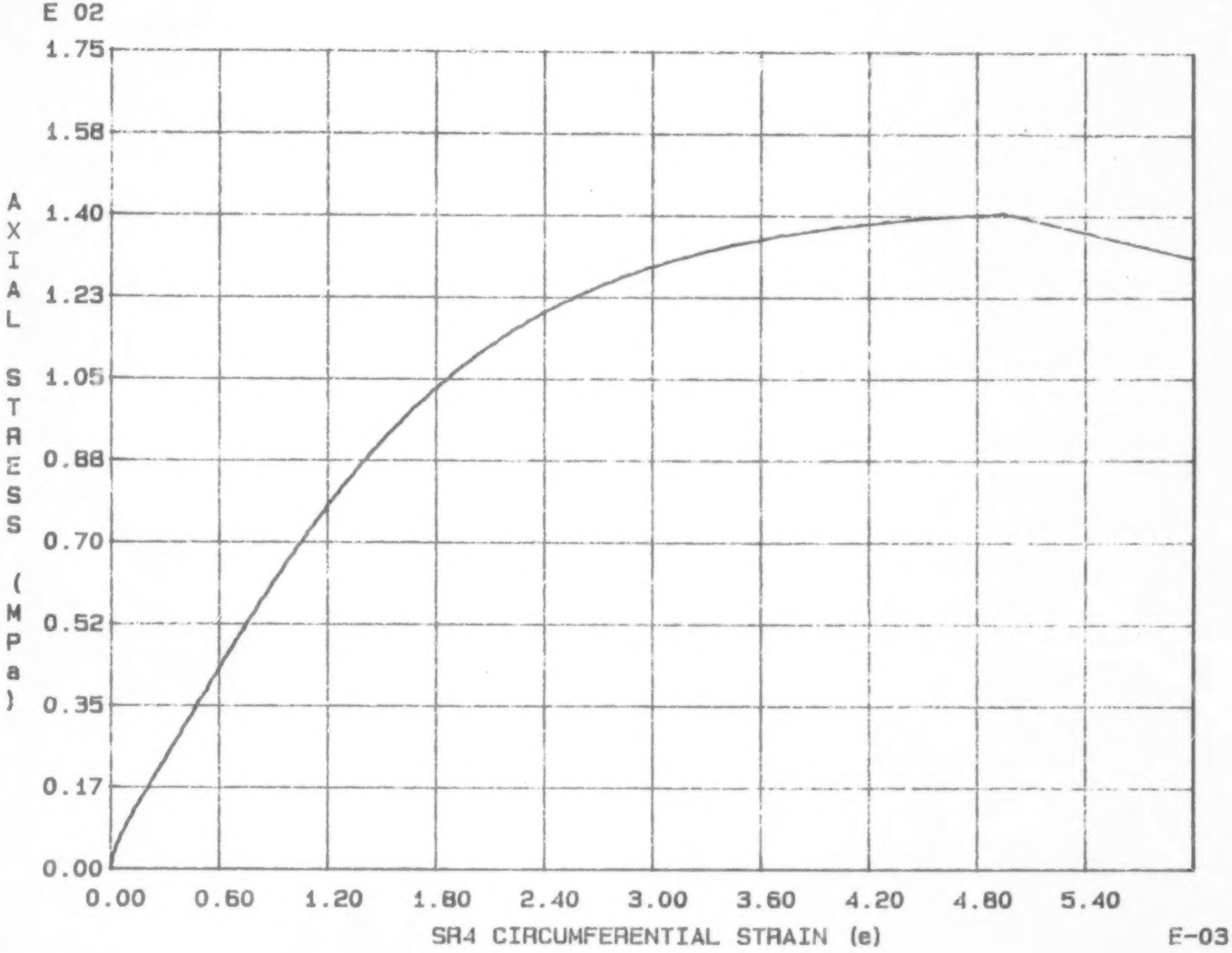
E 02
AXIAL STRESS (MPa)
1.75
1.58
1.40
1.23
1.05
0.88
0.70
0.52
0.35
0.17
0.00
0.00
0.60
1.20
1.80
2.40
3.00
3.60
4.20
4.80
5.40
SR4 CIRCUMFERENTIAL STRAIN (e)
E-03

N2

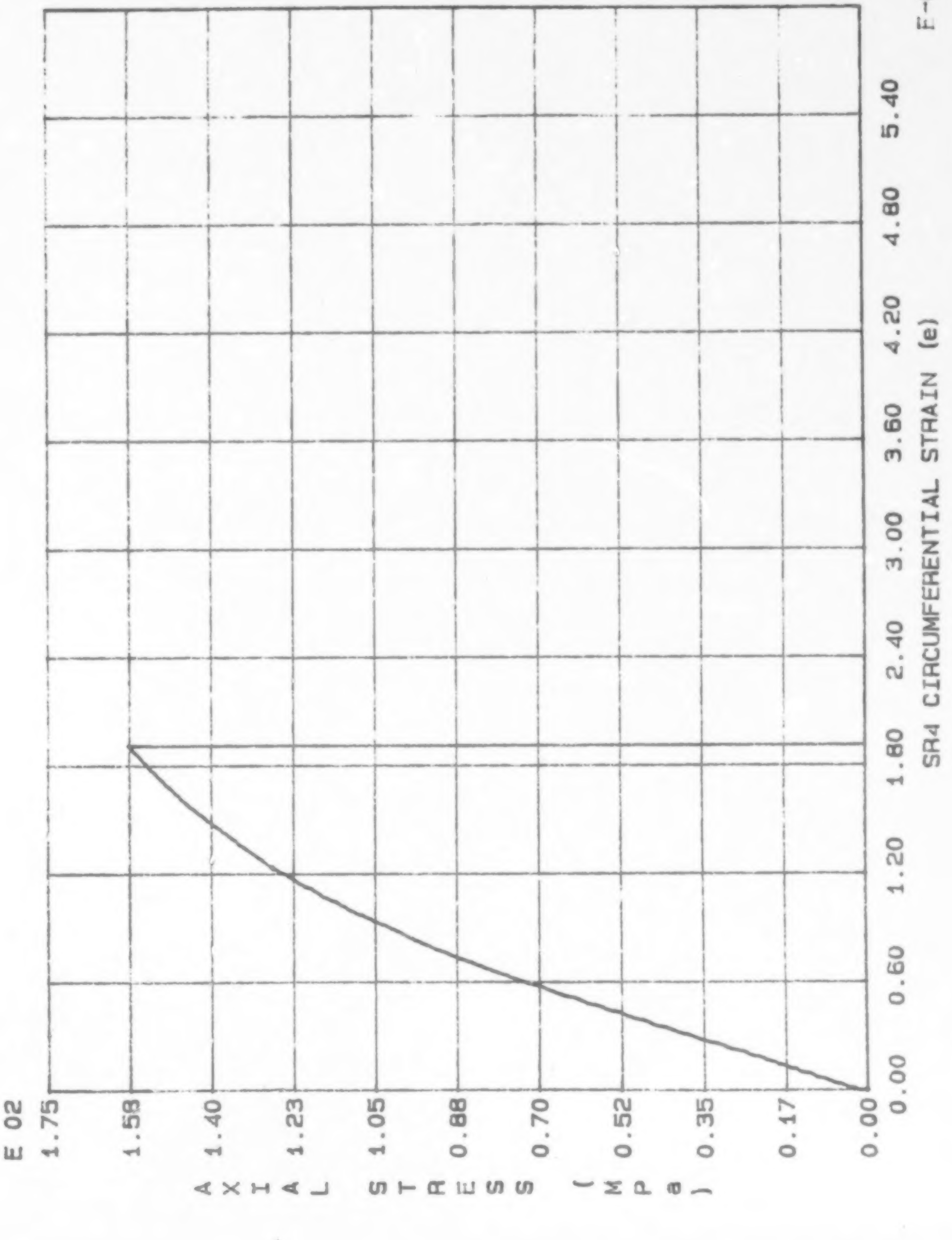
E 02
1.75
1.58
1.40
1.23
1.05
0.88
0.70
0.52
0.35
0.17
0.00
AXIAL STRESS (MPa)
0.00
0.60
1.20
1.80
2.40
3.00
3.60
4.20
4.80
5.40
E-03
SR4 CIRCUMFERENTIAL STRAIN (e)

N3

APPENDIX A-3

Lpost.bas - MTS Basic

```
90 FATALERROR( LINE 5500 )
100 KBINT('B',7, LINE 5500 )
200 KBENB('B')
300 KBINT('A',6, LINE 4200 )
400 KBENB('A')
500 PRINT 'PRESS <ESC> A TO SWITCH TO STRAIN MODE'
600 PRINT 'PRESS <ESC> B TO END TEST'
700 PRINT 'THIS IS A COMPUTER CONTROLLED PROGRAM FOR POST FAILURE UNIAXIAL
TESTS.'
800 PRINT '7 CHANNELS ARE SCANNED:LOAD(CH1),STRAIN(CH2),STROKE(CH3),
STROKE(CH14)'
900 PRINT 'STROKE(CH15),SR4 AXIAL STRAIN(CH8) AND SR4 DIAM STRAIN(CH16).'
1000 PRINT 'STEP1: IN LOAD MODE AT 1 kN/SEC.'
1100 PRINT 'STEP2:IN STRAIN MODE 0-3.81mm IN 50min MAX OR 5kN MIN.'
1200 PRINT 'DATA FROM 7 CHANNELS STORED IN DAT FILE IN 0-1 UNITS OF FULL
RANGE.'
1300 PRINT 'DATA SAMPLED EVERY 1 SECOND'
1400 PRINT 'INPUT LOAD RANGE IN kN'; \ INPUT U
1500 IF U=2500 THEN R=1
1600 IF U=1250 THEN R=2
1700 IF U=500 THEN R=3
1800 IF U=250 THEN R=4
1900 A4=0 \ A5=0 \ A6=0
2000 C0=0 \ C1=0 \ C2=0 \ C3=0 \ C4=0 \ C5=0 \ C6=0 \ C7=0
2100 D4=0 \ D5=0 \ D6=0 \ D7=0
2200 E1=0 \ E2=0 \ E3=0 \ E4=0 \ E5=0
2300 K1=0 \ K2=0 \ K3=0
2400 L0=0 \ L1=0 \ L2=0 \ L3=0 \ L4=0 \ L5=0 \ L6=0 \ L7=0 \ L8=0
2500 S0=0 \ S1=0 \ S2=0 \ S3=0 \ S4=0 \ S5=0 \ S6=0
2520 T1=0 \ T2=0 \ T3=0 \ T4=0 \ T5=0 \ T6=0 \ T7=0
2550 V1=0 \ V2=0 \ V3=0 \ V4=0 \ V5=0 \ V6=0
2560 Y1=0 \ Y2=0 \ Y3=0 \ Y4=0 \ Y5=0 \ Y6=0
2600 CLREMOTESWITCH(1,1,R,0) \ FGSTEP(1,.05/U)
2650 PRINT 'ZERO LVs, CHAIN AND SR4s'
2660 PRINT 'INPUT 1=LOAD CONTROL OR 2=STRAIN CONTROL'; \ INPUT C7
2670 PRINT 'IF BRAZILIAN TEST THEN USE LOAD CONTROL AND RAM LVDT'
2700 PRINT 'PRESS <CR> TO START TEST IN LOAD MODE'; \ INPUT R$
2710 ADIMMED(1,Z1)
2720 B1=-.0167161
2730 B2=.0250557
2740 B3=.0286087
2750 M1=2.90069E-04
2760 M2=2.69138E-04
2770 M3=2.05556E-04
2780 F1=Z1*U*M1+B1
2790 F2=Z1*U*M2+B2
2795 F3=Z1*U*M3+B3
2800 SETDIM VA1(9600,7)
2900 CKTIME(1,.1)
3000 ADTIMED(1,VA1,,1,30,2,3)
3100 ADSLAVE(1,14,15,8,16)
3200 ADINIT
3300 PRINT 'PRESS <CR> TO START LOADING'; \ INPUT R$
3400 FGREAD(1,F)
3500 FGRAMP(1,U,F+1)
3600 ADGO
3700 FGGO
3720 IF C7=1 THEN 4800
3800 ADIMMED(1,C) \ ADIMMED(2,Z) \ IF Z>5.00000E-03 THEN L7=C
\ IF Z>5.00000E-03 THEN 4200
3810 ADIMMED(3,Y1)
3820 ADIMMED(14,Y2)
3830 ADIMMED(15,Y3)
3900 FGSTATUS(1,K) \ IF K<1 THEN 4200
4000 IF C<0 THEN 5500
4100 IF C>0 THEN 3800
```

```
4200 B=4.00000E-03
4250 FGSTOP \ ADIMMED(1,Z) \ FGSTEP(1,Z*.8)
4300 PRINT 'PRESS <CR> TO SWITCH TO STRAIN MODE'; \ INPUT R$
4400 ADIMMED(2,Z) \ CLSWITCH(1,2,1,0) \ FGSTEP(1,Z)
4500 PRINT 'PRESS <CR> TO START TEST IN STRAIN MODE'; \ INPUT R$
4550 FGREAD(1,Y)
4600 FGRAMP(1,3000,Y+.24)
4610 FGGO
4650 Z9=.22
4800 ADIMMED(1,C)
4810 ADIMMED(2,Z)
4820 ADIMMED(3,X)
4830 ADIMMED(8,Y)
4840 ADIMMED(14,T4)
4845 ADIMMED(15,T5)
4848 IF Z>.95 THEN 5500
4849 IF Z>Z9 THEN 5450
4850 IF C<L0 THEN 5200
4900 L0=C
5100 S0=X
5110 L8=Y*(-2)
5120 T6=T4
5130 T7=T5
5200 FGSTATUS(1,K) \ IF K<1 THEN 5500
5300 IF C<-1/U THEN 5500
5320 IF C7=1 THEN 4800
5400 IF Z<.95 THEN 4800
5450 FGSTOP(1)
5452 FGREAD(1,Y)
5454 FGRAMP(1,3000,Y+.7)
5456 FGGO(1)
5458 Z9=2
5460 GO TO 4800
5500 FGSTOP \ ADSTOP
5600 PRINT 'ENTER FILE NAME FOR STORAGE'; \ INPUT F$
5700 OPEN 'DU0:'+F$+'.DAT' FOR OUTPUT AS FILE #1, FILESIZE 2000
5800 PRINT #1:VA1
5900 FOR I=0 TO VA1
6100 PRINT #1:ELEVEL(VA1(I,1))
6110 PRINT #1:ELEVEL(VA1(I,2))
6112 PRINT #1:ELEVEL(VA1(I,3))
6114 PRINT #1:ELEVEL(VA1(I,4))
6116 PRINT #1:ELEVEL(VA1(I,5))
6118 PRINT #1:ELEVEL(VA1(I,6))
6120 PRINT #1:ELEVEL(VA1(I,7))
6122 NEXT I
6200 CLOSE
6250 FATALERROR( LINE 6400 )
6300 CLLOCALSWITCH(1)
6400 SETDIM VA2(9600,7)
6500 PRINT 'ENTER SAMPLE LENGTH IN MM'; \ INPUT Q
6600 PRINT 'ENTER SAMPLE CIRCUMFERENCE IN MM'; \ INPUT R
6700 PRINT 'ENTER SAMPLE X-AREA IN CM SQUARED'; \ INPUT S
6800 PRINT 'ENTER LOAD FULL SCALE IN kN (CH1)'; \ INPUT C
6900 PRINT 'ENTER STRAIN FULL SCALE IN MM (CH2)'; \ INPUT K
7000 PRINT 'ENTER LV#1 FULL SCALE IN MM (CH3)'; \ INPUT D
7100 PRINT 'ENTER AXIAL SR4 STRAIN RANGE IN -STRAIN (CH8)'; \ INPUT L
7200 PRINT 'ENTER DIAM  SR4 STRAIN RANGE IN +STRAIN (CH16)'; \ INPUT M
7250 PRINT 'ENTER LV#2 FULL SCALE IN MM (CH14)'; \ INPUT T1
7300 PRINT 'ENTER LV#3 FULL SCALE IN MM (CH15)'; \ INPUT V
7400 PRINT 'LVs DISP CORRECTED FOR PLATEN COMPRESSION DISP'
7500 OPEN 'DU0:'+F$+'.DAT' FOR INPUT AS FILE #1, FILESIZE 2000
7600 OPEN 'DU0:'+F$+'U.DAT' FOR OUTPUT AS FILE #2, FILESIZE 2000
7700 PRINT 'OUTPUT FILE IS ';F$;'U.DAT'
7800 INPUT #1:A \ VA2=A
8455 L7=L7*C*10/S
```

```
8500 L1=L0*C*10/S
8600 L2=L1*.45
8700 L3=L1*.55
9660 S1=(S0*D-(M1*L0*C+B1)+F1)*100/Q
9662 T6=(T6*T1-(M2*L0*C+B2)+F2)*100/Q
9664 T7=(T7*V-(M2*L0*C+B3)+F3)*100/Q
9666 S1=(S1+T6+T7)/3
9700 FOR I=1 TO VA2
9800 INPUT #1:E \ E=E*C*10/S \ PRINT E;
10200 INPUT #1:J \ J=(J*K)/R \ PRINT J;
10300 INPUT #1:G \ G=(G*D-(M1*E*S/10+B1)+F1)/Q \ PRINT G;
10350 INPUT #1:T3 \ T3=(T3*T1-(M2*E*S/10+B2)+F2)/Q \ PRINT T3;
10400 INPUT #1:U \ U=(U*V-(M3*E*S/10+B3)+F3)/Q \ PRINT U;
10500 INPUT #1:W \ W=W*L \ PRINT W;
10600 INPUT #1:Y \ Y=Y*M \ PRINT Y
10604 IF K2=1 THEN 10700
10605 IF K1=1 THEN 10650
10606 IF K3=1 THEN 10610
10607 IF E>L7*.8 THEN D7=Y
10608 IF E>L7*.8 THEN L7=E
10609 IF L7=E THEN K3=1
10610 IF E>L2 THEN L4=E
10620 IF E>L2 THEN C4=J
10630 IF E>L2 THEN S4=(G+U+T3)/3
10635 IF E>L2 THEN A4=W
10640 IF E>L2 THEN D4=Y
10645 IF E>L2 THEN K1=1
10650 IF E>L3 THEN L5=E
10655 IF E>L3 THEN C5=J
10660 IF E>L3 THEN S5=(G+U+T3)/3
10665 IF E>L3 THEN A5=W
10670 IF E>L3 THEN D5=Y
10675 IF E>L3 THEN K2=1
10700 PRINT #2:E;J;G;T3;U;W;Y
10800 NEXT I
10900 CLOSE
11000 PRINT 'STRESS (MPa), CIRCUM (e), LV#1 (e), LV#2 (e), LV#3 (e),
SR4-A (e), SR4-C (e)'
11005 L6=L5-L4
11010 C6=C5-C4
11015 S6=S5-S4
11020 A6=A5-A4
11025 D6=D5-D4
11030 E1=L6/A6/1000
11035 E2=L6/D6/1000
11036 E3=L4/D4/1000
11037 E4=L6/S6/1000
11038 E5=L7/D7/1000
11040 V1=E1/E2
11045 V2=E1/E3
11046 V3=E4/E2
11047 V4=E4/E3
11048 V5=E1/E5
11049 V6=E4/E5
11100 PRINT '----------------------------- Qu     = ';L1;' MPa'
11200 PRINT 'Average LVs----------------- e_peak = ';S1;' %'
11205 PRINT 'SR4-A----------------------- e_peak = ';L8;' %'
11210 PRINT 'Slope 3 using         SR4-A--- E      = ';E1;' GPa'
11212 PRINT 'Slope 3 using         LVs----- E      = ';E4;' GPa'
11215 PRINT 'Slope 3 using SR4-A & SR4-C--- v      = ';V1
11216 PRINT 'Slope 2 using SR4-A & SR4-C--- v      = ';V2
11217 PRINT 'Slope 3 using LVs   & SR4-C--- v      = ';V3
11218 PRINT 'Slope 2 using LVs   & SR4-C--- v      = ';V4
11219 PRINT 'Slope 1 using SR4-A & SR4-C--- v      = ';V5
11220 PRINT 'Slope 1 using LVs   & SR4-C--- v      = ';V6
11221 PRINT 'Slope 1 is SR4-C E_o modulus'
```

```
11222 PRINT 'Slope 2 is SR4-C 0.5Qu secant modulus'
11223 PRINT 'Slope 3 is SR4-C 0.5Qu tangent modulus'
11300 END
```

APPENDIX A-4

Uplot.bas - MTS Basic

```
50 KBINT('A',7, LINE 7200 )
60 KBENB
100 SETDIM VA2(9600,7)
200 PRINT 'INPUT RAWDATA FILE NAME'; \ INPUT F$
300 PRINT 'ENTER SAMPLE LENGTH IN MM'; \ INPUT Q
400 PRINT 'ENTER SAMPLE CIRCUMFERENCE IN MM'; \ INPUT R
500 PRINT 'ENTER SAMPLE X-AREA IN CM SQUARED'; \ INPUT S
600 PRINT 'ENTER LOAD FULL SCALE IN kN (CH1)'; \ INPUT C
700 PRINT 'ENTER STRAIN FULL SCALE IN MM (CH2)'; \ INPUT K
800 PRINT 'ENTER LV#1 FULL SCALE IN MM (CH3)'; \ INPUT D
900 PRINT 'ENTER AXIAL SR4 STRAIN RANGE IN -STRAIN (CH8)'; \ INPUT L
1000 PRINT 'ENTER DIAM SR4 STRAIN RANGE IN +STRAIN (CH16)'; \ INPUT M
1100 PRINT 'ENTER LV#2 FULL SCALE IN MM (CH14)'; \ INPUT T1
1200 PRINT 'ENTER LV#3 FULL SCALE IN MM (CH15)'; \ INPUT V
1300 PRINT 'LVs DISP CORRECTED FOR PLATEN COMPRESSION DISP'
1400 OPEN 'DU0:'+F$+'.DAT' FOR INPUT AS FILE #2, FILESIZE 2000
1500 PRINT
1600 S1=S
1700 INPUT #2:A \ VA2=A
1800 INPUT #2:Z1
1900 CLOSE
2000 OPEN 'DU0:'+F$+'.DAT' FOR INPUT AS FILE #1, FILESIZE 2000
2100 INPUT #1:A
2200 B1=-.0167161
2300 B2=.0250557
2400 B3=.0286087
2500 M1=.000290069
2600 M2=.000269138
2650 M3=.000205556
2700 E1=Z1*C*M1+B1
2800 E2=Z1*C*M2+B3
2900 E3=Z1*C*M3+B3
3400 PRINT 'INPUT Y MAX SCALE IN STRESS (MPa)'; \ INPUT Y1
3500 Y2=Y1/10
3600 PRINT 'INPUT 1,2,3,4,5,6 OR 7 FOR STRESS VS LV1,CHAIN,SRA,SRC,LV3
,LV2 OR LV_av'; \ INPUT S
3700 IF S=1 THEN A$='LV#1 AXIAL STRAIN (e)'
3800 IF S=2 THEN A$='CIRCUMFERENTIAL STRAIN (e)'
3900 IF S=3 THEN A$='SR4 AXIAL STRAIN (e)'
4000 IF S=4 THEN A$='SR4 CIRCUMFERENTIAL STRAIN (e)'
4100 IF S=5 THEN A$='LV#3 AXIAL STRAIN (e)'
4200 IF S=6 THEN A$='LV#2 AXIAL STRAIN (e)'
4300 IF S=7 THEN A$='LV_av AXIAL STRAIN (e)'
4400 PRINT 'INPUT X MAX SCALE IN STRAIN '; \ INPUT X1
4500 X2=X1/10
4600 PRINT 'INPUT X SCALE LEFT START IN STRAIN '; \ INPUT X3
4700 PRINT 'PRESS <CR> AFTER PLOT PAPER INSTALLED'; \ INPUT R1$
4800 GRATTACH(2,2) \ GRON(2) \ COLORLINE(2,1)
4900 PHYL(2,5,90,10,95) \ SCALE(2,0,X3,X1,0,Y1)
5000 LABEL(2,A$,'AXIAL STRESS (MPa)',X2,Y2,0)
5100 COLORLINE(2,4)
5200 INVEC(2)
5300 PLOT(2,0,H)
5400 FOR I=1 TO VA2
5500 INPUT #1:E \ E=E*C*10/S1
5800 INPUT #1:J \ J=(J*K)/R
5900 INPUT #1:G \ G=(G*D-(M1*E*S1/10+B1)+E1)/Q
6000 INPUT #1:T3 \ T3=(T3*T1-(M2*E*S1/10+B2)+E2)/Q
6100 INPUT #1:U \ U=(U*V-(M3*E*S1/10+B3)+E3)/Q
6200 INPUT #1:W \ W=W*L
6300 INPUT #1:Y \ Y=Y*M
6400 IF S=1 THEN PLOT(2,G,E)
6500 IF S=2 THEN PLOT(2,J,E)
6600 IF S=3 THEN PLOT(2,W,E)
6700 IF S=4 THEN PLOT(2,Y,E)
6800 IF S=5 THEN PLOT(2,U,E)
```

```
6900 IF S=6 THEN PLOT(2,T3,E)
7000 IF S=7 THEN PLOT(2,(T3+G+U)/3,E)
7100 NEXT I
7200 CLOSE
7300 IF S=1 THEN PLOT(2,G,0)
7400 IF S=2 THEN PLOT(2,J,0)
7500 IF S=3 THEN PLOT(2,W,0)
7600 IF S=4 THEN PLOT(2,Y,0)
7700 IF S=5 THEN PLOT(2,U,0)
7750 IF S=6 THEN PLOT(2,T3,0)
7760 IF S=7 THEN PLOT(2,(T3+G+U)/3,0)
7800 PLOT(2,X1,0)
7900 PLOT(2,X1,Y1)
8000 PLOT(2,X1,0)
8100 PLOT(2,0,0)
8200 VTMODE
8300 GRDETACH(2)
8400 PRINT 'DO YOU WISH MORE PLOTS  (Y/N) ?'; \ INPUT I$
8500 GRATTACH(2,2)
8600 GRON(2)
8700 COLORLINE(2,1)
8800 PHYL(2,5,95,5,95) \ SCALE(2,0,0,100,0,100)
8900 LABEL(2,F$,,100,100,3)
9000 VTMODE
9100 GRDETACH(2)
9200 OPEN 'DU0:'+F$+'.DAT' FOR INPUT AS FILE #1, FILESIZE 2000
9300 INPUT #1:A \ VA2=A
9400 IF I$='Y' THEN GO TO 3600
9500 CLOSE
9600 END
```

APPENDIX B

Uniaxial tests - circumferential control

APPENDIX B-1

Stress vs. strain - axial strain gauges

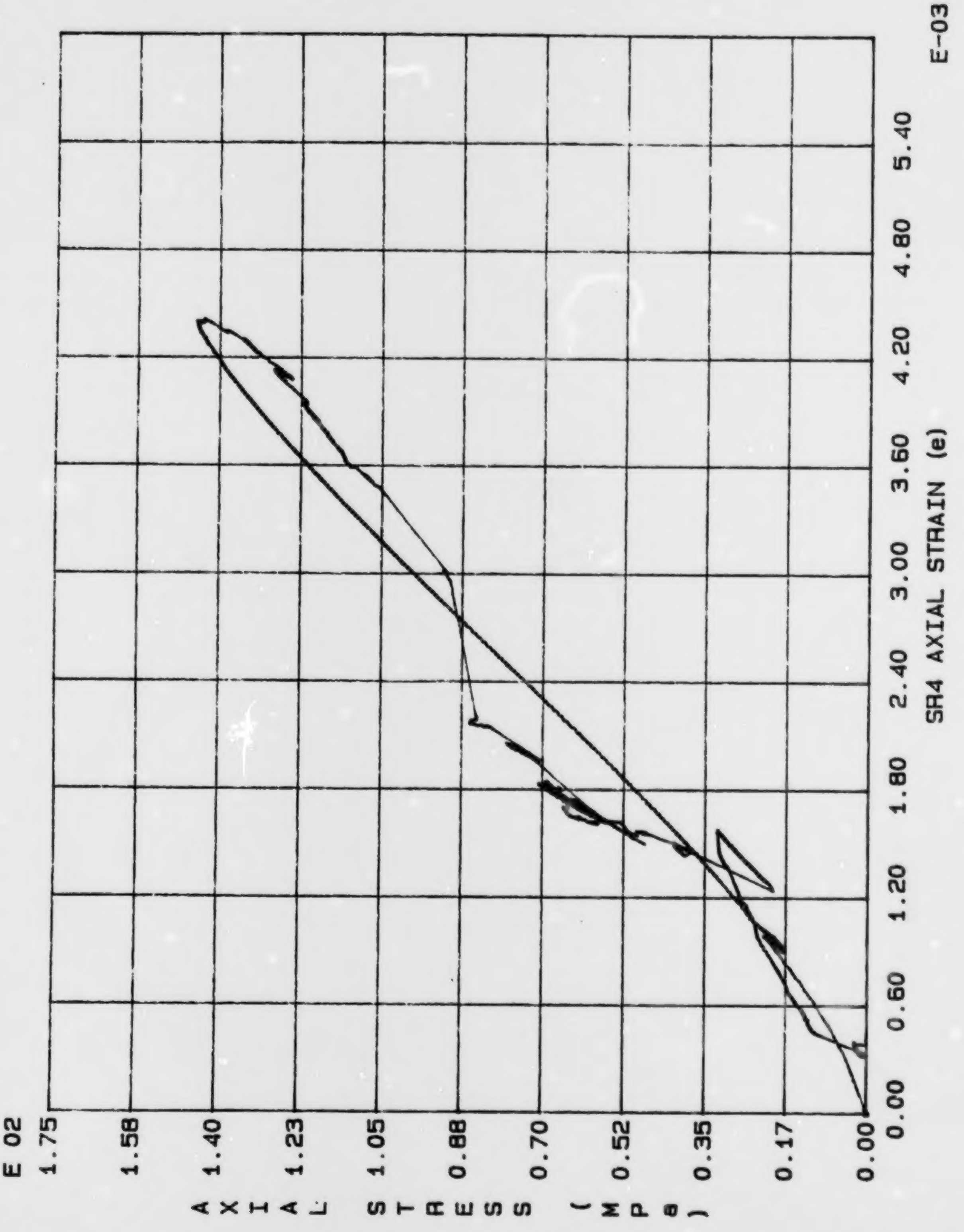
E 02
1.75
1.58
1.40
1.23
1.05
0.88
0.70
0.52
0.35
0.17
0.00
AXIAL STRESS (MPa)
0.00
0.60
1.20
1.80
2.40
3.00
3.60
4.20
4.80
5.40
E-03
SR4 AXIAL STRAIN (e)

N4

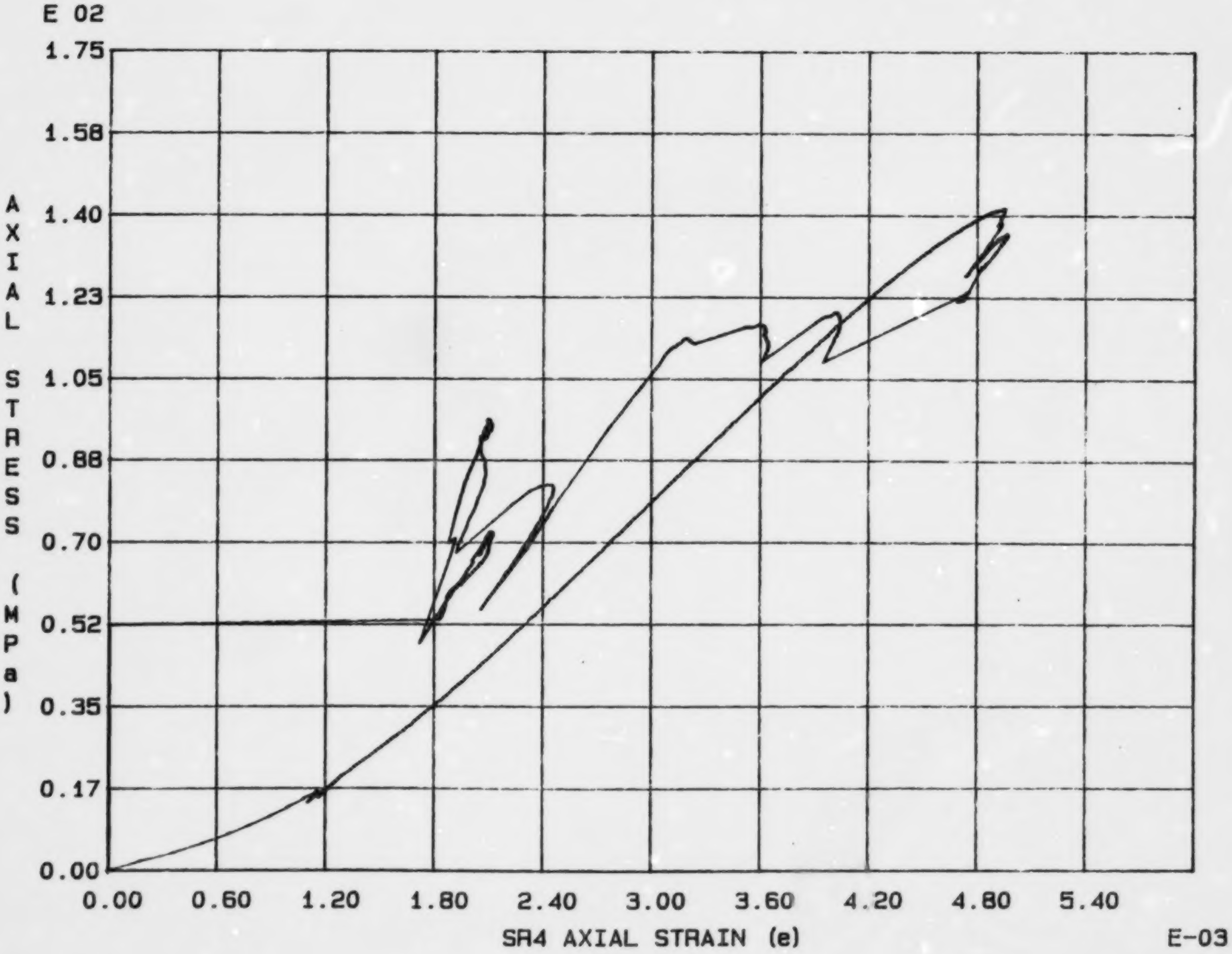
E 02
1.75
1.58
1.40
1.23
1.05
0.88
0.70
0.52
0.35
0.17
0.00
AXIAL STRESS (MPa)
0.00
0.60
1.20
1.80
2.40
3.00
3.60
4.20
4.80
5.40
SR4 AXIAL STRAIN (e)
E-03

N5

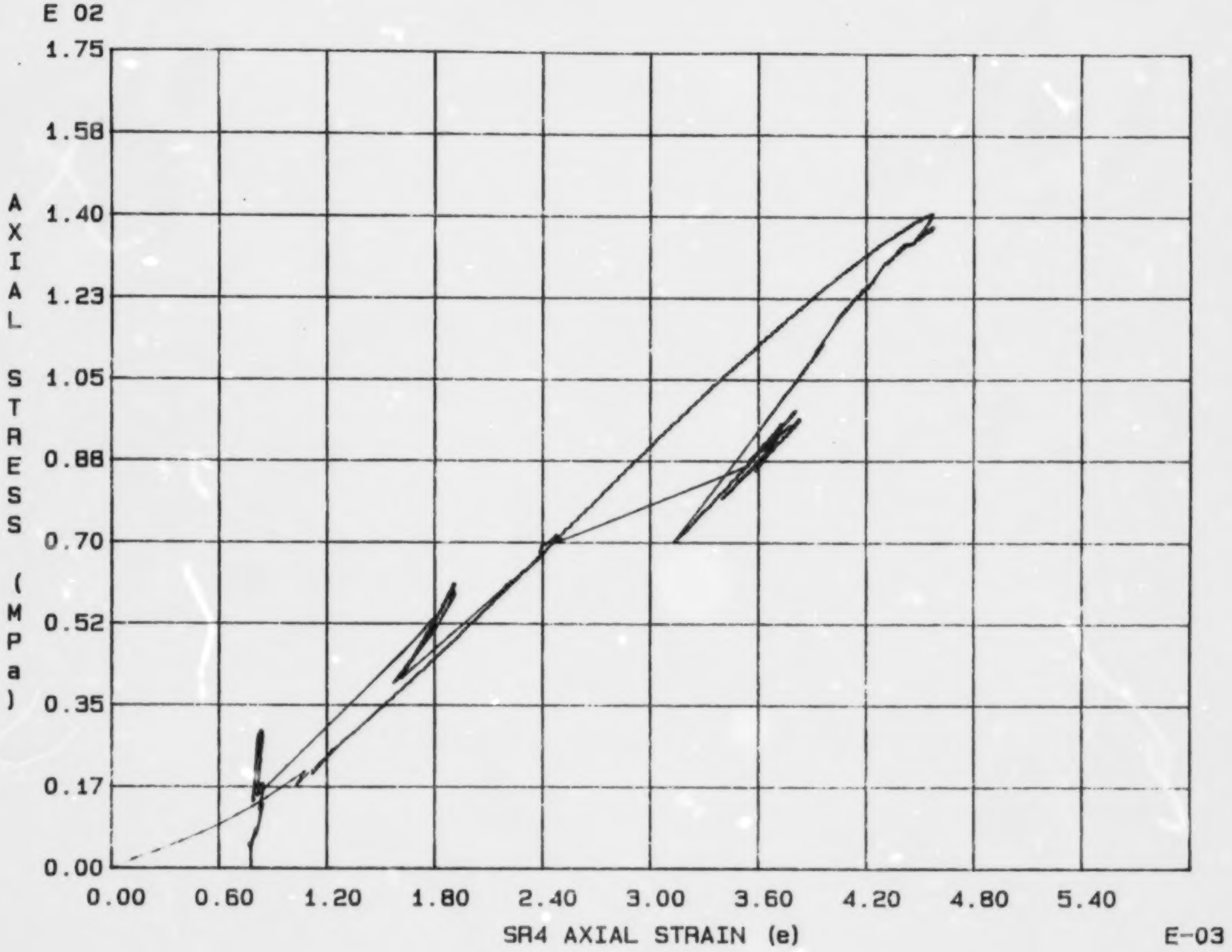
E 02
1.75
1.58
1.40
1.23
1.05
0.88
0.70
0.52
0.35
0.17
0.00
AXIAL STRESS (MPa)
0.00
0.60
1.20
1.80
2.40
3.00
3.60
4.20
4.80
5.40
SR4 AXIAL STRAIN (e)
E-03

N6

APPENDIX B-2

Stress vs. strain - axial lvdts

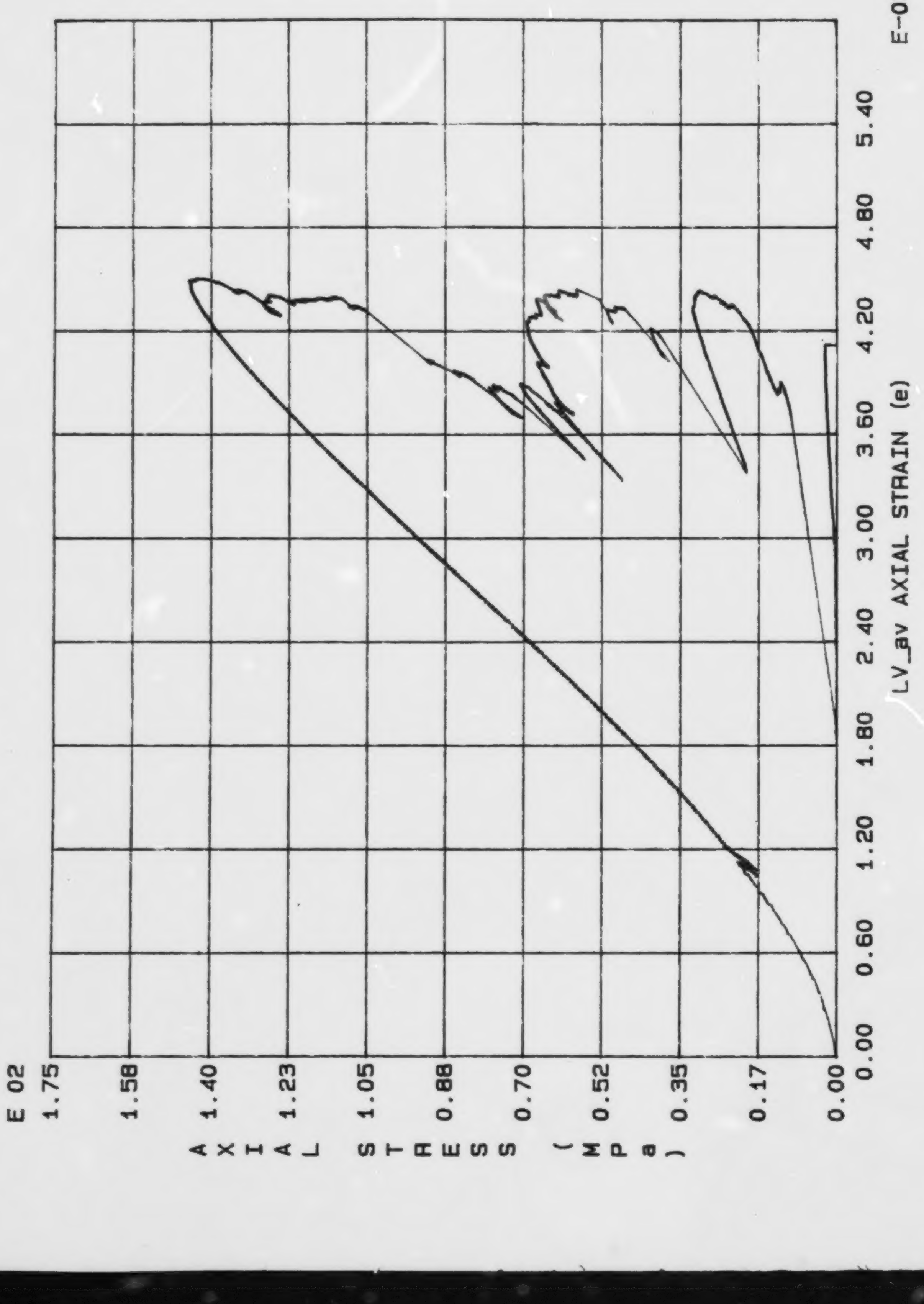
E 02
1.75
1.58
1.40
1.23
1.05
0.88
0.70
0.52
0.35
0.17
0.00
AXIAL STRESS (MPa)
0.00
0.60
1.20
1.80
2.40
3.00
3.60
4.20
4.80
5.40
E-03
LV_av AXIAL STRAIN (e)
N4

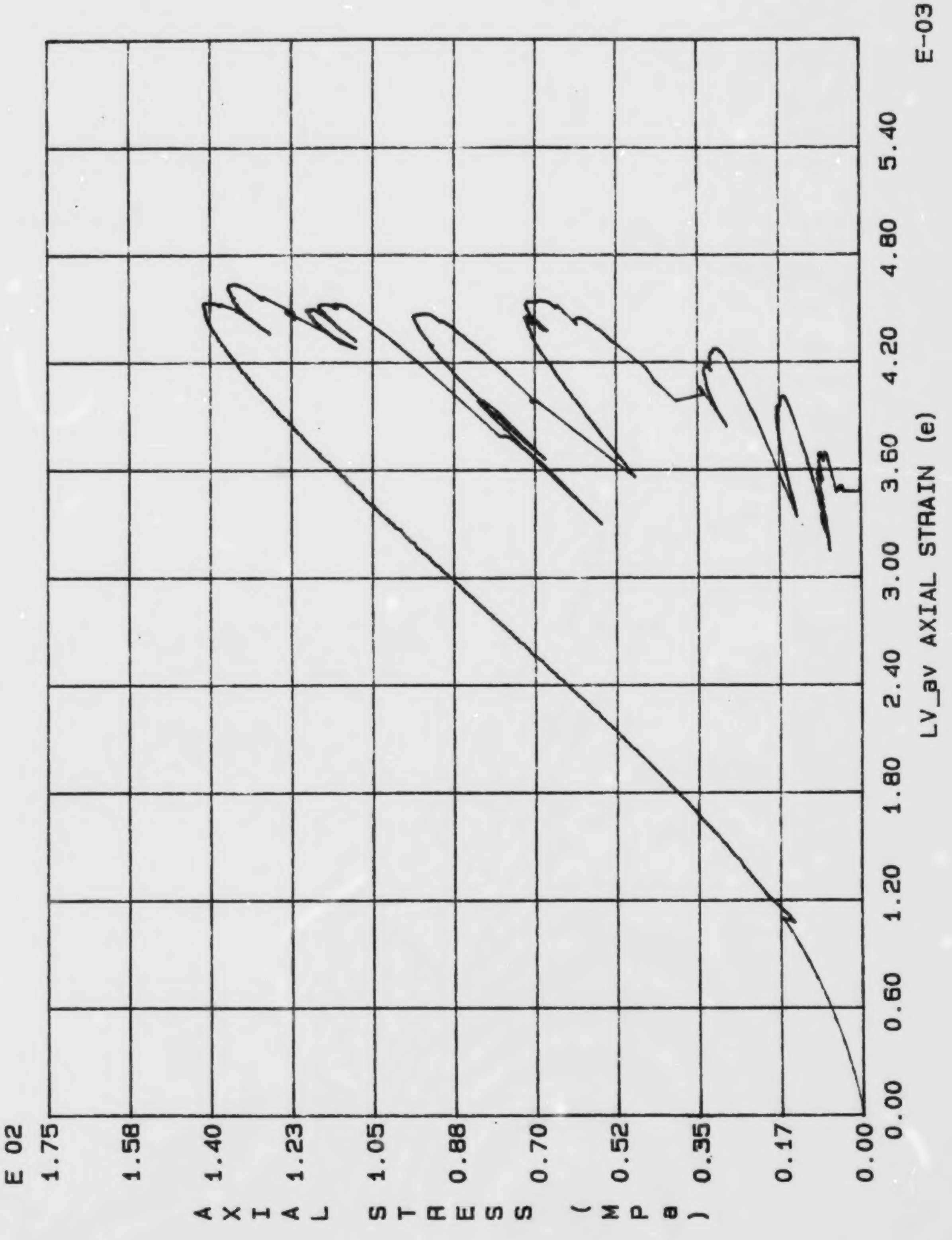
AXIAL STRESS (MPa)
E 02
1.75
1.58
1.40
1.23
1.05
0.88
0.70
0.52
0.35
0.17
0.00
0.00
0.60
1.20
1.80
2.40
3.00
3.60
4.20
4.80
5.40
E-03
LV_av AXIAL STRAIN (e)

N5

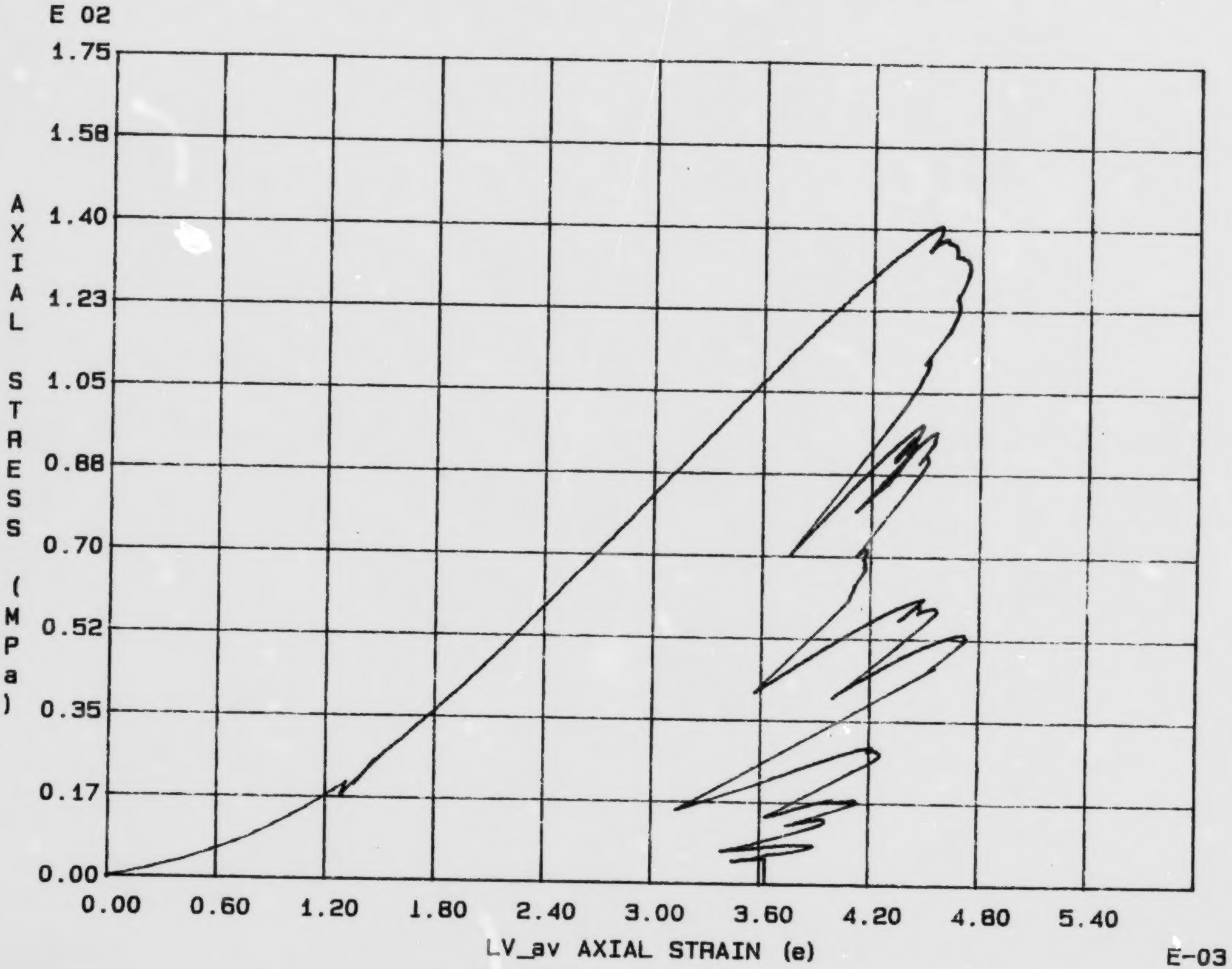
E 02
1.75
1.58
1.40
1.23
1.05
0.88
0.70
0.52
0.35
0.17
0.00
AXIAL STRESS (MPa)
0.00
0.60
1.20
1.80
2.40
3.00
3.60
4.20
4.80
5.40
LV_av AXIAL STRAIN (e)
E-03

N6

APPENDIX B-3

Stress vs. strain - circumferential strain gauges

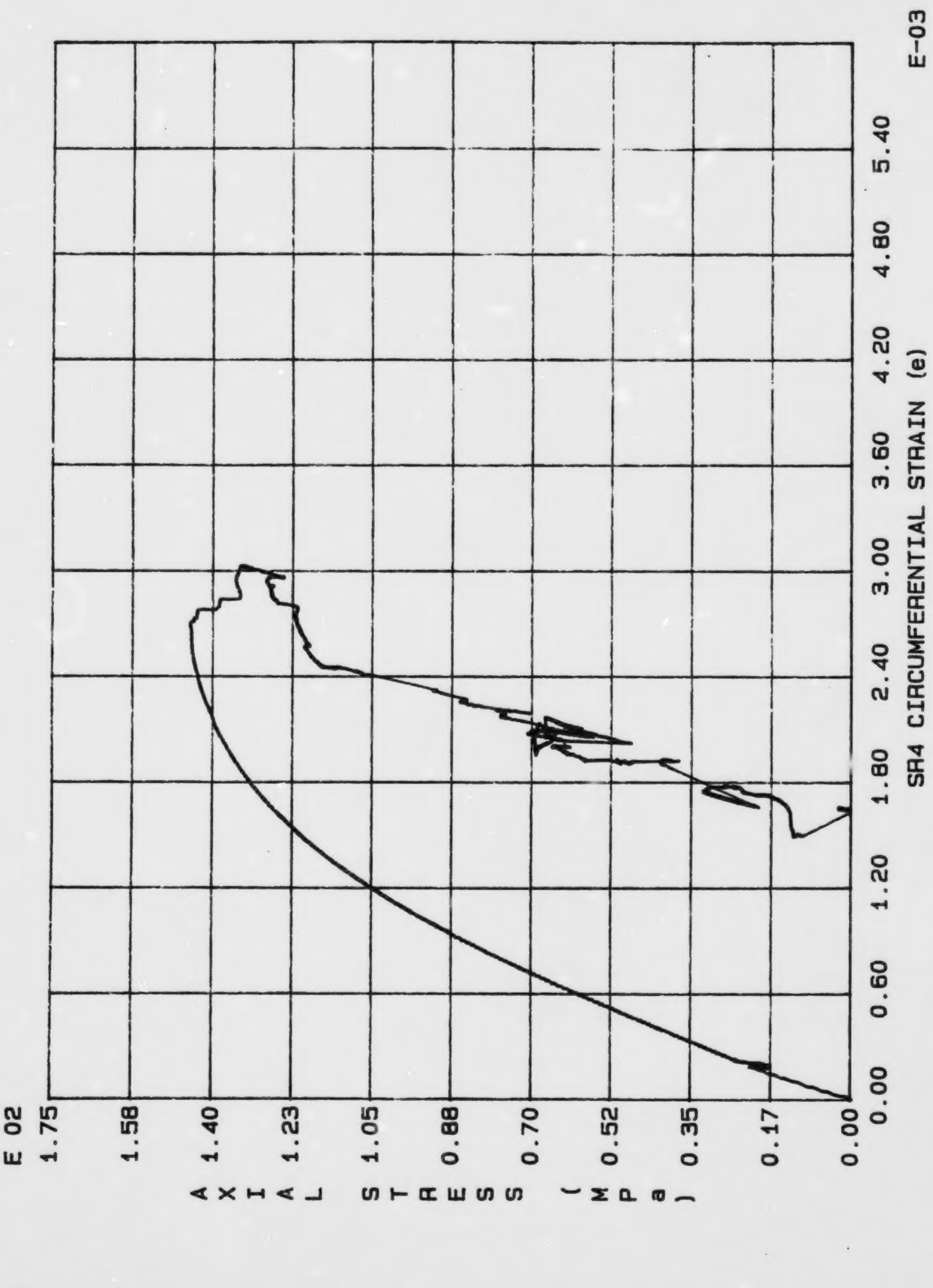
AXIAL STRESS (MPa)
E 02
1.75
1.58
1.40
1.23
1.05
0.88
0.70
0.52
0.35
0.17
0.00
0.00
0.60
1.20
1.80
2.40
3.00
3.60
4.20
4.80
5.40
E-03
SR4 CIRCUMFERENTIAL STRAIN (e)

N4

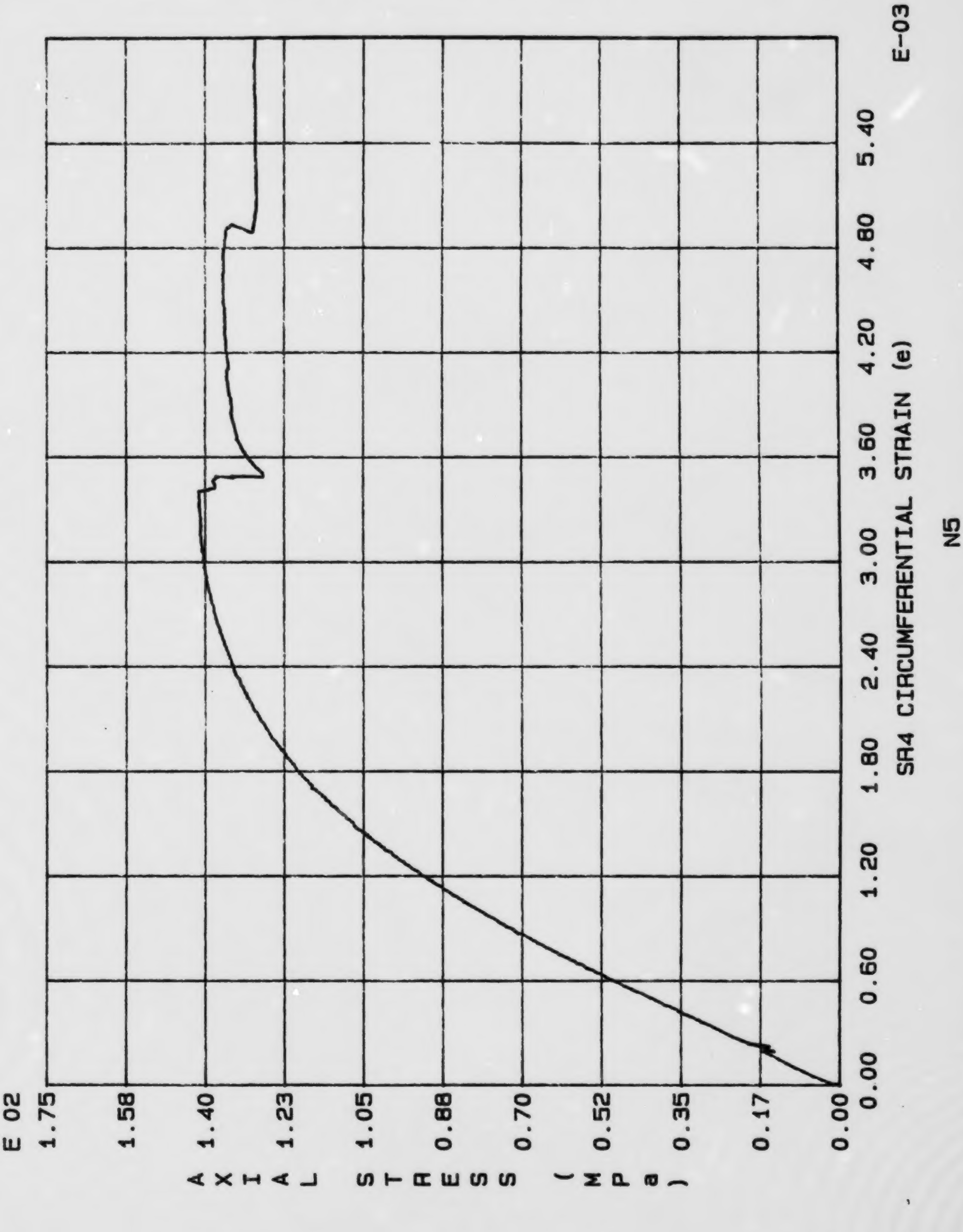
E 02
1.75
1.58
1.40
1.23
1.05
0.88
0.70
0.52
0.35
0.17
0.00
AXIAL STRESS (MPa)
0.00
0.60
1.20
1.80
2.40
3.00
3.60
4.20
4.80
5.40
E-03
SR4 CIRCUMFERENTIAL STRAIN (e)
N5

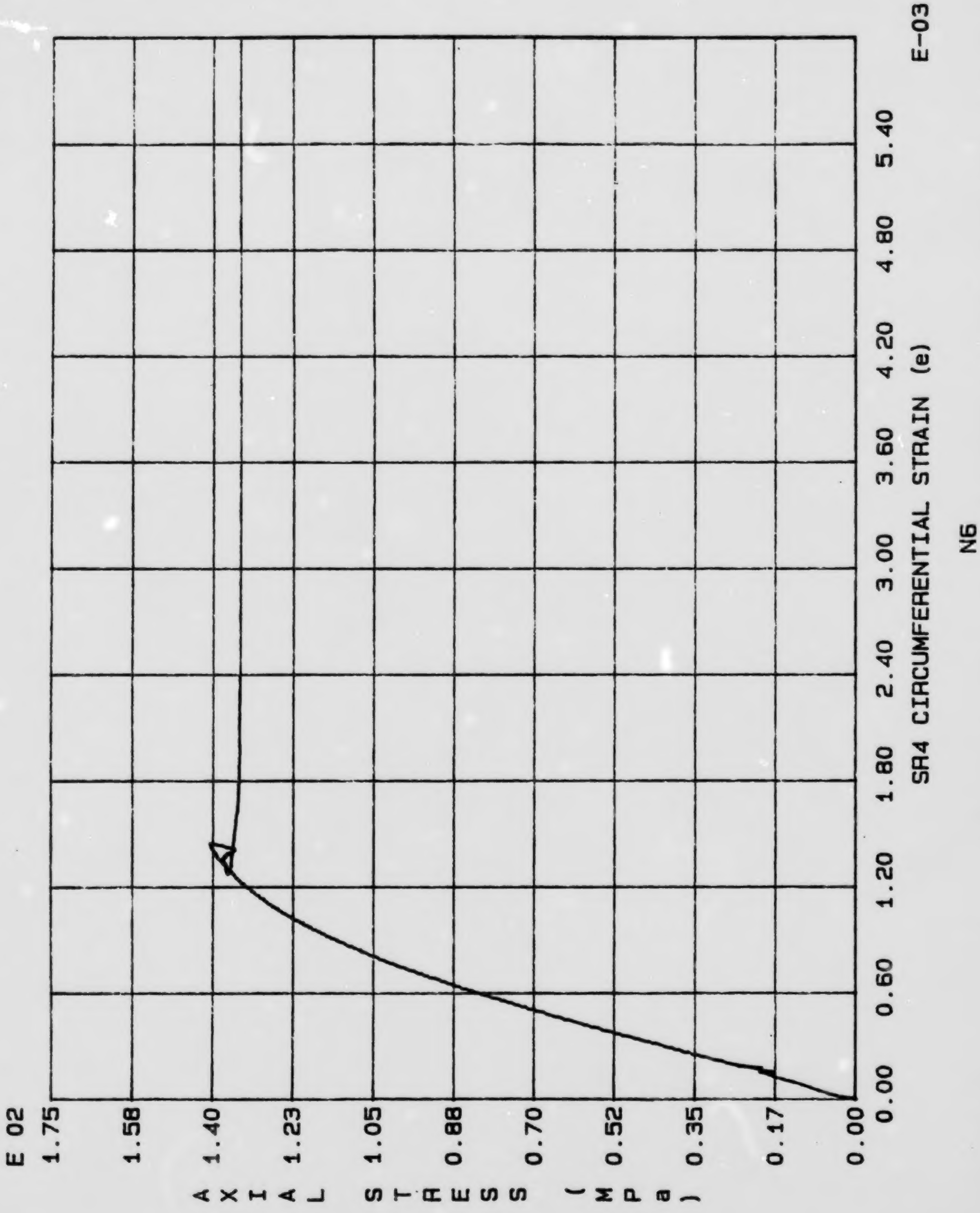
AXIAL STRESS (MPa)
E 02
1.75
1.58
1.40
1.23
1.05
0.88
0.70
0.52
0.35
0.17
0.00
0.00
0.60
1.20
1.80
2.40
3.00
3.60
4.20
4.80
5.40
E-03
SR4 CIRCUMFERENTIAL STRAIN (e)
N6

APPENDIX B-4

Stress vs. strain - circumferential extensometer

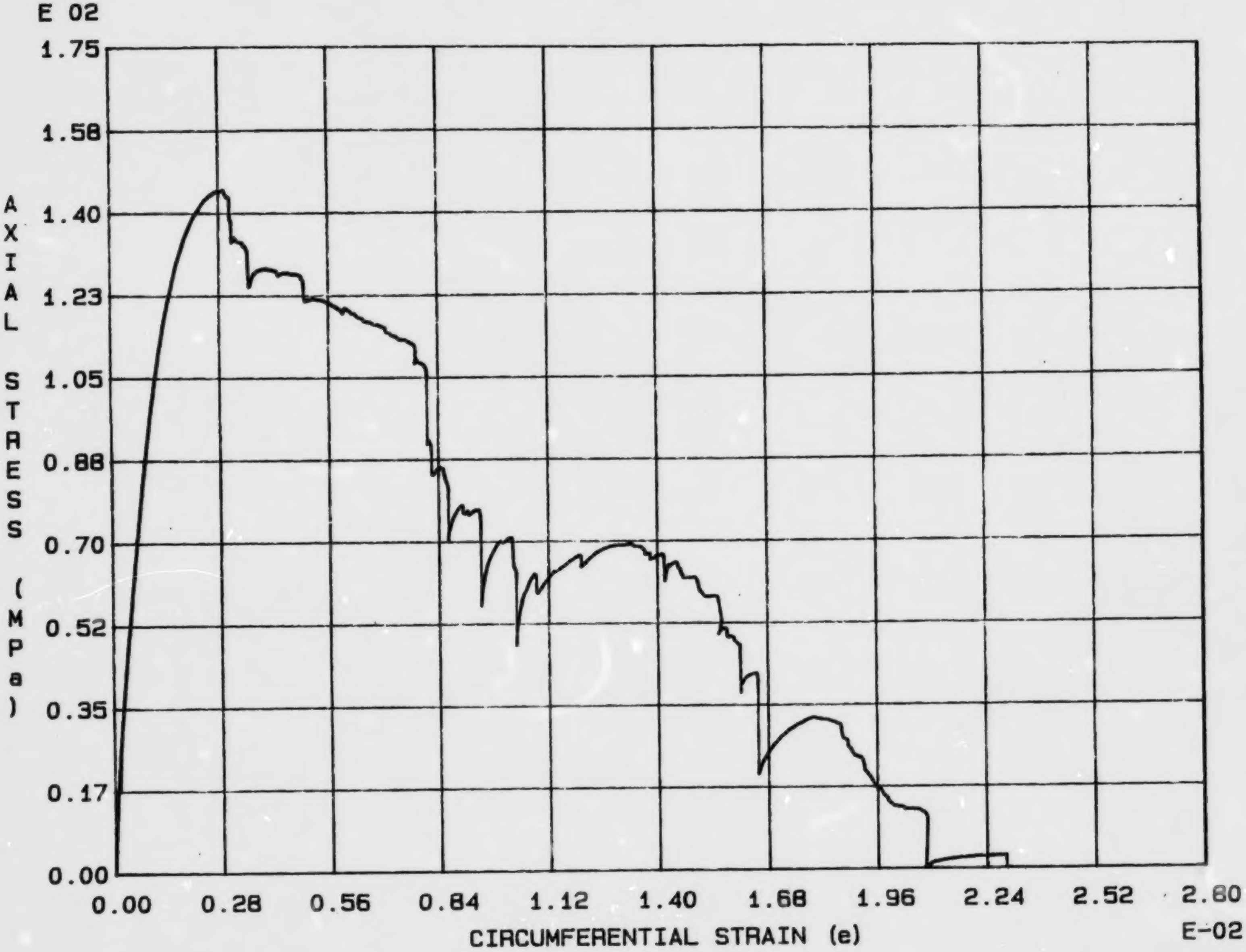
E 02
1.75
1.58
1.40
1.23
1.05
0.88
0.70
0.52
0.35
0.17
0.00
AXIAL STRESS (MPa)
0.00
0.28
0.56
0.84
1.12
1.40
1.68
1.96
2.24
2.52
2.80
E-02
CIRCUMFERENTIAL STRAIN (e)

N4

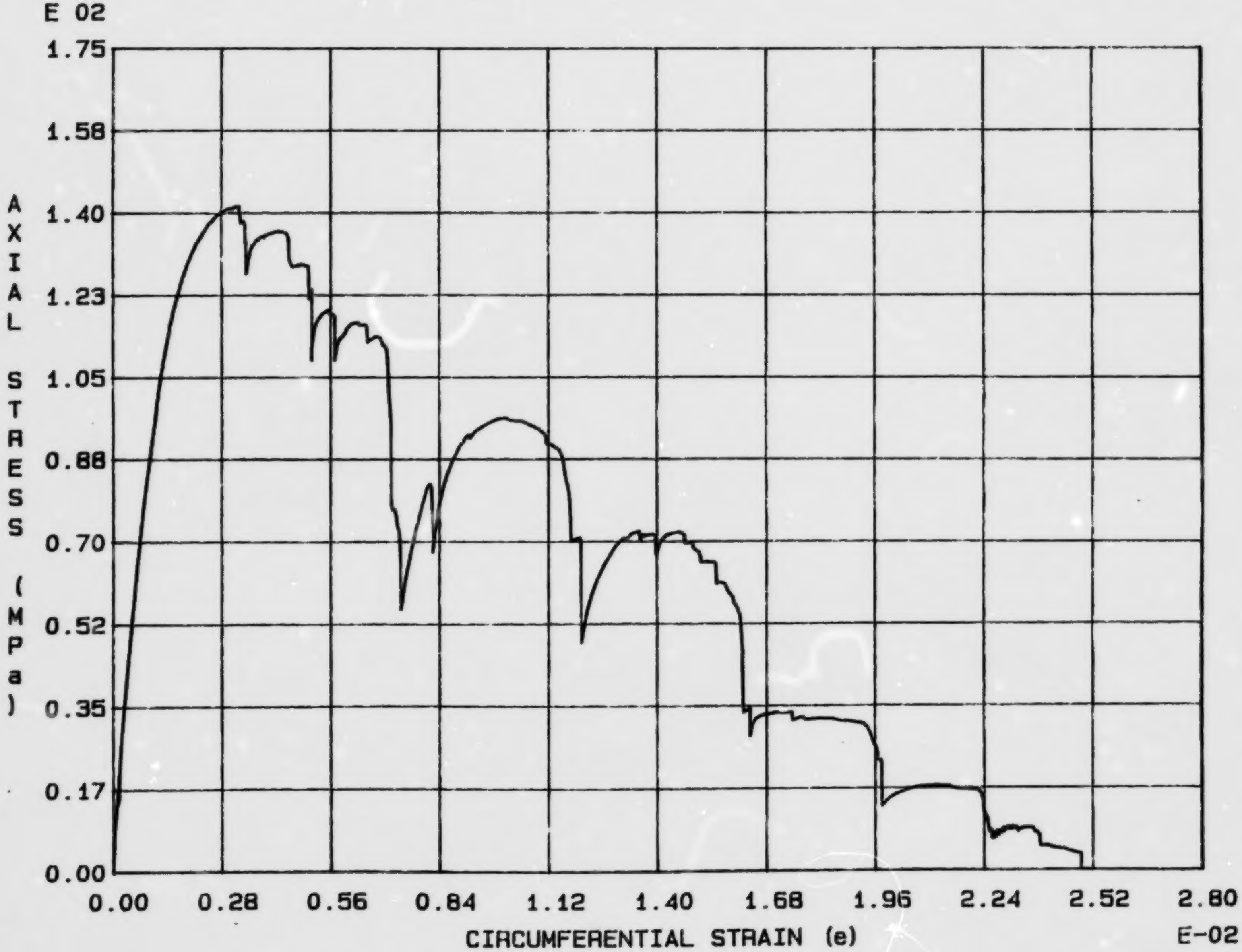
E 02
1.75
1.58
1.40
1.23
1.05
0.88
0.70
0.52
0.35
0.17
0.00
AXIAL STRESS (MPa)
0.00
0.28
0.56
0.84
1.12
1.40
1.68
1.96
2.24
2.52
2.80
E-02
CIRCUMFERENTIAL STRAIN (e)

N5

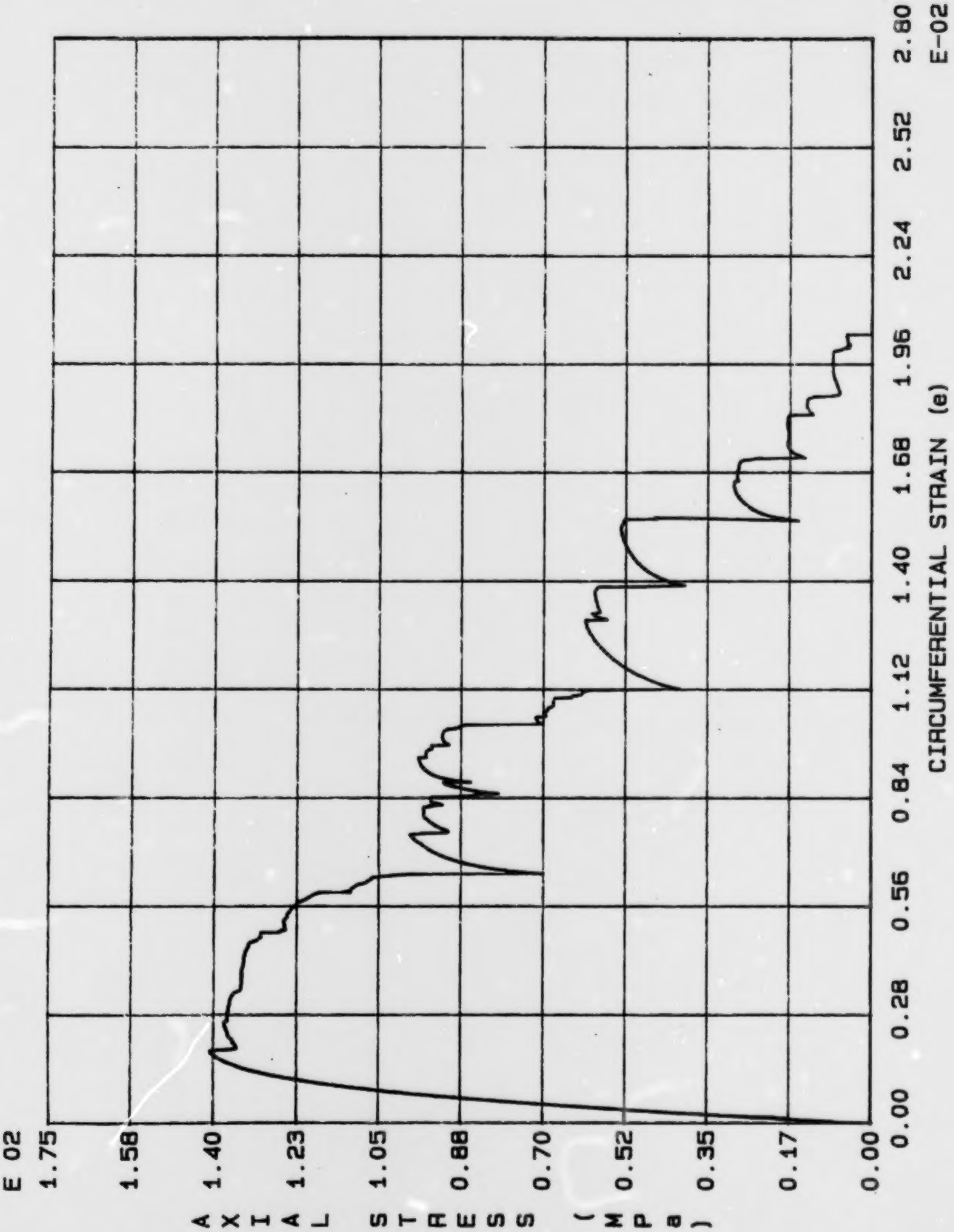
AXIAL STRESS (MPa)
E 02
1.75
1.58
1.40
1.23
1.05
0.88
0.70
0.52
0.35
0.17
0.00
0.00
0.28
0.56
0.84
1.12
1.40
1.68
1.96
2.24
2.52
2.80
E-02
CIRCUMFERENTIAL STRAIN (e)

N6

APPENDIX C

Single stage triaxial tests - load control

APPENDIX C-1

Stress vs. strain - axial lvdts

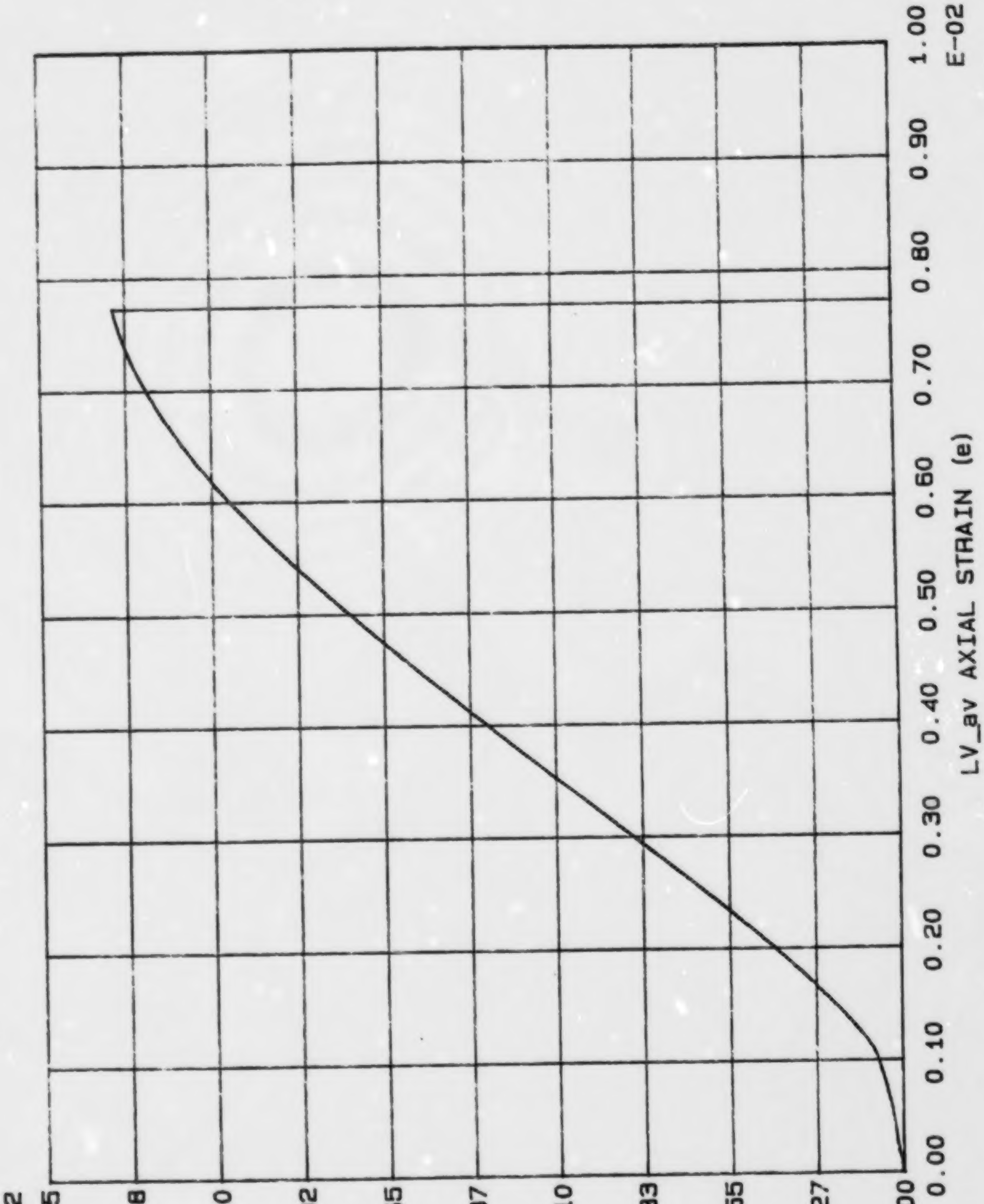
AXIAL STRESS (MPa)
E 02
2.75
2.48
2.20
1.92
1.65
1.37
1.10
0.83
0.55
0.27
0.00
0.00
0.10
0.20
0.30
0.40
0.50
0.60
0.70
0.80
0.90
1.00
E-02
LV_av AXIAL STRAIN (e)
N7

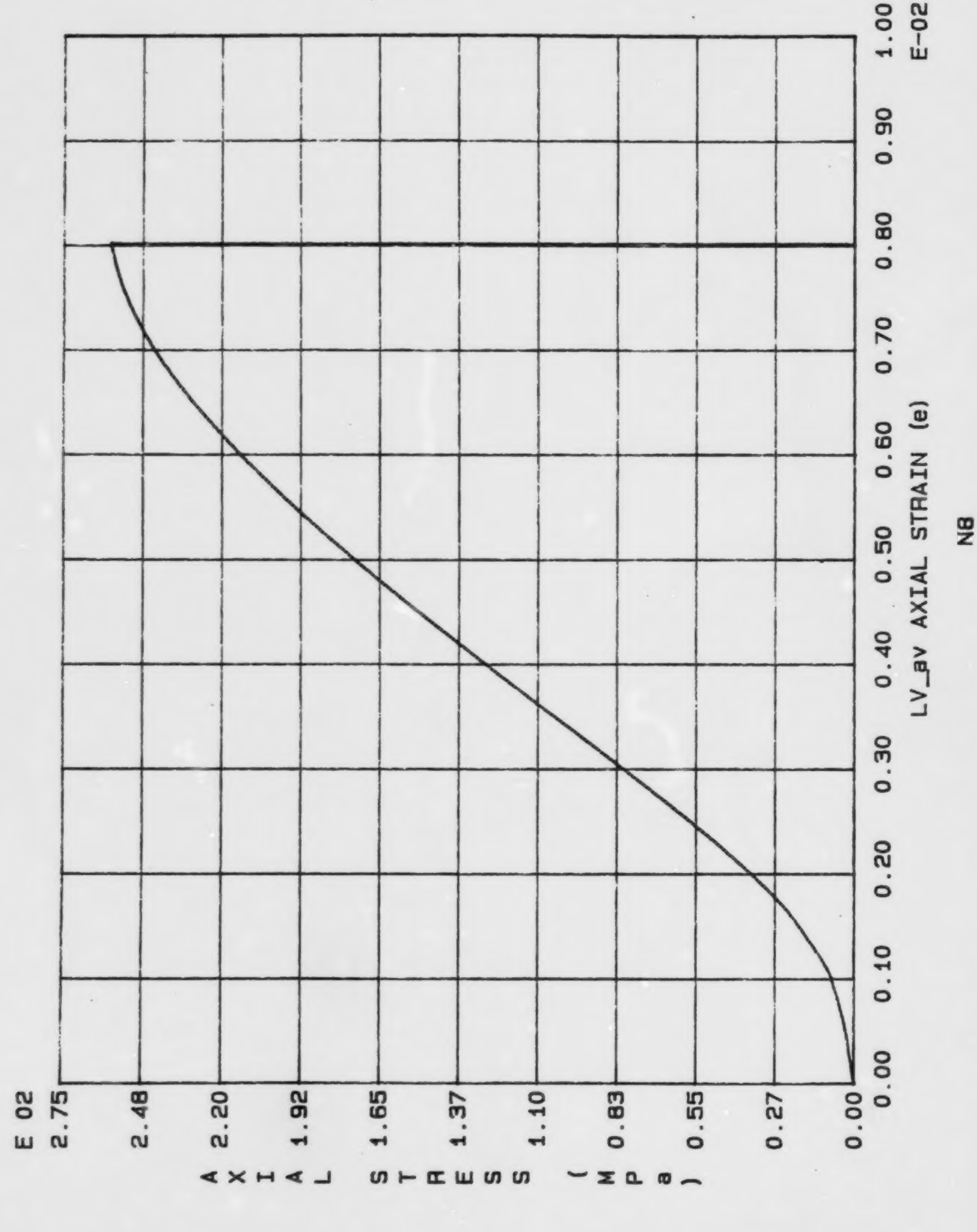
E 02
AXIAL STRESS (MPa)
2.75
2.48
2.20
1.92
1.65
1.37
1.10
0.83
0.55
0.27
0.00
0.00
0.10
0.20
0.30
0.40
0.50
0.60
0.70
0.80
0.90
1.00
E-02
LV_av AXIAL STRAIN (e)
NB

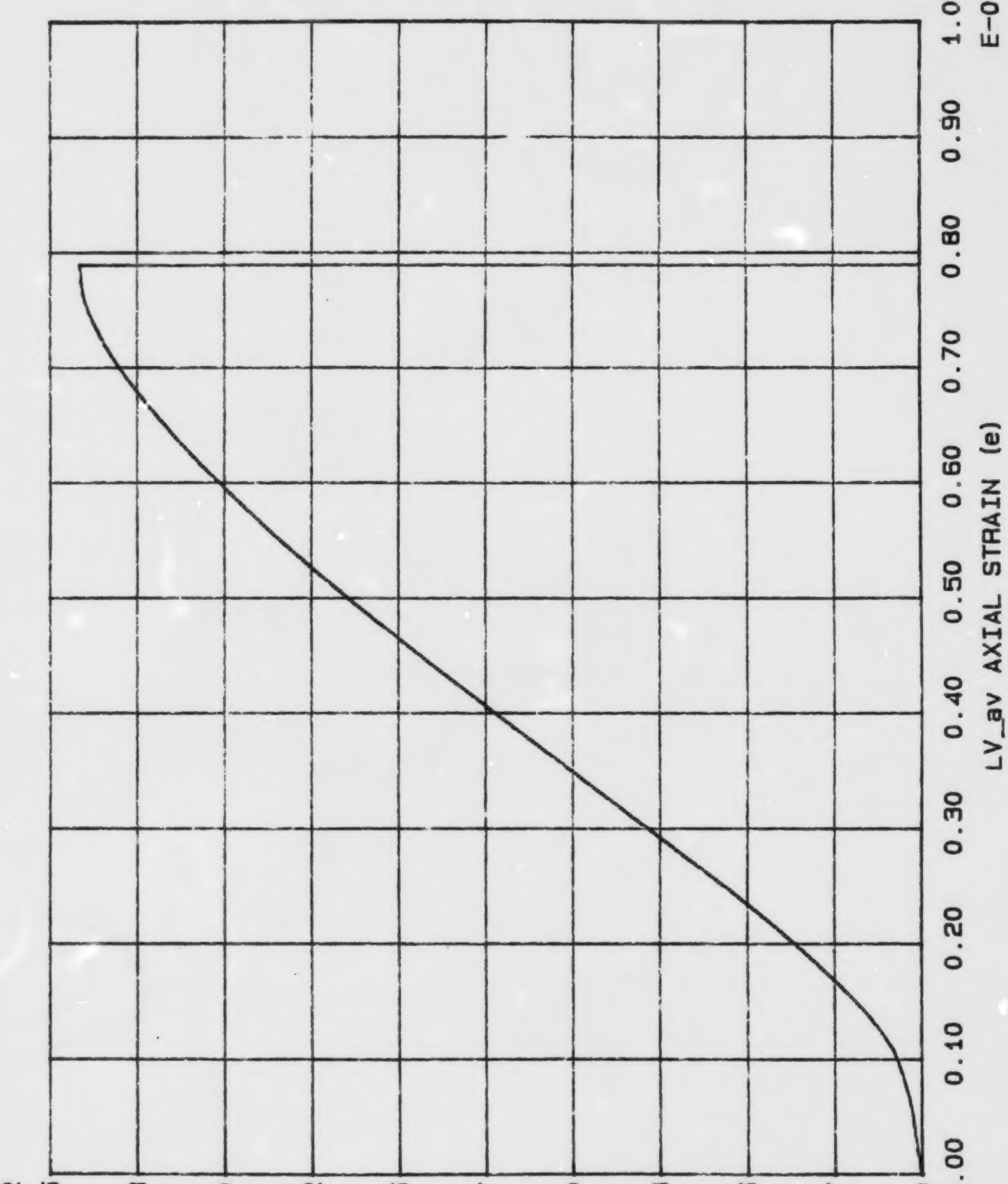
AXIAL STRESS (MPa)
E 02
2.75
2.48
2.20
1.92
1.65
1.37
1.10
0.83
0.55
0.27
0.00
0.00
0.10
0.20
0.30
0.40
0.50
0.60
0.70
0.80
0.90
1.00
E-02
LV_av AXIAL STRAIN (e)
N9

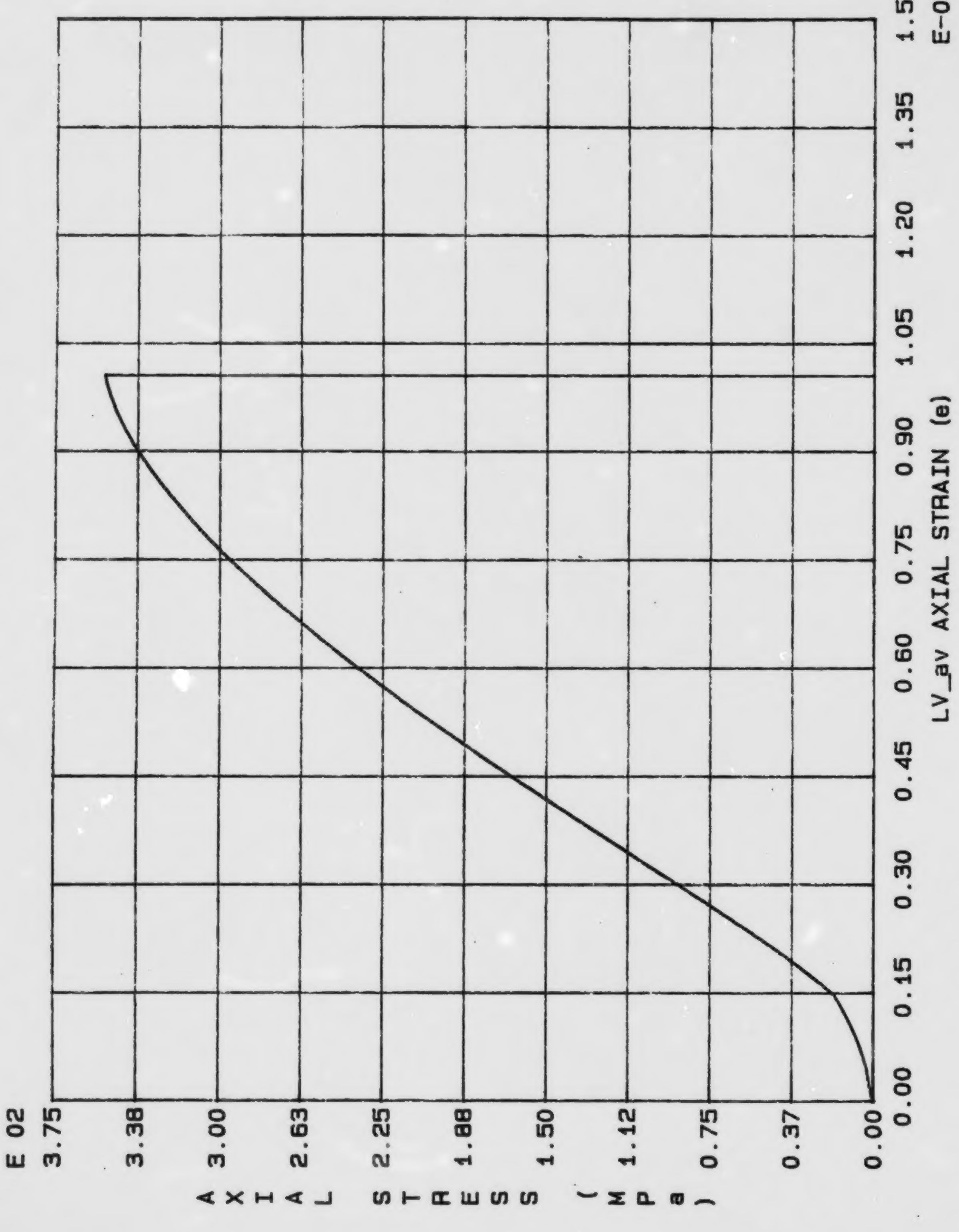
E 02
3.75
3.38
3.00
2.63
2.25
1.88
1.50
1.12
0.75
0.37
0.00
AXIAL STRESS (MPa)
0.00
0.15
0.30
0.45
0.60
0.75
0.90
1.05
1.20
1.35
1.50
E-02
LV_av AXIAL STRAIN (e)

N10

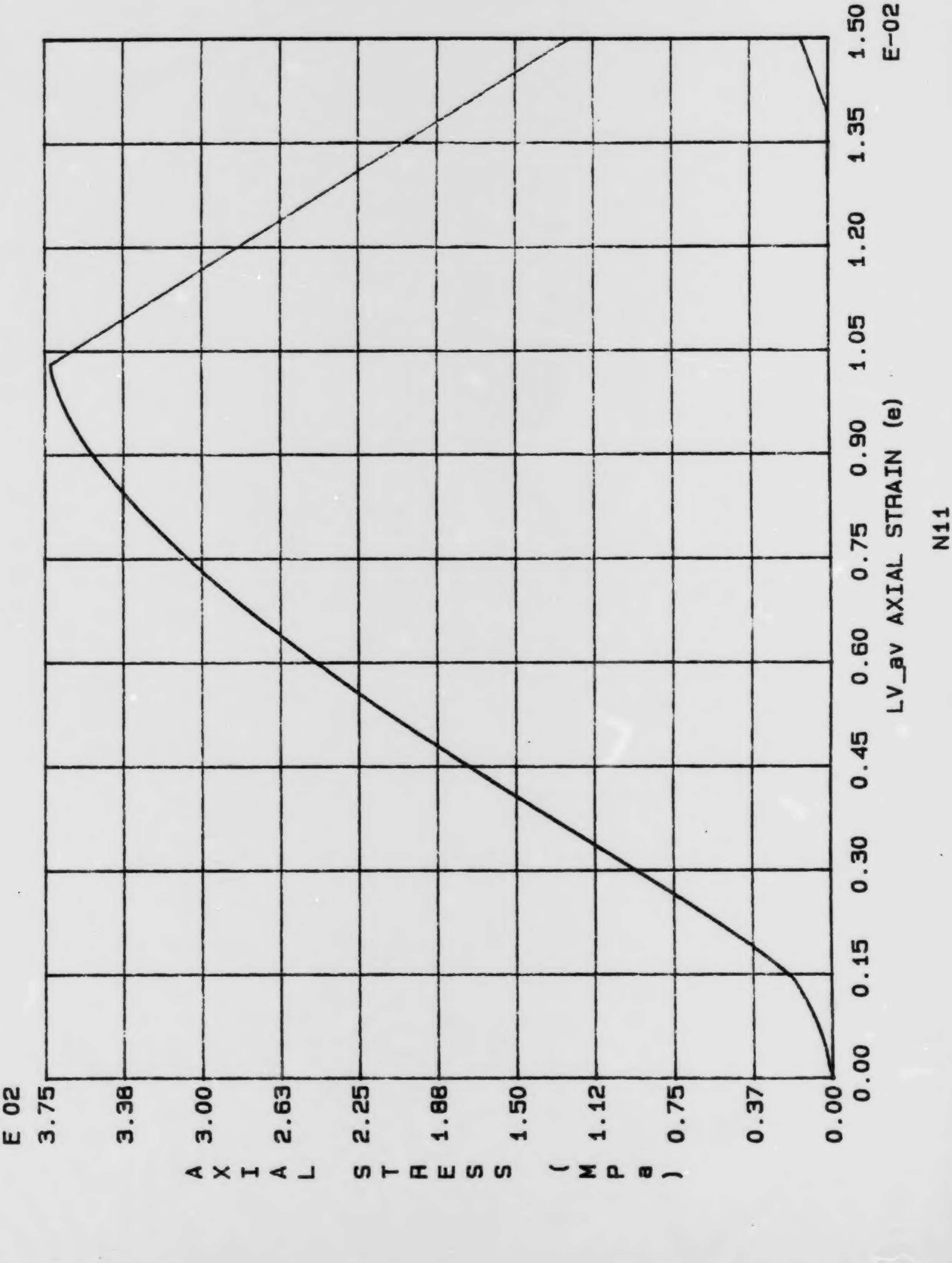
E 02
3.75
3.38
3.00
2.63
2.25
1.88
1.50
1.12
0.75
0.37
0.00
AXIAL STRESS (MPa)
0.00
0.15
0.30
0.45
0.60
0.75
0.90
1.05
1.20
1.35
1.50
E-02
LV_av AXIAL STRAIN (e)
N11

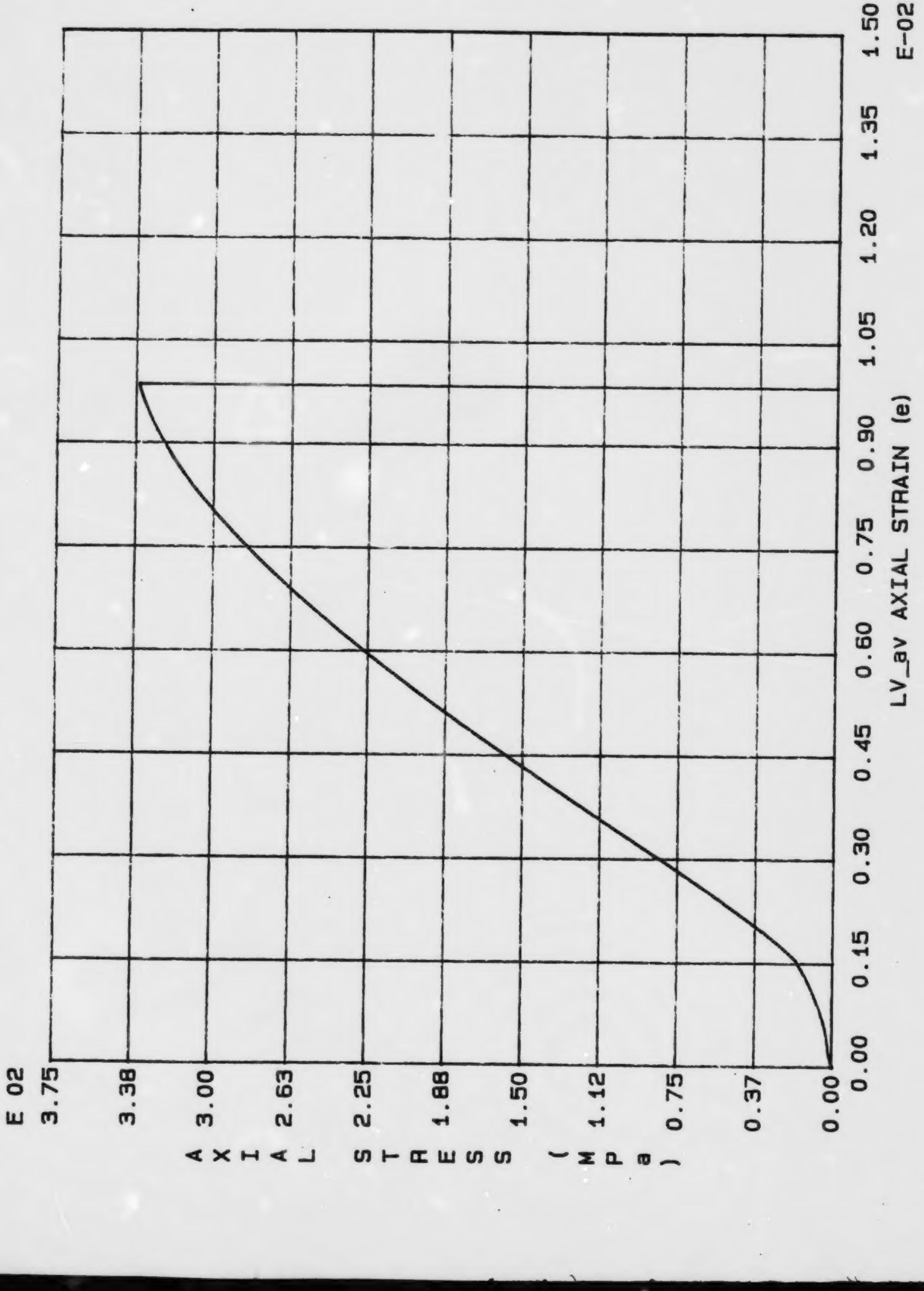
E 02
3.75
3.38
3.00
2.63
2.25
1.88
1.50
1.12
0.75
0.37
0.00
AXIAL STRESS (MPa)
0.00
0.15
0.30
0.45
0.60
0.75
0.90
1.05
1.20
1.35
1.50
E-02
LV_av AXIAL STRAIN (e)

N12

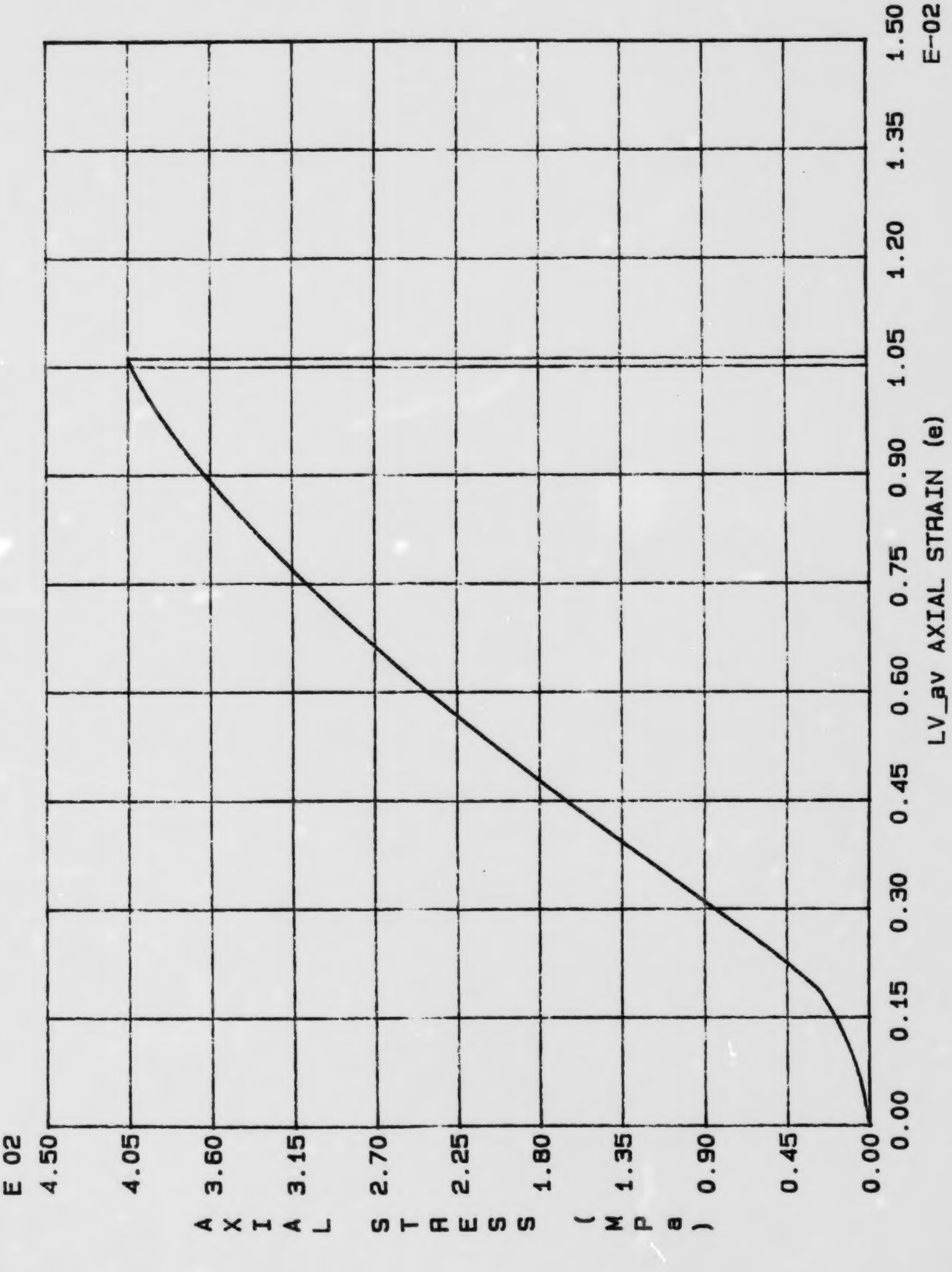
AXIAL STRESS (MPa)
E 02
4.50
4.05
3.60
3.15
2.70
2.25
1.80
1.35
0.90
0.45
0.00
0.00
0.15
0.30
0.45
0.60
0.75
0.90
1.05
1.20
1.35
1.50
E-02
LV_av AXIAL STRAIN (e)
N13

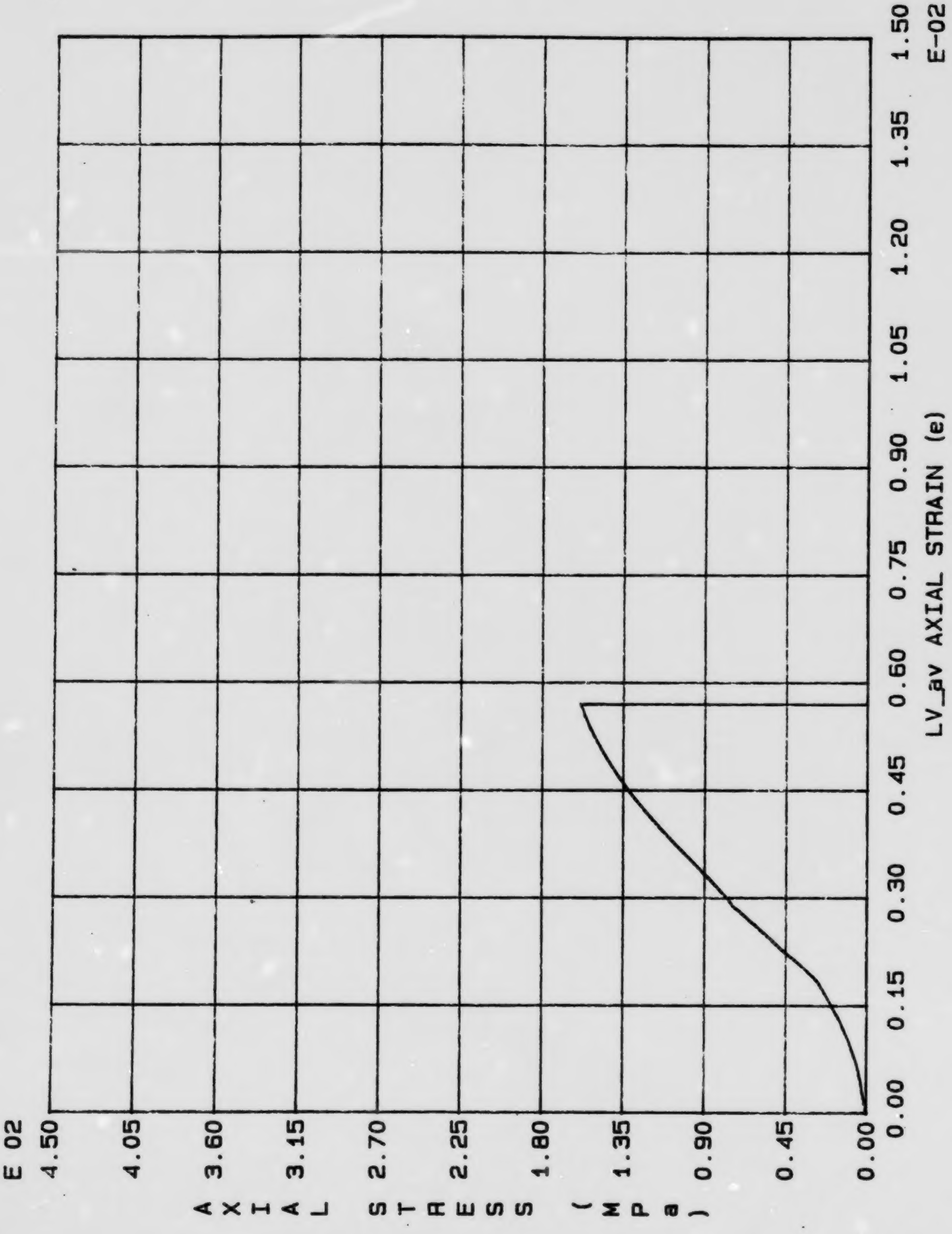
AXIAL STRESS (MPa)
E 02
4.50
4.05
3.60
3.15
2.70
2.25
1.80
1.35
0.90
0.45
0.00
0.00
0.15
0.30
0.45
0.60
0.75
0.90
1.05
1.20
1.35
1.50
E-02
LV_av AXIAL STRAIN (e)
N14

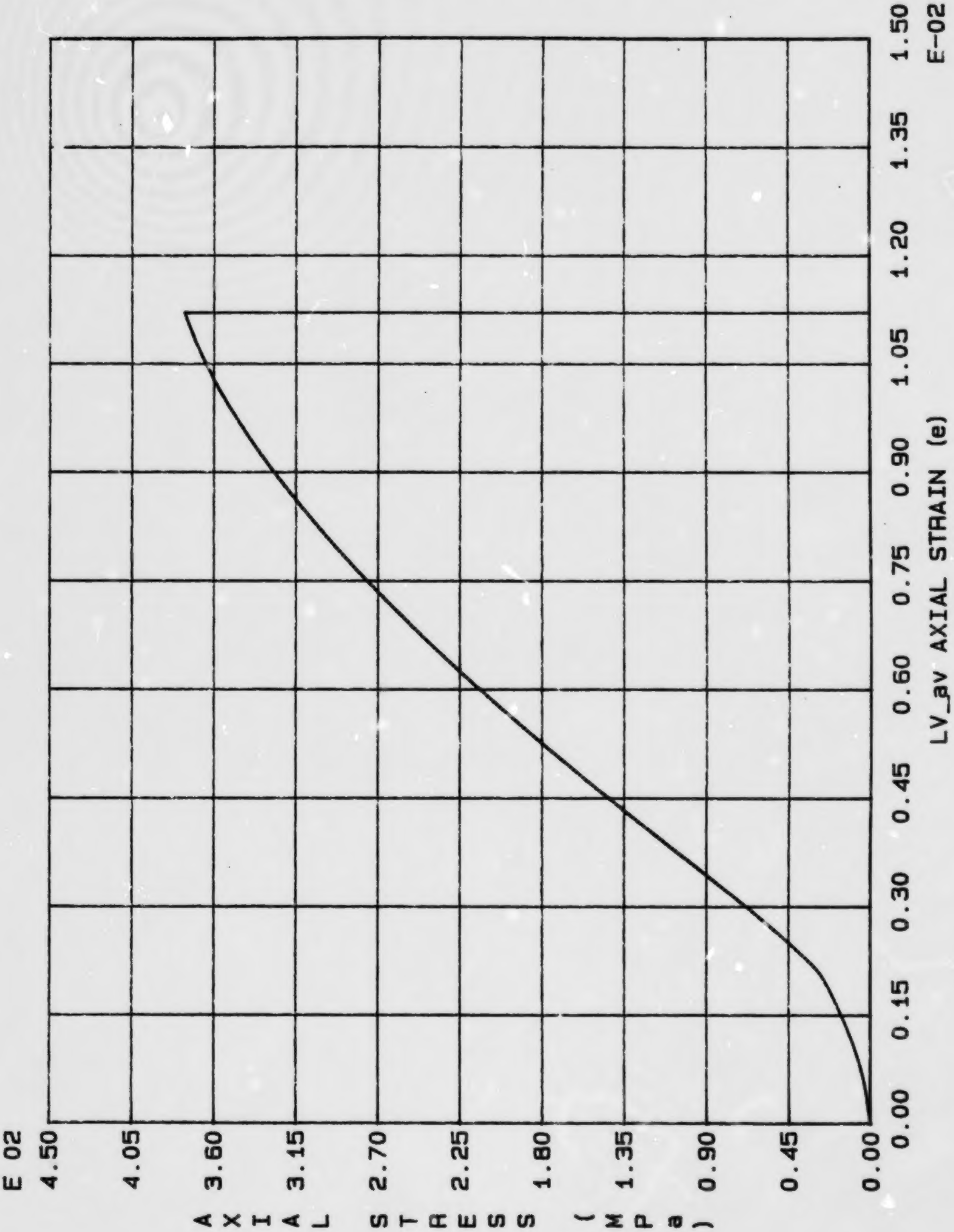
E 02
4.50
4.05
3.60
3.15
2.70
2.25
1.80
1.35
0.90
0.45
0.00
AXIAL STRESS (MPa)
0.00
0.15
0.30
0.45
0.60
0.75
0.90
1.05
1.20
1.35
1.50
E-02
LV_av AXIAL STRAIN (e)

N15

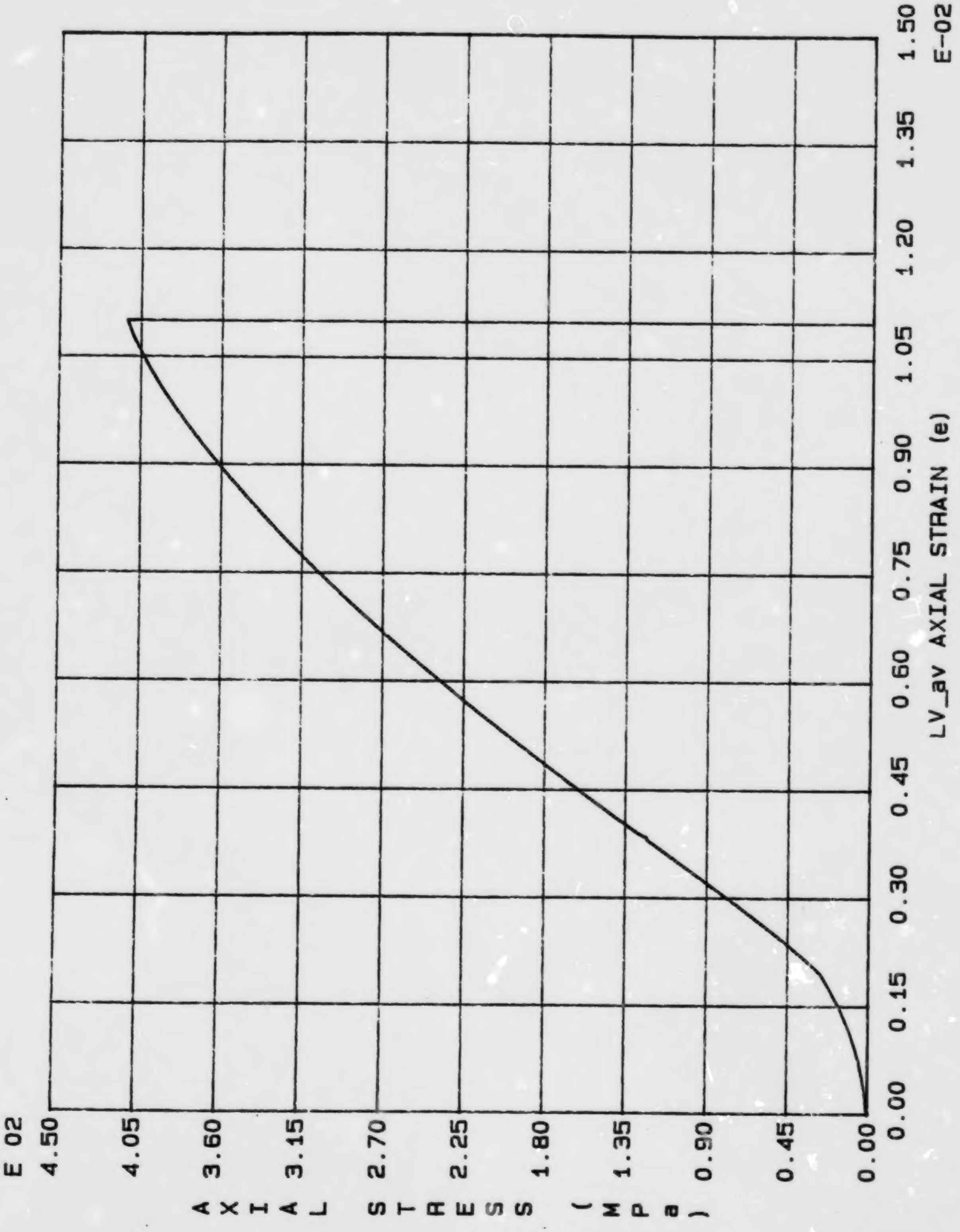
E 02
4.50
4.05
3.60
3.15
2.70
2.25
1.80
1.35
0.90
0.45
0.00
AXIAL STRESS (MPa)
0.00
0.15
0.30
0.45
0.60
0.75
0.90
1.05
1.20
1.35
1.50
E-02
LV_av AXIAL STRAIN (e)

N16

APPENDIX C-2

Stress vs. strain - circumferential extensometer

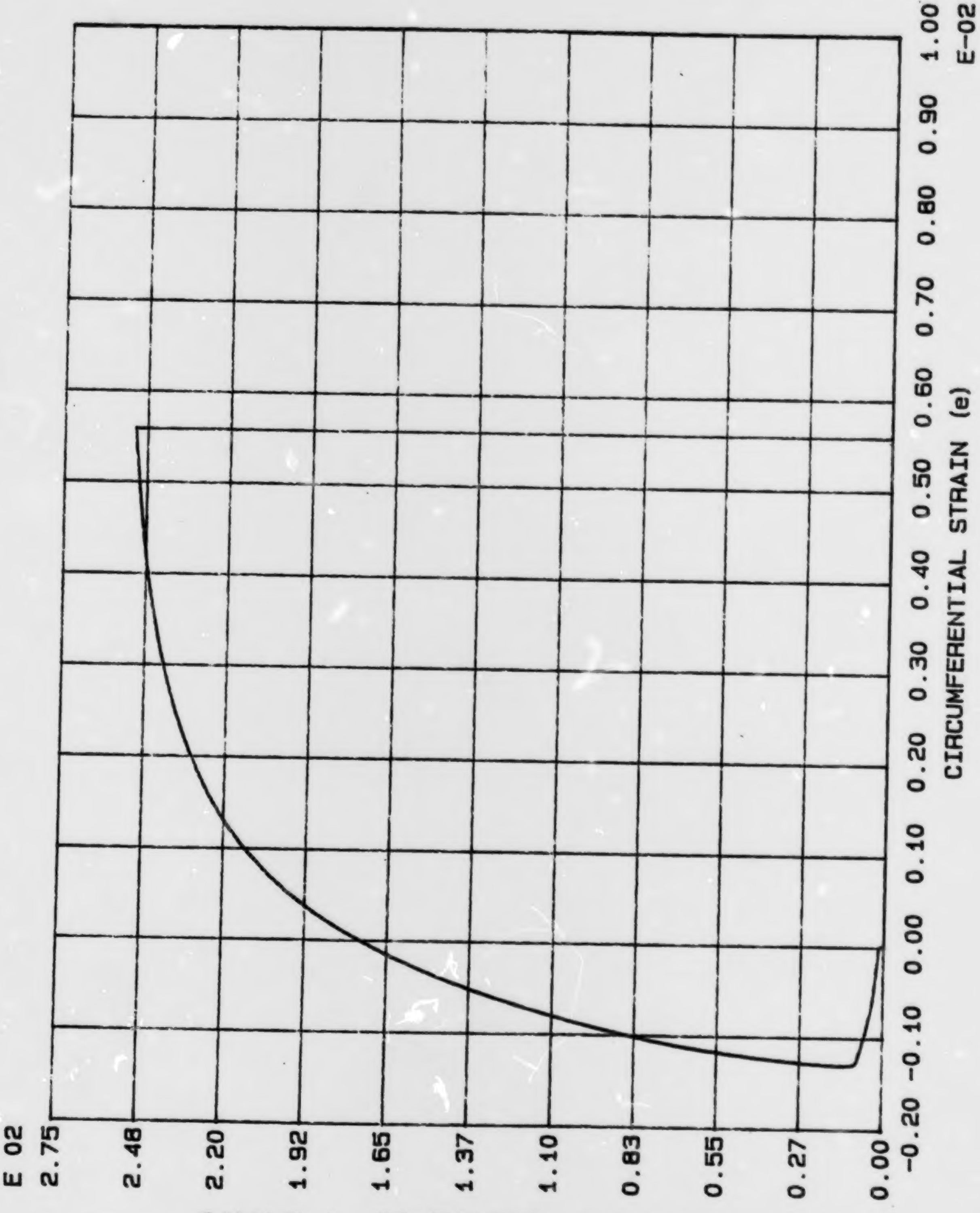
E 02
2.75
2.48
2.20
1.92
1.65
1.37
1.10
0.83
0.55
0.27
0.00
AXIAL STRESS (MPa)
-0.20
-0.10
0.00
0.10
0.20
0.30
0.40
0.50
0.60
0.70
0.80
0.90
1.00
E-02
CIRCUMFERENTIAL STRAIN (e)

N7

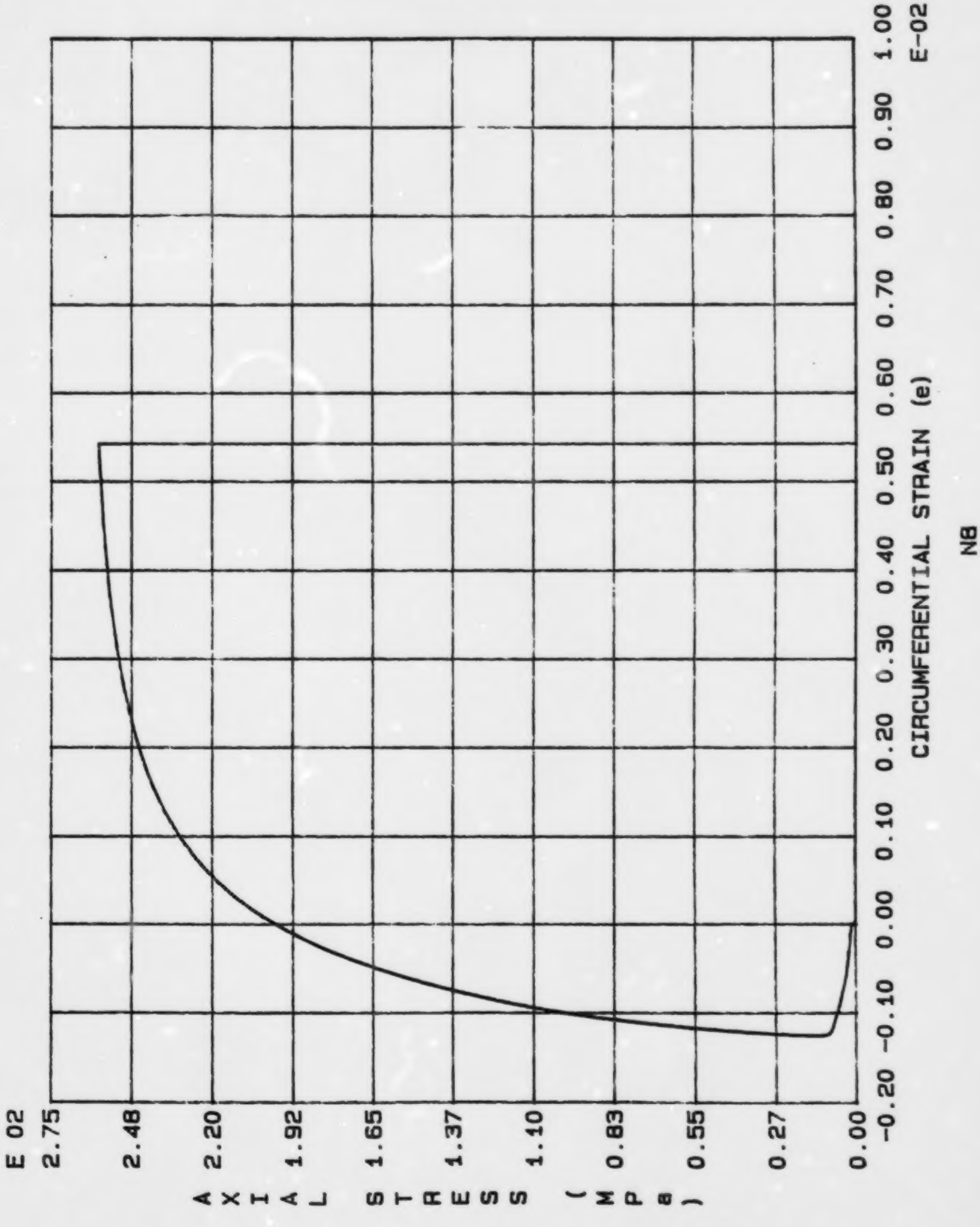
AXIAL STRESS (MPa)
E 02
2.75
2.48
2.20
1.92
1.65
1.37
1.10
0.83
0.55
0.27
0.00
-0.20
-0.10
0.00
0.10
0.20
0.30
0.40
0.50
0.60
0.70
0.80
0.90
1.00
E-02
CIRCUMFERENTIAL STRAIN (e)
NB

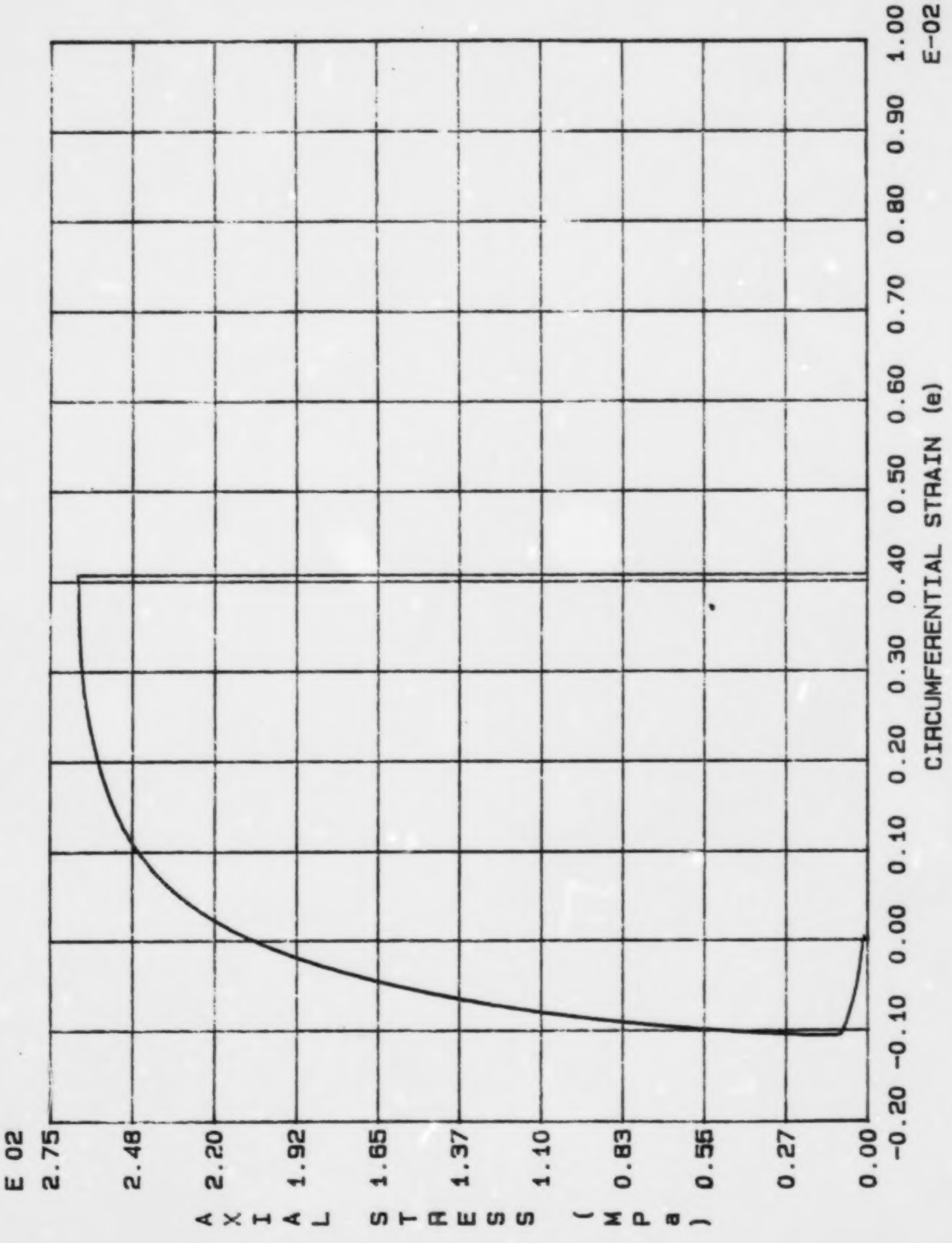
E 02
2.75
2.48
2.20
1.92
1.65
1.37
1.10
0.83
0.56
0.27
0.00
AXIAL STRESS (MPa)
-0.20
-0.10
0.00
0.10
0.20
0.30
0.40
0.50
0.60
0.70
0.80
0.90
1.00
E-02
CIRCUMFERENTIAL STRAIN (e)
N9

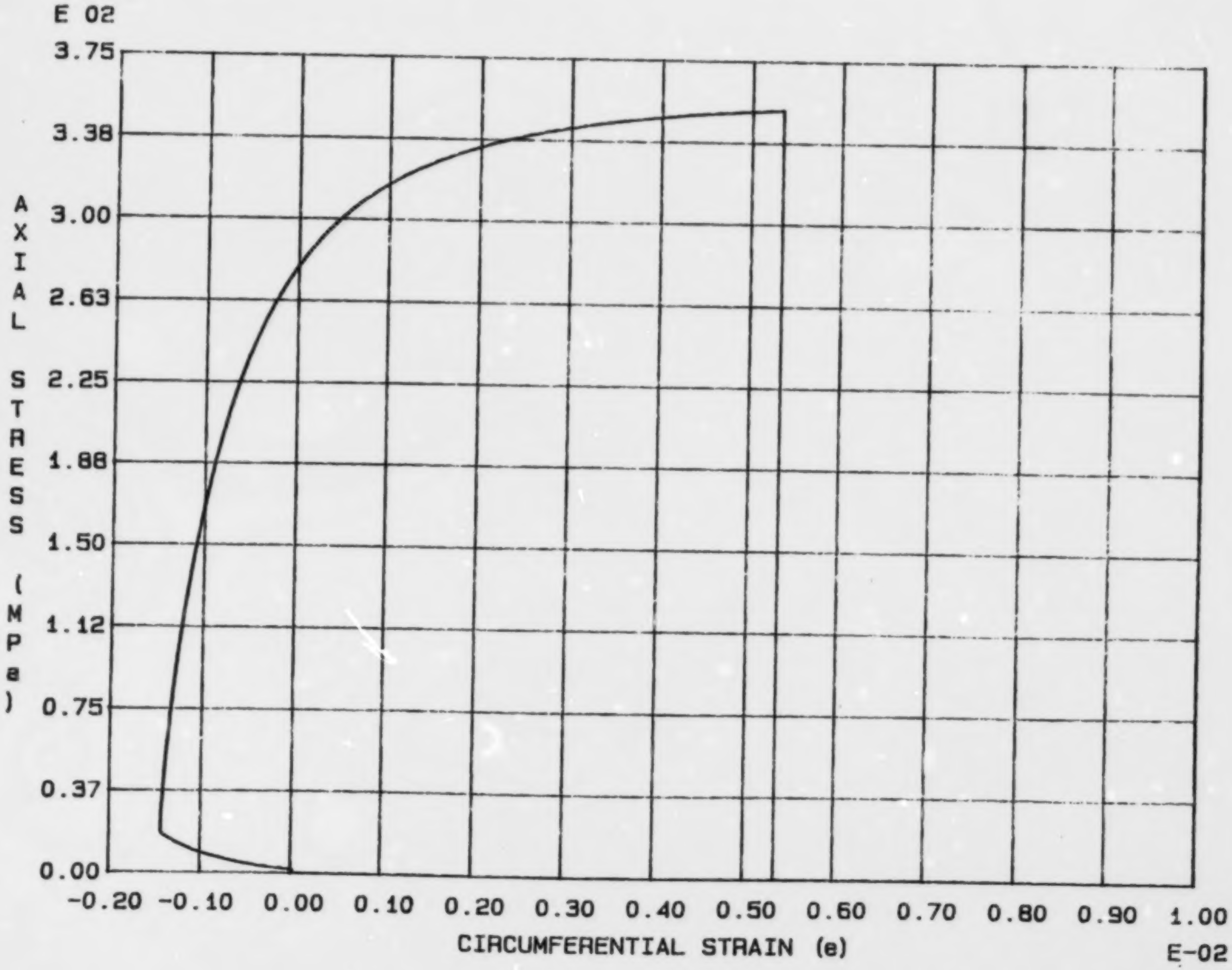
E 02
3.75
3.38
3.00
2.63
2.25
1.88
1.50
1.12
0.75
0.37
0.00
AXIAL STRESS (MPa)
-0.20
-0.10
0.00
0.10
0.20
0.30
0.40
0.50
0.60
0.70
0.80
0.90
1.00
E-02
CIRCUMFERENTIAL STRAIN (e)

N10

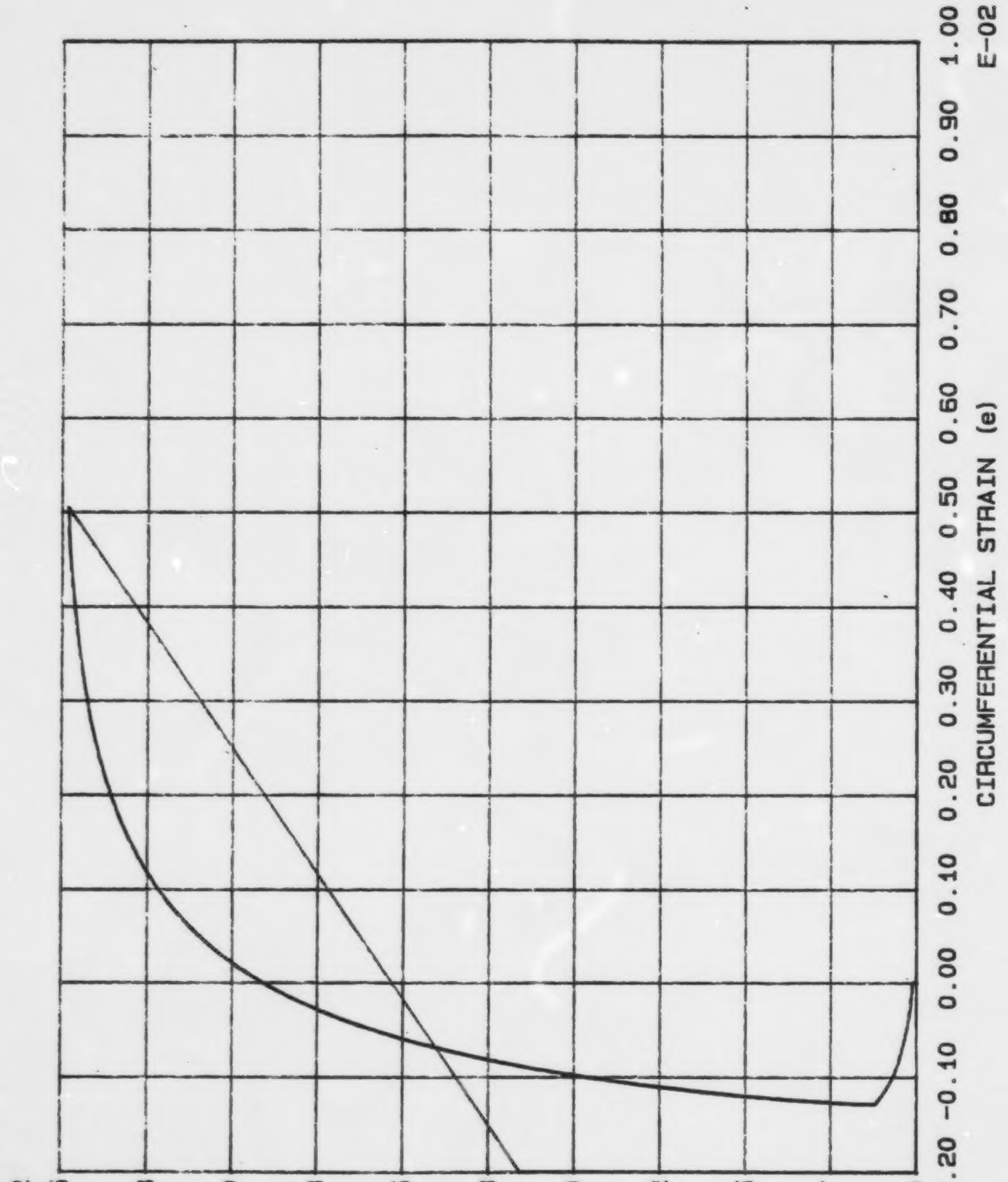
AXIAL STRESS (MPa)
E 02
3.75
3.38
3.00
2.63
2.25
1.88
1.50
1.12
0.75
0.37
0.00
CIRCUMFERENTIAL STRAIN (e)
E-02
-0.20
-0.10
0.00
0.10
0.20
0.30
0.40
0.50
0.60
0.70
0.80
0.90
1.00

N11

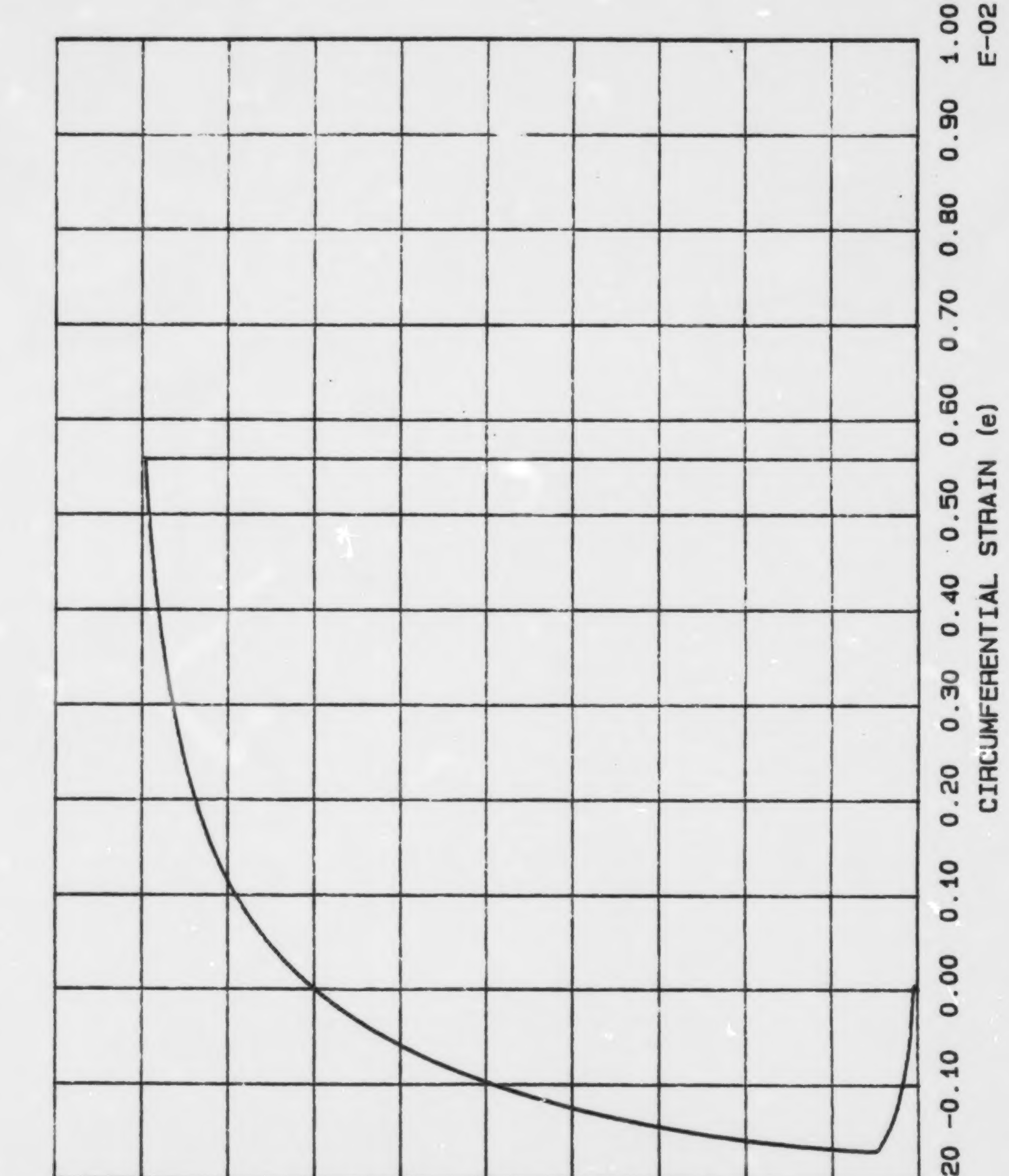
E 02
3.75
3.38
3.00
2.63
2.25
1.88
1.50
1.12
0.75
0.37
0.00
AXIAL STRESS (MPa)
-0.20
-0.10
0.00
0.10
0.20
0.30
0.40
0.50
0.60
0.70
0.80
0.90
1.00
E-02
CIRCUMFERENTIAL STRAIN (e)

N12

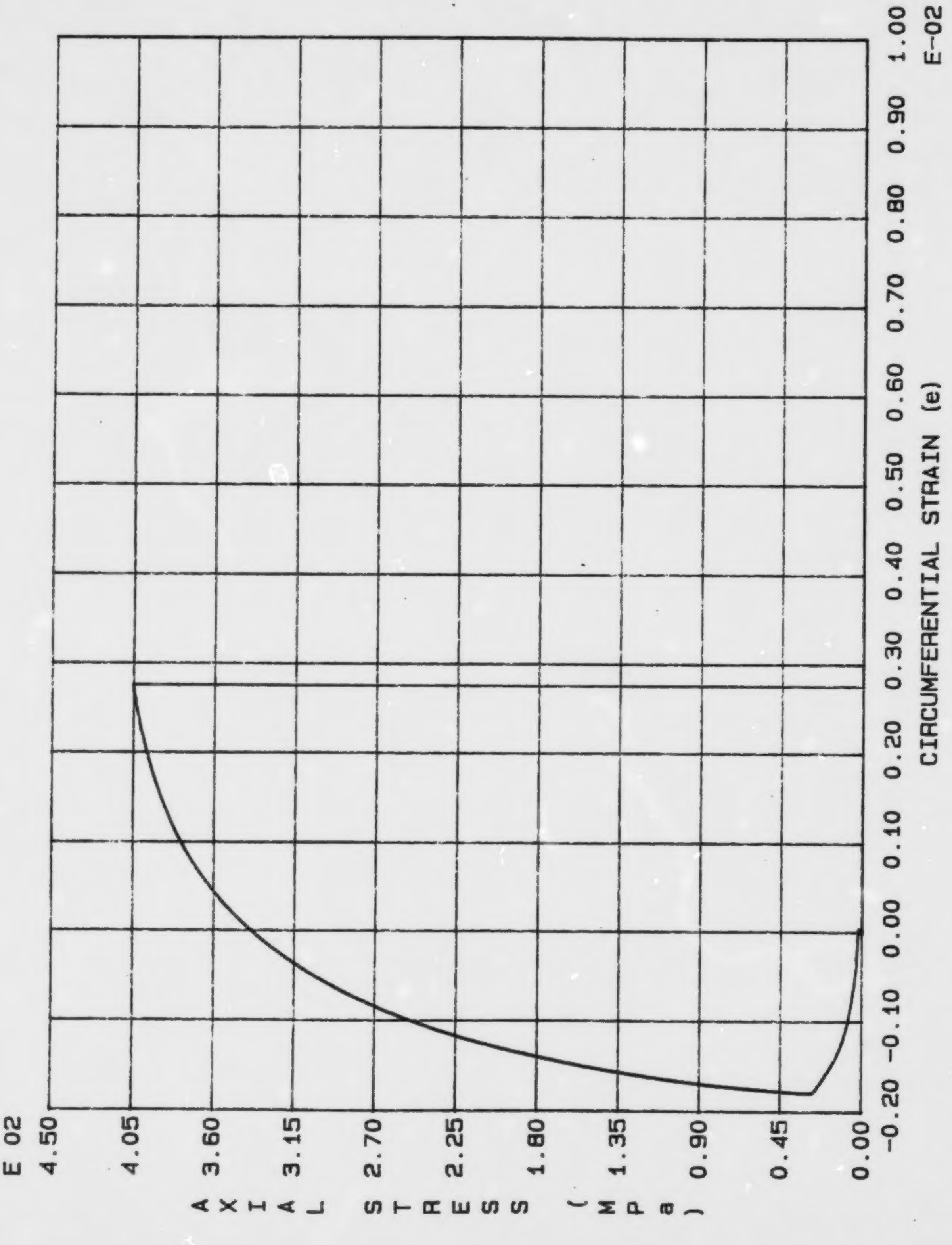
E 02
4.50
4.05
3.60
3.15
2.70
2.25
1.80
1.35
0.90
0.45
0.00
AXIAL STRESS (MPa)
-0.20
-0.10
0.00
0.10
0.20
0.30
0.40
0.50
0.60
0.70
0.80
0.90
1.00
E-02
CIRCUMFERENTIAL STRAIN (e)

N13

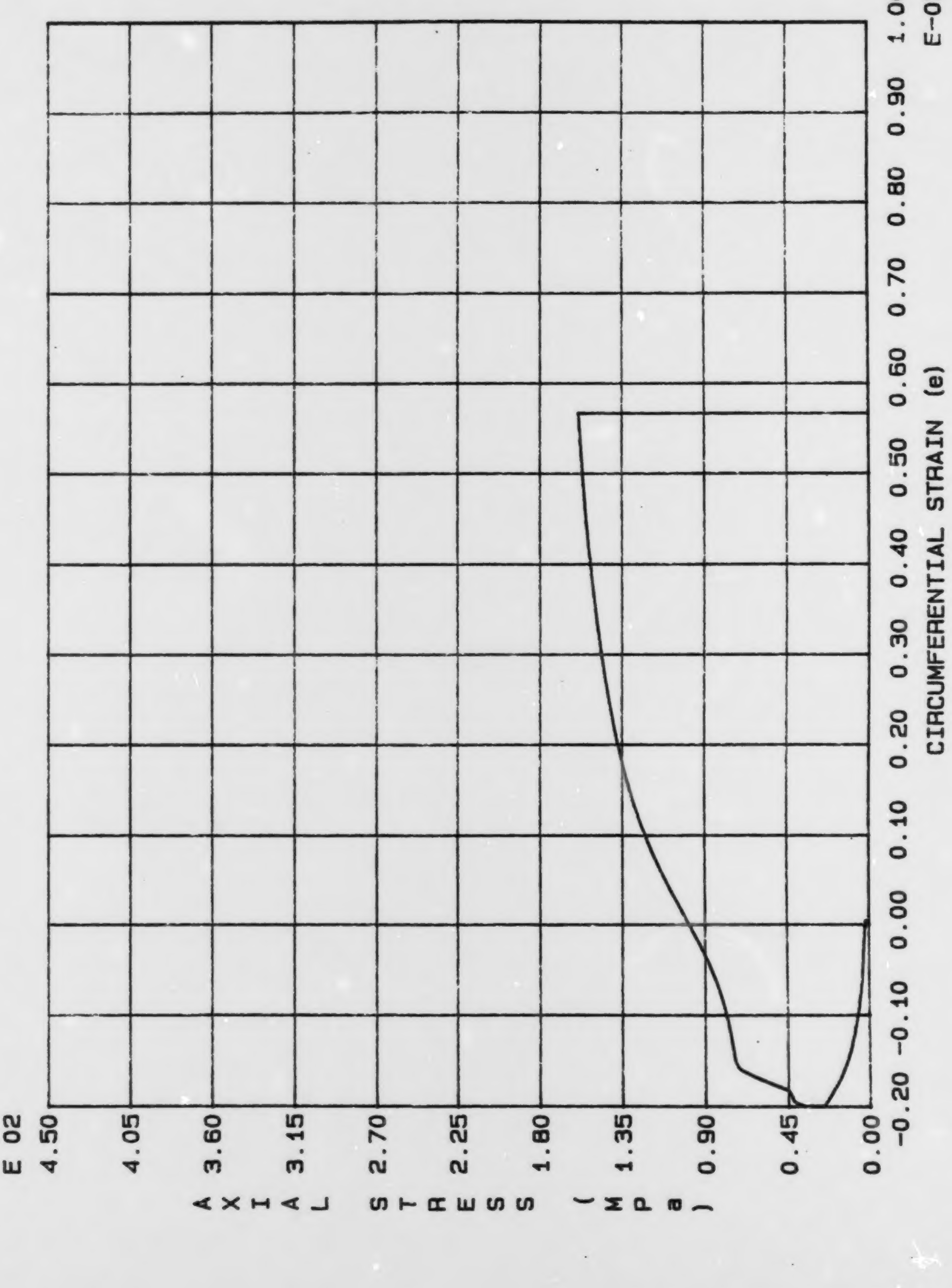
E 02
4.50
4.05
3.60
3.15
2.70
2.25
1.80
1.35
0.90
0.45
0.00
AXIAL STRESS (MPa)
-0.20
-0.10
0.00
0.10
0.20
0.30
0.40
0.50
0.60
0.70
0.80
0.90
1.00
E-02
CIRCUMFERENTIAL STRAIN (e)

N14

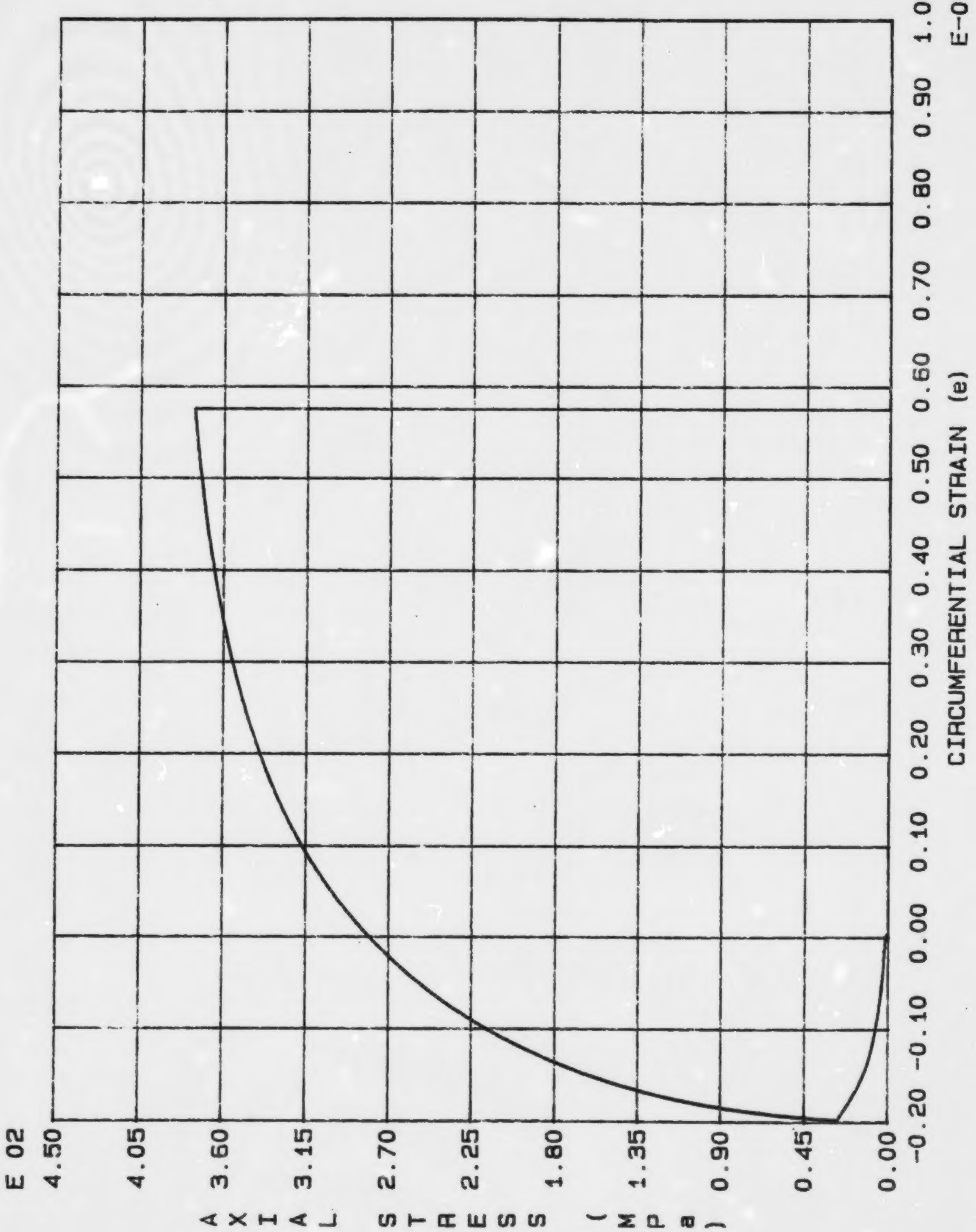
E 02
4.50
4.05
3.60
3.15
2.70
2.25
1.80
1.35
0.90
0.45
0.00
AXIAL STRESS (MPa)
-0.20
-0.10
0.00
0.10
0.20
0.30
0.40
0.50
0.60
0.70
0.80
0.90
1.00
E-02
CIRCUMFERENTIAL STRAIN (e)
N15

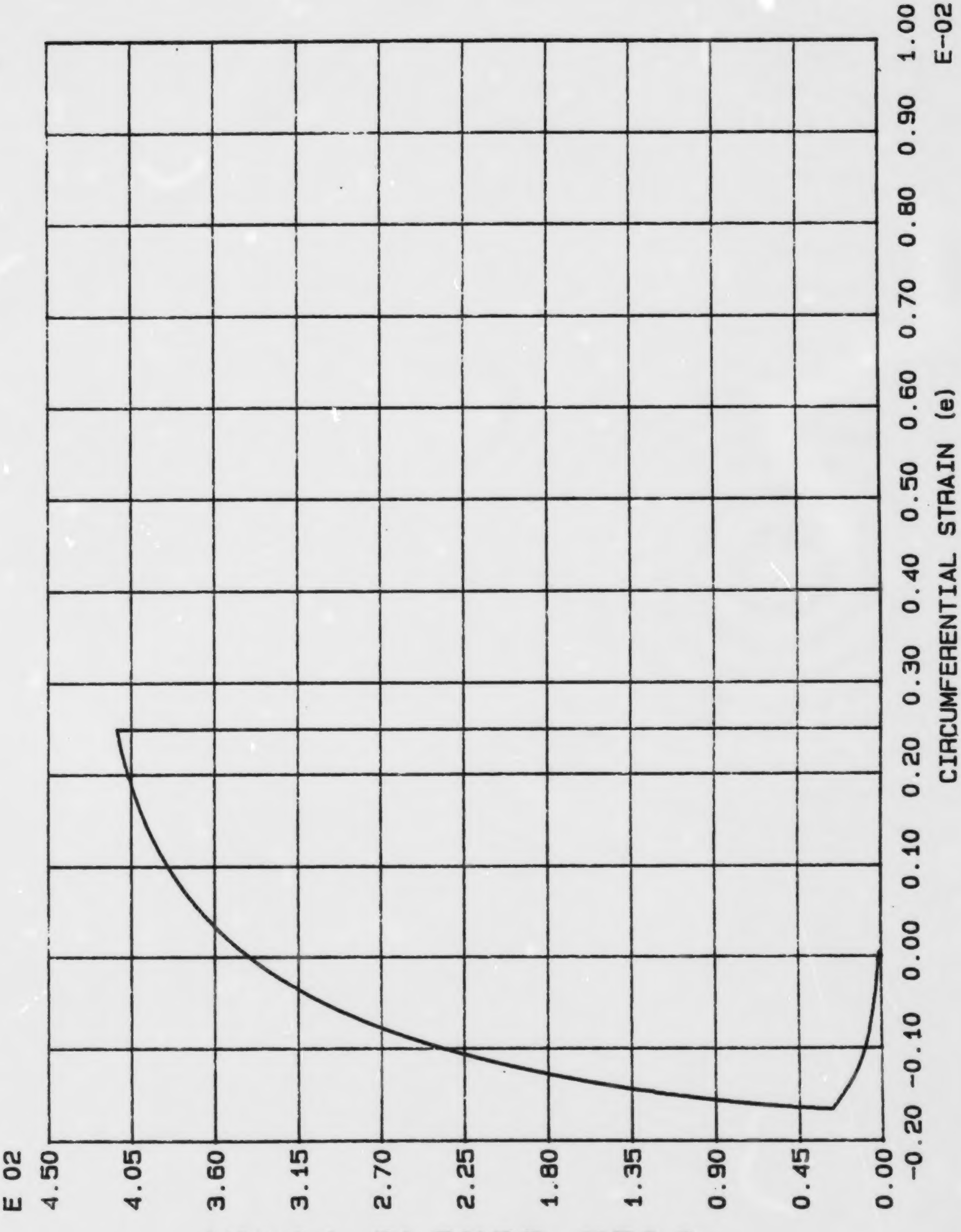
E 02
4.50
4.05
3.60
3.15
2.70
2.25
1.80
1.35
0.90
0.45
0.00
AXIAL STRESS (MPa)
-0.20
-0.10
0.00
0.10
0.20
0.30
0.40
0.50
0.60
0.70
0.80
0.90
1.00
E-02
CIRCUMFERENTIAL STRAIN (e)

N16

APPENDIX C-3

Lmulti.bas - MTS Basic

```
5 PRINT 'PRESS <ESC> <A> TO SWITCH TO STRAIN MODE'
10 KBINT('A',, LINE 290 )
15 PRINT 'PRESS <ESC> <C> TO KICK UP SIG-3 STAGE'
20 KBINT('C',2, LINE 390 )
25 PRINT 'PRESS <ESC> <B> TO SWITCH TO RESIDUAL MODE OR TO END TEST'
30 KBINT('B',3, LINE 570 )
40 KBENB
50 PRINT 'THIS IS A MULTI-STAGE POST-FAILURE TRIAXIAL TEST'
60 PRINT 'INPUT LOAD RANGE IN kN'; \ INPUT U
61 PRINT 'INPUT MAXIMUM CONFINING PRESSURE IN MPa'; \ INPUT E
62 PRINT 'INPUT STARTING CONFINING PRESSURE IN MPa'; \ INPUT T
63 PRINT 'INPUT CONFINING PRESSURE INTERVAL IN MPa'; \ INPUT V
64 PRINT 'INPUT NUMBER OF INTERVALS'; \ INPUT I
65 PRINT 'INPUT CONFINING PRESSURE RANGE CARD IN MPa'; \ INPUT Q
66 PRINT 'INPUT SPECIMEN X-AREA IN CM-SQUARED'; \ INPUT L
67 PRINT 'INPUT SPECIMEN LENGTH IN MM'; \ INPUT L0
68 S=INT((T/10)*L) \ IF S<5 THEN S=5
69 T=T/Q
70 E=E/Q
71 IF U=2500 THEN R=1
80 IF U=1250 THEN R=2
90 IF U=500 THEN R=3
100 IF U=250 THEN R=4
101 B1=-.0167161
102 B2=.0250557
103 B3=.0286087
104 M1=2.90069E-04
105 M2=2.69138E-04
106 M3=2.05556E-04
110 CLREMOTESWITCH(1,1,R,0) \ FGSTEP(1,.05/U)
120 PRINT 'ZERO LVs AND CHAIN'
125 PRINT 'INPUT 1=LOAD CONTROL OR 0=STRAIN CONTROL'; \ INPUT C7
130 PRINT 'PRESS <CR> TO START TEST IN LOAD MODE'; \ INPUT R$
140 SETDIM VA1(9600,6)
150 CKTIME(1,.1)
160 ADTIMED(1,VA1,,1,30,2,3)
170 ADSLAVE(1,9,14,15)
180 ADINIT
200 FGREAD(1,F)
210 FGRAMP(1,U,F+.9)
215 IF T=0 THEN 230
220 FGRAMP(2,S,T)
230 ADGO
240 FGGO
241 ETIME \ SLEEP(S+1) \ ADIMMED(2,H) \ PRINT H*3.81 \ H=H+5.00000E-03
\ PRINT H*3.81
242 ADIMMED(1,Z1)
243 E1=Z1*U*M1+B1
244 E2=Z1*U*M2+B2
245 E3=Z1*U*M3+B3
246 B=4.00000E-03
247 Z9=.45
248 IF C7=1 THEN 540
250 ADIMMED(1,C) \ ADIMMED(2,Z) \ IF Z>1 THEN 670 \ IF Z>H THEN 290
260 FGSTATUS(1,K) \ IF K<1 THEN 670
270 IF C<0 THEN 670
280 IF C>0 THEN 250
290 B=4.00000E-03
300 FGSTOP \ ADIMMED(1,Z) \ FGSTEP(1,Z*.8)
310 A=T
320 J=1
330 PRINT 'PRESS <CR> TO SWITCH TO STRAIN MODE'; \ INPUT R$
340 ADIMMED(2,Z) \ CLSWITCH(1,2,1,0) \ FGSTEP(1,Z)
345 PRINT 'PRESS <CR> TO START TEST IN STRAIN MODE'; \ INPUT R$
360 FGRAMP(1,3000,.5)
365 Z9=.45
```

```
370 FGGO
380 ETIME \ SLEEP(5)
385 IF V=0 THEN 540
390 ADIMMED(1,C) \ ADIMMED(2,Z) \ ADIMMED(3,A0) \ ADIMMED(14,B0)
\ ADIMMED(15,C0)
391 Y1=(A0*5-(M1*C*U+B1)+E1)*100/L0
392 Y2=(B0*5-(M2*C*U+B2)+E2)*100/L0
393 Y3=(C0*5-(M3*C*U+B3)+E3)*100/L0
394 IF Z>1 THEN 670 \ IF C<=B THEN 450
400 FGSTATUS(1,K) \ IF K<1 THEN 670
410 B=C \ C1=C
420 ETIME \ SLEEP(5)
440 IF Z<1 THEN 390
445 GO TO 390
450 FGHOLD(1)
452 L1=(Y1+Y2+Y3)/3
455 PRINT 'Sigma_1=';B*U*10/L;'MPa ';'Sigma_3=';A*Q;'MPa ';'LVs=';L1;'%STRAIN'
456 A=A+(V/Q)
460 J=J+1
470 IF J=I THEN 520 \ IF I=0 THEN 520
480 FGSTEP(2,A)
490 ETIME \ SLEEP(5) \ FGRESUME(1)
500 ADIMMED(1,C) \ B=C \ ETIME \ SLEEP(1)
502 PRINT 'PRESS <ESC> <C> IF LOAD FAILS TO EXCEED LAST STAGE'
505 IF B<C1 THEN 500
510 GO TO 390
520 FGSTEP(2,E)
530 ETIME \ SLEEP(5) \ FGRESUME(1)
540 ADIMMED(1,C) \ ADIMMED(2,Z) \ ADIMMED(3,A0) \ ADIMMED(14,B0)
\ ADIMMED(15,C0)
541 Y1=(A0*5-(M1*C*U+B1)+E1)*100/L0
542 Y2=(B0*5-(M2*C*U+B2)+E2)*100/L0
543 Y3=(C0*5-(M3*C*U*B3)+E3)*100/L0 \ L1=(Y1+Y2+Y3)/3
544 IF Z>.9 THEN 570
552 IF C>B THEN L2=L1
555 IF C>B THEN B=C
556 IF Z>Z9 THEN 562
560 IF Z<.9 THEN 540
561 GO TO 570
562 IF C7=1 THEN 670 \ FGSTOP(1)
563 FGREAD(1,Y)
564 FGRAMP(1,3000,1)
565 FGGO(1)
566 Z9=2
567 GO TO 540
570 FGSTOP \ PRINT 'Sigma_1=';B*U*10/L;'MPa ';'Sigma_3=';E*Q;'MPa ';'LVs='
;L2;'%STRAIN'
575 PRINT 'END TEST ? 1=YES 2=NO'; \ INPUT K1
576 IF K1=1 THEN 670
610 ADIMMED(2,Z)
612 Z=(1-Z)/2+Z
620 FGRAMP(1,60,1)
647 FGRAMP(2,60,0)
648 FGGO
650 ETIME \ SLEEP(60)
670 FGSTOP \ ADSTOP
680 PRINT 'ENTER FILE NAME FOR STORAGE'; \ INPUT F$
690 OPEN 'DU0:'+F$+'.DAT' FOR OUTPUT AS FILE #1, FILESIZE 2000
700 PRINT #1:VA1
710 FOR I=0 TO VA1
720 FOR J=1 TO 6
730 PRINT #1:ELEVEL(VA1(I,J)) \ NEXT J \ NEXT I
740 CLOSE
750 CLLOCALSWITCH(1)
 3010 SETDIM VA2(9600,6)
 3050 PRINT 'ENTER SAMPLE LENGTH IN MM'; \ INPUT Q
```

```
3060 PRINT 'ENTER SAMPLE CIRCUMFERENCE IN MM'; \ INPUT R
3070 PRINT 'ENTER SAMPLE X-AREA IN CM SQUARED'; \ INPUT S
3080 PRINT 'ENTER LOAD FULL SCALE IN MM (CH1)'; \ INPUT C
3090 PRINT 'ENTER STRAIN FULL SCALE IN MM (CH2)'; \ INPUT K
3100 PRINT 'ENTER LV#1 FULL SCALE IN MM (CH3)'; \ INPUT D
3110 PRINT 'ENTER LV#2 FULL SCALE IN MM (CH14)'; \ INPUT L
3120 PRINT 'ENTER LV#3 FULL SCALE IN MM (CH15)'; \ INPUT M
3130 PRINT 'ENTER CONFINING PRESSURE RANGE IN MPa'; \ INPUT V
3140 PRINT 'LVs DISP CORRECTED FOR PLATEN COMPRESSION DISP'
3150 OPEN 'DU0:'+F$+'.DAT' FOR INPUT AS FILE #1, FILESIZE 2000
3170 OPEN 'DU0:'+F$+'M.DAT' FOR OUTPUT AS FILE #2, FILESIZE 2000
3175 PRINT 'OUTPUT FILE IS ';F$;'M.DAT'
3180 INPUT #1:A \ VA2=A
3340 FOR I=1 TO VA2
3350 INPUT #1:E \ E=E*C*10/S \ PRINT E;
3380 INPUT #1:J \ J=(J*K)/R \ PRINT J;
3390 INPUT #1:G \ G=(G*D-(M1*E*S/10+B1)+E1)/Q \ PRINT G;
3400 INPUT #1:U \ U=U*V \ PRINT U;
3410 INPUT #1:W \ W=(W*L-(M2*E*S/10+B2)+E2)/Q \ PRINT W;
3420 INPUT #1:Y \ Y=(Y*M-(M3*E*S/10+B3)+E3)/Q \ PRINT Y
3430 PRINT #2:E;J;G;U;W;Y
3440 NEXT I
3450 CLOSE
3460 PRINT 'STRESS (MPa)   ';'CIRCUM (e)   ';'LV#1 (e)   ';'SIGMA-3 (MPa)   '
;'LV#2 (e)   ';'LV#3 (e)   '
3470 END
```

APPENDIX C-4

Tplot.bas - MTS Basic

```
100 SETDIM VA2(14400,6)
200 PRINT 'INPUT FILE NAME'; \ INPUT F$
300 PRINT 'ENTER SAMPLE LENGTH IN MM'; \ INPUT Q
400 PRINT 'ENTER SAMPLE CIRCUMFERENCE IN MM'; \ INPUT R
500 PRINT 'ENTER SAMPLE X-AREA IN CM SQUARED'; \ INPUT S
600 PRINT 'ENTER LOAD FULL SCALE IN kN (CH1)'; \ INPUT C
700 PRINT 'ENTER STRAIN FULL SCALE IN MM (CH2)'; \ INPUT K
800 PRINT 'ENTER LV#1 FULL SCALE IN MM (CH3)'; \ INPUT D
900 PRINT 'ENTER LV#2 FULL SCALE IN MM (CH14)'; \ INPUT L
1000 PRINT 'ENTER LV#3 FULL SCALE IN MM (CH15)'; \ INPUT M
1100 PRINT 'ENTER CONFINING PRESSURE RANGE IN MPa'; \ INPUT V
1200 PRINT 'LVDTs DISP CORRECTED FOR PLATEN COMPRESSION DISP'
1300 OPEN 'DU0:'+F$+'.DAT' FOR INPUT AS FILE #2, FILESIZE 2000
1400 PRINT
1500 S1=S
1600 INPUT #2:A \ VA2=A
1700 INPUT #2:Z1
1800 CLOSE
1900 OPEN 'DU0:'+F$+'.DAT' FOR INPUT AS FILE #1, FILESIZE 2000
2000 INPUT #1:A
2100 B1=-.0167161
2200 B2=.0250557
2300 B3=.0286087
2400 M1=.000290069
2500 M2=.000269138
2600 M3=.000205556
2700 E1=Z1*C*M1+B1
2800 E2=Z1*C*M2+B2
2900 E3=Z1*C*M3+B3
3100 PRINT 'INPUT Y MAX SCALE IN STRESS (MPa)'; \ INPUT Y1
3200 Y2=Y1/10
3300 PRINT 'INPUT 1,2,3,4,5 OR 6 FOR STRESS VS LV#1,CHAIN,LV#2,LV#3,SIGMA3
OR LVs'; \ INPUT S
3400 IF S=1 THEN A$='LV#1 AXIAL STRAIN (e)'
3500 IF S=2 THEN A$='CIRCUMFERENTIAL STRAIN (e)'
3600 IF S=3 THEN A$='LV#2 AXIAL STRAIN (e)'
3700 IF S=4 THEN A$='LV#3 AXIAL STRAIN (e)'
3800 IF S=5 THEN A$='CONFINING PRESSURE (MPa)'
3900 IF S=6 THEN A$='LV_av AXIAL STRAIN (e)'
4000 PRINT 'INPUT X MAX SCALE IN STRAIN OR MPa'; \ INPUT X1
4100 X2=X1/10
4200 PRINT 'INPUT X SCALE LEFT START IN STRAIN OR MPa'; \ INPUT X3
4300 PRINT 'PRESS <CR> AFTER PLOT PAPER INSTALLED'; \ INPUT R1$
4400 GRATTACH(2,2) \ GRON(2) \ COLORLINE(2,1)
4500 PHYL(2,5,90,10,95) \ SCALE(2,0,X3,X1,0,Y1)
4600 LABEL(2,A$,'AXIAL STRESS (MPa)',X2,Y2,0)
4700 COLORLINE(2,4)
4800 INVEC(2)
4900 PLOT(2,0,H)
5000 FOR I=1 TO VA2
5100 INPUT #1:E \ E=E*C*10/S1
5400 INPUT #1:J \ J=(J*K-N)/R
5500 INPUT #1:G \ G=(G*D-(M1*E*S1/10+B1)+E1)/Q
5600 INPUT #1:U \ U=U*V
5700 INPUT #1:W \ W=(W*L-(M2*E*S1/10+B2)+E2)/Q
5800 INPUT #1:Y \ Y=(Y*M-(M3*E*S1/10+B3)+E3)/Q
5900 IF S=1 THEN PLOT(2,G,E)
6000 IF S=2 THEN PLOT(2,J,E)
6100 IF S=3 THEN PLOT(2,W,E)
6200 IF S=4 THEN PLOT(2,Y,E)
6300 IF S=5 THEN PLOT(2,U,E)
6400 IF S=6 THEN PLOT(2,(G+W+Y)/3,E)
6500 NEXT I
6600 CLOSE
6700 IF S=1 THEN PLOT(2,G,0)
6800 IF S=2 THEN PLOT(2,J,0)
```

```
6900 IF S=3 THEN PLOT(2,W,0)
7000 IF S=4 THEN PLOT(2,Y,0)
7100 IF S=5 THEN PLOT(2,U,0)
7110 IF S=6 THEN PLOT(2,(G+W+Y)/3,0)
7200 PLOT(2,X1,0)
7300 PLOT(2,X1,Y1)
7400 PLOT(2,X1,0)
7500 PLOT(2,0,0)
7600 VTMODE
7700 GRDETACH(2)
7800 PRINT 'DO YOU WISH MORE PLOTS  (Y/N) ?'; \ INPUT I$
7900 GRATTACH(2,2)
8000 GRON(2)
8100 COLORLINE(2,1)
8200 PHYL(2,5,95,5,95) \ SCALE(2,0,0,100,0,100)
8300 LABEL(2,F$,,100,100,3)
8400 VTMODE
8500 GRDETACH(2)
8600 OPEN 'DU0:'+F$+'.DAT' FOR INPUT AS FILE #1, FILESIZE 2000
8700 INPUT #1:A \ VA2=A
8800 IF I$='Y' THEN GO TO 3300
8900 CLOSE
9000 END
```

APPENDIX D

Single stage triaxial tests - circumferential control

APPENDIX D-1

Stress vs. strain - axial lvdts

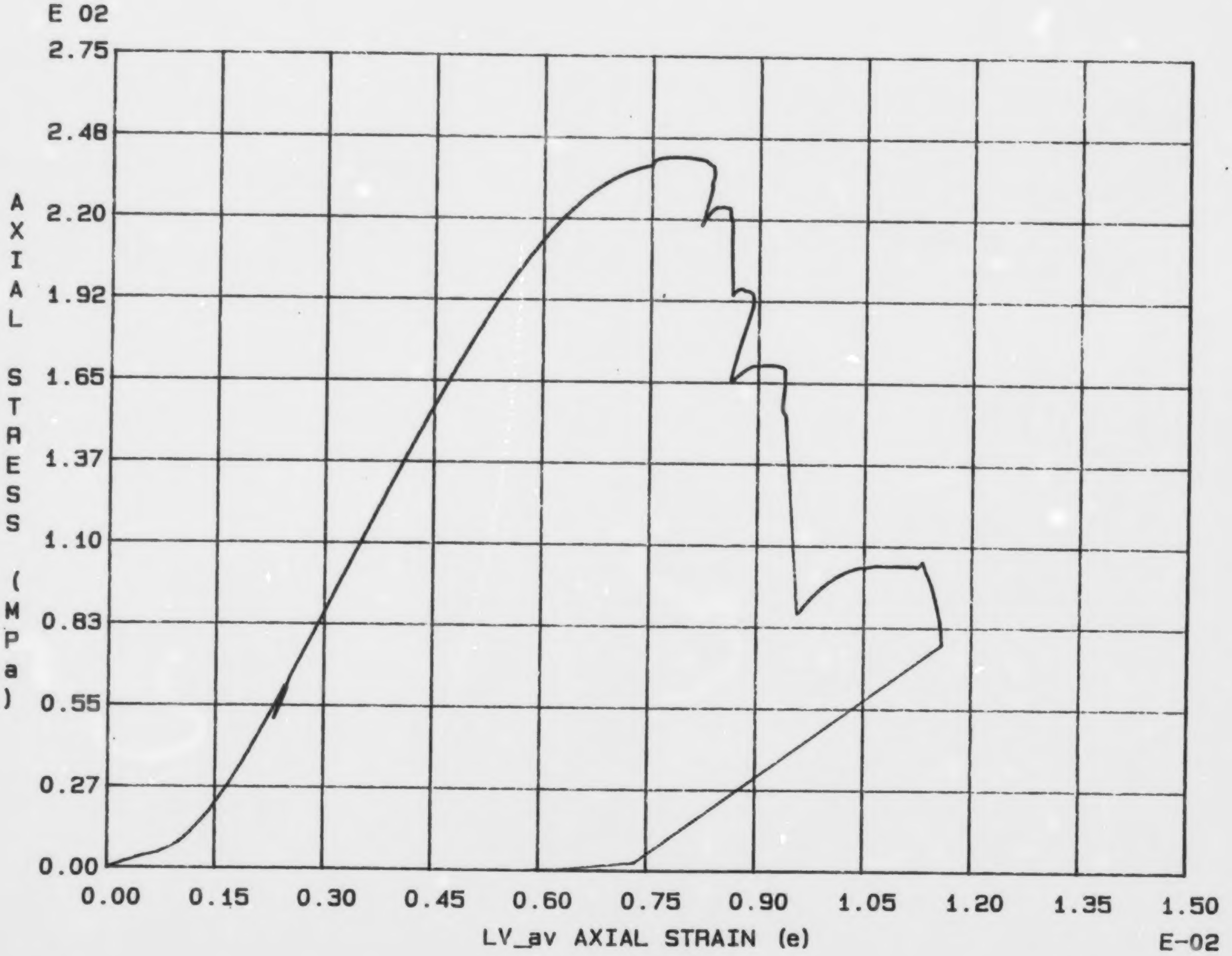
E 02
2.75
2.48
2.20
1.92
1.65
1.37
1.10
0.83
0.55
0.27
0.00
AXIAL STRESS (MPa)
0.00
0.15
0.30
0.45
0.60
0.75
0.90
1.05
1.20
1.35
1.50
E-02
LV_av AXIAL STRAIN (e)

N17

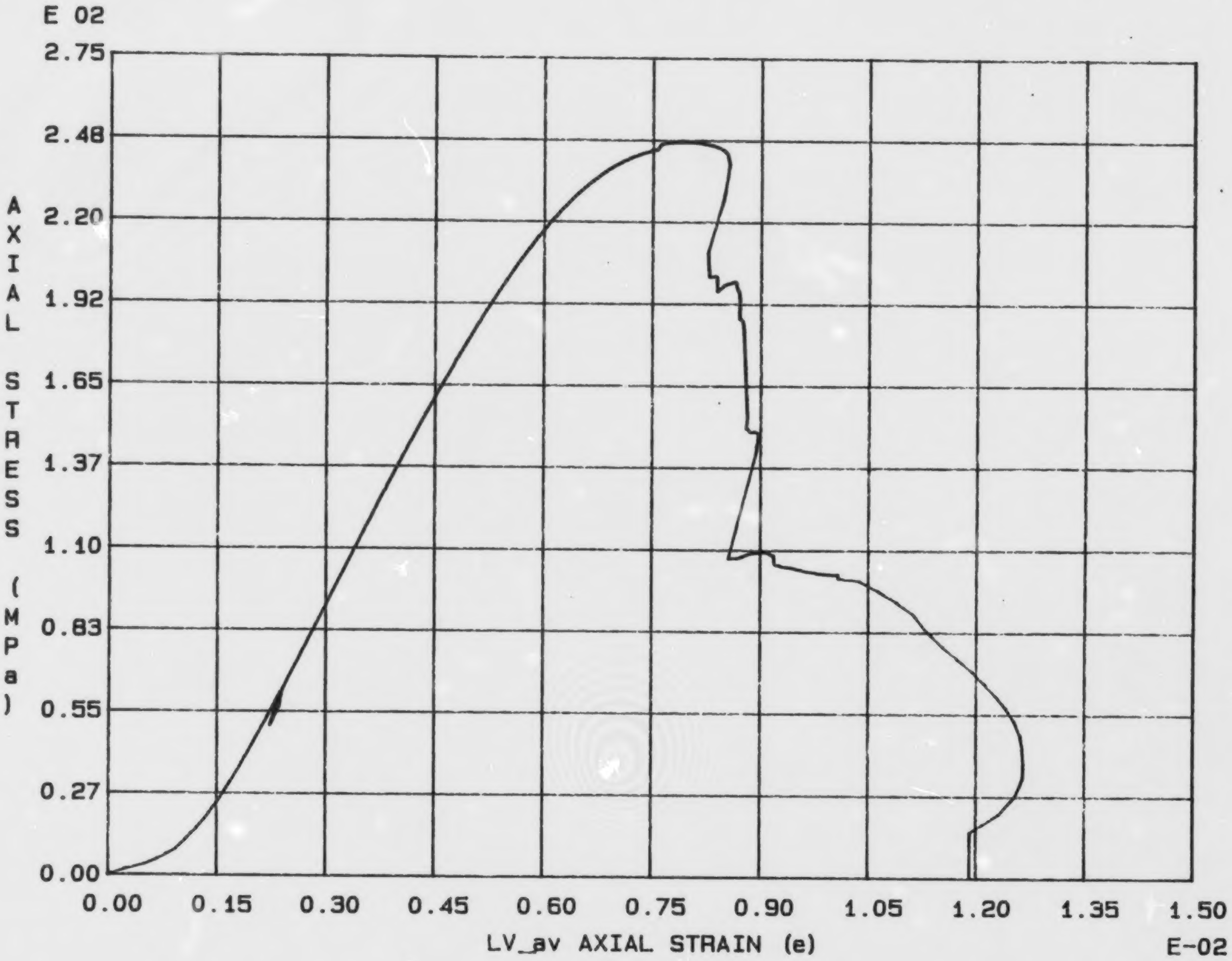
E 02
2.75
2.48
2.20
1.92
1.65
1.37
1.10
0.83
0.55
0.27
0.00
AXIAL STRESS (MPa)
0.00
0.15
0.30
0.45
0.60
0.75
0.90
1.05
1.20
1.35
1.50
E-02
LV_av AXIAL STRAIN (e)

N18

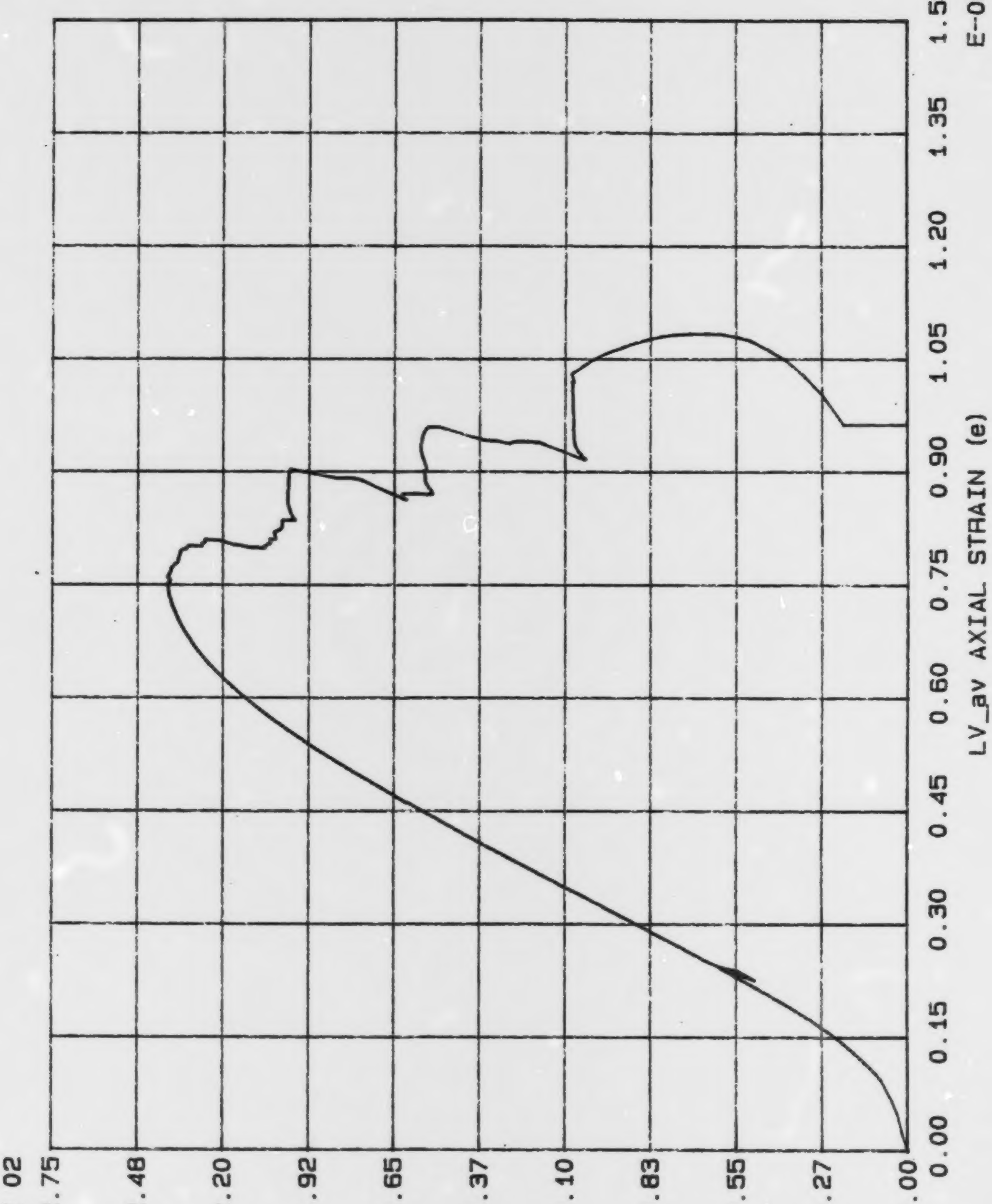
E 02
2.75
2.48
2.20
1.92
1.65
1.37
1.10
0.83
0.55
0.27
0.00
AXIAL STRESS (MPa)
0.00
0.15
0.30
0.45
0.60
0.75
0.90
1.05
1.20
1.35
1.50
E-02
LV_av AXIAL STRAIN (e)
N19

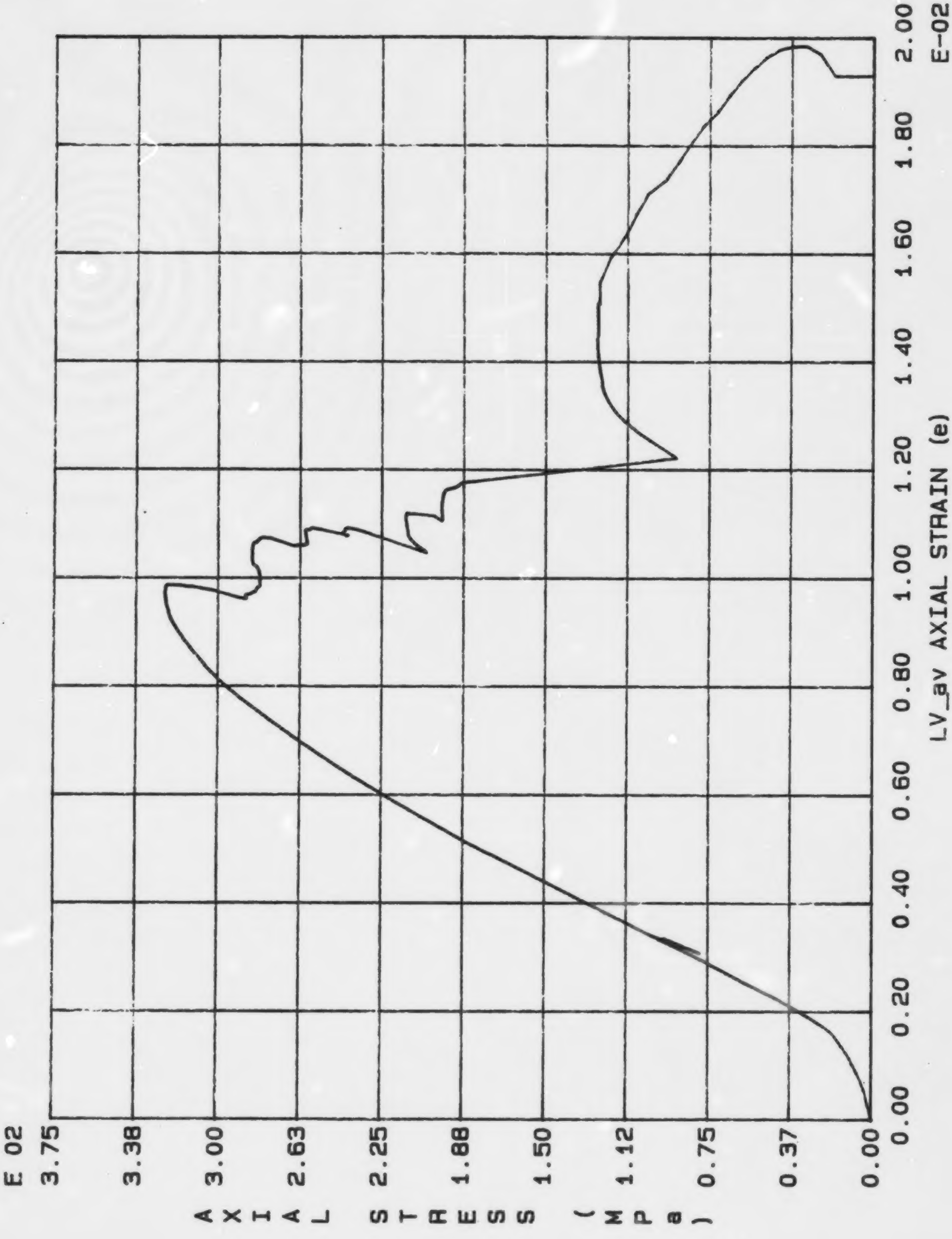
AXIAL STRESS (MPa)
E 02
3.75
3.38
3.00
2.63
2.25
1.88
1.50
1.12
0.75
0.37
0.00
0.00
0.20
0.40
0.60
0.80
1.00
1.20
1.40
1.60
1.80
2.00
E-02
LV_av AXIAL STRAIN (e)

N20

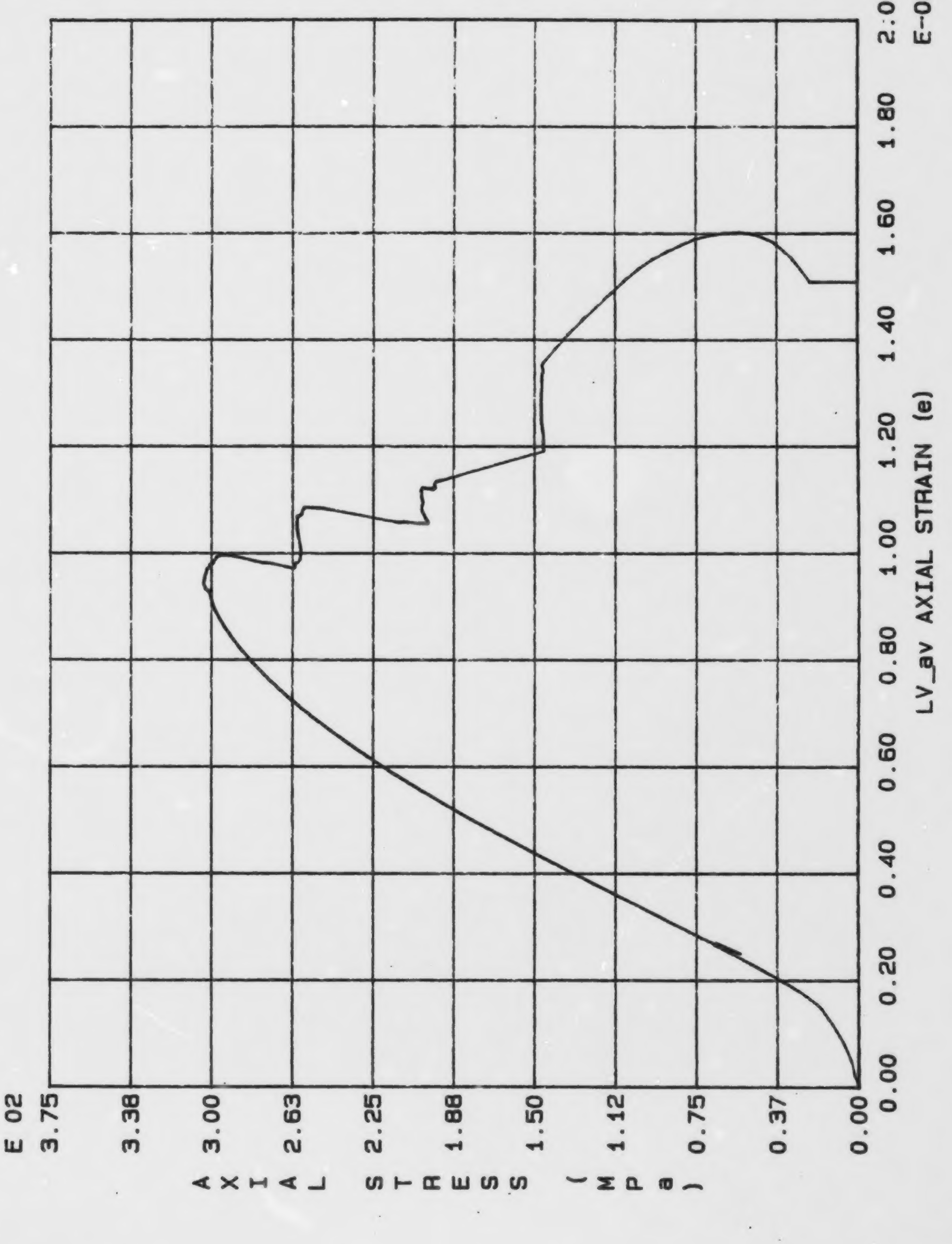
E 02
3.75
3.38
3.00
2.63
2.25
1.88
1.50
1.12
0.75
0.37
0.00
AXIAL STRESS (MPa)
0.00
0.20
0.40
0.60
0.80
1.00
1.20
1.40
1.60
1.80
2.00
E-02
LV_av AXIAL STRAIN (e)

N21

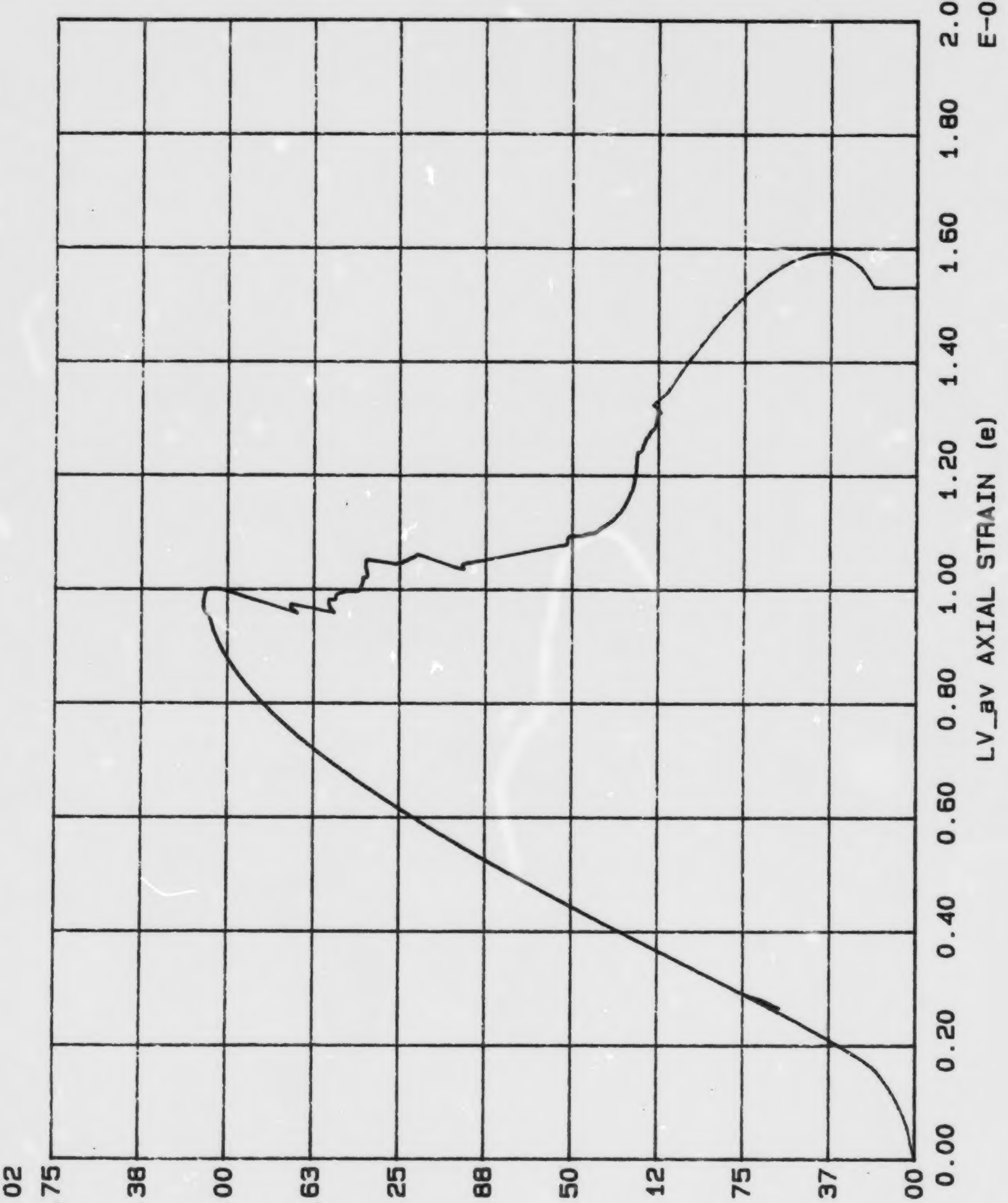
AXIAL STRESS (MPa)
E 02
3.75
3.38
3.00
2.63
2.25
1.88
1.50
1.12
0.75
0.37
0.00
0.00
0.20
0.40
0.60
0.80
1.00
1.20
1.40
1.60
1.80
2.00
E-02
LV_av AXIAL STRAIN (e)
N22

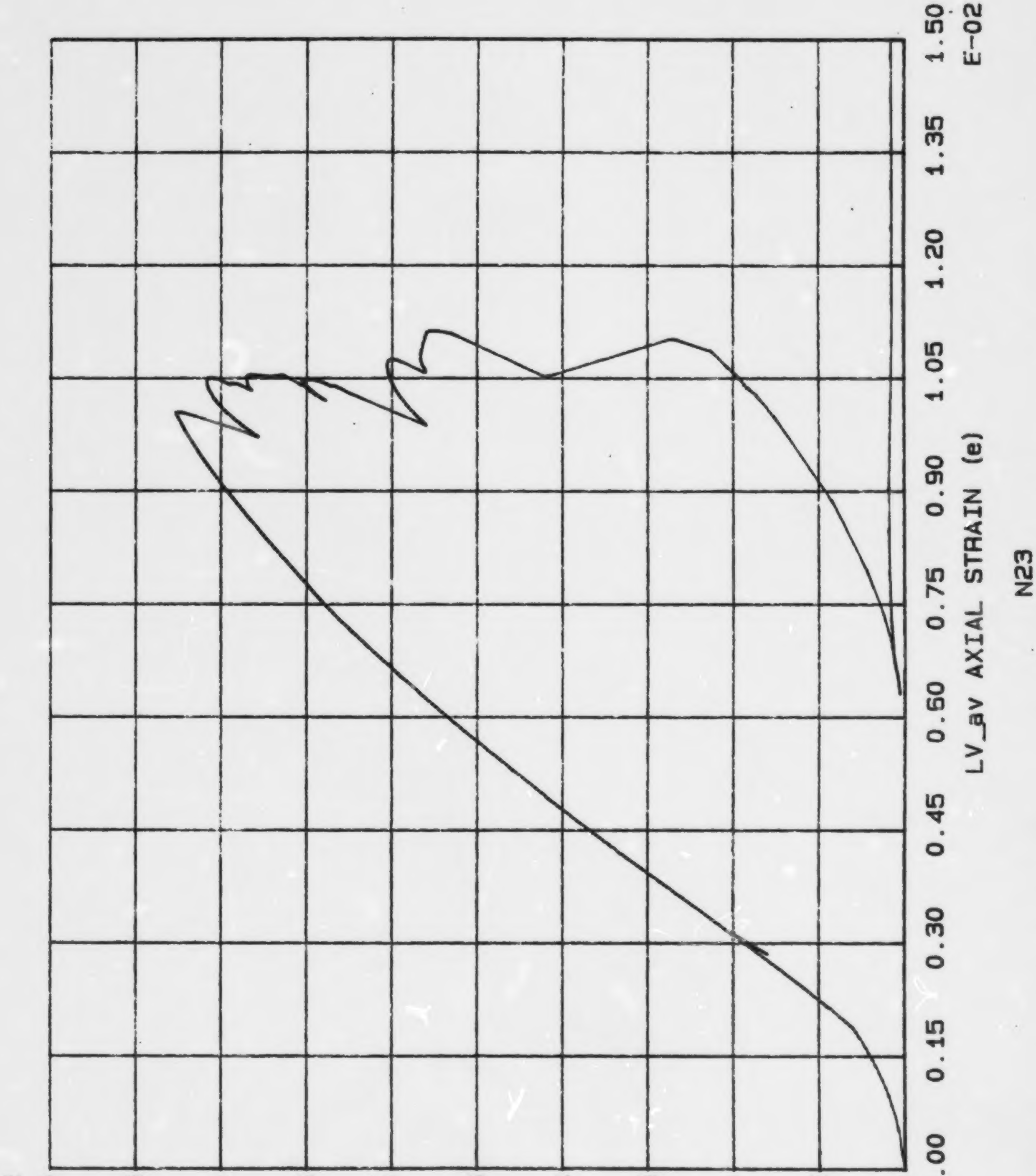
E 02
4.50
4.05
3.60
3.15
2.70
2.25
1.80
1.35
0.90
0.45
0.00
AXIAL STRESS (MPa)
0.00
0.15
0.30
0.45
0.60
0.75
0.90
1.05
1.20
1.35
1.50
E-02
LV_av AXIAL STRAIN (e)
N23

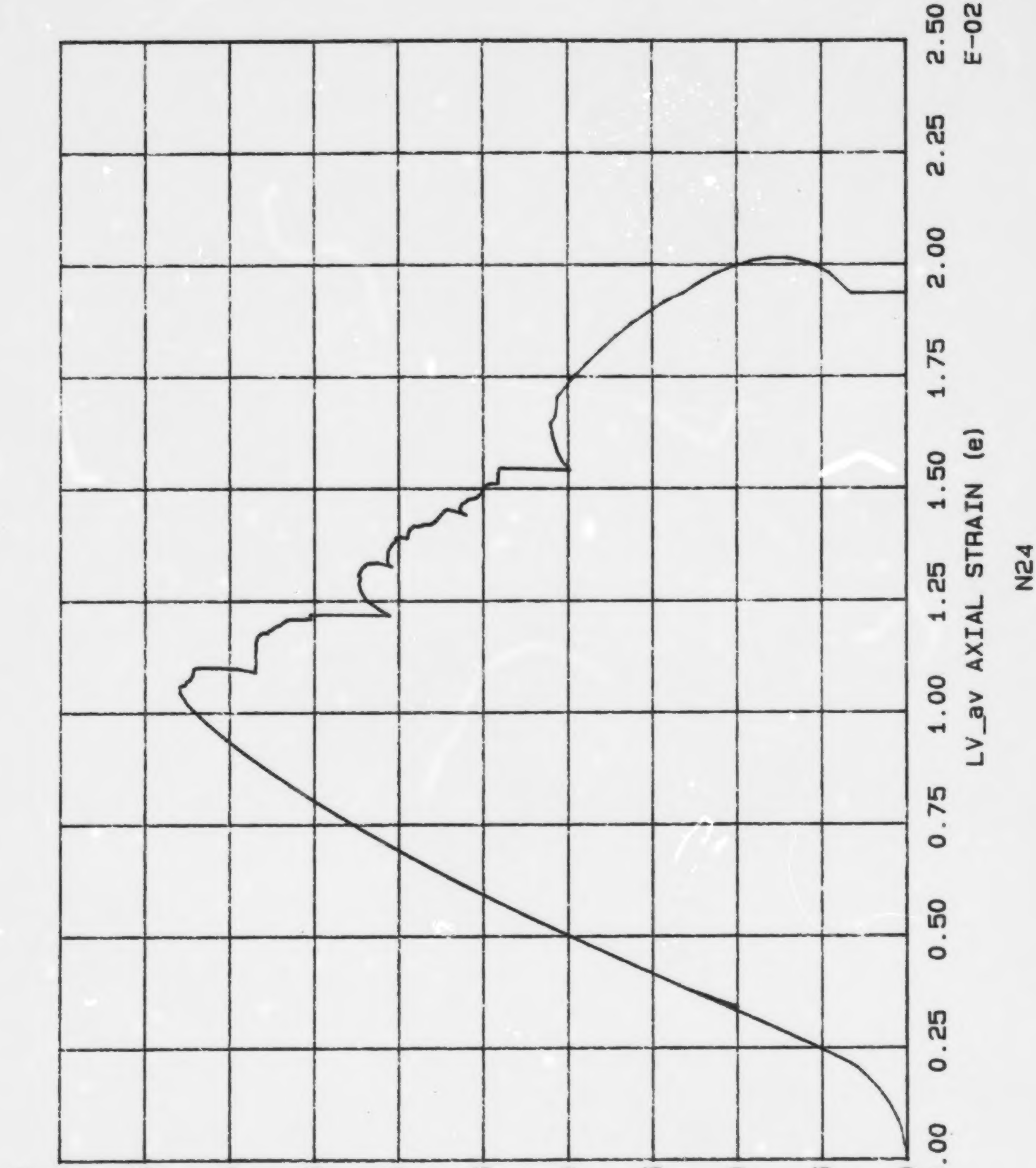
E 02
4.50
4.05
3.60
3.15
2.70
2.25
1.80
1.35
0.90
0.45
0.00
AXIAL STRESS (MPa)
0.00
0.25
0.50
0.75
1.00
1.25
1.50
1.75
2.00
2.25
2.50
E-02
LV_av AXIAL STRAIN (e)
N24

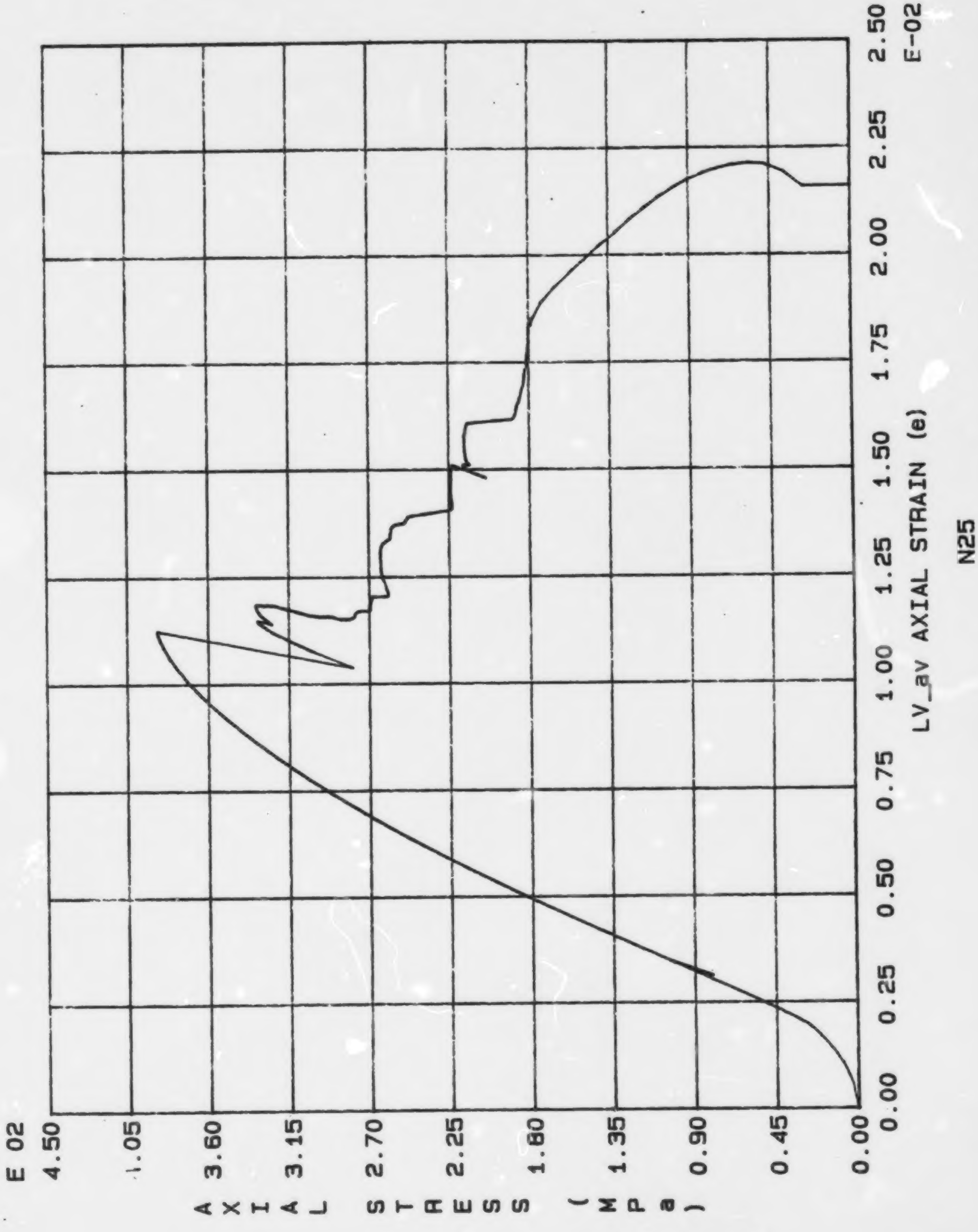
E 02
4.50
4.05
3.60
3.15
2.70
2.25
1.80
1.35
0.90
0.45
0.00
AXIAL STRESS (MPa)
0.00
0.25
0.50
0.75
1.00
1.25
1.50
1.75
2.00
2.25
2.50
E-02
LV_av AXIAL STRAIN (e)
N25

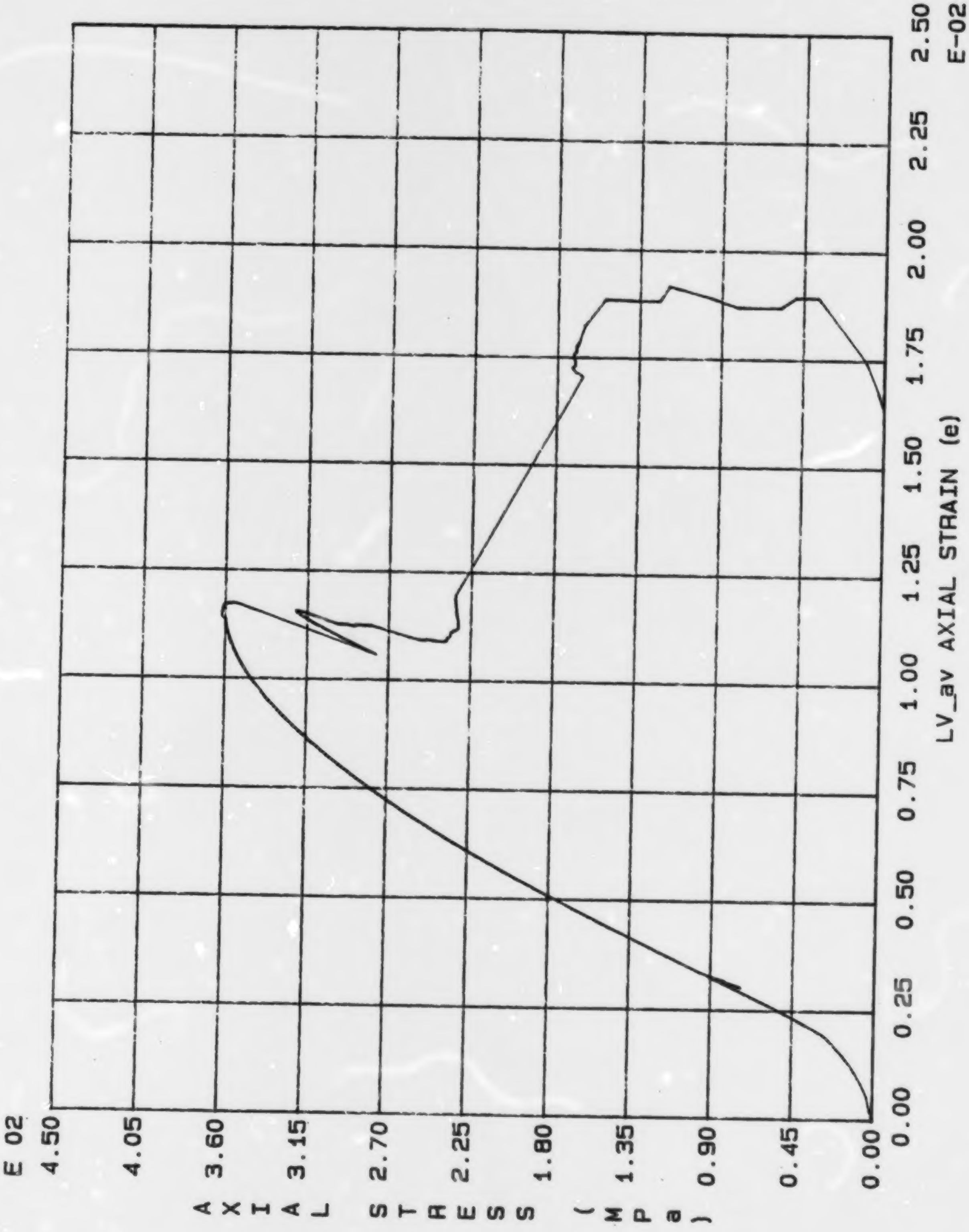
E 02
4.50
4.05
3.60
3.15
2.70
2.25
1.80
1.35
0.90
0.45
0.00
AXIAL STRESS (MPa)
0.00
0.25
0.50
0.75
1.00
1.25
1.50
1.75
2.00
2.25
2.50
E-02
LV_av AXIAL STRAIN (e)
N26

APPENDIX D-2

Stress vs. strain - circumferential extensometer

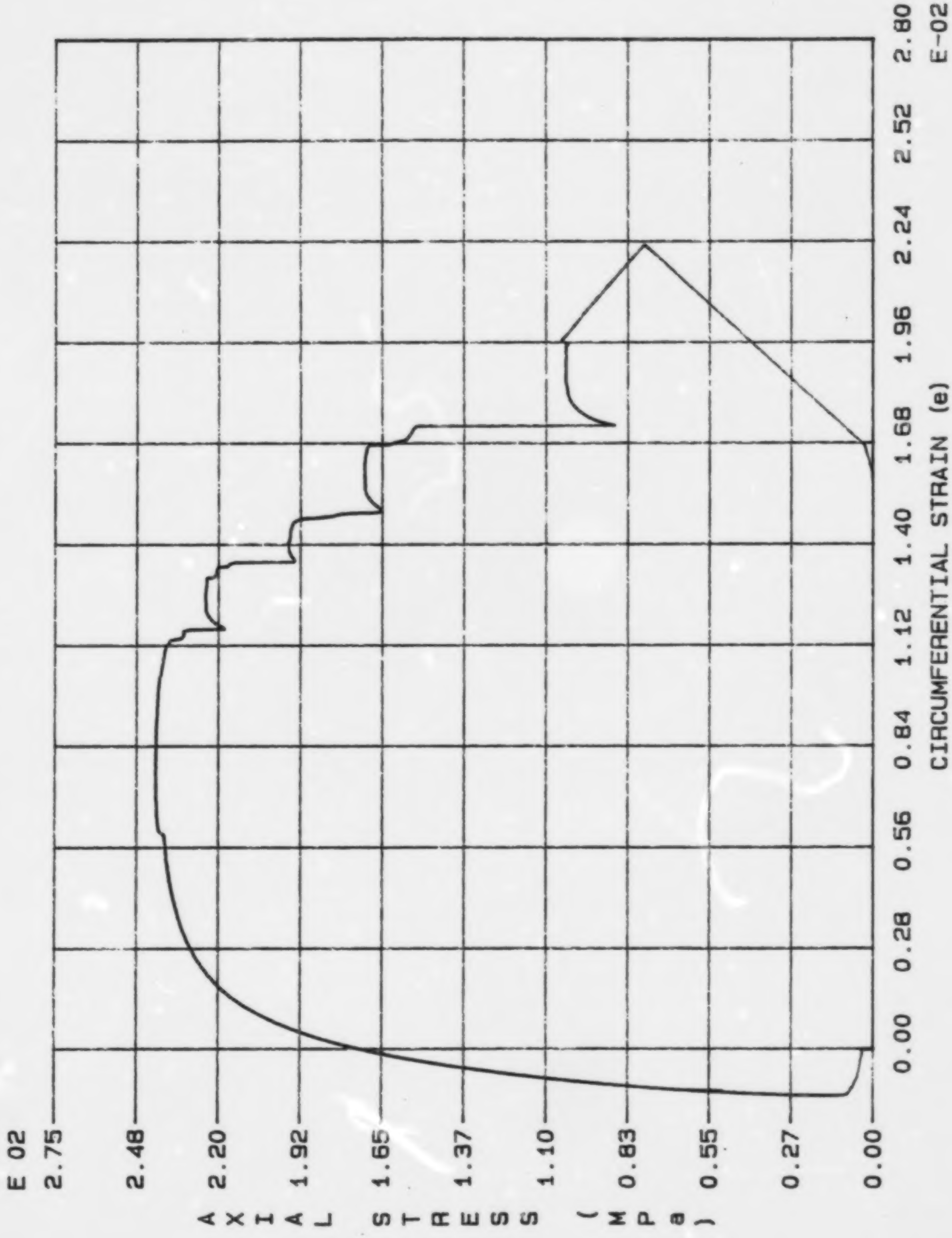
AXIAL STRESS (MPa)
E 02
2.75
2.48
2.20
1.92
1.65
1.37
1.10
0.83
0.55
0.27
0.00
0.00
0.28
0.56
0.84
1.12
1.40
1.68
1.96
2.24
2.52
2.80
E-02
CIRCUMFERENTIAL STRAIN (e)

N17

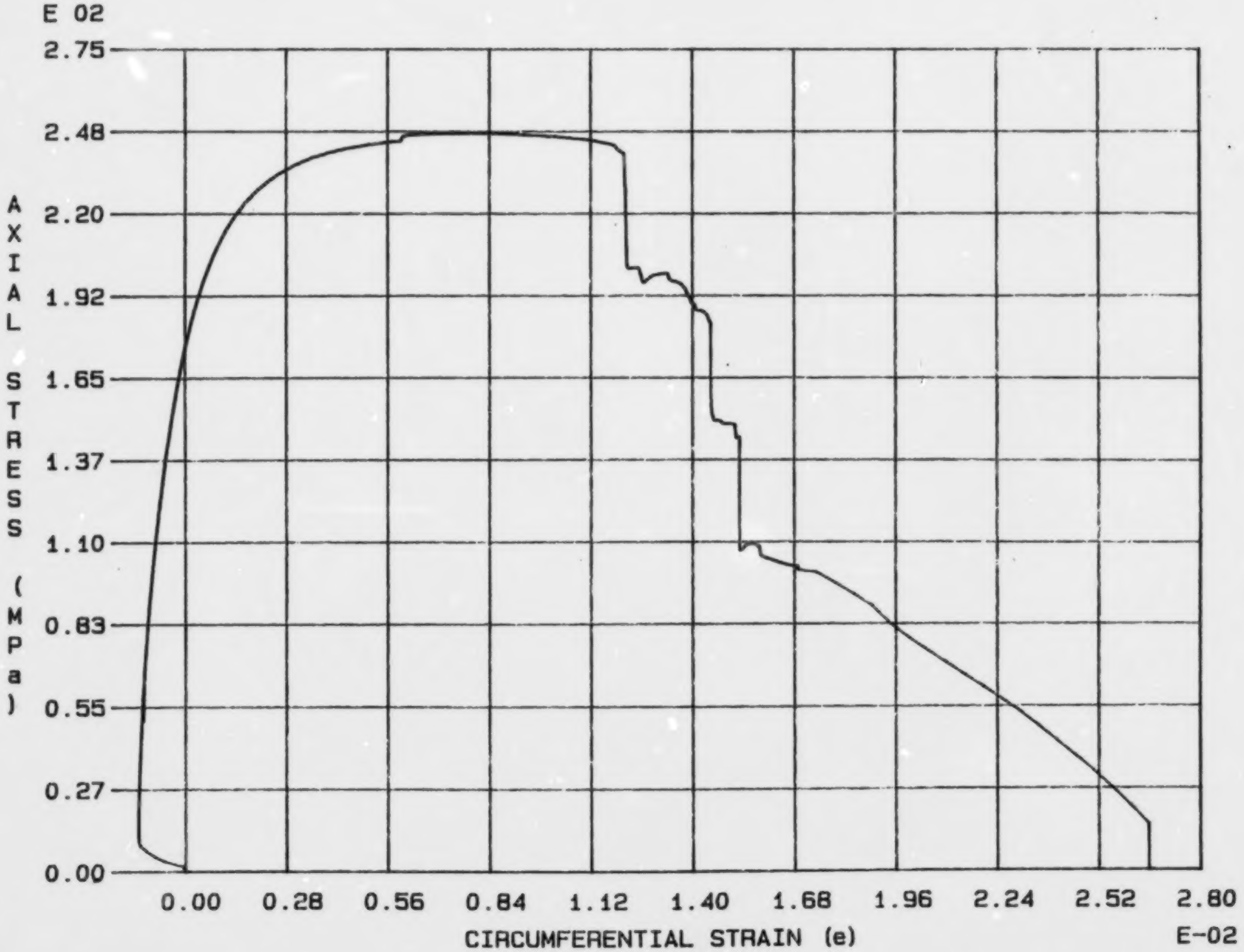
E 02
2.75
2.48
2.20
1.92
1.65
1.37
1.10
0.83
0.55
0.27
0.00
AXIAL STRESS (MPa)
0.00
0.28
0.56
0.84
1.12
1.40
1.68
1.96
2.24
2.52
2.80
E-02
CIRCUMFERENTIAL STRAIN (e)

N18

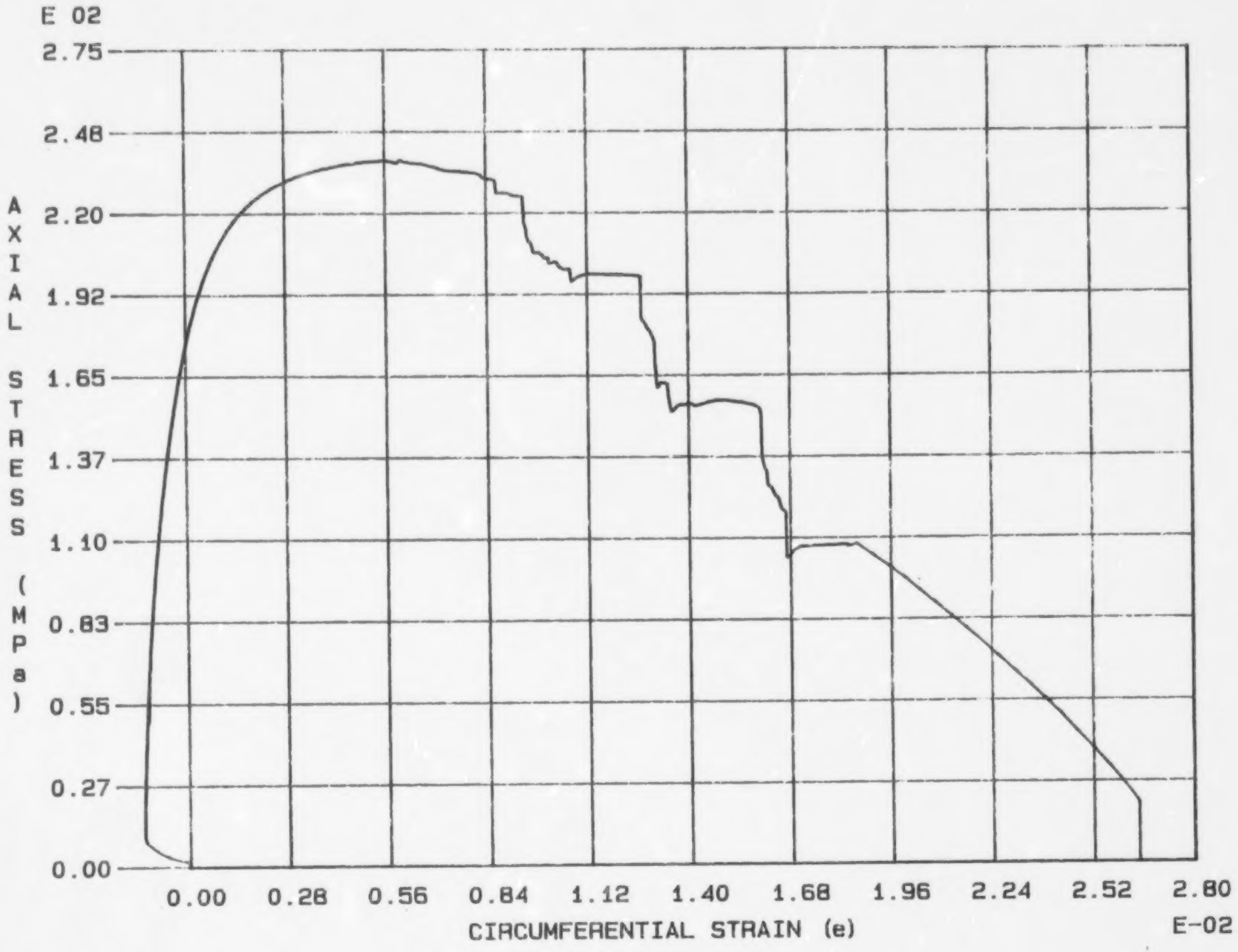
E 02
2.75
2.48
2.20
1.92
1.65
1.37
1.10
0.83
0.55
0.27
0.00
AXIAL STRESS (MPa)
0.00
0.28
0.56
0.84
1.12
1.40
1.68
1.96
2.24
2.52
2.80
E-02
CIRCUMFERENTIAL STRAIN (e)

N19

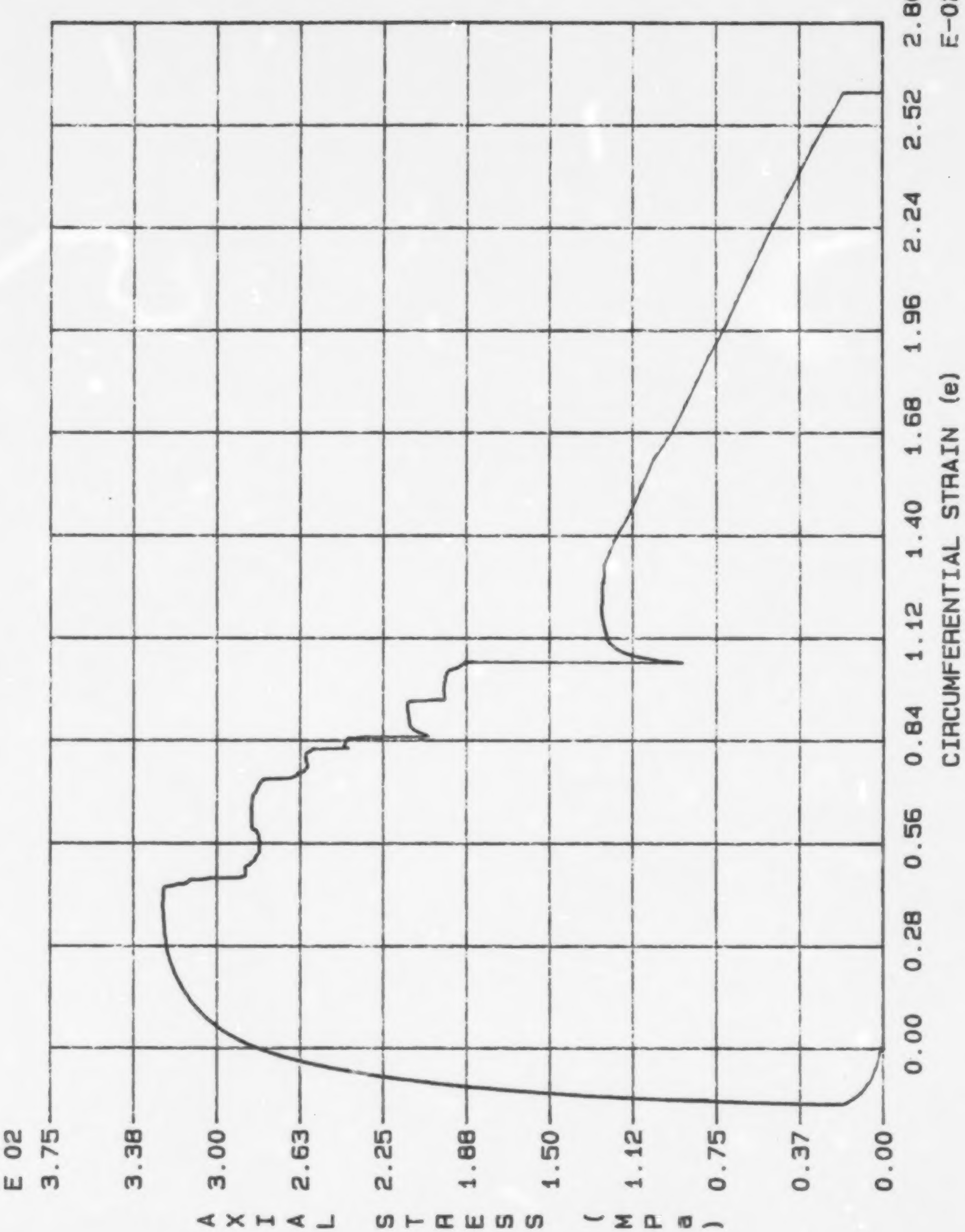
E 02
3.75
3.38
3.00
2.63
2.25
1.88
1.50
1.12
0.75
0.37
0.00
AXIAL STRESS (MPa)
0.00
0.28
0.56
0.84
1.12
1.40
1.68
1.96
2.24
2.52
2.80
E-02
CIRCUMFERENTIAL STRAIN (e)

N20

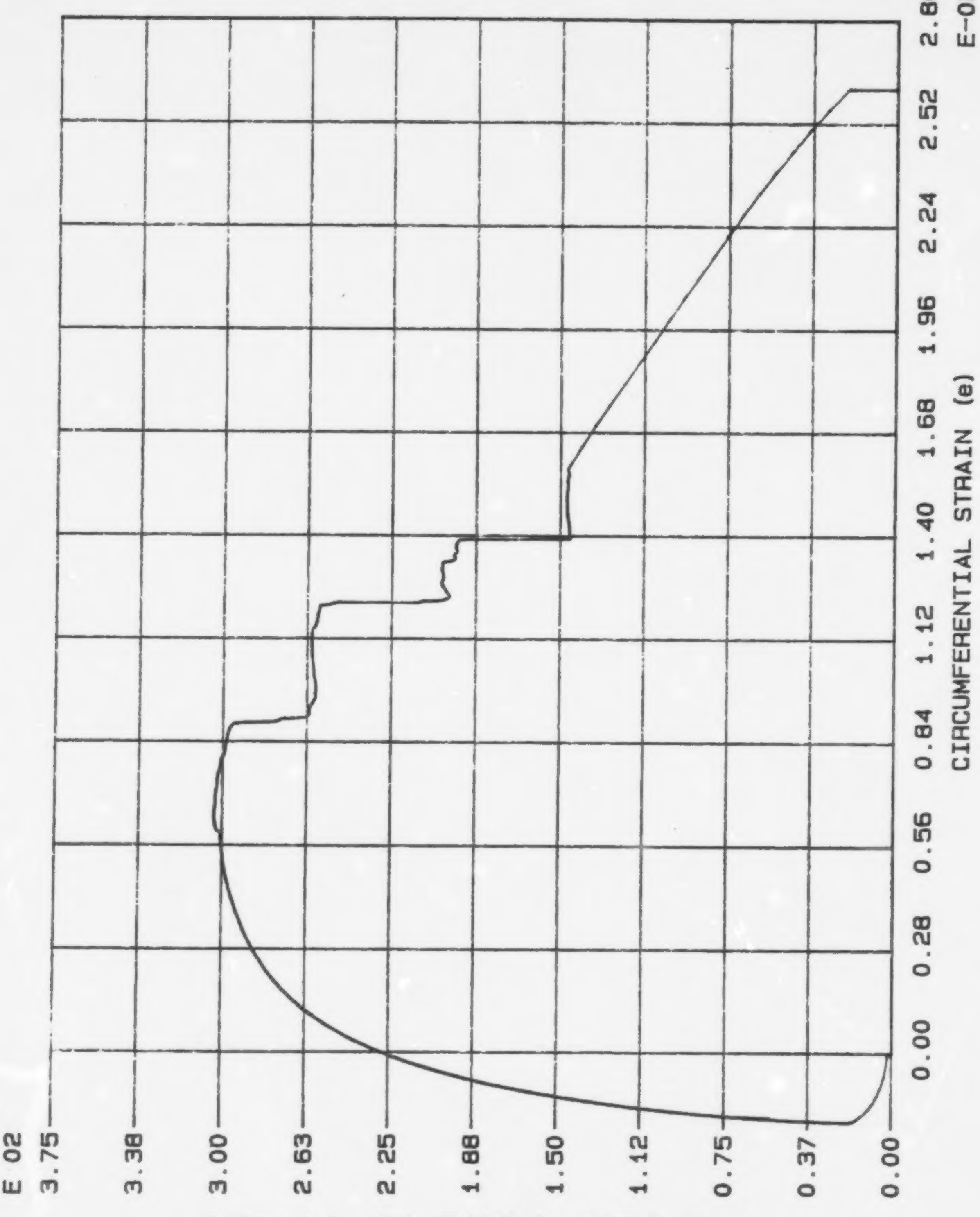
E 02
3.75
3.38
3.00
2.63
2.25
1.88
1.50
1.12
0.75
0.37
0.00
AXIAL STRESS (MPa)
0.00
0.28
0.56
0.84
1.12
1.40
1.68
1.96
2.24
2.52
2.80
E-02
CIRCUMFERENTIAL STRAIN (e)
N21

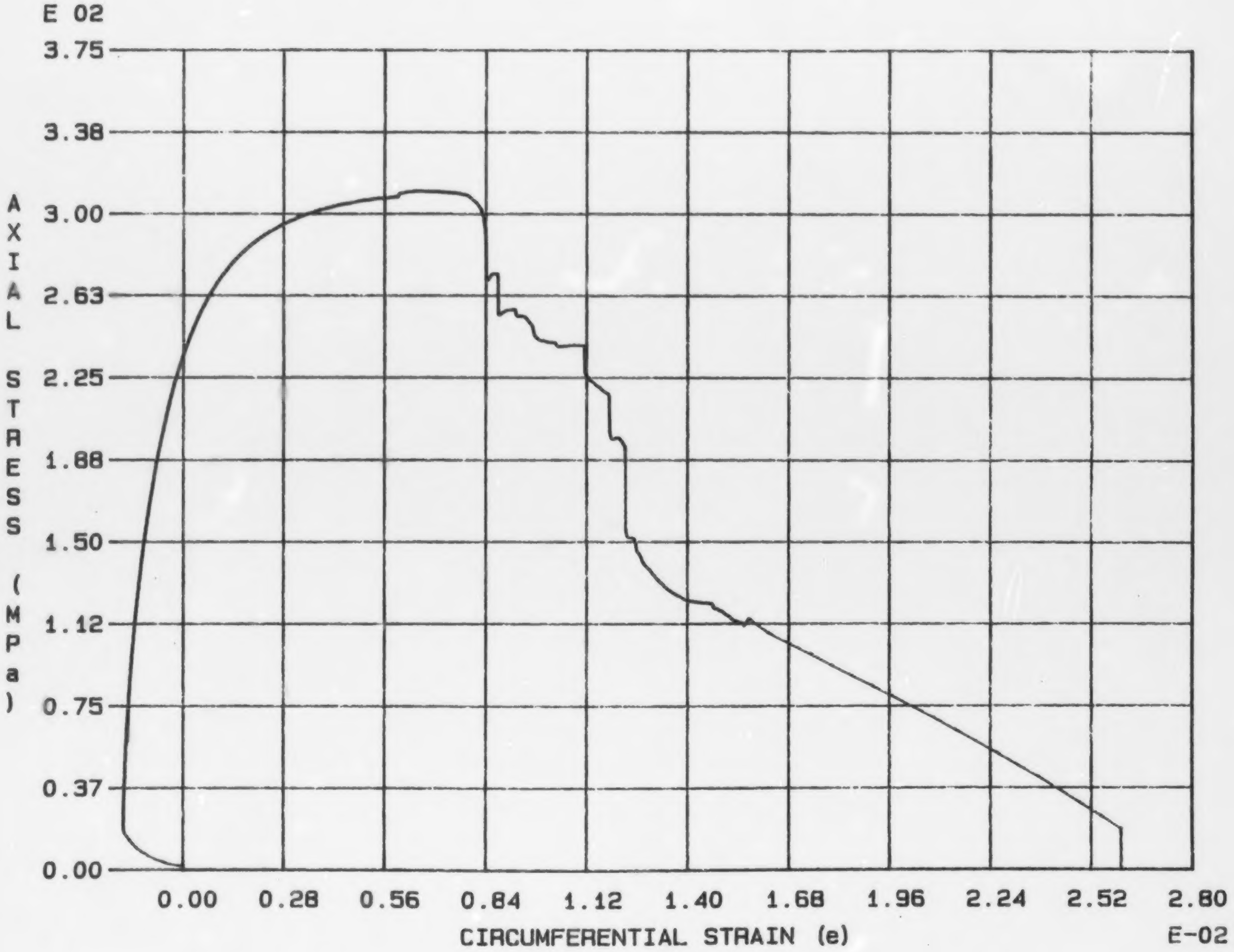
E 02
3.75
3.38
3.00
2.63
2.25
1.88
1.50
1.12
0.75
0.37
0.00
AXIAL STRESS (MPa)
0.00
0.28
0.56
0.84
1.12
1.40
1.68
1.96
2.24
2.52
2.80
E-02
CIRCUMFERENTIAL STRAIN (e)

N22

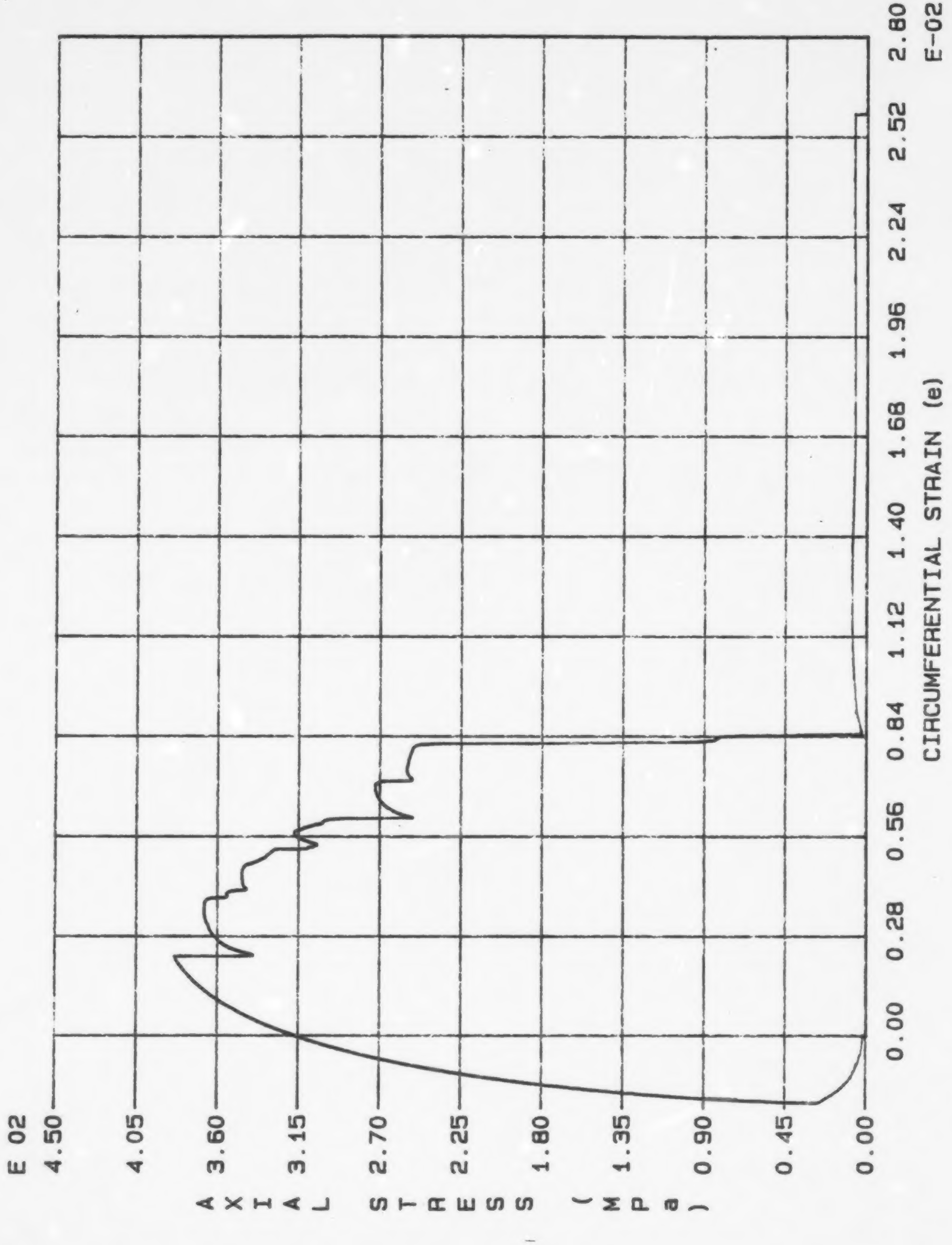
AXIAL STRESS (MPa)
E 02
4.50
4.05
3.60
3.15
2.70
2.25
1.80
1.35
0.90
0.45
0.00
CIRCUMFERENTIAL STRAIN (e)
E-02
0.00
0.28
0.56
0.84
1.12
1.40
1.68
1.96
2.24
2.52
2.80

N23

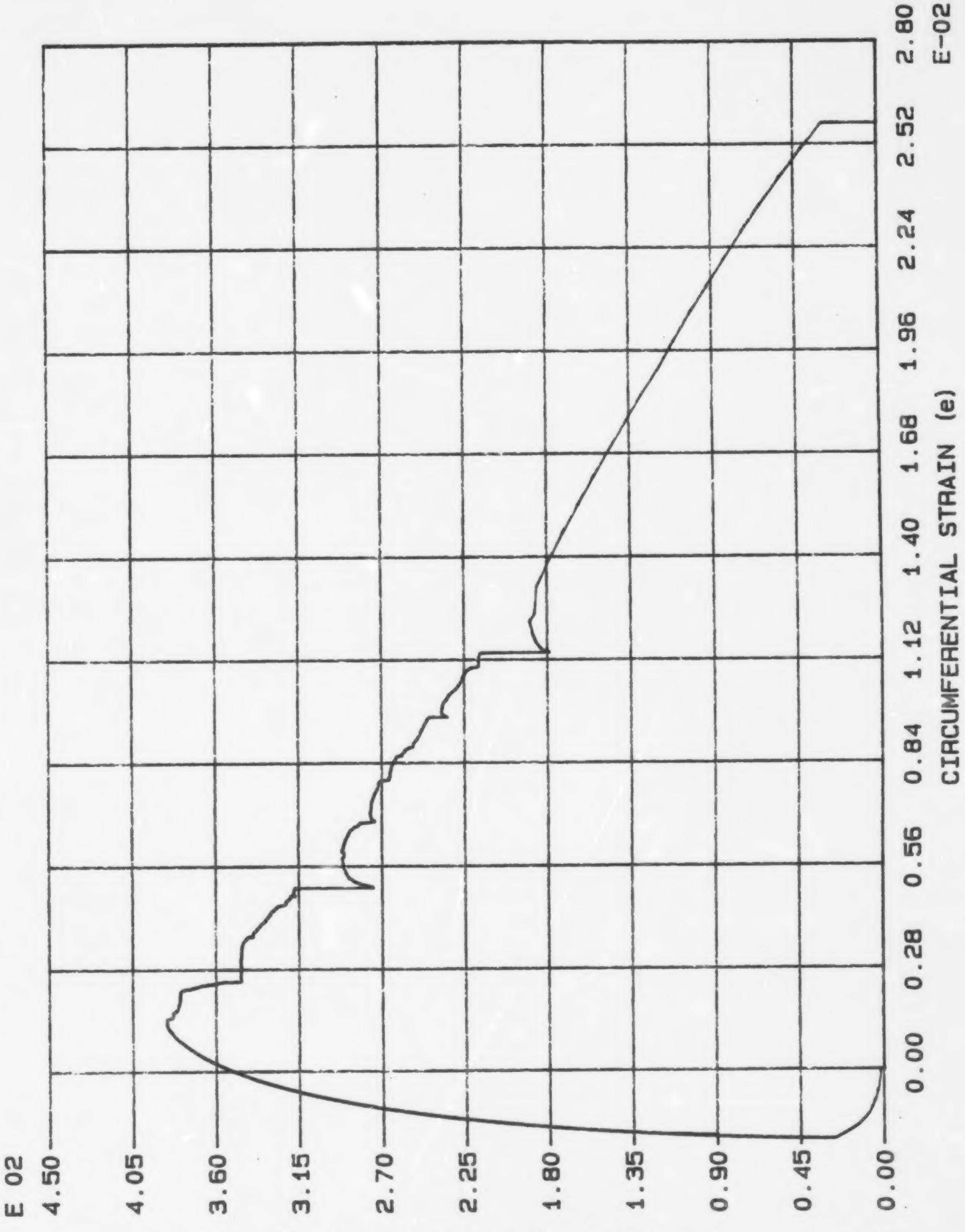
AXIAL STRESS (MPa)
E 02
4.50
4.05
3.60
3.15
2.70
2.25
1.80
1.35
0.90
0.45
0.00
0.00
0.28
0.56
0.84
1.12
1.40
1.68
1.96
2.24
2.52
2.80
E-02
CIRCUMFERENTIAL STRAIN (e)

N24

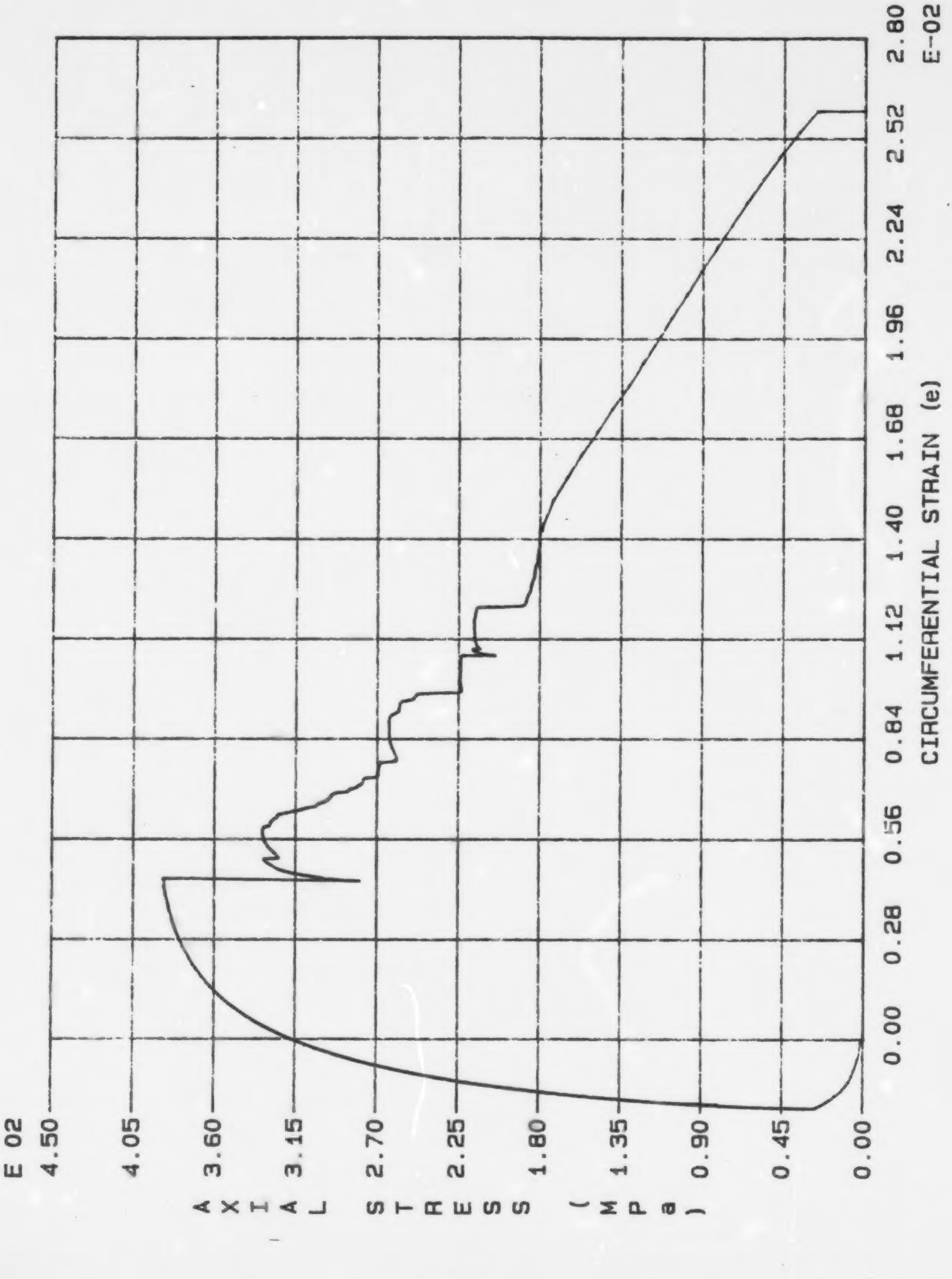
E 02
4.50
4.05
3.60
3.15
2.70
2.25
1.80
1.35
0.90
0.45
0.00
AXIAL STRESS (MPa)
0.00
0.28
0.56
0.84
1.12
1.40
1.68
1.96
2.24
2.52
2.80
E-02
CIRCUMFERENTIAL STRAIN (e)

N25

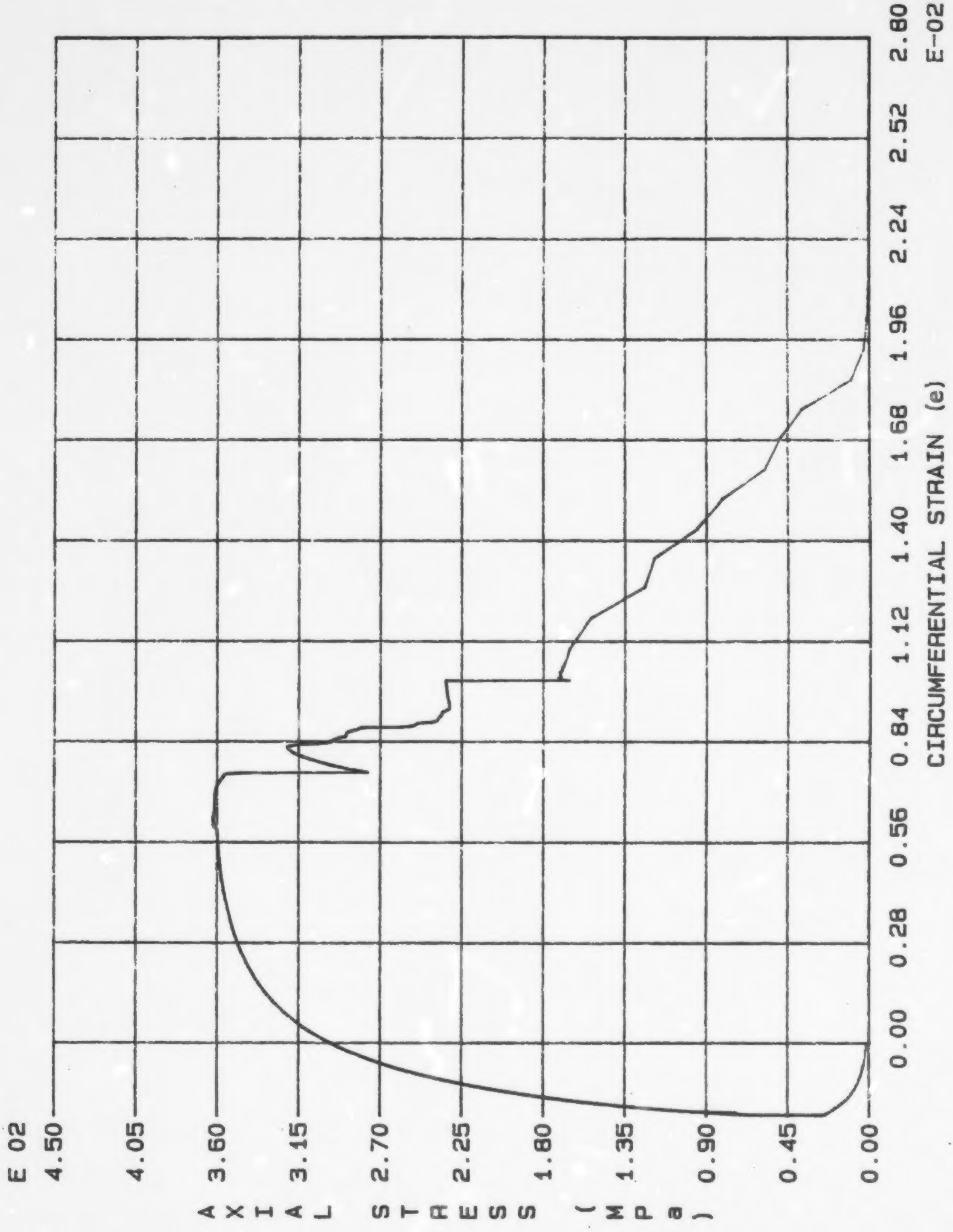
AXIAL STRESS (MPa)
E 02
4.50
4.05
3.60
3.15
2.70
2.25
1.80
1.35
0.90
0.45
0.00
0.00
0.28
0.56
0.84
1.12
1.40
1.68
1.96
2.24
2.52
2.80
E-02
CIRCUMFERENTIAL STRAIN (e)

N26

APPENDIX E

Multi stage triaxial tests - circumferential control

APPENDIX E-1

Stress vs. strain - axial lvdts

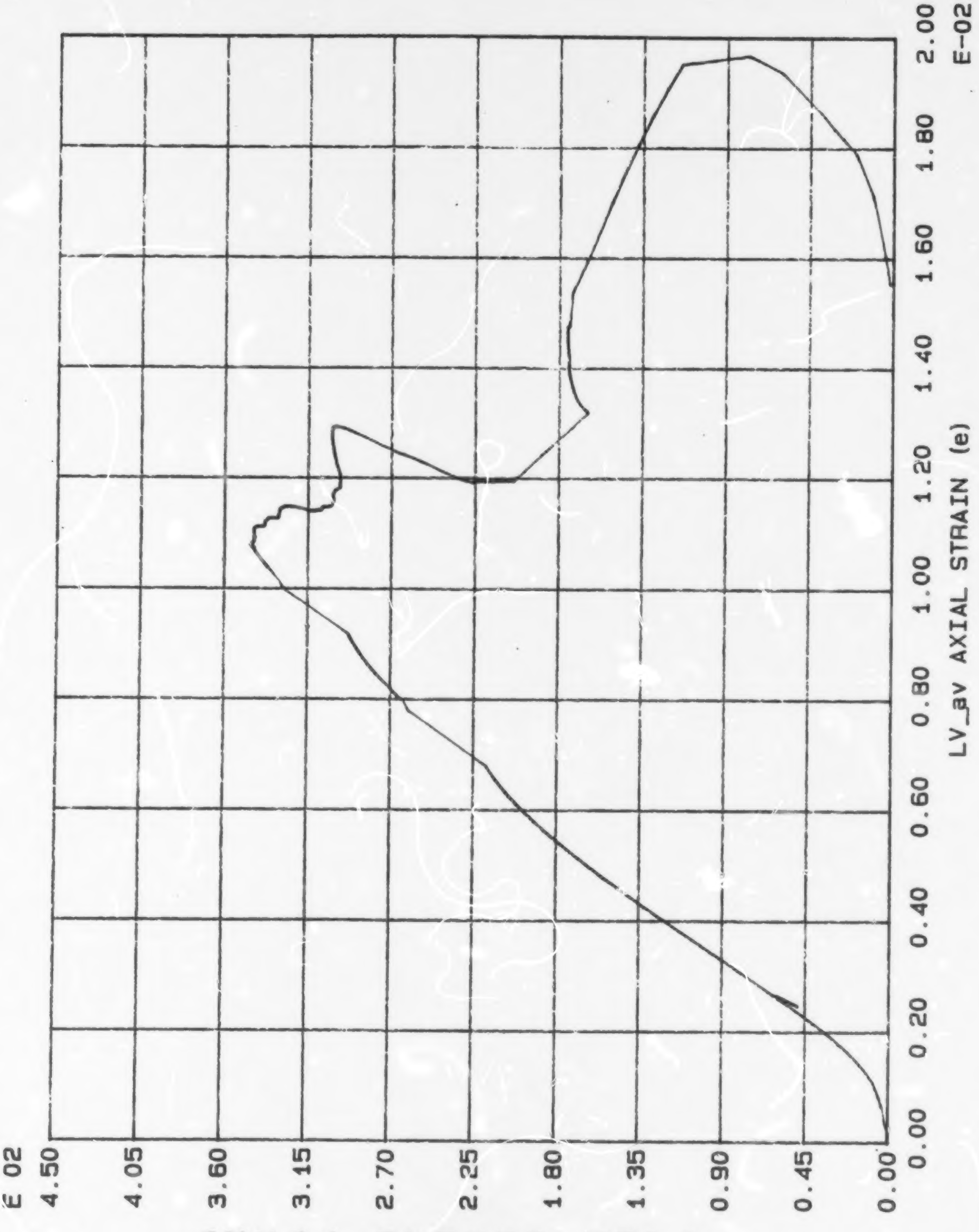
AXIAL STRESS (MPa)
E 02
4.50
4.05
3.60
3.15
2.70
2.25
1.80
1.35
0.90
0.45
0.00
0.00
0.20
0.40
0.60
0.80
1.00
1.20
1.40
1.60
1.80
2.00
E-02
LV_av AXIAL STRAIN (e)
N27

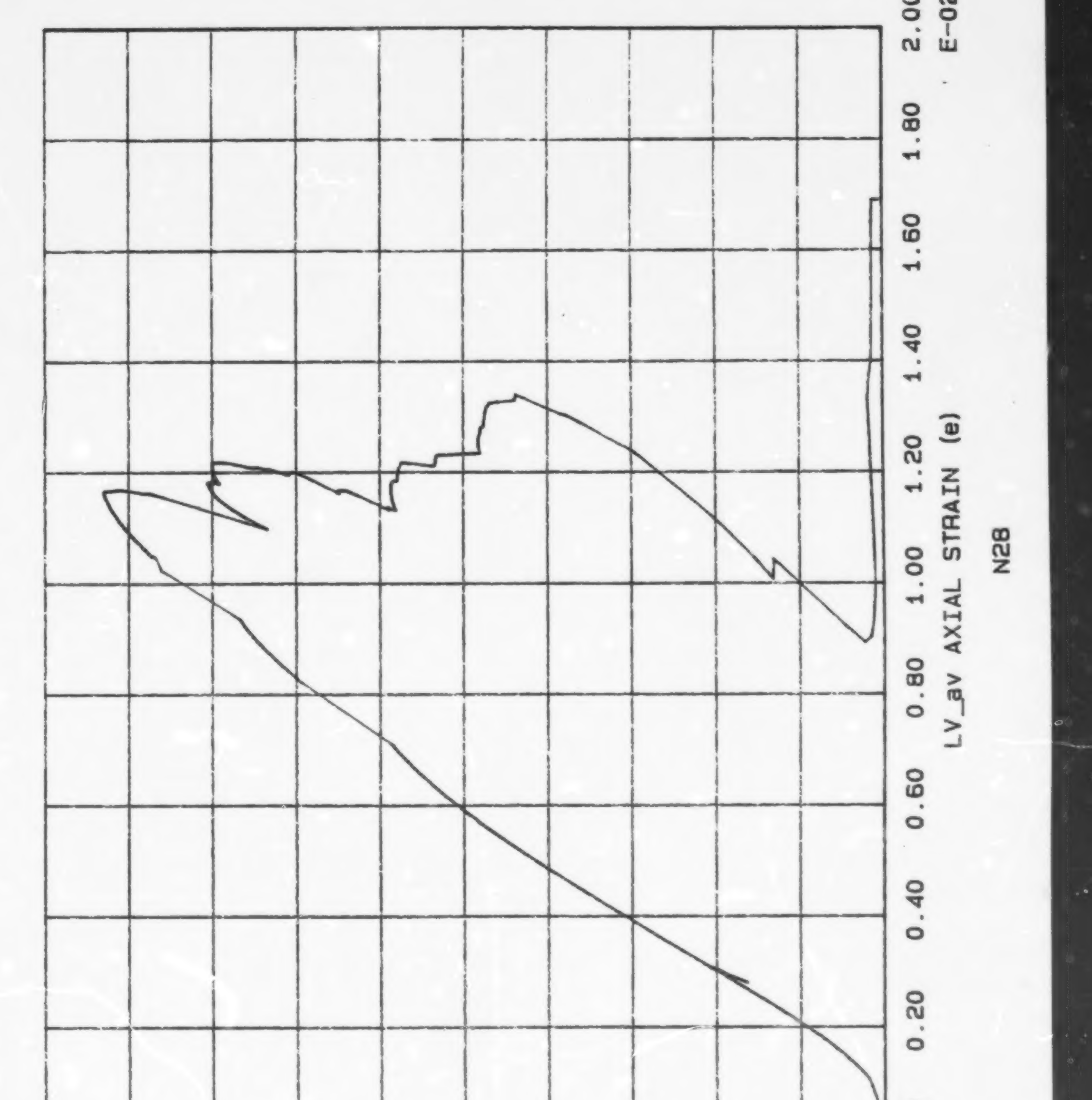
E 02
4.50
4.05
3.60
3.15
2.70
2.25
1.80
1.35
0.90
0.45
0.00
AXIAL STRESS (MPa)
0.00
0.20
0.40
0.60
0.80
1.00
1.20
1.40
1.60
1.80
2.00
E-02
LV_av AXIAL STRAIN (e)
N28

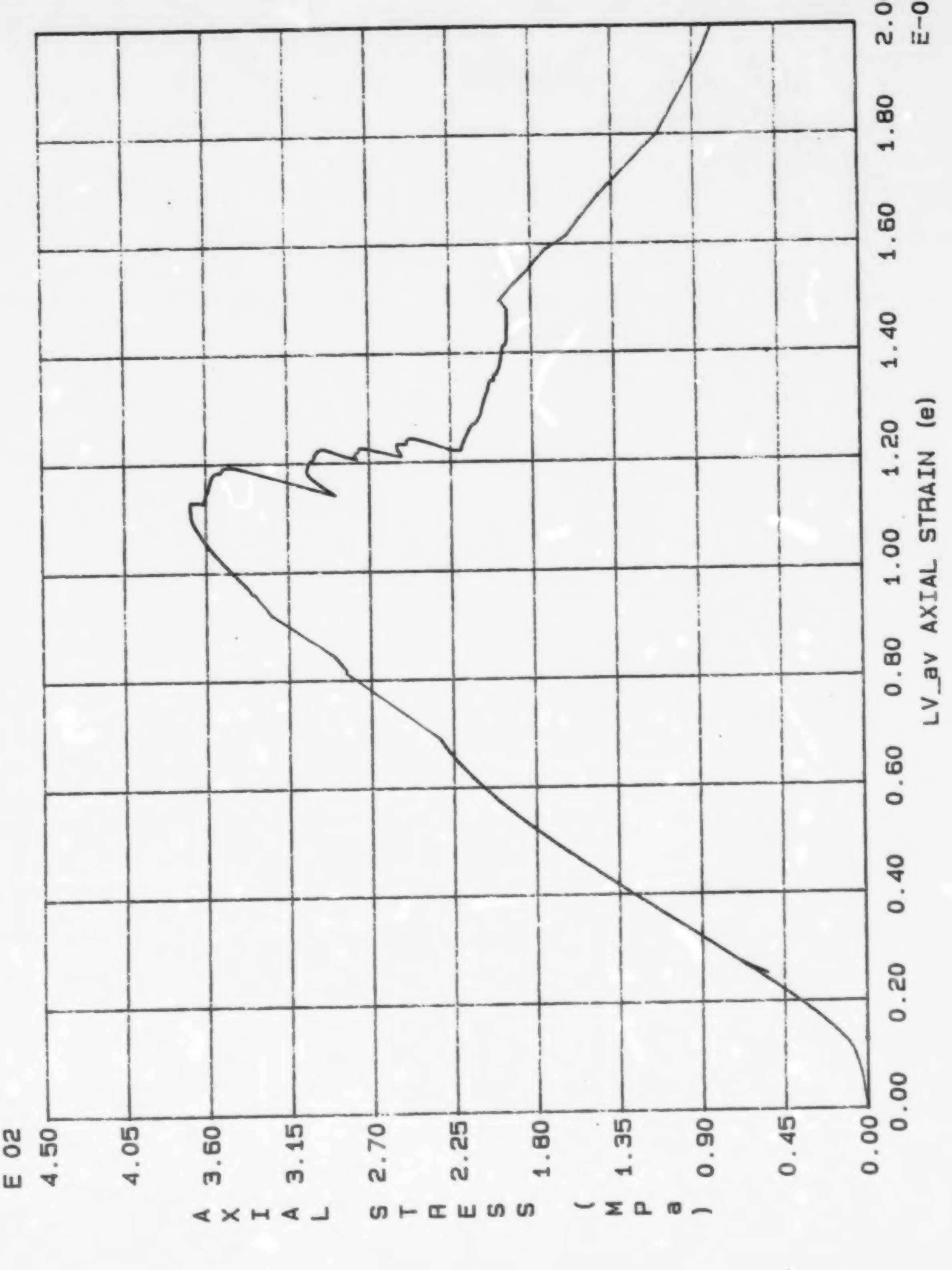
E 02
4.50
4.05
3.60
3.15
2.70
2.25
1.80
1.35
0.90
0.45
0.00
AXIAL STRESS (MPa)
0.00
0.20
0.40
0.60
0.80
1.00
1.20
1.40
1.60
1.80
2.00
E-02
LV_av AXIAL STRAIN (e)

N29

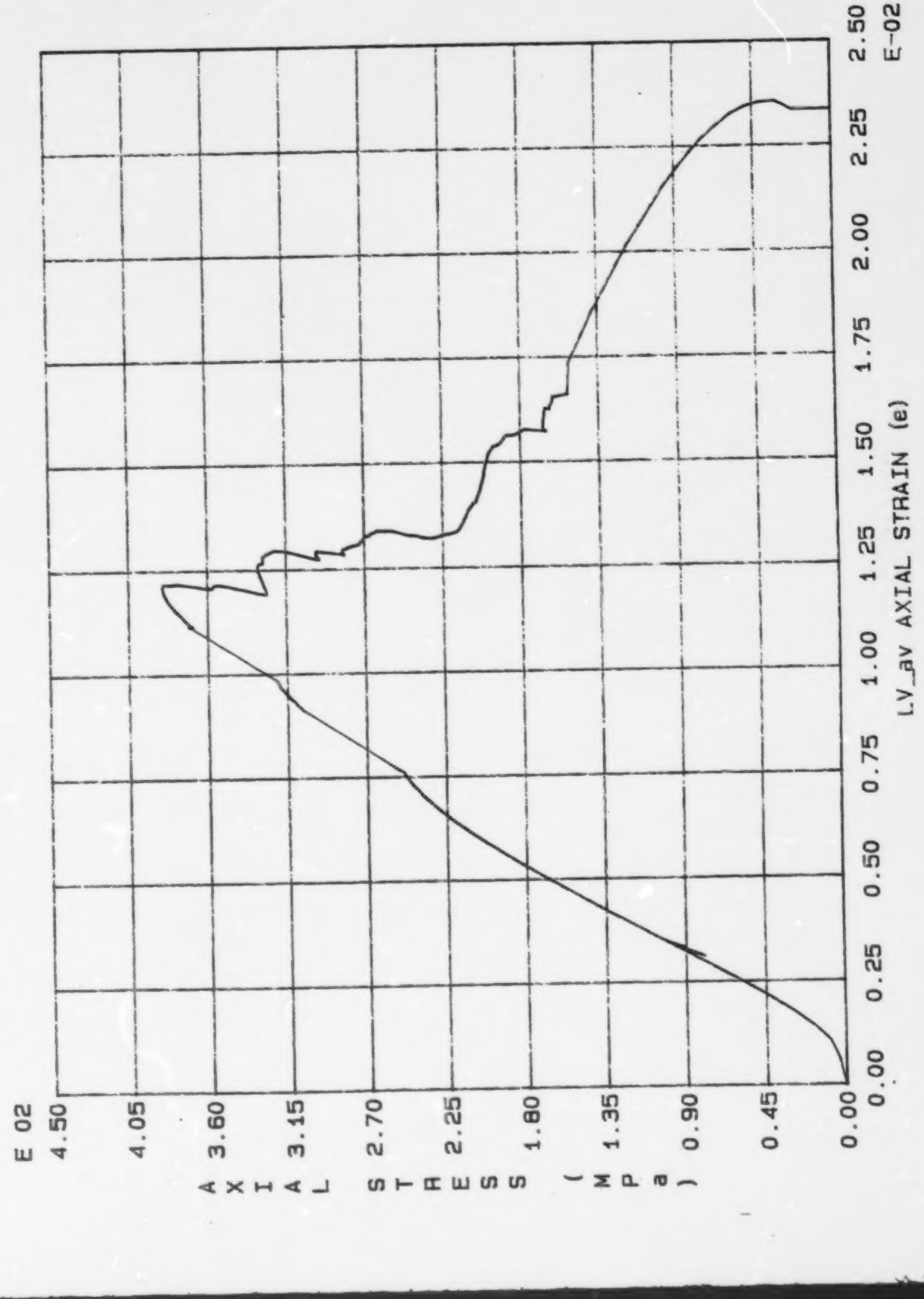
AXIAL STRESS (MPa)
E 02
4.50
4.05
3.60
3.15
2.70
2.25
1.80
1.35
0.90
0.45
0.00
0.00
0.25
0.50
0.75
1.00
1.25
1.50
1.75
2.00
2.25
2.50
E-02
LV_av AXIAL STRAIN (e)

N30

APPENDIX E-2

Stress vs. strain - circumferential extensometer

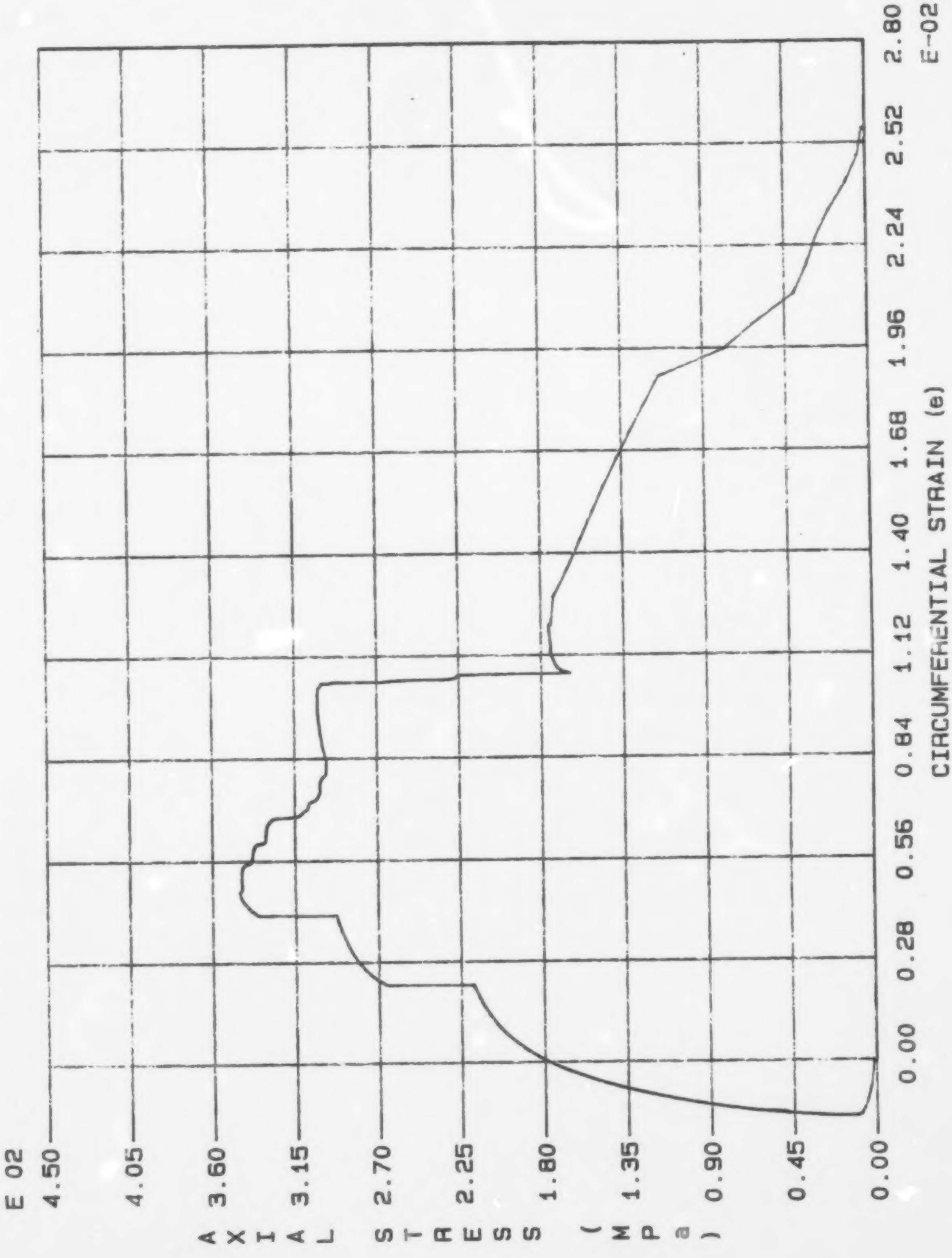
E 02
4.50
4.05
3.60
3.15
2.70
2.25
1.80
1.35
0.90
0.45
0.00
AXIAL STRESS (MPa)
0.00
0.28
0.56
0.84
1.12
1.40
1.68
1.96
2.24
2.52
2.80
E-02
CIRCUMFERENTIAL STRAIN (e)

N27

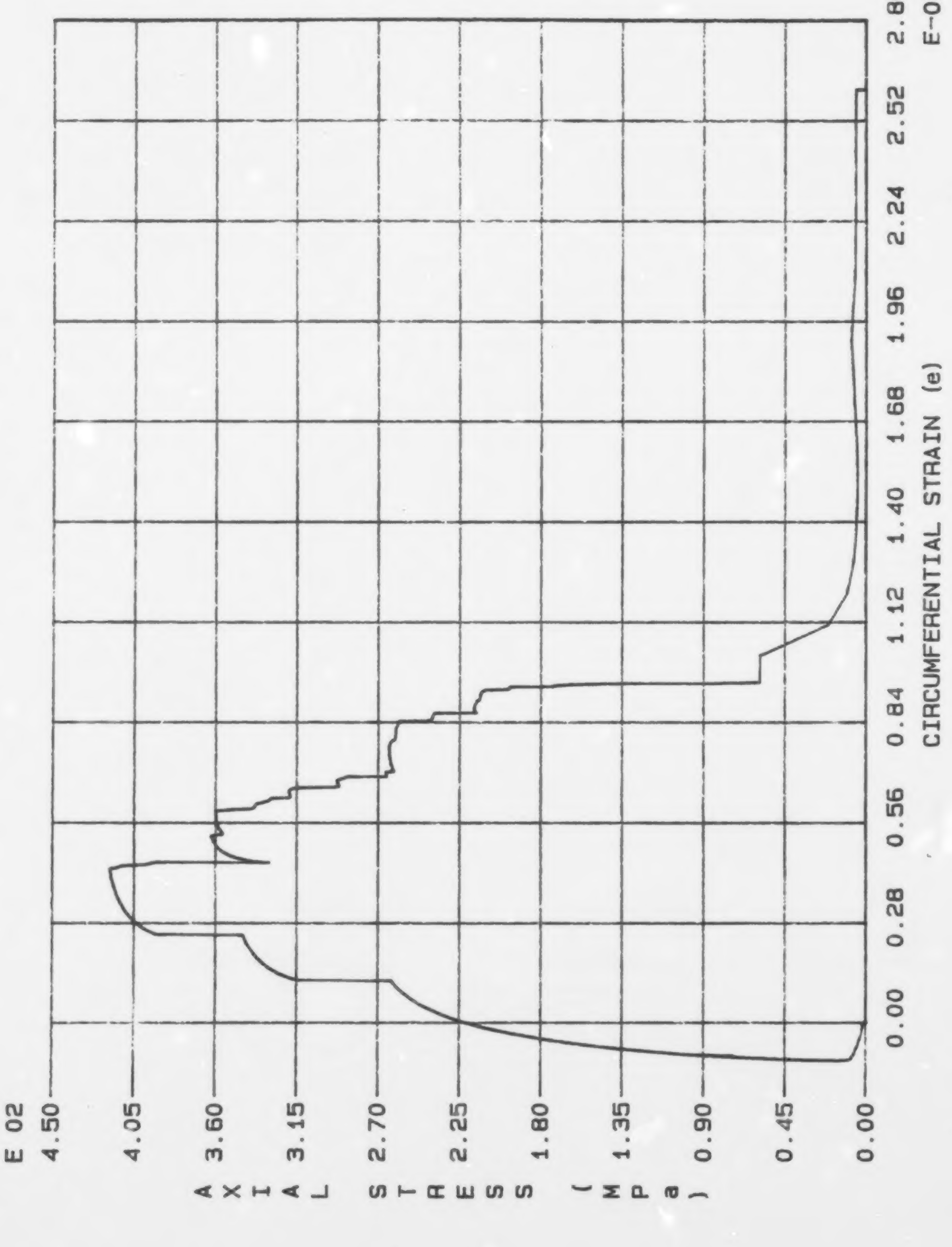
AXIAL STRESS (MPa)
E 02
4.50
4.05
3.60
3.15
2.70
2.25
1.80
1.35
0.90
0.45
0.00
CIRCUMFERENTIAL STRAIN (e)
0.00
0.28
0.56
0.84
1.12
1.40
1.68
1.96
2.24
2.52
2.80
E-02

N28

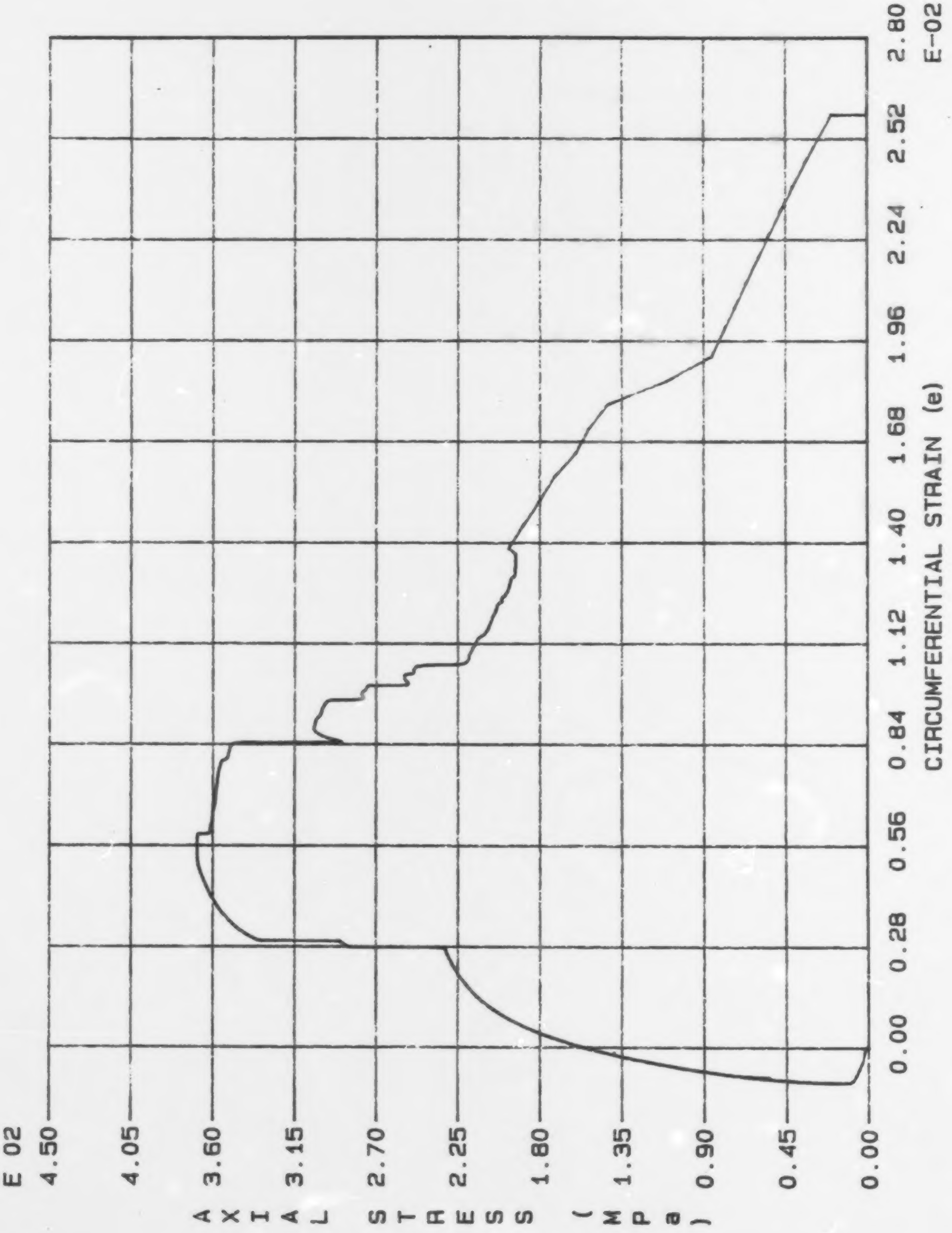
AXIAL STRESS (MPa)
E 02
4.50
4.05
3.60
3.15
2.70
2.25
1.80
1.35
0.90
0.45
0.00
0.00
0.28
0.56
0.84
1.12
1.40
1.68
1.96
2.24
2.52
2.80
E-02
CIRCUMFERENTIAL STRAIN (e)

N29

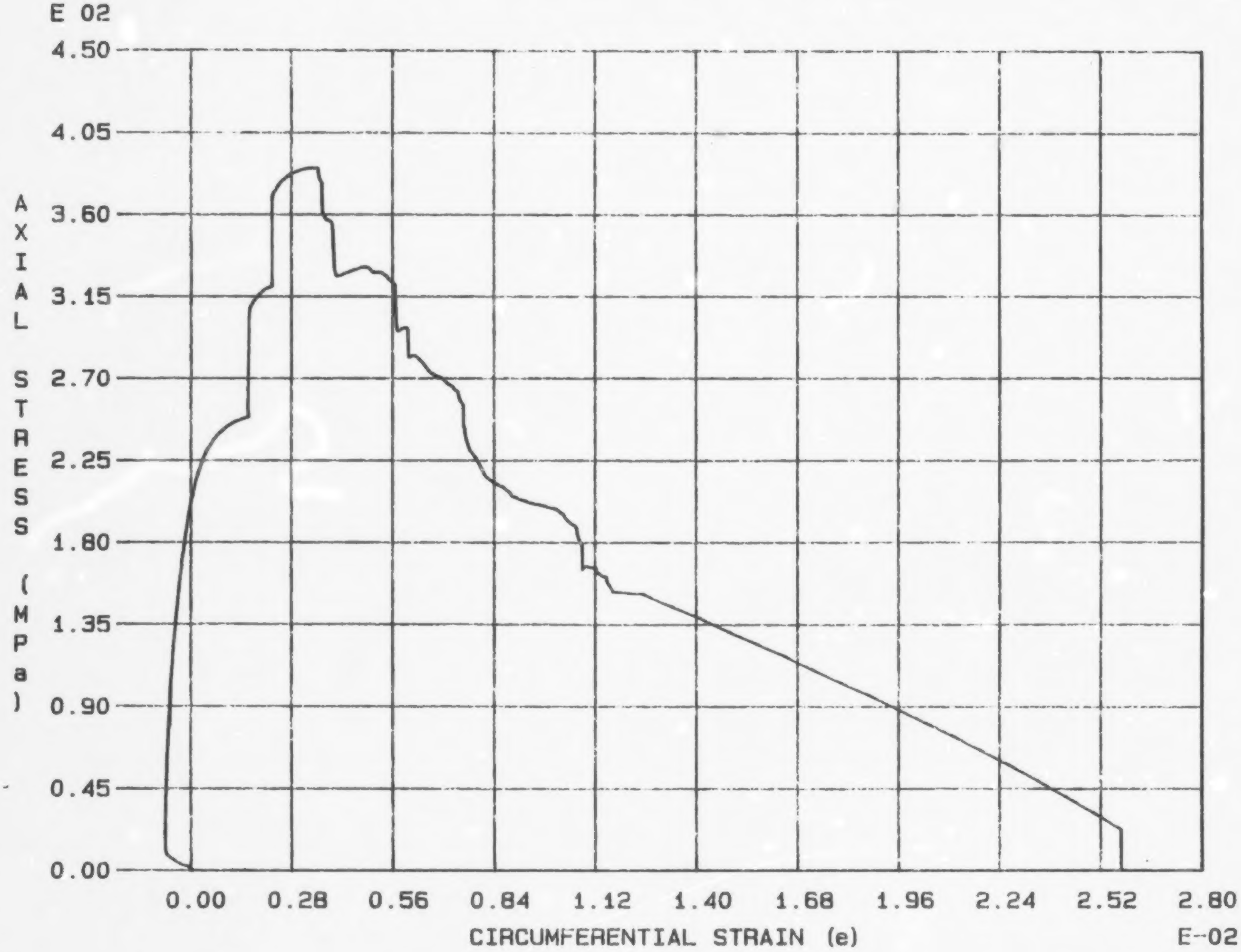
E 02
4.50
4.05
3.60
3.15
2.70
2.25
1.80
1.35
0.90
0.45
0.00
AXIAL STRESS (MPa)
0.00
0.28
0.56
0.84
1.12
1.40
1.68
1.96
2.24
2.52
2.80
E-02
CIRCUMFERENTIAL STRAIN (e)

N30

APPENDIX E-3

Stress vs. confining pressure

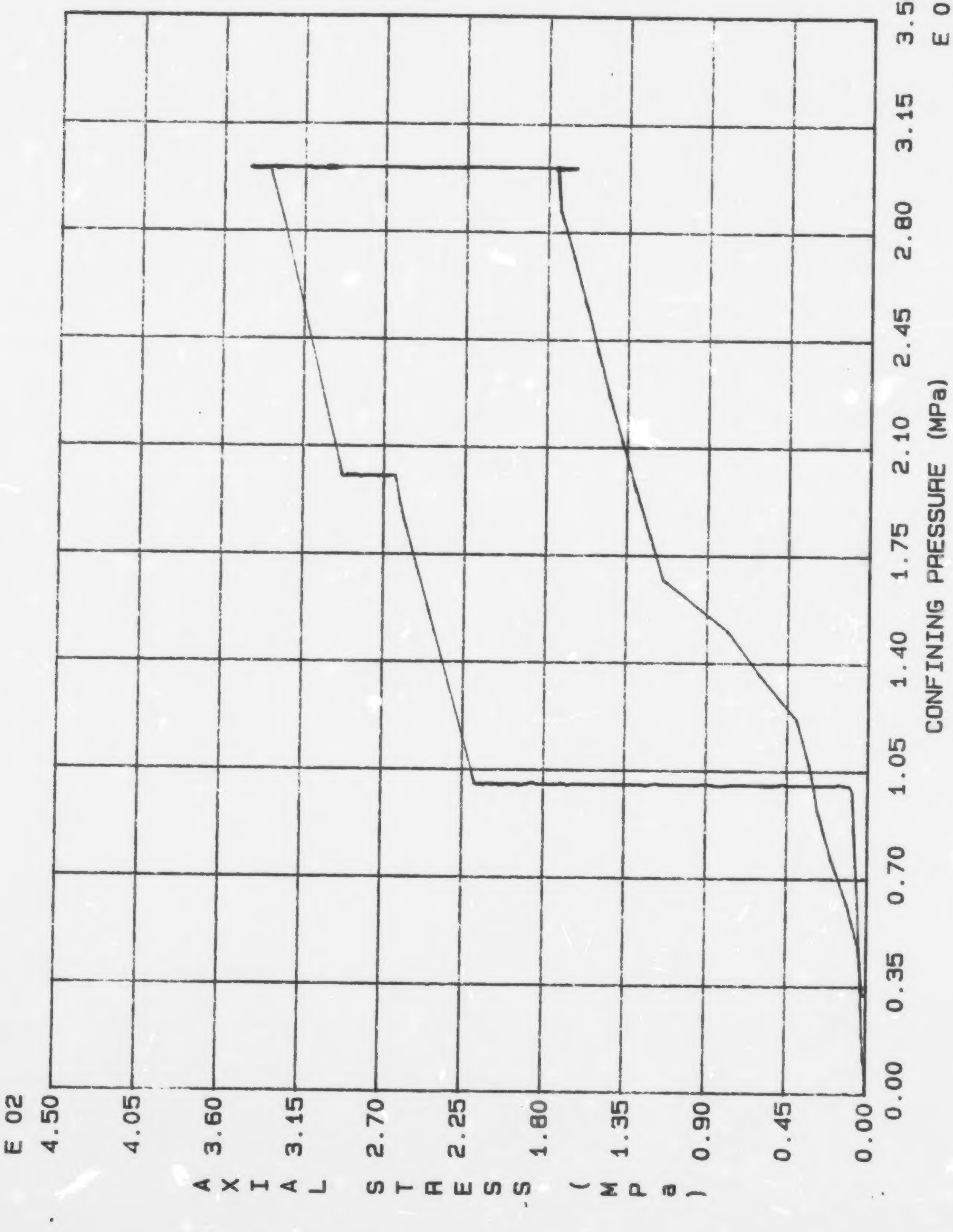
AXIAL STRESS (MPa)
E 02
4.50
4.05
3.60
3.15
2.70
2.25
1.80
1.35
0.90
0.45
0.00
CONFINING PRESSURE (MPa)
E 01
0.00
0.35
0.70
1.05
1.40
1.75
2.10
2.45
2.80
3.15
3.50

N27

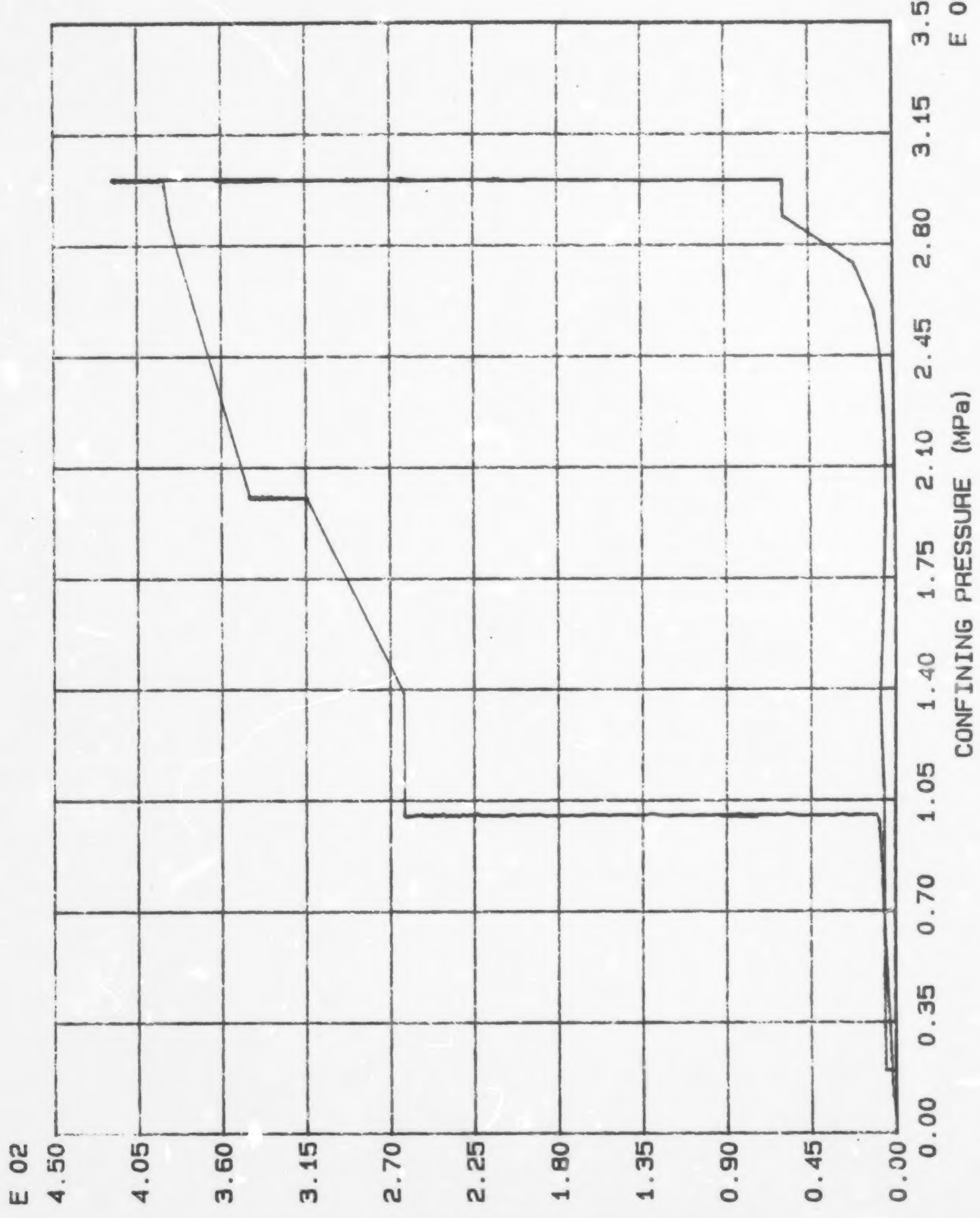
E 02
4.50
4.05
3.60
3.15
2.70
2.25
1.80
1.35
0.90
0.45
0.00
AXIAL STRESS (MPa)
0.00
0.35
0.70
1.05
1.40
1.75
2.10
2.45
2.80
3.15
3.50
E 01
CONFINING PRESSURE (MPa)
N28

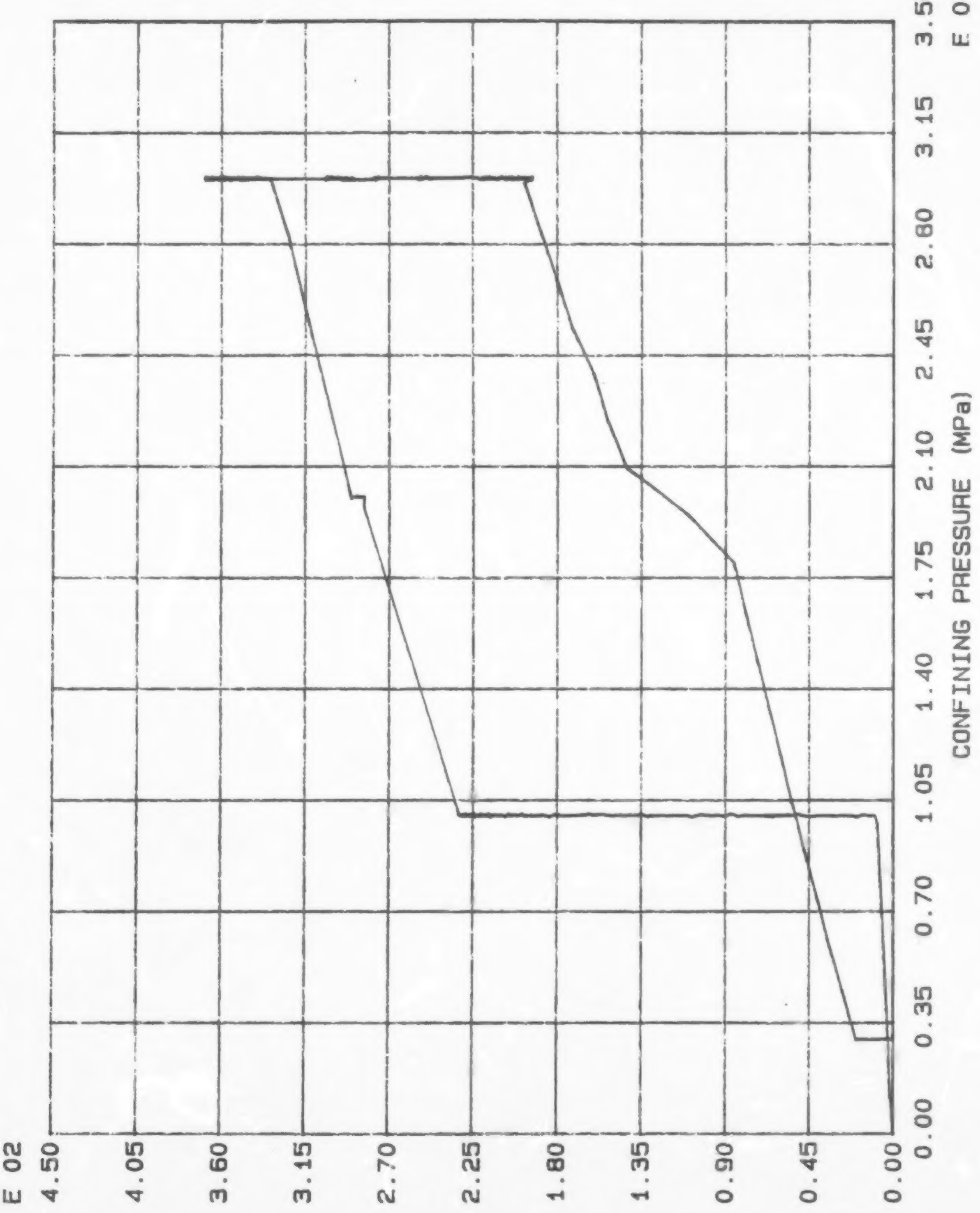
E 02
4.50
4.05
3.60
3.15
2.70
2.25
1.80
1.35
0.90
0.45
0.00
AXIAL STRESS (MPa)
0.00
0.35
0.70
1.05
1.40
1.75
2.10
2.45
2.80
3.15
3.50
E 01
CONFINING PRESSURE (MPa)

N29

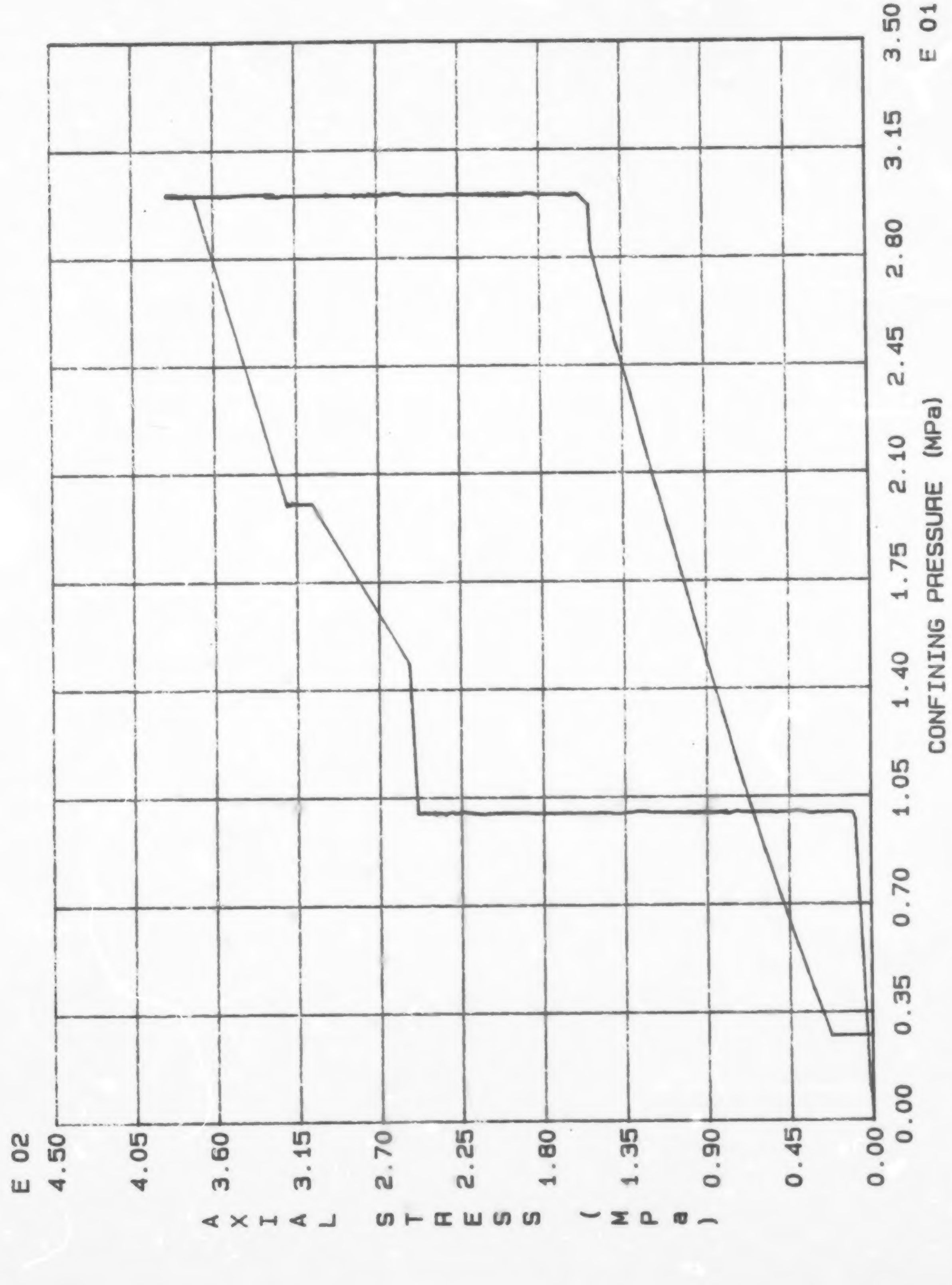
E 02
4.50
4.05
3.60
3.15
2.70
2.25
1.80
1.35
0.90
0.45
0.00
AXIAL STRESS (MPa)
0.00
0.35
0.70
1.05
1.40
1.75
2.10
2.45
2.80
3.15
3.50
E 01
CONFINING PRESSURE (MPa)

N30

APPENDIX F

Additional software

APPENDIX F-1

Mean.for - Fortran 77

```
           REAL X,Y,M,S,SM,INT,X2,R,Z
           INTEGER N
           OPEN (UNIT=5)
C          assign input file 'for005'
           N=0
           Y=0.0
10         READ(5,*,END=15) X
           N=N+1
           Y=Y+X
           GOTO 10
15         M=Y/N
C          m is the mean of the input data
           INT=0.0
           REWIND 5
20         READ(5,*,END=25) X2
           INT=INT + (M-X2)**2
           GOTO 20
25         S= SQRT(INT/(N-1))
           Z= N**0.5
           SM= S/Z
           PRINT*, 'MEAN:',M
           PRINT*, 'STANDARD DEVIATION:',S
           PRINT*, 'STANDARD DEVIATION OF MEAN:',SM
           STOP
           END
```

APPENDIX F-2

Slope.bas - MTS Basic

```
10 SETDIM VA2(3600,6)
15 PRINT 'INPUT FILE NAME'; \ INPUT F$
20 OPEN 'DU0:'+F$+'.DAT' FOR INPUT AS FILE #1, FILESIZE 300
25 PRINT 'ENTER LOAD FULL SCALE IN kN'; \ INPUT C
27 PRINT 'ENTER LV1 FULL SCALE IN mm'; \ INPUT D
28 PRINT 'ENTER LV2 FULL SCALE IN mm'; \ INPUT L
30 PRINT 'ENTER LV3 FULL SCALE IN mm'; \ INPUT M
32 PRINT 'ENTER SPECIMEN LENGTH IN mm'; \ INPUT Q
33 PRINT 'ENTER START LOAD IN kN'; \ INPUT S
35 INPUT #1:A \ VA2=A
36 INPUT #1:A1
37 INPUT #1:A2
38 INPUT #1:A3
39 INPUT #1:A4
40 INPUT #1:A5
41 INPUT #1:A6
50 FOR I=1 TO VA2
60 INPUT #1:X \ X=(X-A1)*C
70 INPUT #1:J
80 INPUT #1:G \ G=(G-A3)*D
90 INPUT #1:R \ R=(R-A4)*-.02*Q
100 INPUT #1:W \ W=(W-A5)*L
110 INPUT #1:Z \ Z=(Z-A6)*M
111 IF X<S THEN 285
120 G=G-R
130 W=W-R
140 Z=Z-R
150 A7=(G+W+Z)/3
155 T=T+1
157 X1=X1+X
160 Y1=Y1+G
170 Y2=Y2+W
180 Y3=Y3+Z
190 Y4=Y4+A7
210 X5=X5+X*G
220 X6=X6+X*W
230 X7=X7+X*Z
240 X8=X8+X*A7
250 X2=X2+X*X
285 NEXT I
287 CLOSE
290 X3=X1/T
300 X4=X3*X3
310 Y5=Y1/T
320 Y6=Y2/T
330 Y7=Y3/T
340 Y8=Y4/T
350 C1=X3*Y5
360 C2=X3*Y6
380 C3=X3*Y7
390 C4=X3*Y8
400 D1=X5/T
410 D2=X6/T
420 D3=X7/T
430 D4=X8/T
440 X2=X2/T
450 S1=X2-X4
550 M1=(D1-C1)/S1
560 M2=(D2-C2)/S1
570 M3=(D3-C3)/S1
580 M4=(D4-C4)/S1
600 B1=Y5-M1*X3
610 B2=Y6-M2*X3
620 B3=Y7-M3*X3
630 B4=Y8-M4*X3
640 PRINT 'FOR LV1 PLATEN DISP CORR IN mm=';M1;'* LOAD +';B1
```

```
650 PRINT 'FOR LV2 PLATEN DISP CORR IN mm=';M2;'* LOAD +';B2
660 PRINT 'FOR LV3 PLATEN DISP CORR IN mm=';M3;'* LOAD +';B3
670 PRINT 'FOR LVs PLATEN DISP CORR IN mm=';M4;'* LOAD +';B4
700 END
```

APPENDIX F-3

Failure.for - Fortran 77

```
      program FAILURE
      REAL a,b,c,d,e,f,g,h,i,j,k,l,m,n,o,p,q,r,t,u,v,w,x,y,z
      REAL DESTRES1,DESTRES2,DESTRES3,CONF1,CONF2,CONF3
      REAL XF,X1,Y1,X2,X4,Y5,X5,X3,C1,B1,M1,D1,Y2
      REAL XI,YI,XIYIT,XXT,YYT,S3MAX,SDMAX,SD,S3,TN,XITYIT,XIXI
      REAL YIYI,R2,TM,XE,YE,TWOB,PHI,PHID,BE,BASE,BC,COHE,W1,XN
      REAL XS,S1,YS,W2,QU,THETA,TAU,SN,W4,V1,QA,XSLICE
      intrinsic asin,ATAN
      character*80 filein,fileout,name
C
C     GENERATES POINTS FOR MOHR CIRCLES
C
      type*,'enter mine name and rock type (in single quotes)'
      accept*,name
      print*,name
      print*,' '
      a=0.0
      b=0.0
      c=0.0
      d=100.0
      e=0.0
      f=0.0
      type *, 'enter input data file (embedded with single quotes)'
      accept *,filein
      open (unit=5, file=filein, status='unknown')
      fileout='cirdata.out'
      open (unit=2, file=fileout, status='unknown')
      write (2,11) a,b
11    format(2f10.3)
      write (2,12) c,d
12    format(2f10.3)
      write (2,13) e,f
13    format(2f10.3)
      XSLICE=0.0
16    READ(5,*,END=17)DSTRES1,CONF1
      XSLICE=XSLICE+DSTRES1
      GOTO 16
17    REWIND 5
      XSLICE=XSLICE/800.0
1     READ(5,*,END=2)DSTRES1,CONF1
      DSTRES1=DSTRES1-CONF1
      r=dstres1/2.
      x=conf1
      h=r+x
      xf=conf1+dstres1
3     y=sqrt(abs(r*r-(x-h)**2))
      j=j+1
      if(j.gt.898)goto 2
      if(x.gt.xf)goto 5
      write (2,4) x,y
4     format(2f10.3)
      x=x+XSLICE
      goto 3
5     X=XF
      Y=0.0
      write (2,6) X,Y
6     FORMAT(2F10.3)
      GOTO 1
2     REWIND 5
      close (unit=2)
C
C     HOEK AND BROWN INTACT FAILURE ENVELOPE ANALYSIS
C
      N=0
      xi=0.
      yi=0.
      xiyit=0.
      xxt=0.
      yyt=0.
      s3max=0.
      sdmax=0.
20    type*,'EXCLUDE UNIAXIAL VALUE ? yes=1 no=0'
      accept*,w
300   READ(5,*,END=600)SD,S3
      if (s3.lt.0)qt=s3
      if (s3.lt.0) goto 300
      if (s3.eq.0)qu=sd
      if (w.eq.1.and.s3.eq.0) goto 300
      N=N+1
      SD=SD-S3
      tn=n
      xi=xi+s3
      y=sd*sd
      yi=yi+y
      xiyit=xiyit+s3*y
      xxt=xxt+s3*s3
      yyt=yyt+y*y
      GOTO 300
600   rewind 5
      xityit=xi*yi
      xixi=xi*xi
      yiyi=yi*yi
      c=sqrt(abs(yi/tn-((xiyit-(xityit/tn))/(xxt-(xixi/tn)))*xi/tn))
      a=(1.0/c)*((xiyit-(xityit/tn))/(xxt-(xixi/tn)))
      r2=((xiyit-(xityit/tn))**2)/((xxt-(xixi/tn))*(yyt-(yiyi/tn)))
      s=(1.0/c/c)*((yi/tn)-(a*c*xi/tn))
      IF(S.LE.0.0)A=YI/C/XI
      IF(S.LE.0.0)S=0.0
      print*,'Brazilian Tensile Strength =               ',qt
      print*,'Uniaxial Compressive Strength =            ',qu
      print*,'Hoek and Brown Intact Failure Envelope Analysis'
      print*,'Computer Uniaxial Compressive Strength = ',c
      print*,'Constant m =                               ',a
      print*,'Constant s =                               ',s
      print*,'Coefficient of Determination =             ',r2
      print*,' '
      sdmax=sd
      s3max=s3
      FILEOUT='COULOMB.OUT'
C
C     HOEK AND BROWN INTACT PARAMETERS
C
      OPEN (UNIT=2, FILE=FILEOUT, STATUS='UNKNOWN')
500   read(5,*,end=700)sd,s3
      if(s3.lt.0)goto 500
      if(s3.eq.0.AND.W.EQ.1)goto 500
      S1=S3+SQRT(A*C*S3+C*C)
      sd=S1-s3
      tm=(0.5)*sd
      xe=s3+tm*tm/(tm+a*c/8.)
      ye=(xe-s3)*sqrt(1+(a*c/(4.*tm)))
      twob=ye/tm
      phi=(90./57.2957)-asin(twob)
      phid=phi*(180./3.14159)
      be=45.+phid/2.
      base=tm/sin(phi)
      bc=base-s3-tm
      cohe=bc*tan(phi)
      print*,'sigma3 =         ',s3,'  failure angle = ',be
      print*,'sigma1 =         ',s1,'  friction angle =',phid
      print*,'shear stress =  ',ye,'  cohesion =       ',cohe
      print*,'normal stress = ',xe
      print*,' '
      WRITE (2,111) S3,XE,YE
111   FORMAT(3F10.3)
      goto 500
700   rewind 5
      rewind 2
      close (unit=2)
      close (unit=5)
C
C     GENERATES POINTS FOR HOEK AND BROWN INTACT FAILURE ENVELOPE
C
      d=s3max
      e=sdmax
      t=s
      F=D+E/2.0
      z=-2.0
      xn=0.0
      IF(T.LE.0.9)XN=-1.0
      y=0.0
      fileout='msdata.out'
      open (unit=2, file=fileout, status='unknown')
77    s9=xs
76    IF(T.LE.0.9)XN=XN+1.01
      IF(T.LE.0.9)GOTO 33
      xn=xn-1.0
33    sl=xn+sqrt(abs(a*c*xn+c*c*T))
      tm=.5*(sl-xn)
      xs=xn+tm*tm/(tm+a*c/8.)
      IF(T.LE.0.9.AND.XS.GT.F)GOTO 21
      ys=(xs-xn)*sqrt(1.+(a*c/(4.*tm)))
      y=y+1.0
      if(y.gt.100.0)goto 21
      IF(T.LE.0.9)GOTO 43
      if(xs.gt.s9.and.xs.lt.0.0)goto 99
43    write (2,50) xs,ys
50    format(2f10.3)
      IF(T.LE.0.9)GOTO 76
99    if(xs.gt.0.0.and.xn.lt.0.0)goto 77
      if(xs.gt.s9.and.xn.lt.0.0)goto 44
      if(xs.lt.0.0.and.xn.lt.0.0)goto 77
44    xn=z+2.0
      z=z+2.0
      IF(XS.GT.F)GOTO 21
      goto 33
21    close (unit=2)
      a=0.0
      r2=0.0
      s=0.0
      type*,'IF NO RESIDUAL DATA FILE ENTER 1, ELSE 2'
      accept*,w2
      if(w2.eq.1.)goto 42
C
C     HOEK AND BROWN RESIDUAL FAILURE ENVELOPE ANALYSIS
C
      N=0
      sdmax=0.0
      s3max=0.0
      xi=0.
      yi=0.
      xiyit=0.
      xxt=0.
      yyt=0.
      v=qu
      type *, 'enter input residual file (embedded with single quotes)'
      accept *,filein
      open (unit=5, file=filein, status='unknown')
```

```
10      READ(5,*,END=15)SD,S3
        N=N+1
        if(sd.gt.sdmax)sdmax=sd
        if(s3.gt.s3max)s3max=s3
        SD=SD-S3
        tn=n
        xi=xi+s3
        y=sd*sd
        yi=yi+y
        xiyit=xiyit+s3*y
        xxt=xxt+s3*s3
        yyt=yyt+y*y
        GOTO 10
15      xityit=xi*yi
        REWIND 5
        xixi=xi*xi
        yiyi=yi*yi
        c=sqrt(abs(yi/tn-((xiyit-(xityit/tn))/(xxt-(xixi/tn)))*xi/tn))
        c=v
        a=(1.0/c)*((xiyit-(xityit/tn))/(xxt-(xixi/tn)))
        r2=((xiyit-(xityit/tn))**2)/((xxt-(xixi/tn))*(yyt-(yiyi/tn)))
        s=(1.0/c/c)*((yi/tn)-(a*c*xi/tn))
        if(s.le.0.0)a=yi/c/xi
        if(s.le.0.0)s=0.0
        GOTO 46
42      type*,'IF RESIDUAL PARAMETERS ENTER 1, ELSE 2'
        accept*,w5
        if(w5.eq.2.)goto 52
        type*,'input m_r'
        accept*,a
        type*,'input s_r'
        accept*,s
        type*,'input intact Qu'
        accept*,qu
        type*,'input coefficient of determination'
        accept*,r2
C
C       GENERATES POINTS FOR HOEK AND BROWN RESIDUAL FAILURE ENVELOPE
C
46      d=s3max
        e=sdmax-s3max
        c=qu
        t=s
        F=D+E/2.0
        z=-2.0
        xn=0.0
        y=0.0
        xn=-1.0
        fileout='r.out'
        open (unit=2, file=fileout, status='unknown')
101     xn=xn+1.01
        sl=xn+sqrt(abs(a*c*xn+c*c*t))
        tm=.5*(sl-xn)
        xs=xn+tm*tm/(tm+a*c/8.)
        if(xs.gt.f)goto 51
        ys=(xs-xn)*sqrt(1.+(a*c/(4.*tm)))
        y=y+3.0
        if(y.gt.100.0)goto 51
        write (2,103) xs,ys
103     format(2f10.3)
        goto 101
51      close (unit=2)
C
C       HOEK AND BROWN RESIDUAL PARAMETERS
C
        print*,'Hoek and Brown Residual Failure Envelope Analysis'
```

```
      print*,'Intact Uniaxial Compressive Strength =',qu
      print*,'Material Constant m_r =              ',a
      print*,'Material Constant s_r =              ',s
      print*,'Coefficient of Determination =       ',r2
      if(w2.eq.1.0.and.w5.eq.2.0)goto 52
      filein='coulomb.out'
      fileout='coulombr.out'
      open (unit=5, file=filein, status='unknown')
      open (unit=2, file=fileout, status='unknown')
302   read(5,*,end=301)s3,s5,s6
306   sl=s3+sqrt(a*qu*s3+qu*qu*s)
      if(sl.gt.0.0)goto 307
      if(sl.eq.0.0)s3=0.001
      if(sl.eq.0.0)goto 306
307   sd=sl-s3
      tm=(0.5)*sd
      xe=s3+tm*tm/(tm+a*qu/8.)
      ye=(xe-s3)*sqrt(1.+(a*qu/(4.*tm)))
      twob=ye/tm
      phi=(90./57.2957)-asin(twob)
      phid=phi*(180./3.14159)
      be=45.+phid/2.
      base=tm/sin(phi)
      bc=base-s3-tm
      cohe=bc*tan(phi)
      print*,'sigma3r =           ',s3,' failure angler =  ',be
      print*,'sigmalr =           ',sl,' friction angler = ',phid
      print*,'shearr stress =     ',ye,' cohesion =        ',cohe
      print*,'normalr stress = ',xe
      print*,' '
      write(2,303)s3,xe,ye
303   format(3f10.3)
      goto 302
301   rewind 2
      rewind 5
      close (unit=2)
      close (unit=5)
52    FILEIN='COULOMB.OUT'
      OPEN (UNIT=5, FILE=FILEIN, STATUS='UNKNOWN')
C
C     MOHR-COULOMB INTACT FAILURE ENVELOPE ANALYSIS
C
      T=0.0
      X1=0.0
      Y1=0.0
      X5=0.0
      X2=0.0
      Y2=0.0
530   READ(5,*,END=909)A,X,G
      T=T+1
      X1=X1+X
      Y1=Y1+G
      X5=X5+X*G
      Y2=Y2+G*G
      X2=X2+X*X
      GOTO 530
909   REWIND 5
      R2=X5/SQRT(Y2*X2)
      X3=X1/T
      X4=X3*X3
      Y5=Y1/T
      C1=X3*Y5
      D1=X5/T
      X2=X2/T
      S1=X2-X4
      M1=(D1-C1)/S1
      M=M1
      B1=Y5-M1*X3
      M1=(ATAN(M1))*(180./3.14159)
      C1=45.+M1/2.
C
C     MOHR-COULOMB INTACT PARAMETERS
C
      print*,' '
      print*,'Mohr-Coulomb Failure Envelope Analysis'
      print*,'Friction Angle =          ',m1
      print*,'Failure Angle =           ',c1
      print*,'Cohesion =                ',b1
      print*,'Correlation Coefficient =',r2
      print*,' '
      c=B1
      phi=M1*3.14159/180.
      print*,'  Sigma3         Sigma1          Shear             Normal'
      FILEOUT='MOHR.OUT'
      OPEN(UNIT=2, FILE=FILEOUT, STATUS='UNKNOWN')
      XS=0.0
      DO 1006 I=1,2
      YS=M*XS+B1
      WRITE(2,1005) XS,YS
1005  FORMAT(2F10.3)
1006  XS=SDMAX
      REWIND 2
      CLOSE (UNIT=2)
1002  READ(5,*,END=1001) S3,S4,S5
      a=(tan(3.14159/4+phi/2.))**2.
      s1=s3*a+c*(a-1)/tan(phi)
      theta=3.14159/4-phi/2.
      tau=(s1-s3)/2*sin(2*theta)
      sn=s3+(s1-s3)*(sin(theta))**2
      print*,s3,s1,tau,sn
      GOTO 1002
1001  REWIND 5
      CLOSE (UNIT=5)
      if(w2.eq.1.and.w5.eq.2.)goto 2004
C
C     MOHR-COULOMB RESIDUAL FAILURE ENVELOPE ANALYSIS
C
      FILEIN='COULOMBR.OUT'
      OPEN (UNIT=5, FILE=FILEIN, STATUS='UNKNOWN')
      T=0.0
      X1=0.0
      Y1=0.0
      X5=0.0
      X2=0.0
      Y2=0.0
2002  READ(5,*,END=2001)A,X,G
      T=T+1
      X1=X1+X
      Y1=Y1+G
      X5=X5+X*G
      Y2=Y2+G*G
      X2=X2+X*X
      GOTO 2002
2001  REWIND 5
      R2=X5/SQRT(Y2*X2)
      X3=X1/T
      X4=X3*X3
      Y5=Y1/T
      C1=X3*Y5
      D1=X5/T
      X2=X2/T
      S1=X2-X4
      Ml=(Dl-Cl)/Sl
      M=Ml
      Bl=Y5-Ml*X3
      Ml=(ATAN(Ml))*(180./3.14159)
      Cl=45+Ml/2.
C
C     MOHR-COULOMB RESIDUAL PARAMETERS
C
      print*,' '
      print*,'Mohr-Coulomb Residual Failure Envelope Analysis'
      print*,'Friction Angler =           ',ml
      print*,'Failure Angler =            ',cl
      print*,'Cohesionr =                 ',bl
      print*,'Correlation Coefficientr =',r2
      print*,' '
      c=Bl
      phi=Ml*3.14159/180.
      print*,'  Sigma3r        Sigmalr        Shearr         Normalr'
      FILEOUT='MOHRR.OUT'
      OPEN(UNIT=2, FILE=FILEOUT, STATUS='UNKNOWN')
      XR=0.0
      DO 2006 I=1,2
      YR=M*XR+Bl
      WRITE(2,2005) XR,YR
2005  FORMAT(2F10.3)
2006  XR=SDMAX
      REWIND 2
      CLOSE (UNIT=2)
2003  READ(5,*,END=2004) S3,S4,S5
      a=(tan(3.14159/4+phi/2.))**2.
      sl=s3*a+c*(a-1)/tan(phi)
      theta=3.14159/4.-phi/2.
      tau=(sl-s3)/2.*sin(2.*theta)
      sn=s3+(sl-s3)*(sin(theta))**2.
      print*,s3,sl,tau,sn
      GOTO 2003
2004  REWIND 5
      CLOSE (UNIT=5)
      stop
      end
```

APPENDIX F-4

Perm.bas - MTS Basic

```
30 PRINT 'THIS IS A CONFINED PERMEABILITY TEST'
35 PRINT 'P-up = 0.5sigma_3'
40 PRINT 'INPUT LOAD RANGE IN kN';\ INPUT L1
42 IF L1=4400 THEN R=1
44 IF L1=2200 THEN R=2
46 IF L1=880 THEN R=3
48 IF L1=440 THEN R=4
70 CKTIME(1,.1)
90 CLREMOTESWITCH(1,1,R,0)
100 FGSTEP(1,1/L1)
105 PRINT 'ZERO LVDTs'
106 PRINT 'INPUT CONFINING PRESSURE RANGE CARD IN MPa';\INPUT C6
107 PRINT 'INPUT SPECIMEN X-AREA IN CM-SQUARED';\INPUT L
110 PRINT 'INPUT DESIRED CONFINING PRESSURE IN MPa'; \ INPUT E
115 PRINT '  PRESS <CR> TO INITIATE RAMP TO EQUILIBRIUM'; \ INPUT I$
130 D=((E/10)*L)/L1
140 E=E/C6
160 FGRAMP(1,60,D)
170 FGRAMP(2,60,E)
180 FGGO
190 ETIME
200 SLEEP(70)
210 FGSTOP
215 PRINT 'SPECIMEN HOLDING AT EQUILIBRIUM'
216 PRINT'ENTER 1 FOR ANOTHER STRESS LEVEL ELSE 2';\INPUT L3
217 IF L3=1 THEN 110
890 CLLOCALSWITCH(1)
900 END
```

APPENDIX G

Geologic rock classification

APPENDIX G-1

Sedimentary rock classification

CLASSIFICATION OF SEDIMENTARY ROCKS

By Russell B. Travis

	TEXTURE →	GRAIN SIZE <1/256 mm.		GRAIN SIZE 1/256-2 mm.								GRAIN SIZE >2 mm.	
		CRYSTALLINE, CLASTIC OR AMORPHOUS		CRYSTALLINE, CLASTIC, BIOCLASTIC, OOLITIC, ETC.		CLASTIC UNCONSOLIDATED - silt, sand CONSOLIDATED - siltstone, sandstone SIZE GRADES (mm.) 1/256 - 1/16, silt. 1/16 - 1/8 very fine sand. 1/8 - 1/4, fine sand; 1/4 - 1/2, medium sand. 1/2 - 1, coarse sand; 1-2, very coarse sand						CLASTIC UNCONSOLIDATED - gravel (rounded), rubble (angular) CONSOLIDATED - conglomerate (rounded), breccia (angular) SIZE GRADES (mm.) - 2-4, granules; 4-64, pebbles; 64-256 cobbles; >256 boulders	
	COMPOSITION OF MAJOR FRACTION →	Composition as Indicated in left column (prefix appropriate names for mixtures)	Clay Minerals or Clay-Size Material	Composition as Indicated in left column (prefix appropriate names for mixtures)	Chiefly Calcite or Dolomite	Chiefly Quartz			Quartz and >25% Feldspar	Quartz, Feldspar, Rock Chips, Pelitic Matrix, Angular grains, Tough.	Volcanic Ejecta	CHIEFLY ONE CONSTITUENT Especially quartz, chert, or quartzite. Also shale or limestone. Homogeneous conglomerates and breccias.	SEVERAL CONSTITUENTS Usually including unstable constituents. Mixed conglomerates and breccias.
						>90% Quartz	Feldspar 10-25%	Rock Chips >10%					
COMPOSITION OF MINOR FRACTION	<10% Minor Fraction				LIMESTONE DOLOMITE ETC. All varieties in the Calcite-Dolomite horizontal column are possible here	QUARTZ SANDSTONE (Quartzose sandstone)	FELDSPATHIC SANDSTONE	LITHIC SANDSTONE	ARKOSE (Arkosic sandstone) Normally pink, red or light gray	GRAYWACKE—normally greenish gray SUBGRAYWACKE—low in feldspar, rock chips, or less angular grains. Tendency to chemical cement	ASH—unconsolidated fragments under 4 mm TUFF—consolidated ash VOLCANIC BRECCIA—angular fragments over 4 mm AGGLOMERATE—large proportion (>25%) of bombs These rocks are classified on the proportions of vitric, crystal (mineral), or lithic material they contain, for example "vitric lithic ash," or "crystal vitric tuff." If the mineralogy of the crystal or lithic fragments can be determined, the name of the appropriate volcanic rock can be prefixed as, "rhyolite vitric crystal tuff," or simply, "rhyolite tuff."	Name consists of chief constituent and size grade, for example QUARTZ PEBBLE CONGLOMERATE CHERT COBBLE CONGLOMERATE LIMESTONE PEBBLE BRECCIA ETC	Name consists of "mixed" or "polycomponent" and size grade, for example MIXED PEBBLE CONGLOMERATE or MIXED COBBLE CONGLOMERATE Name may include composition as GRAYWACKE-ANDESITE-CHERT PEBBLE CONGLOMERATE
	Clay Minerals or Clay-Size Materials	CLAYSTONE—massive, blocky structure MUDSTONE—indurated mud. Includes claystone and siltstone SHALE—finely fissile. May include much silt CLAY SHALE (Argillaceous shale)—chiefly clay minerals ARGILLITE—highly indurated. Incipiently recrystallized BENTONITE—swells and disaggregates in water			ARGILLACEOUS LIMESTONE ETC. All varieties in the Calcite-Dolomite horizontal column are possible here.	ARGILLACEOUS QUARTZ SANDSTONE	ARGILLACEOUS FELDSPATHIC SANDSTONE LOESS—fine sand or silt. Massive, porous, coherent	ARGILLACEOUS LITHIC SANDSTONE	ARGILLACEOUS ARKOSE	ARGILLACEOUS GRAYWACKE ARGILLACEOUS SUBGRAYWACKE		ARGILLACEOUS (rock, grade) CONGLOMERATE—uncommon with stable constituent	ARGILLACEOUS MIXED (grade) CONGLOMERATE GLACIAL TILL—chaotic mixture of clay, sand and gravel TILLITE—indurated till FANGLOMERATE—alluvial fan material
	SILICA Opal Chalcedony Quartz	CHERT—chalcedony or opal. Bedded, nodular, massive DIATOMITE (Diatomaceous earth)—diatom tests RADIOLARITE (Tripoli, in part)—radiolarian tests SILICEOUS SINTER (Geyserite)—porous geyser deposit PORCELLANITE—argillaceous or silty chert	SILICIOUS SHALE " CLAYSTONE " MUDSTONE ETC.	SILICEOUS OOLITE—>50% oolitic OOLITIC CHERT—<50% oolitic DIATOMITE—diatom tests RADIOLARITE—radiolarian tests	SILICEOUS LIMESTONE—disseminated silica CHERTY LIMESTONE—containing chert nodules ETC. All varieties in the Calcite-Dolomite horizontal column are possible here	ORTHOQUARTZITE (Sedimentary quartzite) (Siliceous quartz sandstone)	FELDSPATHIC ORTHOQUARTZITE (Siliceous feldspathic sandstone)	LITHIC ORTHOQUARTZITE (Siliceous lithic sandstone)	SILICEOUS ARKOSE (Quartzitic arkose)	SILICIOUS SUBGRAYWACKE		SILICEOUS (rock, grade) CONGLOMERATE (Orthoquartzitic [rock, grade] conglomerate)	SILICEOUS MIXED (grade) CONGLOMERATE
	CALCITE OR DOLOMITE	LIMESTONE—chiefly calcite, massive DOLOMITE (Dolostone)—chiefly dolomite, massive. CHALK—chalky texture TUFA—very porous, friable TRAVERTINE—banded, coherent, denser than tufa CALICHE—lime-rich deposit formed near surface	CALCAREOUS SHALE (Limy shale) etc MARLSTONE 25-75% carbonate	LIMESTONE — chiefly calcite, crystalline DOLOMITE (Dolostone) — chiefly dolomite, crystalline CLASTIC LIMESTONE (Calcarenite or calcite sandstone) — clastic CALCAREOUS OOLITE — > 50% oolitic OOLITIC LIMESTONE — < 50% oolitic COQUINA — shells, little cement ORGANIC LIMESTONE — Richly fossiliferous		CALCAREOUS QUARTZ SANDSTONE	CALCAREOUS FELDSPATHIC SANDSTONE	CALCAREOUS LITHIC SANDSTONE	CALCAREOUS ARKOSE	CALCAREOUS SUBGRAYWACKE		CALCAREOUS (rock, grade) CONGLOMERATE	CALCAREOUS MIXED (grade) CONGLOMERATE
	IRON MINERALS Chiefly: Limonite Siderite Goethite Chamosite Hematite	HEMATITE ROCK—massive hematite LIMONITE ROCK—massive limonite BOG IRON ORE—earthy, impure, limonite IRONSTONE (Clay ironstone) — coherent mixture of iron, silica, clay, and carbonate SIDERITE (Iron carbonate)—massive siderite	LIMONITIC or HEMATITIC (Ferruginous) SHALE ETC.	HEMATITE OOLITE—>50% oolitic LIMONITE OOLITE—>50% oolitic OOLITIC IRON ORE—<50% oolitic SIDERITE (Iron carbonate)—chiefly siderite, crystalline	LIMONITIC or HEMATITIC (Ferruginous) LIMESTONE ETC. All varieties in the Calcite-Dolomite horizontal column are possible here	LIMONITIC or HEMATITIC (Ferruginous) QUARTZ SANDSTONE	LIMONITIC or HEMATITIC (Ferruginous) FELDSPATHIC SANDSTONE	LIMONITIC or HEMATITIC (Ferruginous) LITHIC SANDSTONE	LIMONITIC or HEMATITIC (Ferruginous) ARKOSE	LIMONITIC or HEMATITIC (Ferruginous) GRAYWACKE LIMONITIC or HEMATITIC (Ferruginous) SUBGRAYWACKE		LIMONITIC or HEMATITIC (Ferruginous) (rock, grade) CONGLOMERATE	LIMONITIC or HEMATITIC (Ferruginous) MIXED (grade) CONGLOMERATE
	CARBON Humus-Yields carbonaceous derivatives Sapropel-Yields bituminous derivatives	COAL BITUMINOUS—Hackly fracture ANTHRACITE—conchoidal fracture ASPHALT—asphaltic GILSONITE—black, high luster, amorphous	CARBONACEOUS SHALE, ETC.—carbonized remains BITUMINOUS SHALE (Oil shale) ETC.—sapropelic	PEAT—dark semi-carbonized plant remains LIGNITE—brown-black well-carbonized plant remains	CARBONACEOUS LIMESTONE BITUMINOUS LIMESTONE ETC. All varieties in the Calcite-Dolomite horizontal column are possible here	CARBONACEOUS QUARTZ SANDSTONE BITUMINOUS QUARTZ SANDSTONE	CARBONACEOUS FELDSPATHIC SANDSTONE BITUMINOUS FELSPATHIC SANDSTONE	CARBONACEOUS LITHIC SANDSTONE BITUMINOUS LITHIC SANDSTONE	CARBONACEOUS ARKOSE BITUMINOUS ARKOSE	CARBONACEOUS GRAYWACKE ETC. CARBONACEOUS SUBGRAYWACKE ETC.		CARBONACEOUS (rock, grade) CONGLOMERATE BITUMINOUS (rock, grade) CONGLOMERATE	CARBONACEOUS MIXED (grade) CONGLOMERATE BITUMINOUS MIXED (grade) CONGLOMERATE
	MISCELLANEOUS Phosphate (Collophane) Evaporites Halite and Sylvite Anhydrite Gypsum	PHOSPHORITE—phosphate rock ROCK SALT—massive halite or sylvite ROCK ANHYDRITE—massive anhydrite ROCK GYPSUM—massive gypsum	PHOSPHATIC SHALE, ETC.	PHOSPHATIC OOLITE—>50% oolitic ROCK SALT—crystalline ROCK ANHYDRITE—crystalline ROCK GYPSUM—crystalline GYPSUM SAND—clastic	PHOSPHATIC LIMESTONE ETC. All varieties in the Calcite-Dolomite horizontal column are possible here	PHOSPHATIC QUARTZ SANDSTONE ETC.	PHOSPHATIC FELDSPATHIC SANDSTONE ETC.	PHOSPHATIC LITHIC SANDSTONE ETC.	PHOSPHATIC ARKOSE ETC.	PHOSPHATIC SUBGRAYWACKE ETC.		PHOSPHATIC (rock, grade) CONGLOMERATE	PHOSPHATIC MIXED (grade) CONGLOMERATE

The names in the above chart are root names and should be preceded by appropriate terms for any significant feature of the rock. The proper order is color, structure, grain size (sandstones only), minor constituents, cement, and root name. Structure includes, for example, "thin-bedded," "massive," "cross-bedded," "thinly laminated," etc. The size grade for conglomerates should immediately precede "conglomerate." Some common nonmineral minor constituent terms are "tuffaceous," "cherty," "fossiliferous," "crinoidal," "coralline," "clayey (argillaceous)," "silty," "shaly," "sandy (arenaceous)," and "conglomeratic." Minor mineralogy should follow the nonmineral composition and should be restricted to one conspicuous mineral not implied in the root name. It should be applied in adjective form as "micaceous," "chloritic," "glauconitic," and "pyritic." The most common cement terms are given in the chart with the root names. Some typical rock names are "black thin-bedded micaceous shale," "gray massive, medium-grained glauconitic quartz sandstone," "tan siliceous quartz pebble conglomerate," and "white vuggy foraminiferal limestone."

Graywacke currently has two meanings. To some, it denotes a feldspar quartz sandstone with more than 20 (or 15) percent pelitic matrix. To many others, it has retained its original meaning that is a very hard, firm sandstone without porosity or chemical cement. In addition these "true" graywackes typically have extremely angular grains, a pelitic matrix, and a dark color.

FREQUENCY OF OCCURRENCE
This size type indicates **COMMON ROCKS.**
This size type indicates **UNCOMMON ROCKS.**
This size type indicates **RARE ROCKS.**

APPENDIX G-2

Igneous rock classification

ESSENTIAL MINERALS		POTASH FELDSPAR > ⅔ TOTAL FELDSPAR			POTASH FELDSPAR ⅓ – ⅔ TOTAL FELDSPAR			POTASH >10% T FELDSPA
		QUARTZ >10%	QUARTZ <10% FELDSPATHOID <10%	FELDSPATHOID >10%	QUARTZ >10%	QUARTZ <10% FELDSPATHOID <10%	FELDSPATHOID >10%	QUAR
CHARACTERIZING ACCESSORY MINERALS		CHIEFLY: HORNBLENDE, BIOTITE, PYROXENE, MUSCOVITE ALSO: SODIC AMPHIBOLES, AEGIRINE, CANCRINITE, SODALITE, TOURMALINE			CHIEFLY: HORNBLENDE, BIOTITE, PYROXENE ALSO: SODIC AMPHIBOLES, AEGIRINE			
COLOR INDEX		10	15	20	20	25	30	
AVERAGE CHEMICAL COMPOSITION (DALY)	SiO_2	71.5	60.4	56.0	66.8	57.0	54.1	
	Al_2O_3	14.0	17.0	19.2	15.8	17.1	21.0	
	Fe_2O_3	1.5	2.7	2.9	2.3	3.4	1.8	
	FeO	1.4	2.9	1.6	1.3	3.6	3.3	
	MgO	0.6	1.8	0.6	1.0	2.3	1.1	
	CaO	1.6	3.7	2.0	2.8	5.4	3.2	
	Na_2O	3.4	4.2	8.5	3.7	4.7	6.2	
	K_2O	4.3	5.1	5.3	4.2	3.7	5.9	
PHANERITIC	**EQUIGRANULAR** Batholiths, lapoliths, stocks, large laccoliths, thick dikes, and sills	**GRANITE** ALASKITE—few dark minerals GRAPHIC GRANITE—graphic texture ALKALI GRANITE—abundant albite and sodic amphibole or pyroxene CHARNOCKITE—with orthopyroxene LUXULLIANITE—tourmalinized	**SYENITE** QUARTZ SYENITE—a little quartz ALKALI SYENITE—no plagioclase except albite PULASKITE—a little nepheline NORDMARKITE—a little quartz LARVIKITE—with "blue" feldspar SHONKINITE—abundant FeMg minerals	**NEPHELINE SYENITE** LEUCITE SYENITE—pseudoleucite only feldspathoid SODALITE SYENITE—sodalite only feldspathoid FOYAITE—abundant feldspar MALIGNITE—abundant FeMg minerals DITROITE—with nepheline and sodalite	**QUARTZ MONZONITE (ADAMELLITE)**	**MONZONITE**	**NEPHELINE MONZONITE**	**GRANO**
PORPHYRITIC	**PHANERITIC GROUNDMASS** Laccoliths, dikes, sills, plugs, small stocks, margins of larger masses	**GRANITE PORPHYRY**	**SYENITE PORPHYRY**	**NEPHELINE SYENITE PORPHYRY**	**QUARTZ MONZONITE PORPHYRY**	**MONZONITE PORPHYRY**	**NEPHELINE MONZONITE PORPHYRY**	**GRANO PORP**
	APHANITIC GROUNDMASS Dikes, sills, laccoliths, surface flows, margins of larger masses, welded tuffs	**RHYOLITE PORPHYRY**	**TRACHYTE PORPHYRY**	**PHONOLITE PORPHYRY**	**QUARTZ LATITE PORPHYRY**	**LATITE PORPHYRY**	**NEPHELINE LATITE PORPHYRY**	
APHANITIC	**MICROCRYSTALLINE** Dikes, sills, surface flows, margins of larger masses, welded tuffs	**RHYOLITE**	**TRACHYTE**	**PHONOLITE** LEUCITE PHONOLITE (Leucite trachyte)—leucite only feldspathoid TINGUAITE—abundant aegirine WYOMINGITE—leucite and phlogopite	**QUARTZ LATITE (DELLENITE)**	**LATITE (TRACHY-ANDESITE)**	**NEPHELINE LATITE**	
	GLASSY Surface flows, margins of dikes and sills, welded tuffs	**OBSIDIAN**—black **PITCHSTONE**—resinous **VITROPHYRE**—porphyritic **PERLITE**—concentric fractures **PUMICE**—finely cellular, light colored **SCORIA**—coarsely cellular, dark colored			Normally it is not possible to determine the composition of these rocks. They are customarily designated by the names at the left of this column. Basic glass is rare so rocks named, except scoria, will normally be silicic. If the approximate composition (by close association) or silica content (by refractive index or analysis), can be determined, the name may be prefixed by the name of the appropriate aphanitic rock, for example, "trachyte obsidian," or "latite vitrophyre." In general, scoria is basic; basic obsidian is called "tachylite"; and spherulitic tachylite is "variolite."			

CLASSIFICATION OF IGNEOUS ROCKS

Russell B. Travis

PLAGIOCLASE FELDSPAR >⅔ TOTAL FELDSPAR						LITTLE OR NO FELDSPAR		SPECIAL TYPES
SH FELDSPAR TOTAL PAR	POTASH FELDSPAR <10% TOTAL FELDSPAR					CHIEFLY PYROXENE AND/OR OLIVINE	CHIEFLY FERRO-MAGNESIAN MINERALS AND FELDSPATHOIDS	
	SODIC PLAGIOCLASE		CALCIC PLAGIOCLASE					
ARTZ >10%	QUARTZ > 10%	QUARTZ <10% FELDSPATHOID <10%	QUARTZ <10% FELDSPATHOID <10%		FELDSPATHOID >10% PYROXENE >10%			
CHIEFLY: HORNBLENDE, BIOTITE, PYROXENE (IN ANDESITE) ALSO: PYROXENE FELDSPATHOID SODIC AMPHIBOLES			CHIEFLY PYROXENE URALITE, OLIVINE ALSO HORNBLENDE, BIOTITE, QUARTZ, ANALCITE, AEGIRINE, SODIC AMPHIBOLES			CHIEFLY SERPENTINE, IRON ORE ALSO HORNBLENDE, BIOTITE	HORNBLENDE BIOTITE IRON ORE	
20	20	25	50		60	95	55	
65.3 16.1 2.1 2.3 1.7 3.9 3.8 2.7	61.6 16.2 2.5 3.8 2.8 5.4 3.4 2.1	58.2 17.0 3.2 3.7 3.5 6.3 3.5 2.1	48.6 16.8 4.8 6.0 5.1 8.9 3.7 1.9		47.4 15.4 4.9 5.4 5.0 9.7 3.8 3.5	41.1 4.8 4.0 7.1 32.2 4.4 0.5 1.0	42.0 17.9 5.7 5.7 3.4 10.3 8.0 2.4	
ANODIORITE	QUARTZ DIORITE (TONALITE)	DIORITE	GABBRO GABBRO—with clinopyroxene NORITE—with orthopyroxene OLIVINE GABBRO—with olivine TROCTOLITE—olivine and plagioclase only ANORTHOSITE—plagioclase only QUARTZ GABBRO—with quartz	DIABASE (Dolerite of British) Phaneritic diabasic texture, normally medium or fine-grained	THERALITE ESSEXITE NEPHELINE GABBRO TESCHENITE—analcite only feldspathoid OLIVINE THERALITE—with olivine	PERIDOTITE PERIDOTITE—clinopyroxene and olivine HARZBURGITE—orthopyroxene and olivine PICRITE—pyroxene and olivine with some plagioclase DUNITE—olivine only PYROXENITE—pyroxene only SERPENTINE (SERPENTINITE)—chiefly serpentine	MISSOURITE—pyroxene, olivine, and pseudoleucite IJOLITE—pyroxene and nepheline FERGUSITE—pyroxene and pseudoleucite UNCOMPAHGRITE (MELILITE PYROXENITE)—pyroxene and melilite	**PEGMATITE**—phanerocrystalline, normally silicic, dike rock (or small irregular mass) having a conspicuously coarser texture than parent. **APLITE**—phanerocrystalline rock having sugary (fine-grained allotriomorphic-granular) texture. **LAMPROPHYRE**—dark dike rock with euhedral mafic phenocrysts and/or euhedral mafic minerals in groundmass.
ANODIORITE PORPHYRY	QUARTZ DIORITE PORPHYRY	DIORITE PORPHYRY	GABBRO PORPHYRY		THERALITE PORPHYRY	PERIDOTITE PORPHYRY KIMBERLITE—peridotite porphyry or breccia		
DACITE PORPHYRY		ANDESITE PORPHYRY	BASALT PORPHYRY		TEPHRITE PORPHYRY	LIMBURGITE PORPHYRY		**TRAP**—dark-colored aphanitic rock. **FELSITE**—light-colored aphanitic rock.
DACITE		ANDESITE	BASALT OLIVINE BASALT—with olivine ANALCITE BASALT—with analcite QUARTZ BASALT—with quartz OCEANITE—with abundant olivine		TEPHRITE LEUCITE TEPHRITE—leucite only feldspathoid BASANITE—with olivine LEUCITE BASANITE—with olivine and leucite	LIMBURGITE	NEPHELINITE—pyroxene and nepheline LEUCITITE—pyroxene and leucite MELILITITE—pyroxene and melilite OLIVINE NEPHELINITE (NEPHELINE BASALT)—pyroxene, nepheline, and olivine ETC	
nily ept ico the ro- ny.			FREQUENCY OF OCCURRENCE This size type indicates COMMON ROCKS. This size type indicates UNCOMMON ROCKS. This size type indicates RARE ROCKS.					

APPENDIX G-3

Metamorphic rock classification

CLASSIFICATION OF METAMORPHIC ROCKS

By Russell B. Travis

COLOR	CHIEF MINERALS	CHARACTERIZING ACCESSORY MINERALS	NONDIRECTIONAL STRUCTURE Massive or Granulose		DIRECTIONAL STRUCTURE (Lineate or Foliate)					
			Contact Metamorphism*		Mechanical Metamorphism	Regional Metamorphism				Plutonic Metamorphism
			Fine Grained (Aphanitic)	Medium or Coarse Grained (Phaneritic)	Cataclastic	Slaty	Phyllitic	Schistose	Gneissose	Migmatitic
LIGHT	QUARTZ FELDSPAR CALCITE DOLOMITE TALC MUSCOVITE SERICITE	Muscovite Sericite Sillimanite Kyanite Cordierite Tremolite Wollastonite Albite Andalusite Garnet Phlogopite Diopside Enstatite Staurolite Glaucophane Anthophyllite Pyrophyllite Chloritoid Actinolite Tourmaline Epidote Chiastolite Olivine Serpentine Chlorite Biotite Graphite Chondrodite Scapolite	METAQUARTZITE MARBLE BRUCITE MARBLE SOAPSTONE—chiefly talc HORNFELS—any metamorphic rock with nondirectional structure	METAQUARTZITE MARBLE BRUCITE MARBLE TREMOLITE MARBLE WOLLASTONITE MARBLE TREMOLITE HORNFELS WOLLASTONITE HORNFELS CALC-SILICATE HORNFELS—chiefly calc-silicate minerals	These rocks are formed by crushing and shearing with only minor recrystallization. If there are no conspicuous directional features, the rock is called "crush breccia" if coarse grained, and "cataclasite" if fine grained. Most of them, however, are foliate. MYLONITE—finely ground, foliate FLASER GRANITE, FLASER DIORITE, FLASER CONGLOMERATE, ETC.—flaser structure AUGEN GNEISS—augen structure ULTRAMYLONITE—partially fused mylonite Rocks with only minor deformation may be called "schistose," for example "schistose sandstone," "schistose rhyolite," etc., but these are not properly metamorphic rocks	Most slates are dark colored	PHYLLITE is intermediate between slate and schist. It differs from slate in that crystallization of micaceous minerals imparts a sheen to the rock; it differs from schist in that grains are too small for megascopic identification. PHYLLONITE—a phyllite owing its fine grain to mylonitization	QUARTZ-MICA SCHIST TALC SCHIST SILLIMANITE SCHIST ALBITE-MICA SCHIST QUARTZ-SERICITE SCHIST KYANITE SCHIST CALCITE SCHIST (Schistose marble)	RHYOLITE GNEISS QUARTZ PORPHYRY GNEISS QUARTZITE GNEISS SILLIMANITE GNEISS GRANULITE—banding due to elongated quartz or feldspar grains	These rocks have a gneissose, streaked, or irregular structure produced by intimate mixing of metamorphic and magmatic materials. When they can be recognized as "mixed rock," they are called migmatite or migmatite gneiss. They may originate by injection (injection migmatite, injection gneiss, or lit-par-lit gneiss), or by differential fusion. Many so-called migmatites probably originate by partial granitization or by metamorphic differentiation. But at great depth these processes apparently do not differ substantially from the igneous processes forming migmatite, so the products are usually indistinguishable. Migmatites are named by prefixing the rock name of the granitic material to the appropriate root as "granite migmatite," "monzonite injection migmatite," etc.
INTERMEDIATE (Includes Red or Brown)	ABOUT EQUAL PROPORTIONS OF LIGHT-COLORED AND DARK-COLORED MINERALS		METAQUARTZITE MARBLE SKARN—pyroxene-garnet-carbonate hornfels SOAPSTONE—chiefly talc HORNFELS—any metamorphic rock with nondirectional structure SERPENTINE*	METAQUARTZITE MARBLE DIOPSIDE MARBLE CHONDRODITE MARBLE ANDALUSITE HORNFELS SKARN—pyroxene-garnet-carbonate hornfels GARNET HORNFELS KYANITE HORNFELS ANTHOPHYLLITE HORNFELS CALC-SILICATE HORNFELS SERPENTINE* CORDIERITE-ANTHOPHYLLITE HORNFELS				MICA SCHIST CHIASTOLITE SCHIST ANDALUSITE SCHIST STAUROLITE SCHIST KYANITE SCHIST PYROPHYLLITE SCHIST GARNET-MICA SCHIST SERPENTINE* TOURMALINE-MICA SCHIST ANTHOPHYLLITE SCHIST STAUROLITE-KYANITE SCHIST SILLIMANITE-GARNET SCHIST GRAPHITE SCHIST CALCITE SCHIST (Schistose marble) SCHISTOSE QUARTZITE	GRANITE GNEISS SYENITE GNEISS MONZONITE GNEISS GRANODIORITE GNEISS ANORTHOSITE GNEISS TRACHYTE GNEISS CONGLOMERATE GNEISS ARKOSE GNEISS SANDSTONE GNEISS AUGEN GNEISS—augen structure BIOTITE GNEISS STAUROLITE GNEISS PLAGIOCLASE GNEISS GARNET GNEISS MUSCOVITE-BIOTITE-QUARTZ GNEISS KYANITE GNEISS GRANULITE—banding due to elongated quartz or feldspar grains	
DARK (Includes Green)	QUARTZ CALCITE DOLOMITE FELDSPAR CHLORITE HORNBLENDE SERPENTINE BIOTITE PYROXENE ACTINOLITE EPIDOTE OLIVINE MAGNETITE		METAQUARTZITE MARBLE SKARN—pyroxene-garnet-carbonate hornfels GRAPHITE MARBLE CHLORITE MARBLE SERPENTINE MARBLE (Ophicalcite) HORNFELS—any metamorphic rock with nondirectional structure SERPENTINE*	METAQUARTZITE MARBLE GRAPHITE MARBLE CHLORITE MARBLE OLIVINE MARBLE SKARN—pyroxene-garnet-carbonate hornfels ACTINOLITE MARBLE ACTINOLITE-EPIDOTE HORNFELS ACTINOLITE HORNFELS PYROXENE HORNFELS EPIDOTE HORNFELS TOURMALINE HORNFELS ANDALUSITE-BIOTITE HORNFELS SERPENTINE* ECLOGITE—pyrope-omphacite hornfels MAGNETITE ROCK CORDIERITE HORNFELS AMPHIBOLITE—chiefly hornblende and or plagioclase		SILTY SLATE GREEN SLATE BLACK SLATE SPOTTED SLATE ANDALUSITE SPOTTED SLATE CHIASTOLITE SPOTTED SLATE BIOTITE SPOTTED SLATE CARBONACEOUS SLATE CALCAREOUS SLATE		GREENSCHIST CHLORITE SCHIST CHLORITOID SCHIST GLAUCOPHANE SCHIST AMPHIBOLITE (HORNBLENDE SCHIST) ACTINOLITE SCHIST GRAPHITE SCHIST PYROXENE SCHIST EPIDOTE-CHLORITE SCHIST HORNBLENDE- BIOTITE SCHIST BIOTITE-CHLORITE SCHIST SERPENTINE* TOURMALINE SCHIST EPIDOTE AMPHIBOLITE GARNET-PYROXENE AMPHIBOLITE GARNET-CHLORITE SCHIST	QUARTZ DIORITE GNEISS DIORITE GNEISS GABBRO GNEISS PERIDOTITE GNEISS DIABASE GNEISS PYROXENE GNEISS GRAYWACKE GNEISS EPIDOTE GNEISS GARNET-BIOTITE GNEISS SKARN GNEISS AMPHIBOLITE GNEISS	

As can be noted from the chart, naming a metamorphic rock consists chiefly of prefixing the structural term with mineral names or an appropriate rock name. The rock name indicates either the original rock, if recognizable, or the new mineral composition. The prefix "meta," as "metagabbro," "metasandstone," "metatuff," etc., is applied to rocks that have undergone considerable recrystallization but have largely retained their original fabric. Most of the minerals listed as accessories are genetically important and if present should be included in the rock name regardless of their quantity.

* **SERPENTINE** is a product of hydrothermal alteration which some authorities consider to be an igneous process and others a metamorphic process. For this reason, serpentine appears both on this chart and on the igneous rock chart.

FREQUENCY OF OCCURRENCE

This size type indicates COMMON ROCKS.
This size type indicates UNCOMMON ROCKS.
This size type indicates RARE ROCKS